HEAT TRANSFER IN MIXING VESSELS AT LOW REYNOLDS NUMBERS

An experimental study of temperature profiles, heat transfer rates and power requirements for mechanically agitated vessels operating at low Reynolds numbers.

by

P. Ayazi Shamlou B.Tech.
Parviz

A thesis presented for the Degree of Doctor of Philosophy

Postgraduate Studies in
Schools of Chemical Engineering,
University of Bradford,
Bradford, BD7 1DP.

December , 1980

To Monir and Naby

ABSTRACT

The present study investigates experimentally the laminar mixing and heat transfer of a range of helical ribbon and anchor impellers for both Newtonian and inelastic non-Newtonian fluids. The work also correlates the experimental data empirically in the form of dimensionless groups.

In order to estimate the relative importance and the effect of all the geometrical parameters on the mixing power and heat transfer, data from the published literature sources will be utilized and combined with the results from this study. Thus, reliable empirical correlations will be obtained which are applicable over the widest range of operating conditions.

The study also investigates the ablity of the various impellers to level out temerature distributions. The measurement of these temperature gradients and the impeller power requirements gives a measure of the mixing efficiency of the impeller used.

ACKNOWLEDGEMENT

I wish to express my profoundest appreciation to Dr. M.F. Edwards for his help and supervision throughout the research period.

I would also like to thank other members of the teaching staff, notably, Mr. J.C. Godfrey and Dr. W.C. Macsporran for their helpful suggestions and advice during the study.

Special thanks must go to Mr. R. Peel for his help in the design, selection and construction of the experimental equipment.

Finally the author extends fis grateful thanks to the Science Research Council for granting him financial assistance for the period of this work.

CONTENTS

SUMMARY

The present work is concerned with an experimental study of the heat transfer characteristics of various Newtonian and non-Newtonian fluids in mechanically agitated vessels under laminar conditions for close-clearance impellers.

Measurements have been taken of the power requirements, temperature distributions and rates of heat transfer in a 0.4m and a smaller 0.15m diameter vessel fitted with a cooling jacket. Heat addition was provided by an immersion heater. Agitation was provided by a variety of helical ribbon and anchor impellers.

Isothermal power input measurements were taken in both laminar and turbulent regions for all the impellers using several Newtonian fluids. These power data together with power input data for a number of time-independent non-Newtonian fluids were, then, used to obtain impeller shear rate constants, k_s, for all the agitators. Using these k_s values, average shear rates, $\dot{\gamma}_A$, and hence average apparent viscosities, μ_A, could be obtained. Average apparent viscosities obtained in this way were used in all subsequent experiments to correlate power and heat transfer data for the non-Newtonian liquids.

Experimental power input data for both Newtonian and non-Newtonian fluids recorded in the present study were combined with results extracted from literature and the following correlations were developed for anchor and helical ribbon impellers:

$$P_o = 85\ (C/D_T)^{-0.314}(h/D)^{0.476}\ \ Re^{-1}$$

for anchors and

$$P_o = 150\ (C/D)^{-0.2774}(P/D)^{-0.5332}(h/D)(W/D)^{0.325}\ (Nb)^{0.54}\ \ Re^{-1}$$

for helical ribbons.

Large temperature gradients were recorded in the core region of the agitated Newtonian and non-Newtonian fluids at low Reynolds numbers for both helical ribbon and anchor impellers. Temperature profiles were established for a number of fluids of widely different physical properties. The following empirical correlations were obtained for the critical Reynolds numbers, Re_c, below which large temperature variations existed in the bulk of the agitated liquid:

$$Re_c = 1.84 \times 10^{8} (P/D)^{0.428} (C/D)^{1.261} (Nb)^{-1.42} Pr^{-1.3}$$

for helical ribbons and

$$Re_c = 5 \times 10^{5} Pr^{-1}$$

for anchor impellers.

For Reynolds numbers above the critical value required to eliminate large temperature gradients, the following equations have been developed for heat transfer:

$$Nu = 0.171 (Re)^{0.16} (Pr)^{0.336} (Vis)^{0.188} (C/D)^{-0.452} (P/D)^{-0.235} (Nb)^{0.222}$$

in the range $Re < 1.0$

and

$$Nu = 0.45 (re)^{0.598} (Pr)^{0.336} (Vis)^{0.188}$$

in the range $10 < Re < 10^3$

for helical ribbons and

$$Nu = 0.1 (Re)^{0.653} (Pr)^{0.333} (Vis)^{0.18} (C/D)^{-0.363}$$

in the range $20 < Re < 10^3$

for anchors.

Alternative correlations relating the Nusselt number to the power input of the impellers have also been developed

CHAPTER 1

INTRODUCTION

Highly viscous Newtonian and non-Newtonian fluids are frequently encountered in the process industries and the production of many such materials often involves heat transfer and accurate temperature control in a mixing vessel. Examples of such processes include the production of foodstuffs, pharmaceuticals, detergents, rubber, plastics, synthetic fibres, paints, cement, paper pulp, soap, petroleum and heavy chemicals. Due to the high viscosity of these materials the mixing operation, in most cases, is carried out at low Reynolds numbers giving rise to laminar or,at best, transitional conditions. If this is the case, then significant temperature gradients may exist within the vessel during both heating and cooling operations. This fact has been confirmed in a few limited experimental studies (1 - 6).

The presence of such temperature variations within the vessel leads directly to several problems for the equipment designer;

(i) What heat transfer correlations should be used in this region to calculate appropriate heat transfer surface area?

(ii) What will be the magnitude of the impeller power requirement which determines the motor size?

(iii) What is the quantitative temperature distribution and how will this affect criteria such as reaction yields, or will any thermal degradation, e.g. of foodstuffs, be produced?

There is available in the literature much data on heat transfer rates and power requirements in agitated vessels in the turbulent region, particularly for open-proximity impellers. Unfortunately, however, there is insufficient information in the literature to predict quantitatively the probable temperature distributions for any type of impeller in the laminar and transitional region. As a result it is not possible to define bulk liquid temperatures and hence meaningful heat transfer coefficients which can be incorporated into design correlations. Further, no work has been done on the prediction of power requirements in the presence of temperature gradients. This final point is of significance because many viscous liquids exhibit a highly temperature sensitive viscosity and thus the power requirement in the laminar and transitional regions will be affected strongly by viscosity variations.

The accurate thermal design and analysis of mixing vessels operating in the laminar region is clearly held back by a lack of quantitative information. This contrasts sharply with the position in the turbulent region where the designer will find an abundance of relevant publications giving design correlations.. Paradoxically, the most difficult mixing and heat transfer operations are to be found in the laminar and transitional regions.

In theory, the exact understanding of the kinematics and dynamics of the flow could be achieved by solving the equation of motion and the equation of continuity for known boundary conditions. However, due to the complexities in the geometry, the solution of such problems involves enormous mathematical difficulties. In the case of non-Newtonian liquids the non-linearities in the constitutive equations make the problem almost intractable . Numerical solutions may be possible, but they do not offer general relationships. Therefore the obvious trend in the study of mixing is to collect extensive experimental data and then interpret them so as to deduce any possible generalisation.

Studies by Nagata(1), Zlokarnik(4), Gray(7), and Hoogendorn and Den-Hartog(8) indicated the suitablity of anchor and helical ribbon impellers for mixing of highly viscous Newtonian and inelastic non-Newtonian liquids.

Scope and objectives of the present investigation;

The present study investigates experimentally the laminar mixing and heat transfer of a range of helical ribbon and anchor impellers for both Newtonian and inelastic non-Newtonian fluids. The work also correlates the experimental data empirically in the form of dimensionless groups.

In order to estimate the relative importance and the effect of all the geometrical parameters on the mixing power and heat transfer, data from the published literature sources will be utilized and combined with the results from this study. Thus, reliable empirical correlations will be obtained which are applicable over the widest range of operating conditions.

The study also investigates the ablity of the various impellers to level out temerature distributions. The measurement of these temperature gradients and the impeller power requirements gives a measure of the mixing efficiency of the impeller used.

CHAPTER 2

LITERATURE SURVEY

Despite the importance of laminar mixing and heat transfer in many industrial processes, reports on the mixing performance and heat transfer coefficients from the vessel wall agitated by both large and close-clearnce impellers are few and agreement of data among investigators is poor.

There are excellent reviews in the literature on power requirements and turbulent heat transfer using various combinations of impeller (i.e. turbines, anchors, paddles and propellers) (9 - 11). Attention is focussed in this chapter upon power requirement and heat transfer in agitated vessels containing Newtonian and non-Newtonian liquids in the laminar and transition regions using helical ribbon and anchor impellers.

The review has been structured in two parts. Part 1 presents a summary and critical review of literature pertaining to power requirements for clos-clearnce impellers, while the published literature on heat transfer in agitated systems for these impellers is critically reviewed and compared in part 2.

2.1 Power Consumption

Slow moving agitators with large surface areas are generally recommended for mixing and performing other operations in the processing of various materials. Metzner and co-workers(12,13) have effectively demonstrated the inadequacy of open impellers such as propellers and turbines for these tasks. Anchor impellers are often used for mixing viscous liquids of upto 10^6 cps.(2). They exhibit very little axial mixing (14,15) and have stagnant zones behind the agitator blades and near the shaft (14).

Helical ribbon and related design agitators, on the other hand, promote excellent top to bottom circulation and are the recommended agitators for materials having consistencies between mobile fluids and extremely high-consistency materials which are generally palstic in character (2,6,15).

2.1.1 Theoretical Prediction of Power Requirement

In theory the equations for the conservation of mass, momentum and energy may be written to describe the system (16,17.18). The general solution of these equations, however, involves enormous mathematical difficulties even for Newtonian fluids. The complexities are essentially

due to the complicated shape of the agitator and vessel. Numerical methods may be used to solve the problem for some agitator shapes. However, such a solution has extremely limited utility in that it is linked to one particular set of boundary conditions.

Most of the work on impeller power requirement reported in the literature has, therefore, been concerned with fitting dimensionless parameters to experimental data.

The power requirement for a Newtonian liquid in an agitated vessel in the laminar region depend upon many variables, some of which are listed below;

a) System variables: Viscosity, density, etc.

b) Operating variables: Impeller speed, liquid depth, etc.

c) Equipment variables: Impeller type and diameter, tank diameter, etc.

Under isothermal conditions and for a single phase system, the relationship between the power, P, and the variables may simply be written as;

$$P = f(\mu, \varrho, N, g, D, \text{other geometric dimensions}) \qquad \text{---------- 2.1}$$

The geometrical dimensions, other than the impeller diameter, D, could include clearance between impeller

blade and the vessel wall, impeller pitch and width and number of blades.

By dimensional analysis, equation 2.1 may be reduced to give:

$$P_o = f\ (\ Re,\ Fr,\ \text{other dimensionless geometrical factors}\ ) \quad \text{----------} \quad 2.2$$

where P_o is the Power number ($P/\varrho N^3D^5$), Re is the Reynolds number ($\varrho ND^2/\mu$), and Fr is the Froude number (N^2D/g).

The Froude number characterises uneven surfaces which are produced by vortexing. Skelland (19) reports that in agitated systems, Froude effects can be neglected at values of Reynolds number less than about 300. Since close-clearance impellers generally operate at Reynolds numbers less than this value, the effect of Fr may be ignored.

For geometrically similar systems, therefore, equation 2.2 reduces to

$$P_o = f\ (Re) \quad \text{----------} \quad 2.3$$

Dimensional analysis does not give further insight into the form of this function. It might be, for example,

exponential or logarithmic. For the sake of convenience and simplicity, however, equation 2.3 is arbitrarily assumed to have the form:

$$P_o = K_p (Re)^A \quad \text{----------} \quad 2.4$$

where K_p and A are constants that must be determined experimentally.

So, for most non-vortexing single phase mixing systems under isothermal conditions, the Reynolds number is the usual parameter for characterizing the system. A plot of P_o against Re is known as the power curve. Such curves are used, if available for a given geometry, to obtain the power for given agitator speeds and material properties.

Dimensional analysis is successful in so far as the power data for any particular impeller can be correlated for a Newtonian fluid by plotting the conventional power number, P_o, against Reynolds number, Re, and provided complete geometrical similarity is observed. This type of correlative equations can then be used accurately to reflect the effect of fluid properties.

A typical Newtonian power curve is shown in Fig.(2.1). Generally, below a Reynolds number of about 20, the curve has a slope of -1 on log-log paper. This is the

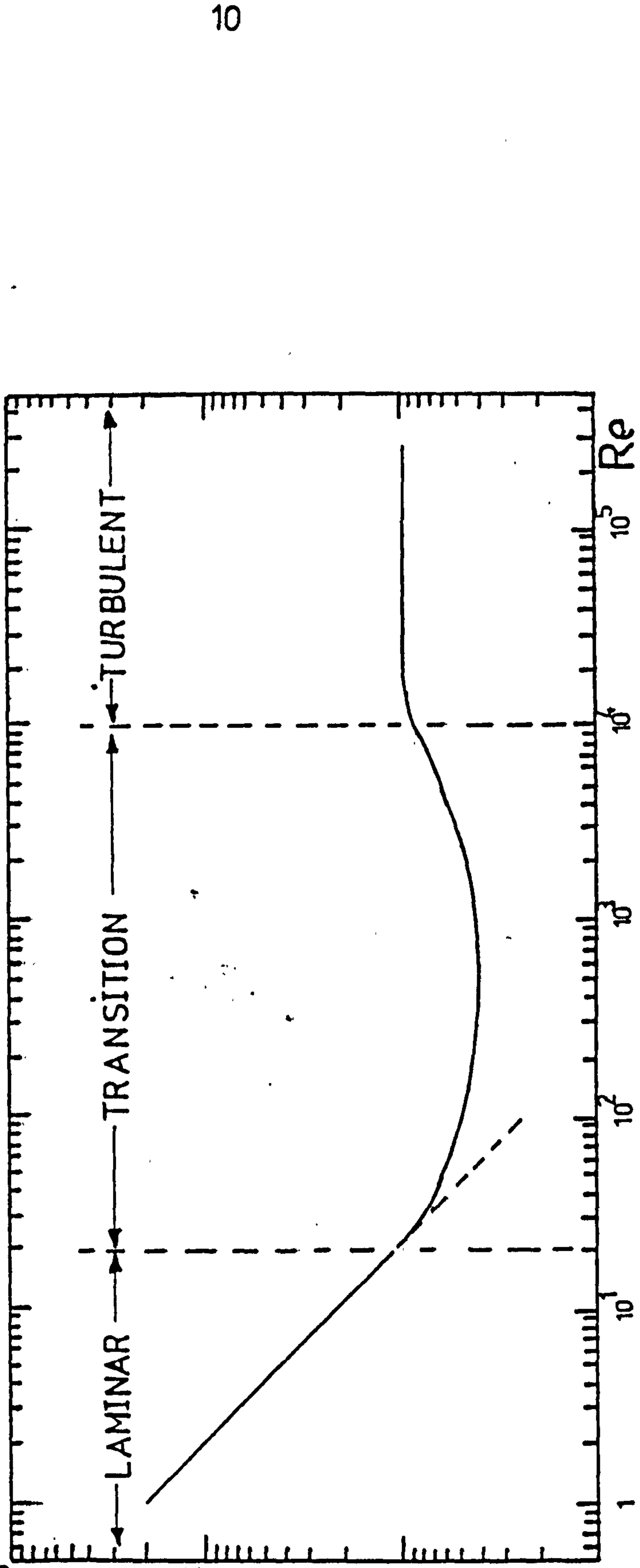

Fig. 2.1 Typical Newtonian Power Curve

laminar region and it is dominated by viscous forces. In this regime, therefore, equation 2.4 may be written as:

$$P_o = K_p \, Re^{-1} \quad \text{----------} \quad 2.5$$

where K_p is a function of impeller and tank geometry.

In the range $20 < Re < 10{,}000$ the slope gradually changes from -1 to 0.0 . This is the transition region where both viscous and inertial effects are important. Uhl and Voznik (3) suggest that turbulence probably starts at about Re = 600. Then laminar extends to Re $\simeq$600. Inertial effects become increasingly important as Re increases; in the range $600 < Re < 10{,}000$ the flow becomes increasingly turbulent as Re increases. Above $Re = 10^4$ the power curve is essentially flat and thus:

$$P_o = \text{Constant} \quad \text{----------} \quad 2.6$$

the value of the constant in equation 2.6 may depend uopn impeller and vessel geometry.

For non-Newtonian liquids equation 2.5 will no longer be valid as the liquid viscosity, μ , used in the Reynolds number term, Re, does not remain constant for all shear rates when agitated at a constant temperature.

For Newtonian liquids:

$$\mu = \frac{\tau}{\dot{\gamma}} \quad \text{----------} \quad 2.7$$

(μ is constant for all $\dot{\gamma}$)

Hence it is a simple task to obtain values for the Reynolds number, Re. In an agitated vessel, however, the shear rate varies throughout the process liquid, thus producing a variation in the apparent viscosity if the fluid is non-Newtonian in character. This makes the specification of a viscosity, which is to be used in the Reynolds number extermely difficult.

Metzner and Otto(12) and Magnusson (13) were the first workers to propose a technique to overcome this difficulty. They proposed the use of an ' average shear rate', $\dot{\gamma}_A$, for the vessel and the apparent viscosity of the non-Newtonian liquid is evaluated at this shear rate. This is done in conjunction with the flow curve (plot of shear stress against shear rate) for the liquid which can be obtained from viscometric data. This value of the apparent viscosity at $\dot{\gamma}_A$ is the ' average apparent viscosity', μ_A.

For small impellers such as turbines and propellers these workers experimentally verified (12,13) that the average shear rate, $\dot{\gamma}_A$, in an agitated liquid is directly proportional to the rotational speed of the impeller, N. Thus:

$$\dot{\gamma}_A = k_s N \qquad \text{----------} \qquad 2.8$$

where k_s is generally known as the ' impeller shear rate

constant'. Its value depends mainly upon the geometry of the equipment and the type of impeller used and is essentially independent of rheological properties.

Having defined an average shear rate and hence an average apparent viscosity for the agitated liquid, a modified Reynolds number, Re_1 , may easily be defined incorporating μ_A :

$$Re_1 = \rho N D^2 / \mu_A \quad \text{----------} \quad 2.9$$

For the special case of power law fluids k_s may be incorporated into the power number - Reynolds number equation. For power law fluids:

$$\tau = K \dot{\gamma}^n \quad \text{----------} \quad 2.10$$

where K is the fluid consistency index and n is the flow behaviour index. A full discussion and classification of non-Newtonian fluids is presented in Appendix (2).

The apparent viscosity, μ_A , may be written as:

$$\mu_A = \frac{\tau}{\dot{\gamma}_A} = K (\dot{\gamma}_A)^{n-1} \quad \text{----------} \quad 2.11$$

Substituting for $\dot{\gamma}_A$ from 2.8 into 2.11

$$\mu_A = K\,(k_s N)^{n-1} \qquad \text{----------} \qquad 2.12$$

This value of μ_A may then be incorporated into equation 2.9 to give:

$$Re_1 = \frac{\varrho N^{2-n} D^2}{K} (k_s)^{1-n} \qquad \text{----------} \qquad 2.13$$

The power number equation may be rewritten as:

$$P_o = K_p \left[\frac{\varrho N^{2-n} D^2}{K} (k_s)^{1-n} \right]^{-1} \qquad \text{-----} \qquad 2.14$$

where the value of of K_p is valid for Newtonian and non-Newtonian fluids. The value of the shear rate constant, k_s, obtained experimentally and to be discussed later in this section have been reported for a number of impellers (1,12,13,19). It is important to note the presence of the impeller shear rate constant, k_s, in the power number equation. The Reynolds number for pseudoplastic fluids is sometimes taken as:

$$Re_2 = \frac{N^{2-n} D^2 \varrho}{K} \qquad \text{----------} \qquad 2.15$$

in which case the power correlation is not achieved. Skelland (19) pointed out that such Reynolds numbers do not give a unique curve for a wide range of flow behaviour index.

An alternative approach has been put forward by Calderbank and Moo-Young (20) for fluids of the power-law type whose rheological behaviour is represented by equation 2.10 . For such fluids these workers propose the following expression for the average shear rate:

$$\dot{\gamma}_A = BN \left[\frac{3n + 1}{4n} \right]^{\frac{n}{n-1}} \qquad \text{----------} \qquad 2.16$$

giving:

$$Re_3 = \frac{\rho N^{2-n} D^2}{K} \; B^{1-n} \left[\frac{4n}{3n + 1} \right]^n \qquad \text{-----} \qquad 2.17$$

For shear thinning fluids with small impellers a value of B = 11 $\pm$ 10% is reported while for the same impellers operating in shear thickening dilatent materials:

$$B = \frac{22 \; (D_T/D)^2}{(D_T/D - 1)^2} \qquad \text{----------} \qquad 2.18$$

For anchor agitators in pseudoplastic materials:

$$B = 9.5 + \frac{9 \; (D_T/D)^2}{(D_T/D - 1)^2} \qquad \text{----------} \qquad 2.19$$

Edwards and Wilkinson (9,10) comparing the average

shear rates proposed by Metzner (12) and Calderbank (20) pointed out that both methods for the evaluation of the average shear rate in the vessel, i.e. equations 2.8 and 2.16 predicted a linear relationship between the average shear rate and the impeller speed. For a wide range of n values ($0.05 < n < 1.68$) the term:

$$\left[\frac{3n + 1}{4n}\right]^{n/n-1} \qquad \text{---------- 2.20}$$

involved in equation 2.16 was found to be close to $0.84 \pm 8.5\%$ and could thus be treated as a constant, if $n \neq 1$.

Skelland (19) presents values of k_s empirically determined for a wide variety of agitator configurations and fluids. A universal value of about 11.0 has been recommended by Metzner for most small impellers such as turbines and propellers.(12).

Beckner and Smith (21) using pseudoplastic fluids and anchor agitation proposed the following expression for the Reynolds number:

$$Re_4 = \frac{\rho N^{2-n} D^2}{K} \left[a\,(1-n)\right]^{n-1} \qquad \text{-------- 2.21}$$

where for anchor agitation with simple arms:

$$a = 37 - 120\ (C/D_T) \quad \text{----------} \quad 2.22$$

and for anchor agitation with oblique arms:

$$a = 106 - 1454\ (C/D_T) \quad \text{----------} \quad 2.23$$

Comparing equation 2.21 with equation 2.13, it is seen that the impeller shear rate constant, k_s, as defined by equation 2.21 is:

$$k_s = a\ (1-n) \quad \text{----------} \quad 2.24$$

which shows the strong dependence of the shear rate constant, k_s, on the flow behaviour index, n, for both standard and pitched blade anchors.

An alternative expression often used for the determination of the average shear rate in the vessel is the following proposed by Gluz and Pavlushenko (17):

$$\dot{\gamma}_A = 4\pi N \quad \text{----------} \quad 2.25$$

giving:

$$Re_5 = \frac{N^{2-n}\ D^2}{K}\ (4\pi)^{1-n} \quad \text{------} \quad 2.26$$

Comparing equation 2.26 with equation 2.13 indicates that:

$$k_s = 4\pi \quad \text{----------} \quad 2.27$$

Equation 2.25 correlates the data for most small impellers where a k_s value of about 4π (i.e. 10 - 14) has been reported by many workers (1,12,13,18,19,20). It, however, tends to underestimate the average shear rate in the mixing vessel when large impellers such as helical ribbons are involved (1,22,23,2,3).

Mitsuishi and Miyairi (24) claimed that the use of equation 2.8 for the determination of average shear rate in the vessel is not valid for geometrically similar but variously sized agitators. These workers using the three-constant Ellis model and a semi-theoretical technique obtained shear rate - rotational speed relationship for various impellers, e.g. by comparing the flow between a vessel wall and a ribbon to the flow between two parallel flat plates, they obtained:

$$\dot{\gamma}_A = \frac{\pi}{\sqrt{2}} \left[\frac{D}{D_T - D}\right] N \quad \text{----------} \quad 2.28$$

Comparing equation 2.28 with equation 2.8 indicates that for this type of impeller:

$$k_s = \frac{\pi}{\sqrt{2}}\left[\frac{D}{D_T - D}\right] \quad \text{----------} \quad 2.29$$

i.e.

$$k_s = 1.1\ (C/D)^{-1} \quad \text{----------} \quad 2.30$$

Carreau et-al (25) using the analogy with pipe flow first suggested by Metzner and Otto (12) used the following expression for the modified Reynolds number:

$$Re_6 = \frac{\rho N^{2-n} D^2}{K} \; 8 \left[\frac{n}{6n+2}\right]^n \qquad \text{---------- 2.31}$$

Skelland (19) pointed out that such Reynolds numbers do not give a unique curve for a wide range of flow behaviour index. Mitsuishi and Hirai (26) claimed that this failure was due to the power-law approximation rather than the analogy. They, thus, analysed their results using Ellis and Sutterby's model and gave:

$$Re_7 = \frac{\rho N D^2}{\mu_o} \left[1 + \frac{4}{\alpha+3} \left\{Fe\left(\alpha, \frac{8N\mu_o}{\tau_o}\right)\right\}^{\alpha-1}\right] \text{---- 2.32}$$

for Ellis model and:

$$Re_8 = \frac{\rho N D^2}{\mu_o} \left(\frac{8NB}{Fs\ (A,\ 8NB)}\right) \qquad \text{---------- 2.33}$$

for Sutterby model.

Functions Fe and Fs are capillary viscometric data. The analysis correlated their results very well but it should be pointed out that:

a) There was not a good variation in the value of α, the rheological constant in the Ellis model.

b) They did not consider Newtonian liquids.

c) Equations 2.32 and 2.33 do not reflect the real situation since functions Fe and Fs are obtained by a capillary viscometer which normally does not give low shear rate data while the systems under investigation are often under low shear rates.

d) There was not a good variation in the values of A and B, the rheological constants in the Sutterby model.

e) Equations 2.32 and 2.33 are restricted to particular fluid models.

Kelkar, Mashelkar and Ulbrecht (27) using Ellis model and studying the rotational flows around simple bodies proposed the following alternative expression for the modified Reynolds number for the case of inelastic non-Newtonian fluids:

$$Re_9 = \frac{\rho N D^2}{\mu_o} \left(\frac{4}{\alpha+3}\right) \left(\frac{N\mu_o}{\tau_o}\right)^{B'(1-\alpha/\alpha)} \qquad \text{--- 2.34}$$

giving:

$$P_o = K_p' \left(\frac{4}{3+\alpha}\right) \left(\frac{N\mu_o}{\tau_o}\right)^{B'(1-\alpha/\alpha)} \left(\frac{D^2 N\rho}{\mu_o}\right)^{-1} \qquad \text{---- 2.35}$$

where K_p' and B' depend upon the type of rotating bodies. It should, however, be pointed out that it is very dangerous for design purposes to extrapolate the results from rotation of simple bodies such as discs and spheres to data

obtained from the rotation of geometrically complex shapes such as impellers.

Equations such as 2.32, 2.33, 2.34 and 2.35 are cumbersome to use and offer no advantage over the simpler, more general average shear rate approach proposed by Metzner and Otto (12). The average shear rate concept in not without disadvantage. Many workers (1,2,11,15,19) have reported different values for k_s for different agitation systems and so the idea of k_s being a universal constant as proposed by Metzner and Otto (12) is no longer valid. In fact equations such as 2.24 and 2.28 indicate that even for a particular agitation system k_s could be function of geometrical variables and rheology of the fluid. However, the concept is simple and as yet there is no convenient and more accurate alternative.(1,9,10,23)

Metzner and Otto (12) carried out the most extensive study to test the concept of the average shear rate and developed a procedure,outlined below,for the determination of k_s:

1. Determine experimentally the power number - Reynolds number curve for the particular vessel and impeller geometry using Newtonian fluids.
2. Determine experimentally the power number for the time-independent non-Newtonian liquid at

various impeller speeds using the term ($P/\varrho N^3D^5$).

3. For the non-Newtonian power numbers, read off the corresponding Reynolds number using the power curve developed in (1).
4. For each Reynolds number obtained in (3), calculate the average apparent viscosity using:

$$\dot{\gamma}_A = \frac{\varrho ND^2}{Re}$$

5. Obtain the flow curve (i.e. plot of shear stress against shear rate) for the particular non-Newtonian liquid using a concentric cylinder viscometer.
6. Evaluate the appropriate average shear rates for the non-Newtonian time-independent liquid from the average apparent viscosity values obtained in (4) and the flow curve obtained in (5)
7. Plot the shear rates determined in (6) against their corresponding impeller speeds, N. The slope of this slope is the value of k_s.

It is important to note that in using the average apparent viscosity concept no particular fluid model is assumed. It should also be pointed out that this technique only applies in the lamiar flow region and could possibly be extended to the transition region. Such measurements are not possible in the turbulent regime since in this region the power number is independent of Reynolds number.

2.1.2 Dimensionless Correlations

The general dimensionless equation describing the power consumption for laminar mixing of Newtonian and inelastic non-Newtonian fluids is:

$$P_o = K_p (Re)^{-1} \quad \text{----------} \quad 2.36$$

where for a Newtonian liquid Re is given by ($\varrho ND^2/\mu$) and for an inelastic non-Newtonian liquid it is given by ($\varrho ND^2/\mu_A$). The value of K_p is a function of geometry.

Equation 2.36 is extremely restrictive as it does not allow for any changes in the geometry of the system. Complete geometrical similarities must be observed or gross errors in the evaluation of the power consumption will result. In order to relax some of these restrictions a number of geometrical factors may be included in the correlation. Equation 2.36 may, thus, be rewritten depending on the number of geometrical factors relaxed as:

$$P_o = K_p \ (C/D_T)^a \ (h/D)^b \ (W/D)^c \ (H/D_T)^d \left[\begin{array}{l}\text{other geometrical} \\ \text{factors as required}\end{array}\right] Re^{-1} \quad \text{----} \quad 2.37$$

where the value of K_p in equation 2.37 is still a function of geometry (i.e. those geometrical factors

that have not been relaxed) but, obviously, not the same as the value of K_p in equation 2.36 .

It is important to note that the functional relationship given by equation 2.37 is an assumed form used for the sake of convenience and simplicity only. There is no physical justification why the relationship between the power number and the geometrical factors should not be any other form such as exponential, logarithmic or an infinite series.

(i) Anchor Impellers

Foresti and Liu (28) carried out a series of experiments with anchors, a turbine, and two-cone agitators using one Newtonian and three non-Newtonian liquids in the viscous regime. Their data were plotted as P_o against $(\varrho N^{2-n} D^2/K)(H/h)^n(D/D+D_T)$ on log-log paper. Their correlation appears to have brought the data for all agitators together for any value of n; however, a separate curve resulted for each value of n with the curve for n = 1.0 being about 20 times higher than for n = 0.34 . In other words, while their modified Reynolds number, i.e.

$$Re_{lo} = \frac{D^2 N^{2-n} \varrho}{K} \left(\frac{H}{h}\right)^n \left(\frac{D}{D + D_T}\right) \qquad \text{--------- 2.38}$$

seems to have reduced the variation due to different geometries the power curves are very much dependent on

the value of the flow behaviour index, n . In the laminar region all their data were correlated by:

$$P_o = 160\ (50)^{n-1}\ Re_{10}^{-1} \qquad \text{---------- 2.39}$$

comparing equation 2.39 with equation 2.14 indicates that according to these workers the value of $K_p = 160$ while the value of the impeller shear rate constant, $k_s = 50$.

The use of the empirical constant 50 in equation 2.39, i.e. the value of k_s, has not been justified and is very approximate since only two non-Newtonian fluids (n = 0.34 and 0.52) were tested. For Newtonian fluids their plot indicate that:

$$P_o = 320\ (H/h)(1 + C/D)\ Re^{-1} \qquad \text{---------- 2.40}$$

This equation indicates that:

a) power is proportional to liquid height, H; as will be shown later power is almost independent of H .

b) power is essentially independent of clearance, C, for small values of clearance; However, the literature indicates a strong dependence of power on clearance.

Uhl (2) and Uhl and Voznick (3) using a 0.25m diameter dished bottom vessel and anchors with clearance ratios,

C/D_T, of 0.00914, 0.0244, 0.0488 and 0.0732 reported some data on power input for anchor impellers. They tested one Newtonian fluid and presented the data as log P_o against log Re and a separate curve resulted for each clearance. These workers also reported data for a 0.6m diameter dished bottom vessel having clearance ratios of 0.0104, 0.0208 and 0.0416 . They noticed that the curves for the two different diameter vessels did not merge and suggested that better comparison and scale up between different diameter anchor impellers could be made at constant C/D if the power number, P_o, was divided by the ratio of effective peripheral length to vessel diameter. The effective peripheral length was defined as the length of the two vertical blades plus one quarter the length of the bottom blade:

$$\frac{EPL}{D_T} = \frac{2h}{D_T} + \frac{1}{4} \qquad \text{---------- 2.41}$$

where h is the height of the upright anchor arm. Their data agreed within 30% of the Newtonian anchor data of Foresti and Liu (28) .

These workers also noticed that impeller width had negligible effect on power, but more experimental data are required to confirm this since they only tested two impellers (W/D = 0.085 and 0.1276) .

Calderbank and Moo-Young (20) using the data of Uhl and Voznick (3) and Foresti and Liu (28) with their own data obtained a general correlation for anchors which included non-Newtonian behaviour index and some geometrical variables. They used the analogy with pipe flow to define the following Reynolds number:

$$Re_3 = \frac{\rho N^{2-n} D^2}{K} B^{1-n} \left[\frac{4n}{3n+1}\right]^n \qquad \text{------- 2.42}$$

where

$$B = 9.5 + \frac{9\,(C/D_T)^2}{(D_T/D)^2 - 1} \qquad \text{---------- 2.43}$$

Their final correlation for anchor impellers takes the following form:

$$P_o' = (P/\rho\, N^3 D^5)\,(h_e'/D_e')\,\frac{(\Delta W)^{0.5}}{(N_b\, N_s)^{0.67}}$$

$$= 6.3\, Re_3^{-1} \qquad \text{------ 2.44}$$

To simplify the calculation assume that for Newtonian fluids with $W_a = W_1 \ll h$, i.e. impeller width much smaller than impeller height:

$$h_e = h - W/2 \simeq h$$

and

$$D_e^{\cdot} = D - W \simeq D$$

$$\therefore \quad \frac{h_e'}{D_e'} = \frac{4\ N_s h_e + D_e}{N_s\ D_e}$$

$$= \frac{4\ N_s h + D}{N_s D}$$

But for anchor impellers $N_s = N_b = 2$

$$\therefore \quad \frac{h_e'}{D_e'} = \frac{8\ h + D}{2\ D}$$

$$\therefore \quad P_o' = (P/\rho N^3 D^5)\left(\frac{8\ h + D}{2\ D}\right) \frac{\Delta W^{0.5}}{4^{0.67}} = 6.3\ Re^{-1}$$

$$\therefore \quad P/\rho N^3 D^5 = 32\left(\frac{D}{8h + D}\right) (\Delta W)^{-0.5}\ Re^{-1} \quad \text{-----} \quad 2.45$$

But ΔW is defined as:

$$\Delta W = 1/(D_T/D - 1) = 1/(2C/D)$$

where C is the clearance between the impeller blade to vessel wall. Equation 2.45 may, therefore, be written as:

$$P/\rho N^3 D^5 = 45\left(\frac{D}{8h + D}\right) (C/D)^{0.5}\ Re^{-1} \quad \text{----} \quad 2.46$$

If it is further assumed that h = D, i.e. impeller diameter equal impeller height, equation 2.46 will reduce to:

$$P/\rho N^3 D^5 = 5\,(C/D)^{0.5}\ Re^{-1} \quad \text{----------} \quad 2.47$$

This correlation fails completely since it predicts a decrease in power with a decrease in clearance which is inconsistent both with physical reality and results from other published data.

It is also worth noting that for the extreme case of $8h \gg D$, equation 2.46 will reduce to:

$$P = 45\,\frac{\mu N^2 D^4 (C/D)^{0.5}}{8h} \quad \text{----------} \quad 2.48$$

which predicts that:

a) $P \propto D^4$ at constant (C/D) rather than D^3.

b) $P \propto 1/h$ rather than h .

The same problems as outlined for Newtonian fluids are inherent in equation 2.44 when dealing with non-Newtonian materials. The use of equation 2.42 for the modified Reynolds number will result to further errors in the evaluation of the power consumption since the analogy between pipe flow and flow in a tank is an oversimplification.

In order to demonstrate the problems associated with such analogies, a simple example is worked out below;

Calderbank and Moo-Young (20) proposed the following correlation for the average shear rate:

$$\dot{\gamma}_A = BN \left(\frac{4n}{3n+1}\right)^{n/1-n} \quad \text{----------} \quad 2.49$$

where the value of B is given by equation 2.43 . The value of the term $(4n/3n+1)^{n/1-n}$ was found to be close 0.84 $\pm$ 8.4% for a wide range of n values ($0.05 < n < 1.68$) (20,9,10). Equation 2.49 may, therefore, be written as:

$$\dot{\gamma}_A = 0.84 \quad BN \quad \text{----------} \quad 2.50$$

For anchor impellers, using equation 2.43 and taking a $D_T/D = 1.136$, i.e. $C/D_T = 0.06$:

$$\dot{\gamma}_A = 30 \; N \quad \text{----------} \quad 2.51$$

Equation 2.51 compared to equation 2.8 indicates that $k_s = 30$; This is about 23% higher than the normal value of about 23 reported by many workers (1,2,3,12,13) .

Schilo (29) presented the results of his studies on power consumption of an anchor impeller in the form:

$$P_o = 0.7\pi^2 \; (4\pi/n)^n \; (h/D) \frac{(D_T/D)^2}{\left[(D_T/D)^{2/n} - 0.75\right]^n} \left(\frac{\rho N^{2-n} D^2}{K}\right)^{-0.9} \quad \text{---} \quad 2.52$$

This correlation agrees to ±15% with the published work for Newtonian fluids. In this case equation 2.52 takes the following form:

$$P_o = 86.8\ (h/D)\ \frac{(D_T/D)^2}{(D_T/D)^2 - 0.75}\ Re^{-0.9} \quad -- \quad 2.53$$

For non-Newtonian fluids, however, equation 2.52 tends to underestimate the power consumption for most of the published work (1,2,3,9,10,23) by about 70% . This is inherent in the approached used to obtain the correlation. Schilo (29) used a theoretical approach based on power consumption of a rotating cylinder in a tank containing the shear thinning power-law fluid. He, thus, developed the following theoretical correlation for the impeller shear rate constant, k_s:

$$k_s = \left[\frac{(4\pi)^{n-1}}{n^n} \quad \frac{(D_T/D)^2 - 0.75}{[(D_T/D)^{2/n} - 0.75]^n} \right]^{\frac{1}{0.9(n-1)}}$$

-------- 2.54

This correlation tends to overestimate the value of k_s by about 20% for each D_T/D when compared with the published values of k_s (1,2,3, 23) . However the main reason for the inadequacy of equation 2.52 to correlate non-Newtonian data must be related to the coefficient of the term

$(\varrho N^{2-n} D^2/K)^{-0.9}$ in equation 2.52. This is high-lighted by the correlation proposed by Gluz and Pavlushenko (17). i.e.

$$P_o = 198 \left[\frac{\varrho N^{2-n} D^2}{K} (4\pi)^{1-n}\right]^{-1} \quad \text{---------- 2.55}$$

These workers used a theoretical approach to evaluate the value of the impeller shear rate constant, k_s. However, they used dimensional analysis to correlate their power data. Their correlation agrees to $\pm$20% with the published work where a k_s of about 26 has been used in place of 4π. This is partly expained by the fact that for shear thinning materials the term $(k_s)^{1-n}$ is insensitive to moderate changes in k_s. The less pseudoplastic the fluid, the less senstive will this term be to changes in k_s. For example, a 100% change in k_s will only result in 15% change in the value of k_s^{1-n} for $n = 0.8$, to 40% in k_s^{1-n} for $n = 0.5$ and to 74% in k_s^{1-n} for $n = 0.2$. It is, perhaps for this reason that a number of workers (18,27, 30,31,32) treat the term k_s^{1-n} as a constant and hence exclude it from their modified Reynolds number. The practice is both misleading in that it leads to incorrect values of Reynolds numbers and gives rise to unneccessary complications.

Nagata (1) studied the effect of anchor height, h/D, upon power consumption. For a constant C/D_T a separate

power curve resulted for each h/D . They used both Newtonian and non-Newtonian liquids and correlated their data using the apparent viscosity concept. Their correlation, together with those of other workers are given in Table (1) Appendix (1).

Reher and Bohm (33) seem to have studied the effects of some important geometrical factors such as h/D and C/D_T upon power consumption of anchor impellers. They, however, proposed a single correlation which suggests that these geometrical factors have negligible effect on power. This, in the light of other published sources, seems to be very approximate.

Reher and Bohm (33) also employed Calderbank and Moo-Young's approach to evaluate the impeller shear rate constant, k_s, i.e. equations 2.16 and 2.19 . However, they used dimensional analysis to obtain their power correlation. Their power correlation, therefore, does not suffer from the same drawbacks as that of Calderbank and Moo-Young (20). It is, nevertheless, very approximate and overestimates the published Newtonian power data in the laminar region by about 30%. The approximation of the correlation is primarily due to overlooking the significance of important geometrical factors such as h/D and C/D_T .

Beckner and Smith (21) tested the effect of a wide range of geometrical factors on power consumption of

anchor impellers in the laminar region but their final correlation only included the C/D_T term. Their correlation, therefore, brings together most of the data for differing C/D_T but the effect of h/D on power shown to be of significance by Nagata (1) and other workers (20,33,34), was ignored in their final correlation. For non-newtonian shear-thinning fluids, it is interesting to notice that Beckner and Smith (21) found a strong dependence of the impeller shear rate constant, k_s, on both C/D_T and the exponent of power-law fluids, n . These workers, thus, proposed an empirical correlation based on only a very few data for the evaluation of the impeller shear rate constant, k_s, i.e.

$$k_s = a\ (1 - n) \quad \text{----------} \quad 2.56$$

where the value of a is dependent on the type of anchor and takes the form:

$$a = 37 - 120\ (C/D_T) \qquad 0.02 < C/D_T < 0.16 \quad \text{----} \quad 2.57$$

for plain flat-bottom anchors and

$$a = 106 - 1454\ (C/D_T) \qquad 0.02 < C/D_T < 0.05 \quad \text{----} \quad 2.58$$

for pitched-bladed anchors. The range of flow behaviour index, n, covered by these workers was $0.29 < n < 0.73$.

For geometrical variations, the dependence of the impeller shear rate constant, k_s, is described fairly well with

equation of the type given by 2.56 and 2.58 but as Beckner and Smith (21) pointed out correctly a lot more data are required to confirm the numerical constants in these equations. However, as far as the influence of the flow behaviour index, n, upon the mixer shear rate constant, k_s, is concerned, most published data indicate that k_s ia almost independent of the flow behaviour index, n, and an average value is reported in most cases.

The final correlation cited by Beckner and Smith (21) takes the following form:

$$P_o = 82\ (C/D_T)^{-\frac{1}{4}} \left[\frac{\rho N^{2-n} D^2}{K} \left[a(1-n)\right]^{1-n}\right]^{-0.93} \quad \text{---- 2.59}$$

This correlation agrees to $\pm 15\%$ with other published data for Newtonian fluids. It also seems to best fit the data of non-Newtonian fluids with low values of flow behaviour index, n .

Kashani (22) studying the power consumption of anchors and helical ribbons for laminar mixing of both shear-thinning lower-law fluids and thixotropic liquids proposed a correlation that took into consideration the effect of (C/D_T) on power. The exponent of (C/D_T) in his correlation is $-1/3$ as compared to $-\frac{1}{4}$ proposed by Beckner and Smith (21) . Kashani (22) used the Metzner-Otto technique to obtain the modified Reynolds number which was subsequently

employed to fit power data for shear-thinning fluids.

The final correlation reported takes the form:

$$P_o = 90\ (C/D_T)^{-1/3}\left[\frac{\rho N^{2-n} D^2}{K}\ (k_s)^{1-n}\right]^{-1} \quad \text{---} \quad 2.60$$

Appendix(1)

Table (1) is a summary of almost all the correlations reported on power consumption of anchor impellers in the laminar region up to 1980. Wherever possible full details of the geometrical variables tested, fluids used, the range and type of Reynolds number employed in the correlation are included. Correlative equations or the value for the impeller shear rate constant, k_s, are also included for each case when these have been published.

There are about 50 correlations reported in the literature for the power consumption of anchor impellers in the laminar region and the designer is faced with the formidable task of choosing the best one to use. A Table such as the one reported here is rarely published in the literature and yet it is only in the light of such summaries that one might begin the task of comparing the works of different researchers.

The most obvious points high-lighted from Table (1) are:

a) There is a vast amount of information in the literature but,unfortunately, there do not seem

to be any co-ordination of works. So often, the influence of one geometrical variable on power has been studied by a great number of workers and yet the effect of others of equal importance have been ignored.

b) Even when the effect of such geometrical factors has been taken into account, there is rarely enough experimental information to correlate the data. The range of variables tested are often too limited or the correlation has been tested on only a few fluids.

(ii) Helical Ribbon Impellers

The applicablity of equation 2.61 has been confirmed for these impellers in almost all published papers for Reynolds numbers less than 10, and in a few cases up to a Reynolds number of about 100 .

$$P_o = K_p \ Re^{-1} \qquad \text{----------} \quad 2.61$$

Zlokarnik (4) was the first to propose a correlation taking into account a factor for ribbon surface area, F_w, which included some of the geometrical variables:

$$P_o = 1000 \ (F_w/D^2)^{0.187} \ Re^{-1} \qquad \text{--------} \quad 2.62$$

This equation suffers from a number of drawbacks such as the effect of clearance, C/D, impeller height, h/D, shown to be of significance on the evaluation of power. The relation also seems to indicate, as Hall and Godfrey (23) pointed out, that for constant ribbon area, the power consumption is independent of the pitch, P/D, or number of blades, Nb . Furthermore, the correlation was only tested for Newtonian fluids.

Nagata (1,36-38) realising the importance of the effect of some of the geometrical variables missing in equation 2.62 proposed the following:

$$P_o = 52.5 \left(\frac{D_T - D}{D}\right)^{-0.5} (Nb)^{0.5} (P/D)^{-0.5} Re^{-1} \quad \text{--- 2.63}$$

The correlation includes the effect of some important geometrical variables. However, the numerical constants of this equation should be regarded in the light of relatively few data and the narrow range of variables used in its derivation. The correlation also leaves out some of the important variables such as impeller width, W/D, or impeller height, h/d .

The correlation proposed by Hall and Godfrey (23) suffers from some of the drawbacks as equation equation 2.63 put

forward by Nagata (1) and co-workers (36-38) . The correlation suggested by Hall and Godfrey (23) is:

$$P_o = 66\ (P/D)^{-.73}\ (Nb)(h/D)(W/D)^{0.5}(C/D)^{-0.6}\ Re^{-1} \quad \text{---} \quad 2.64$$

The main disadvantages of this correlation are:

1. Evaluation of exponents of (P/D) and (Nb) was based on insufficient data, i.e. to obtain the exponent of these variables these workers compared the results of only two impellers with varying (P/D) and (Nb).
2. Data from literature was not used to evaluate the exponent of (h/D), but a value of 1 was assumed based on a single work of Penny and Bell (39).

Point (1) manifestes itself when one compares the value of K_p provided by equation 2.64 and the expeimental value proposed by Hoo and Wong (40) for a quadruple-helical ribbon agitator, i.e. Nb = 4 . Equation 2.64 overesti-mates the power for this geometry by about 60% . It is also interesting to note that for the same geometry equation 2.63 of Nagata et-al (1) overestimates the power by 40% .

The fact that equation 2.64 overestimates the power is also demonstrated in its ablity to correlate the data of

Johnson (41) and Gray (7) . If the geometry used by Johnson (41) is considered, a higher power consumption is to be expected for his impeller compared to a normal ribbon because of extra attachments on the ribbon employed to promote better mixing. So when equation 2.64 correlates this impeller with an accuracy of -1.7% , it can not be expected to correlate the data from a normal ribbon. The value of K_p reported by Gray (7), i.e. $K_p = 420$, is also questionable since only two points were used in its evaluation . It is also interesting to note that for Johnson's geometry equation 2.63 by Nagata et-al (1) underestimates the power by -15% .

Other workers such as Bourne and Butler (42) derived a theoretical expression for power consumption of helical impellers by comparing the gap between the impeller and the vessel wall with the flow between two concentric cylinders and gave:

$$P_o = \pi^2 \, (h/D)(D_T/D)^2 \left[\frac{4\pi}{n\left[(D_T/D)^{2/n} - 1 \right]} \right]^n \left(\epsilon N^{2-n} \, D^2/K \right)^{-1} \qquad \text{2.65}$$

This correlation does not account for the effects of P/D, Nb, or W/D . It also faied to correlate the data of Bourne and Butler with any degree of accuracy.

The correlation of Bourne and Butler (42) was later modified by Chavan and Ulbrecht (31) who claimed that the failure of equation 2.65 to fit data was due to exclusion of important geometrical factors from the correlation rather than to the analogy with Couette flow. A generalized model was thus developed for both Newtonian and non-Newtonian liquids for Reynolds numbers up to 10 :

$$P_o = \pi(a)\ (De/D)\ \lambda^2 \left[\frac{4\pi}{n\ (\lambda^{2/n} - 1)}\right]^n (\varrho N^{2-n} D^2/K)^{-1} \quad \text{---------- 2.66}$$

where

$$\lambda = D_T/De \quad \text{---------- 2.66a}$$

$$De/D = (D_T/D) - \frac{2(W/D)}{\ln\left[\frac{D_T/D - [1 - 2(W/D)]}{(D_T/D) - 1}\right]} \quad \text{---- 2.66b}$$

and the value of the dimensionless surface area, a, is given by:

$$a = \frac{(h/D)(P/D)}{3\pi}\left(\frac{\pi\sqrt{(P/D) + \pi^2}}{(P/D)^2}\right) + \left(\ln\frac{\pi}{(P/D)}\right) +$$

$$\left(\frac{\pi\sqrt{(P/D) + \pi^2}}{(P/D)}\right)\ [1 - [1 - 2(W/D)]^2\ ] \text{ ----- 2.66c}$$

The corresponding correlation for Newtonian fluids is obtained by putting $n = 1$, and $K = \mu$, in equation 2.66, i.e.

$$P_o = 4\pi^2 (a)(De/D)\left(\frac{\lambda^2}{\lambda^2 - 1}\right) Re^{-1} \quad \text{----- 2.67}$$

Equations such as 2.66 and 2.67 are not only cumbersome to use but also create unnecessary complications and possibilities of errors for the designer who is faced with the difficult task of choosing a correlation to use. Apart from this, equation 2.66 and 2.77 simply fail to fit the data of published work. To demonstarte this point the correlation, equation 2.67, was tested for Nagata's geometry (1), see Table (2) . For this case and using equations 2.66a, 2.66b, 2.66c and 2.67 yields values for K_p about four times below those found experimentally by Nagata (1) .

Chavan and Ulbrecht (43) realising the same discrepancies seem to claim in their later publication (43) that equations 2.66 and 2.67 will be improved if multiplied by a factor of 2.5, i.e. equation 2.66 and 2.67 should now be:

$$P_o = 2.5\,\pi (a)(De/D)\ \lambda^2 \left[\frac{4\pi}{n\,(\lambda^{2/n} - 1)}\right]^n (\varrho N^{2-n} D^2/K)^{-1} \quad \text{---------- 2.68}$$

and

$$P_o = 10\pi^2 (a)(De/D)\left(\frac{\lambda^2}{(\lambda^2 - 1)}\right) Re^{-1} \quad \text{---- 2.69}$$

respectively. However, application of equation 2.69 to Nagata's data revealed that even with these correlations the values of K_p are underestimated by about 40% . It is also suprising to see that the relationship for the dimensionless surface area, a, equation 2.66c , does not involve the number of ribbon blades, Nb . This means that exactly the same power consumption is to be expected for the same values of D_T/D, h/D, W/D, and P/D regardless of the number of blades, Nb, which clearly leads to gross underestimations of power as seen from the above analysis.

So the main point to be made is that although it is desirable and more exact to be able to derive theoretical relationships to describe the mixing systems, it is a very dangerous practice if not backed by ample experimental data and vigrous analysis. In the light of present evidences, therefore, equations such as 2.65 to 2.69 should be used with great caution.

Bourne, Knoepfli and Riesen (44) in a recent publication proposed a new correlation for helical ribbon impellers based on 8 helical ribbons having 3 pitches and various wall clearances, see Table (2) and Table (3) . Their final correlation is:

$$P_o = 134\ (h/D_T)\ (P/D_T)^{-0.3}\ (C/D_T)^{-0.3}\ Re^{-1} \quad \text{---- 2.70}$$

It should be pointed out that the correlation was not

tested against the published work and that the effect of number of blades and impeller width was not studied. They claim an accuracy of ±2% , but a check of this correlation against published data revealed an accuracy of about ±40% . It is also worth noting that this correlation was derived for Newtonian fluids only and as the authors point out should not be applied for non-Newtonian materials.

Kappel and Seibring (45) studying power consumption of a series of impellers, proposed the following correlation for helical ribbons:

$$P_o = 14 \left(\frac{(h/D_T)(P/D)^{-2/3}}{1 - (D/D_T)^2} \right) (Nb)^{0.9} \; Re^{-1} \quad \text{------} \quad 2.71$$

This equation correlates most Newtonian published data in the laminar region to ±30% . Note that the effect of impeller width on power is not included in this correlation.

M. Kappel (46) studying the mixture quality of helical ribbon impellers proposed the following correlation for power consumption of these agitators:

$$P_o = 60 \; (P/D)^{-0.5} \; (C/D)^{-0.3} (Nb)^{0.8} \; Re^{-1} \quad \text{-----} \quad 2.72$$

The correlation is only valid for:

$H/D = 1.1$ $\quad 0.5 \leqslant P/D \leqslant 1$

$W/D = 0.1$ $\quad 0.01 < C/D < 0.5$

$h/D = 1.0$ $\quad 1.0 \leqslant Re \leqslant 30$

Brauer and Schmidt - Traub (47) using six helical ribbon impellers of varying C/D, P/D, W/D and H/D proposed the following semi-theoretical correlation:

$$P_o = 16.9\ (h/D) \left[\frac{1}{1 - (D/D_T)^2} + 11.5\ \frac{(W/D)(D/D_T)}{(P/D)^2} \right] (Nb)^{0.2}\ Re^{-1} \quad ---- \quad 2.73$$

This equation underestimates most of the published power data in the laminar region by as much as 50% . This may, partly, be due to the exponent of Nb . Most workers (1, 23) agree that the exponent of Nb should be higher than 0.2 . Furthermore, the correlation was not tested for non-Newtonian liquids.

Blasinski and Ryzski (48) have, recently, proposed a general correlation for the power consumption of helical impellers by combining their data with those published in the literature:

$$P_o = 34.1\ (C/D)^{-0.53}\ (H/D)^{0.45}\ (P/D)^{-0.63}\ (h/D)^{1.01}\ (W/D)^{0.14}\ (Nb)^{0.79}\ Re^{-1} \quad ---- \quad 2.74$$

This equation predicts the Newtonian power data in the laminar region of most published work to ±20% . It is the most general correlation published to date and reflects the effect of most parameters on power. It does not, however, reflect the true dependence of power on number of impeller blades, Nb . If equation 2.74 is tested against Hoo and Wong's[40] data for Nb = 4 , it will be found that this correlation overestimates the power by about 80% indicating that the exponent of Nb may be too high. The exponent of (H/D) is also questionable because it is based mainly on the work of Gray (7) and Ulbrecht and Schrieber (30) . Gray (7) used a H/D of 1.23 and not 1.41 as claimed by Blasinski and Rzyski (48) . Furthermore, Gray (7) was primarily interested in mixing time and used only two data points to obtain his results for power which is in the form of a graph (the value of K_p has to be obtained roughly from the graph) . The work of Ulbrecht and Schrieber (30) is in German and hard to interpret since neither the impeller geometries, nor the values of K_p are given in tabulated form. The actual value of H/D used in their work, therefore, could be from 1.41 to 1.56, but not 1.64 as used by Blasinski and Rzyski (48).

Gluz and Pavlushenko (17) using the theoretical coefficient for shear rate at the surface of a rotating cylinder

in an infinite Newtonian fluid (i.e. 4π) and discussed in section 2.1.1 defined a modified Reynolds number and proposed the following correlation which does not allow for any changes in geometry:

$$P_o = 235\left[\frac{\rho N^{2-n} D^2}{K}(4\pi)^{1-n}\right]^{-1} \quad \text{-------} \quad 2.75$$

Reher and Bohm (33), on the other hand, used the universal value of 11 for the impeller shear rate constant, k_s. This value of k_s was originally reported by Metzner and Otto (12) for small impellers such as turbines and propellers. However, it has been shown by a number of workers (1,2,3,8,21,22,23, 24) that this value of 11 for k_s is very low for large impellers such as anchors and helical ribbons. A number of investigators (23,22,21) have also found that for large impellers the value of k_s is influenced by impeller geometry. Hall and Godfrey (23), for example,found 17% departure in k_s from the average value of 27 for 2% variation in clearance. in the case of helical ribbon impellers. These workers also noticed a tendency for the value of k_s to decrease with increase in the flow behaviour index, n, but the dependence reported negligible for practical purposes.

Appendix(1)

Table (2) is a summary of all the published correlations to date. The main point to be made is that almost all correlations with the exception of those in Table(3) are for specific geometries. Even the correlations in Table (3),Appendix(1) have been obtained with insufficient data as demonstrated

from their geometries in Table (2) . It should also be mentioned that in order to compare different correlations, it is important to consider all the facts such as power measurement techniques, modifications on the standard geometry, method of determination of impeller shear rate constant, k_s, etc. as these have a profound effect on predicted power consumption.

2.2 Heat Transfer

In a vessel containing an agitated liquid, heat transfer is brought about primarily through conduction and forced convection (1,19,49,50,51) .

Consider an element of a clean vessel wall as shown in Fig. 2.2a and assume a large diameter vessel so that the effect of curvature is negligible . On the outer side of the vessel is a cooling medium such as water, and on the inner is an agitated liquid being cooled. The following equation describe the process:

$$\text{Rate} = \frac{\text{Driving force}}{\text{Resistance}} \qquad \text{---------- 2.76}$$

where the driving force is the temperature difference ΔT in ^{o}C , resistance is the reciprocal of the overall heat transfer coefficient, U in $W/m^2\ ^{o}C$, and rate is heat flow per unit area Q/A in W/m^2 . Therefore equation 2.75 can be written as:

$$\frac{Q}{A} = \frac{\Delta T}{1/U} \qquad \text{----------} \qquad 2.77A$$

i.e.

$$Q = U\ A\ \Delta T \qquad \text{----------} \qquad 2.77B$$

Furthermore, for the purpose of this discussion assume that the material in the tank is heated electrically by an immersion heater. Under steady-state conditions, therefore, applying equation 2.77, in turn, to each of the resistances shown in Fig. 2.2a we may write:

$$Q = M\ Cp\ (T_o - T_i) = V\ I = h_j\ A\ (T_b - T_{wi}) = \frac{k}{x}\ (T_{wi} - T_{wo}) =$$

$$h_c\ A\ (T_{wo} - T_c) \qquad \text{-------} \qquad 2.78$$

where

A = Inside or outside tank area (m^2) . This is true assuming the effect of tank curvature is small and that vessel diameter, D x, tank wall thickness.

h_c = Coolant liquid-film heat transfer coefficient ($W/m^2\ ^oC$)

h_j = Jacket-side process-liquid film heat transfer coefficient ($W/m^2\ ^oC$)

k = Vessel wall thermal conductivity ($W/m\ ^oC$)

M = Coolant liquid flow rate (kg/s)

Cp = Coolant specific heat ($J/kg\ ^oC$)

T_b = Bulk liquid temperature (^oC)

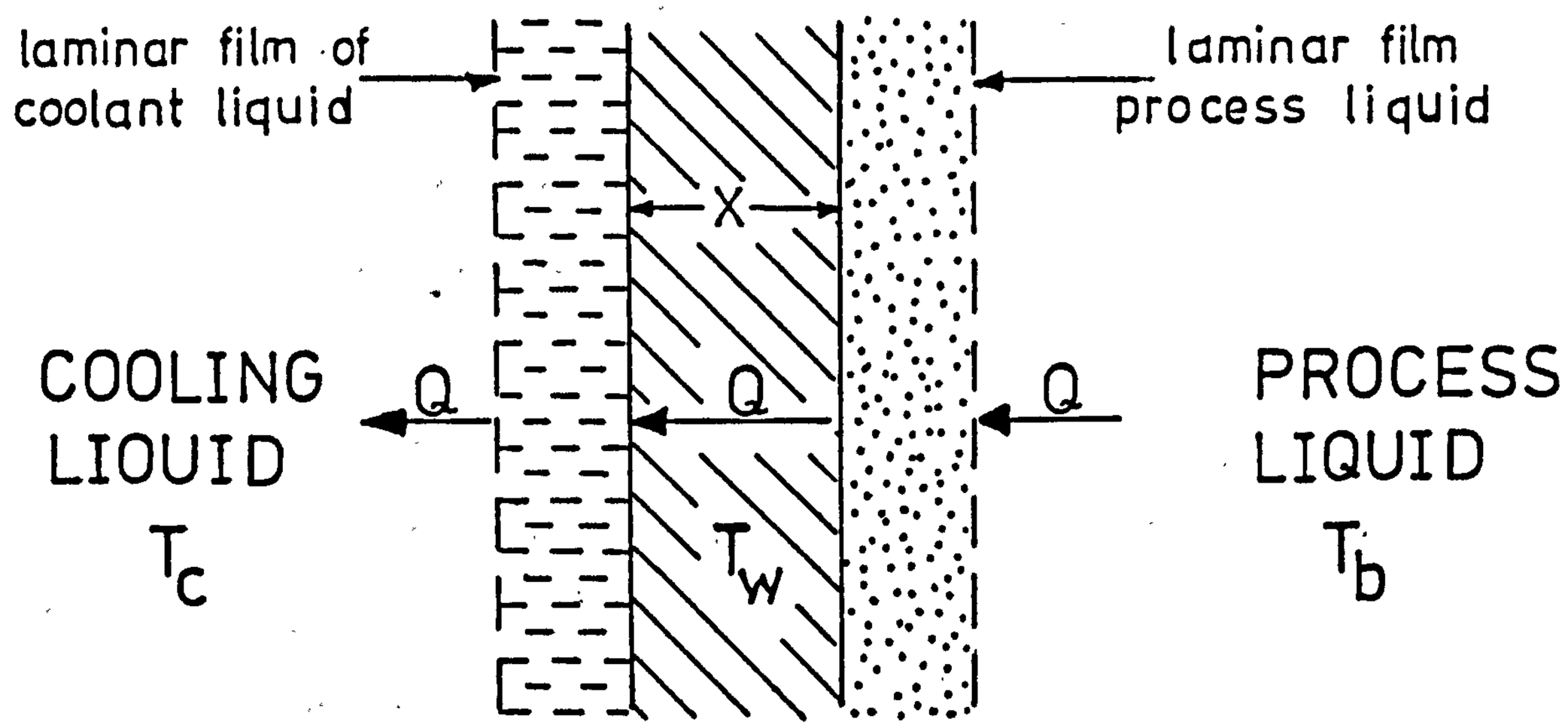

Fig. 2.2a Resistances to heat transfer through a clean tank wall to a liquid being cooled

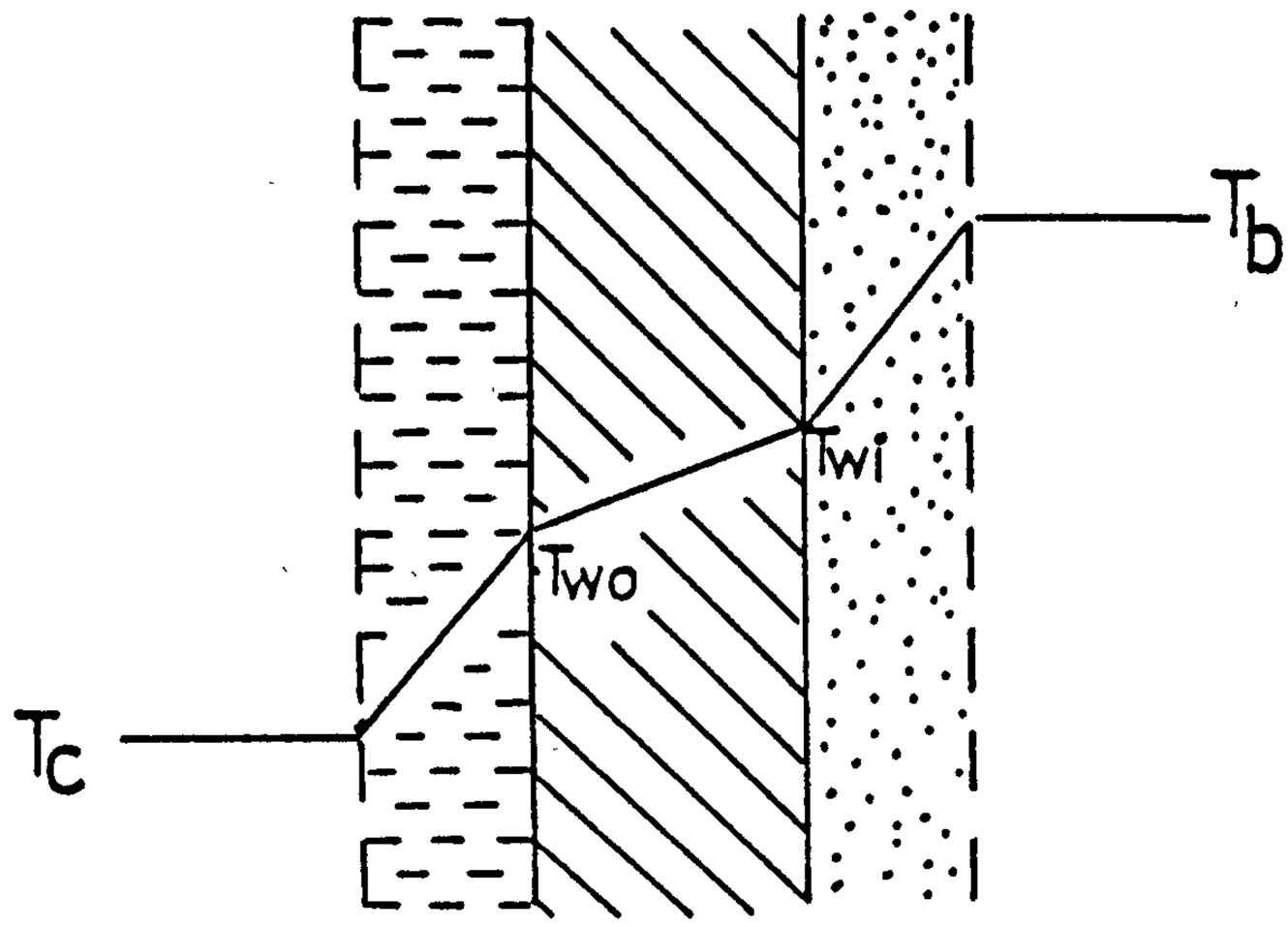

Fig. 2.2b Idealised temperature distribution through a clean tank wall to a liquid being cooled

T_o = Outlet coolant temperature (^oC)

T_i = Inlet coolant temperature (^oC)

T_c = Mean temperature of coolant equal to $\frac{1}{2}(T_i + T_o)$ (^oC)

(This is resonable for high coolant flow rates)

T_{wi} = Inner wall temperature (^oC)

T_{wo} = Outer wall temperature (^oC)

V = Voltage to the immersion heater (volts)

I = Current to the immersion heater (Amp)

x = Vessel wall thickness (m)

Q = Rate of thermal energy flow across a surface (W)

Since the temperature difference between the cold water in the jacket and the agitated liquid in the vessel is the sum of the individual temperature differences across the various resistances, we can write:

$$(T_b - T_c) = (T_b - T_{wi}) + (T_{wi} - T_{wo}) + (T_{wo} - T_c) \quad \text{----} \quad 2.79$$

Equation 2.77 may be written as:

$$\Delta T = \left(\frac{Q}{U\ A}\right) \quad \text{----------} \quad 2.80$$

In terms of equation 2.78 and 2.80, equation 2.79 can be written as

$$\left(\frac{Q}{U\ A}\right) = \left(\frac{Q}{h_j\ A} + \frac{Q\ x}{A\ k} + \frac{Q}{h_c\ A}\right) \quad \text{----------} \quad 2.81$$

The preceding equation reduces to:

$$\frac{1}{U} = \frac{1}{h_j} + \frac{x}{k} + \frac{1}{h_c} \qquad \text{----------} \qquad 2.82$$

In heating or cooling of highly viscous materials the inside heat transfer coefficient, h_j , is small compared to other terms in equation 2.82 and thus is a controlling factor determining the value of the overall heat transfer coefficient.

2.2.1 Theoretical Prediction of the Jacket-side Heat Transfer Coefficient, h_j

In principle the equations for the conservation of momentum, mass and energy may be written to describe the system (1,17,49,51,18) . The general solution of these equations, however, involves enormous mathematical difficulties even for Newtonian fluids. The complexities are essentially due to the complicated shape of the agitator and the vessel. Numerical methods may be used to solve the problem for some agitator shapes. However, such a solution has extremely limited utility in that it is linked to one particular set of boundary conditions. Therefore, the published work on mechanical agitators has been, in the most part, concerned with fitting dimensionless parameters to experimental data.

The jacket side film heat transfer coefficient, h_j , depends upon the fluid properties, the system geometry, and the impeller speed. It is,therefore, possible to write:

$$h_j = f\ (\varrho\ ,\ \mu_b,\ \mu_w,\ Cp,\ k,\ g,\ N,\ \beta,\ \Delta T,\ D,\ D_T,$$

other geometric dimensions) ---------- 2.83

where

h_j = Jacket side film heat transfer coefficient ($W/m^2\ ^oC$)

ϱ = Fluid density at bulk fluid temperature (kg/m^3)

μ_b = Fluid viscosity at bulk fluid temperature (kg/ms)

μ_w = Fluid viscosity at jacket wall temperature (kg/ms)

Cp = Fluid specific heat at bulk fluid temperature ($J/kg\ ^oC$)

k = Fluid thermal conductivity at bulk fluid temperature ($W/m\ ^oC$)

g = Acceleration due to gravity (m/s^2)

β = Coefficient of thermal expansion ($/^oC$)

ΔT = Temperature difference (^oC)

D = Impeller diameter (m)

D_T = Tank diameter (m)

The geometrical dimensions, other than the impeller diameter, D, and tank diameter, D_T, could include clearance between impeller blade and the vessel wall, impeller pitch, and width and number of blades. The fluid properties,ϱ , μ ,

Cp, and k are evaluated at the bulk fluid temperature, T_b , whilst μ_w is the fluid viscosity at the wall temperature, T_w . This parameter, μ_w, is introduced following the work of Sieder and Tate (52) .

By dimensional analysis, equation 2.83 may be reduced to give:

$$Nu = f\ (\ Re,\ Pr,\ Vis,\ Fr,\ Gr,\ \text{dimensionless geometrical factors}) \quad \text{----------} \quad 2.84$$

where

$Nu = \frac{h_j D_T}{k}$, dimensionless Nusselt number

$Re = \frac{\rho N D^2}{\mu}$, dimensionless Reynolds number

$Pr = \frac{Cp\mu}{k}$, dimensionless Prandtl number

$Gr = \frac{gD^3\beta\Delta T\ \rho^2}{\mu^2}$, dimensionless Grashof number

$Vis = \frac{\mu_b}{\mu_w}$, dimensionless viscosity ratio similar to that used by Sieder and Tate (52) in pipes.

Dimensional analysis does not give further insight into the form of this function. It might be, for example, the sum of a few terms; it might be exponential, logarithmic, or an infinite series. For the sake of convenience and

simplicity, however, it has usually been assumed that each of the four groups enters the equation only once, and then as a power function . In other words, equation 2.84 is arbitrarily assumed to have the form:

$$Nu = A\,(Re)^a\,(Pr)^b\,(Vis)^c\,(Fr)^d\,(Gr)^e \quad \text{------ 2.85}$$

where A, a, b, c, d, and e are constants that must be determined experimentally.

The Froude number characterises uneven surfaces which are produced by vortexing. Skelland (19) reports that in agitated systems, Froude effects can be neglected at values of Reynolds number less than about 300 . Since close-clearance impellers generally operate at Reynolds numbers less than this value, the effect of Fr may be ignored.

The Grashof number, Gr, characterises natural convection which results from density variations. A review of the published literature to date reveals that most of the experimental work for the jacket and coil types of heat transfer surfaces has been carried out under conditions where the effect of forced convection, characterised by Reynolds number, on heat transfer has been far greater than that of natural convection.

Under these restrictions equation 2.85 may be reduced to give:

$$Nu = A\ (Re)^{a}\ (Pr)^{b}\ (Vis)^{c} \quad \text{----------} \quad 2.86$$

For turbulet forced convection heat transfer processes, the exponent of Reynolds number in equation 2.86 is usually reported as 0.67 although it varies from 0.5 to 0.75 (53,54,55,56) . Likwise the exponent of the Prandtl number, Pr, is usually reported as 0.333 but varies from 0.25 to 0.50 (57,55,53,54,58). The viscosity ratio exponent varies between 0.14 to 0.97 (1,2,3,59,19,51) with the majority reporting a vlaue of 0.14 based on the work of Sieder and Tate (52) on heat transfer in pipes. The constant, A , varies over a wide range because it is a function of the impeller type and system geometry. In summary, however, the equation usually reported in the turbulent region is. see Table, 4 Appendix (1),

$$Nu = A\ (Re)^{0.67}\ (Pr)^{0.333}\ (Vis)^{0.14} \quad \text{---------} \quad 2.87$$

There are excellent reviews of the many correlations available for various geometries in the turbulent region (9,10,19,51,61) . Here, concentration is focussed in the laminar region where there is a distinct lack of information on rates of heat transfer and the associated power.

In order to highlight this point it is worth going back to our measurement of the characteristic temperature difference $\Delta T = (T_b - T_w)$ used in equation 2.78 and rewritten below to calculate the jacket side film heat transfer coefficient, h_j, i.e.

$$Q = h_j A (T_b - T_w) \quad \text{----------} \quad 2.89$$

The determination of the average wall temperature causes no serious problems provided there is good flow distribution in the jacket (4,61). The same can be said also for the determination of the temperature in the bulk of the liquid in the turbulent flow region where the bulk temperature can be measured accurately by only one measuring instrument arranged at almost any position in the liquid (2,3,4,61).

Contrary to this in the laminar flow region, marked temperature gradients in the bulk liquid have been observed by several investigators (1 - 6) . This makes the determination of an appropriate bulk temperature, T_b, very difficult. Furthermore, without a good definition of T_b, it is extremely difficult to calculate a meaningful jacket side film heat transfer coefficient, h_j, using equation 2.89 .

2.2.2 Temperature Distribution of Agitated Viscous Fluids in the Laminar Region

Coyle et-al (6) studying the cooling of highly viscous materials, observed temperature differences between two thermocouples, one near the edge of the blade and one at the centre of the tank near the shaft. The spread was from 5 - 15 ^{o}C with a helical ribbon impeller, while at the same speed and power, an anchor impeller gave differences from 10 to 20 ^{o}C, with a 50 ^{o}C driving force from the wall to the centre of the vessel (cooler near the wall) .

Uhl (2) also observed that the bulk fluid was not well mixed and tended to stratify when the Reynolds number was less than about 20 . This temperature variation was also recognized by other researchers (4,5) .

An extensive study on temperature distribution of viscous fluids in a vessel agitated by a series of helical ribbons and anchors was carried out by Nagata (1) . His results also indicated a greater temperature distribution in the vessel agitated by an anchor suggesting poorer mixing. This worker obtained an standard deviation smaller than 0.8^{o}C for the liquid temperature at six positions in the mixing vessel agitated by helical ribbons at a Reynolds number less than 50 . For anchor impellers,

however, he reported an standard deviation of 1.5°C at a Reynolds number of 100 and an standard deviation of 2°C at a Reynolds number of 50 . Hence, he argued that defining an average bulk temperature, in the case of anchor impellers, was very difficult. This results in poor correlative equations for anchor impellers in the laminar region.

Nagata (1) also observed that mixing by helical ribbon impellers was poor regardless of the liquid viscosity when the impeller speed was below 6 rpm, but pointed out that this minimum effective impeller speed may change with vessel diameter.

Zlokarnik (4) noticed marked temperature variations in the core region of the agiated vessel at Reynolds numbers less than 100 for anchor agitation and used a heat balance to calculate the bulk fluid temperature. However, he gives no information on technique or the accuracy of this method.

Heinlein and Sandall (62) observing a significant temperature spread at low agitator speeds, measured the bulk fluid temperature by four thermocouples placed at various positions in the tank and took the lowest reading as the bulk fluid temperature when these readings did

not differ by more than 5°C . They observed the same phenomena for both heating and cooling of viscous fluids.

Camurdan (5) observed a temperature decrease with increase in liquid depth and gave an spread of 20 °C between top and bottom of the vessel for anchor agitation. He also noticed a temperature spread of 25 °C between a point near the vessel wall and the inner side of the impeller blade. However, from the inner side of the impeller blade to the centre of the vessel the temperature variation was only about 1°C and the temperature only varied by about ±0.5 °C for any fixed depth but various angular positions. These large temperature variations presented difficulties in defining a bulk fluid temperature.

2.2.3 Dimensionless Correlations

It was stated in section 2.2.1 that the general dimensionless equation describing the heat transfer to both Newtonian and inelastic non-Newtonian fluids for forced convection is:

$$Nu = A\,(Re)^{a}\,(Pr)^{b}\,(Vis)^{c} \qquad \text{----------} \quad 2.90$$

neglecting the effect of natural convection, i.e. Grashof number, Gr, and Froude number, Fr .

Equation 2.90 is very restrictive as it does not allow for any changes in the geometry of the system. Complete geometrical similarity must be observed or gross errors in the evaluation of heat transfer coefficient, h_j, will result. There has been very little attempt in the literature published to date to study systematically the effect of system geometry on heat transfer.

Uhl (2) and Uhl and Voznick (3) carried out extensive investigations of the anchor agitator in the viscous and the lower transition zones. All tests were of the batch type. These workers noticed a tendency for the hot liquid to stratify at the top of the vessel at lower temperatures for both heating and cooling runs. However, they gave no temperature distribution at these low Reynolds numbers. Agitated fluid temperature was measured by two thermocouples only placed at the top and the bottom of the vessel. Their final correlation is:

$$Nu = 1.0 \ (Re)^{0.5} \ (Pr)^{0.33} \ (Vis)^{0.18} \quad \text{-----} \quad 2.91$$

for;

$$30 < Re < 300$$

and

$$Nu = 0.38 \ (Re)^{0.66} \ (Pr)^{0.33} \ (Vis)^{0.18} \quad \text{-----} \quad 2.92$$

for;

$$300 < Re < 4000$$

These workers also studied the effect of clearance factor, C/D, upon heat transfer coefficient and recommended a C/D value of 0.05 to 0.08 . They claimed that these clearance factors gave better heat transfer rate at a lower power requirement than a C/D of 0.01 to 0.02 commonly used.

Their claim was also supported by Heinlein and Sandall (62) who obtained an optimum value of .06 for the clearance factor, C/D . The correlation by these workers is given Table (4) which is a summary of all correlations published to date for anchor and helical ribbon impellers.

Gluz and Pavlushenko (63) using a 0.3m diameter steel cylindrical tank with a jacket for cooling water proposed heat transfer correlations for both anchor and helical ribbon impellers in the laminar and turbulent regions. Their correlations are also included in Table (4). It is, however, important to realise that these workers used an average temperature, T_{av}, for the agitated medium but did not mention anything about the temperature distribution in the vessel at the reported low Reynolds numbers. This may partly explain why these workers proposed a correlation for helical ribbon impellers that predicts heat transfer 58% less than that predicted by the correlation proposed by Uhl (2) for anchor impellers in the anchor transition range.

Tests carried out by Coyle and co-workers (6) in the range of Reynolds number from 0.1 to 1.0 for cooling a pseudoplastic organic fluid with a behaviour index of 0.2 and a viscosity of 1000 poise at a shear rate of 5 sec^{-} for 0.36m and 0.76m diameter vessels indicated that the resistance to heat transfer was virtually independent of both speed, N, and the fluid viscosity but was equal to a static conduction film with a thickness about 2/3 of the clearance . Therefore, for anchor agitation in the laminar region it may be written that:

$$h_j \backsimeq \frac{k}{(2/3)\ C} \qquad \text{----------} \qquad 2.93$$

where

h_j = jacket side film heat transfer coeffecient ($W/m^2\ ^oC$)

k = liquid thermal conductivity ($W/m\ ^oC$)

C = clearance between the impeller blade and vessel wall (m)

Using results from smilar tests carried out by Coyle et-al , Uhl (64) argued that, in the case of a helical ribbon impeller, the resistance to heat transfer could be approximated by a static conduction film equal to $\frac{1}{2}$ the clearance, C, or :

$$h_j \backsimeq \frac{k}{(1/2)\ C} \qquad \text{----------} \qquad 2.94$$

Nagata (1) carried out extensive studies of anchors and helical ribbons in mixing and heat transfer to agitated viscous fluids. As seen from their correlations in Table (4), for helical ribbons the exponent of both the Re and Pr is 1/3 and hence the effect of fluid viscosity, they argue, only appears in the viscosity correction term. They conjectured that this may be due to the film thickness for heat transfer being thicker than the clearance between the wall and the impeller tip, and hence the film thickness is kept constant across the clearance irrespective of the viscosity of the liquid.

These investigators also argued that, in the case of an anchor, the correlative equation was independent of clearance between the vessel wall and the impeller edge. This result is contrary to that obtained by Uhl (2) and others (3,62) who reported that heat transfer for anchor impellers changed markedly with clearance between impeller tip and vessel wall.

There is very little information in the literature to check the validity of equations 2.93 and 2.94 but it is interesting to note that Coyle et-al (6) reported values for h_j varying from about 20 to 32 $W/m^2\ ^oC$ for a speed range of 7 to 50 rpm indicating some effect of agitator speed on h_j for low Reynolds numbers. It is also worth

noting that they reported a heat transfer coefficient, h_j, of about 8.5 $W/m^2\ ^oC$ with the impeller stopped, i.e. N = 0.0 . This is the value for natural convection.

(i) Natural Convection

A close look at the published work indicates that most investigations on heat transfer in stirred vessels have been made in the range of Reynolds numbers greater than 10 . There are only limited data for heat transfer to viscous liquids in the range of Reynolds numbers less than 10 (1,6).

From these limited works, however, it is obvious that the exponent of Reynolds number in equation 2.90 decreases to a value well below 2/3 reported for the turbulent forced convection region. A careful analysis of the published literature, in fact, indicates that for helical ribbon impellers, the exponent of Reynolds number decreases to about $\frac{1}{2}$ for Reynolds numbers between 10 to 100 , and to about 1/3 for Reynolds numbers between 1 to 10 . Coyle et-al (6) and R. Rautenbach (65) indicated that the exponent of Reynolds number decreases to zero for Reynolds numbers less than 1.0 . Their data, however, does show some dependency of heat transfer coefficient upon impeller speed even at these low values of Reynolds numbers. It is expected that the value of the film heat transfer

coefficient, h_j, will approach the natural convection value as speed decreases to zero, but this is hard to find from the cited papers (6,65) .

The data of Coyle et-al (6), Penny and Bell (66) and Rautenback (65) clearly indicate that the contribution of natural convection to heat transfer, at low Reynolds numbers is of significance. Under these conditions, therefore, it may be assumed that equation 2.95 prevails, i.e.

$$Nu = A\,(Re)^a\,(Pr)^b\,(Vis)^c\,(Gr)^d \qquad \text{-------} \quad 2.95$$

where, as stated previously, Gr is the dimensionless Grashof number given, in general, by:

$$Gr = \frac{L^3 \rho^2 \beta g\, \Delta T}{\mu^2} \propto \frac{\text{buoyancy force}}{\text{viscous force}}$$

The term L in Grashof number is a linear dimension of the heating surface, whose precise definition varies with the geometry of the situtation. For horizontal cylinders, L is the outside diameter of the cylinder. For vertical flat plates and cylinders, L is usually the height of the heating surface.

Little information could be found, in the literature, on natural convection heat transfer to high viscosity fluids in tanks at Prandtl numbers in the range of practical interest to the present problem. For steady-state free-convection heat transfer at moderate Prandtl numbers both analytical studies (67,69) and empirical correlations (70,71,72,73) led to a simple relationship between the Nusselt, Grashof and Prandtl numbers:

$$Nu = C\,(Gr\ Pr)^{\frac{1}{4}} \qquad \text{----------} \qquad 2.96$$

This correlation represents the free convection heat transfer in laminar flow on simple surfaces within generally acceptable engineering accuracy. In this flow region the value of the constant C has been shown to be almost independent of the Prandtl number. Schuh (68) showed that the value of C in equation 2.96 varies from 0.612 to 0.653 , i.e. by about 7% over the range of Prandtl numbers between 10 and 1000 . LeFevre and Ede(74) found an asymptotic value of $C = 0.67$ for $Pr \rightarrow \infty$. The value of the constant C in equation 2.96 is also affected by the condition of heat transfer on vertical surfaces, whether it occurs at uniform heat flux or at uniform surface temperature (75).

It is also important to point out that most analytical solutions and empirical correlations are obtained under

the simplifying assumptions of constant,temperature - independent fluid properties throughout the boundary layer. However, since real fluids of high viscosity often feature a strong dependence of the viscosity on temperature, the reported equations for constant fluid properties may lead to unrealistic predictions .

Experimental studies of free-convection heat transfer on vertical plates in lubrication oil of Prandtl numbers up to 500 were reported by Lorenz (76) . His values of the constant C for the heat transfer were about 35% lower than the analytical values for this region reported by Schuh (68) .

There is no published work which offers any analysis of the combined natural and forced convection heat transfer in tanks under the conditions of interest in the present work. Acrivos (75) studying combined natural and forced convection heat transfer to Newtonian fluids under laminar boundary-layer flows, established that, for simple surfaces, two different controlling parameters exist ;

a) $\frac{Gr}{Re^2}$, i.e. $\frac{\text{buoyancy force}}{\text{inertia force}}$ for $Pr \to 0$

b) $\frac{Gr}{Re^2\ Pr^{1/3}}$ for $Pr \to \infty$

Gryzagoridis (77) , however, proposed that Gr/Re^2 is the main controlling parameter. This worker studying combined heat transfer over vertical plates, argues that the term Gr/Re^2 gives a qualitative indication of the influence of forced flow in a natural convection process. The regimes of convection are classified as:

a) Free convection: $Gr/Re^2 \geqslant 3.0$

b) Forced convection: $Gr/Re^2 \leqslant 1.0$

Gryzagoridis, therefore, concluded that the external flow aided and increased the heat transfer in the region of $0.1 \quad Gr/Re^2 \quad 3.0$. Furthermore, his data suggests that at any value of Gr/Re^2 between the limits of purely forced and purely free convection flows, the Nusselt number is higher than it would be in either of these modes alone.

(ii) Penetration Model

A number of investigators (78,65) have attempted to correlate their heat transfer data at low Reynolds numbers using the penetration theory developed for turbulent heat transfer (49). A full discussion of the theory is given elsewhere (49,79), but Harriott pointed out that the simple penetration theory successfully correlated the data of scraped surface heat exchangers, but it greatly overestimates the heat transfer coefficient for close-clearance impellers

handling viscous materials. The correlation proposed by Harriott for scraped-surface heat exchangers is:

$$h_j = \left(\frac{2}{\sqrt{\pi}}\right) \sqrt{\varrho Cp\ k\ N\ Nb} \qquad \text{---------- 2.97}$$

where

Cp = fluid heat capacity (J/kg)

= fluid density (kg/m^3)

k = fluid thermal conductivity (W/m ^oC)

N = impeller speed (rps)

Nb = number of impeller blades

h_j = average heat transfer coefficient ($W/m^2\ ^oC$)

Equation 2.97 in dimensionless form may be written as:

$$\left(\frac{h_j D_T}{k}\right) = 1.13 \left(\frac{\varrho N D^2}{\mu}\right)\left(\frac{Cp\mu}{k}\right) (Nb)^{0.5} \qquad \text{------- 2.98}$$

Rautenback (65) using a helical ribbon impeller with a 2mm clearance between the impeller blade and the vessel wall calculated that equation 2.98 overestimated the inside film heat transfer coefficient by 700% for N = 10 rpm . He argued that this large discrepency between the predicted and calculated value of h_j is inherent in the penetration when the liquid layer between the wall and the stirrer is not taken into account. By allowing for

this liquid layer, Rautenback (65) modified the simple penetration theory and proposed the following equation for heat transfer to viscous materials at low Reynolds numbers:

$$Nu = 0.568 \quad (C/D_T)^{-1} \left[\frac{\left(\frac{k}{Cp\mu}\right)}{\left(C^2 \; N \; Nb\right)} \right]^{-0.23} \qquad \text{-----} \qquad 2.99$$

This equation may be written in dimensionless form:

$$Nu = 0.568 \; (\rho ND^2/\mu)^{0.23} \; (Cp\mu/k)^{0.23} \; (Nb)^{0.23} \; (C/D_T)^{-0.54}$$

$$\text{----------} \qquad 2.100$$

It is difficult to check this correlation as it stands since this investigator does not give any information on the system geometry apart from a clearance of 2mm and $Nb = 2$. From the cited paper it appears as if only one impeller was used to test the theory. It is, however, interesting to note that the exponent of Reynolds number has shown a further decrease to 0.23 from 0.333 reported by Nagata (1) and others (3,62,63) to exist up to $Re = 1.0$.

In summary it may be stated that much study has been done on the correlation of heat transfer coefficients in agitated vessels, but that many differences or even contradictions exist among the present correlations. Some

of the difficulty may be due to the problems of obtaining accurate data. The data of Chilton et-al (53) for heating and cooling of water, for example, could only be duplicated to an average deviation of 17.5% . Brooks and Su (80) reported reproducibility of ±20% for water and corn syrup and ±5% for mobil oil . Cummings and West (81) claimed that their correlation in 90% of the cases it was used, predicted the batch heat transfer coefficient to within 20% of its true value . Correlation proposed by Zlokarnik (4) predicts heat transfer coefficient to an accuracy of ±20% .

CHAPTER 3

EXPERIMENTAL EQUIPMENT & PROCEDURE

Experimentation was primarily carried out in a 0.4m diameter vessel . For the purpose of this chapter this vessel is dessignated vessel 1 . Limited work was also carried out both by the author and others (85, 86) in a smaller 0.15m diameter vessel . This tank is dessignated as vessel 2 . All Figures are given in Appendix(1) .

3.1 General Description of Vessel 1

Essentially the equipment consisted of a jacketed vessel containing a centrally placed heating coil. Metered cold water was pumped through the baffled jacket (see Fig. 3.3) at the top and was withdrawn from the bottom. Heating was provided electrically by a small immersion heater. This was replaced by a hot water heating coil in the case of non-Newtonian materials where localized heating caused severe thermal degradation of the fluids. A line diagram of the vessel and its ancillary equipment is presented in Fig. 3.1 . Plate 3.2 is a photograph of the vessel and its ancillary equipment.

3.2 Technical Specification of Equipment

3.2.1 Vessel 1

This consisted of a dished bottom 0.4m diameter by 0.5m deep tank, fabricated from stainless steel plate having a thickness of 0.005m . The capacity of the

tank at an operating level of 0.43m was 0.054 m^3, see Fig. 3.3 .

The vessel was provided with a mild steel baffled jacket, as shown in Fig. 3.3 , to facilitate cooling. The baffles provided good distribution of the coolant through the jacket. Two 12.7mm diameter holes were positioned 180^o away from each other at the top of the jacket and served as cold water inlets, while a 25.4mm diameter hole at the bottom served as water outlet.

3.2.2 Agitators

Agitation was provided by a variety of anchor and helical ribbon impellers fabricated from stainless steel and having geometrical configuration as shown in Fig 3.4, Fig. 3.5, Plate 3.6 and Plate 3.7 . Each impeller was mounted on a 25.4mm diameter stainless steel shaft. The impeller was driven by a 3KW motor with infinitely variable speed between zero and 300 rpm . The whole drive unit was vertically mounted on a thrust bearing, thus permitting the torque on the shaft to be measured . Details of the torque measuring devices are discussed later in the chapter.

3.2.3 Electrical Immersion Heater and Heating Coil

For the purpose of experimentation in vessel 1, a 2KW

electrical immersion heater having a mean helix diameter of 0.1m was used. The heating element, fabricated from copper of 8mm external diameter, had three turns and a pitch between the centres was 0.05m . The total length of the heating element was 1.4m .

The electrical immersion heater was replaced by a heating coil for the steady-state heat transfer experiments with non-Newtonian materials. This had to be done since the electrical immersion heater caused localized heating and severe degradation of viscous non-Newtonian materials. The heating coil had the same configuration of the electrical immersion heater. All experiments were conducted with hot water entering at the bottom of the helical coil.

3.2.4 Torque Measuring Devices

To obtain data on the power consumption of the impellers, the free torque, T, on the shaft was measured using a 0-81 Nm shaft-mounted torque transducer . The transducer utilises a network of bonded foil strain gauges as the torsion sensing element. The gauges are cemented to a high tensile torsion shaft and are protected for life by a resin film . The gauges are connected in a full bridge circuit in such a way that an electrical bridge unbalance is caused by torsional strain. The arrangement is such that the shaft strains due to bending, thrust and temperature, within the quoted limits, are self-cancelling and

do not contribute to the electrical output . Connection between the stator and the gauges on the rotor is affected by a system of silver sliprings and silver graphite brushes. The electrical signal taken off through the sliprings and monitored on a milivoltmeter is directly proportional to the torque, T .

In addition, the motor was mounted on essentially frictionless bearings to enable the reaction torque to be measured as an independent check on impeller power. The device consisted of a fixed base plate with a ball race on which was placed the whole motor assembly with the agitator shaft . The ball race was well greased so that the motor assembly could rotate on it with minimum friction . The torque produced on the shaft resulted in an equal and opposite torque on the motor assembly, resulting in an anti-clockwise rotation of the motor assembly, when the rotation of the shaft was clockwise. To prevent this anti-clockwise motion of the motor assembly, it was provided with a lever arm pressing against a load cell. The reading taken from the load cell meter was the force required to prevent the motion of the motor assembly as shown in Plate 3.2 .

Assuming that the friction loss on the ball race was negligible (checked during initial runs), for equilibrium

the torque on the shaft will equal the torque on the load cell. Thus, the torque, T, on the shaft is given by:

$$T = F \times d \quad \text{----------} \quad 3.1$$

where

F = force on the load cell in Newton

d = distance from the centre of the tank to the point where the force acts (m)

The power consumed, P, by the impeller is given by:

$$P = T \times 2\pi N \quad \text{----------} \quad 3.2$$

where

N = rotational speed of impeller (rps)

This value of P is used in power number, i.e.

$$P_o = \frac{P}{\rho N^3 D^5}$$

3.2.5 Temperature Measurement

Copper-constantan (36 gauge) thermocouples were used for the measurement of all temperatures.

Two small-bore copper tubes each carrying six thermocouples

were used to measure temperature distribution in the tank, see Plate 3.8 . The copper tubing was screwed on to the perspex lead of the vessel . This lead had groves to enable the thermocouples to be moved in any direction. Radial, angular and vertical variations in the bulk fluid temperature could, thus, be measured at any position in the tank by these travelling thermocouples without incersion of too many stationary units. A direct digital thermometer was used to monitor the thermocouples outputs .

Four copper-constantan thermocouples placed at various positions on the agitators were used to monitor the temperature of the fluid adjacent to the rotating impeller, see Plate 3.7 . The signal from these four thermocouples was removed by a slipring unit mounted at the top of the shaft as shown in Plate 3.2 . No difficulty was encountered in using thermocouples to measure temperature of the rotating impellers at the operating speeds . Thermistor temperature sensors, however, have advantages for use with slipring systems at high impeller speeds . This is because changes in the slipring contact and lead resistance will have noticeable effect on thermocouple sensors which have a small coefficient of resistance . The thermocouple output would, thus, become very irratic above a certain impeller speed . Thermistor temperature sensors, on the other hand, have a relatively large temperature coefficient of

resistance of the order of tens or hundreds of Ohms per Centigrade degree . Thus changes in slipring and lead resistance will not affect their reading at high impeller speeds. For the purpose of steady-state heat transfer experiments at low impeller speeds carried out in this study, thermocouples were used used to measure the temperature of fluids at various positions along the impeller. Care was taken to thermally insulate the thermocouple probes from both the copper tubing and impeller blade .

The temperature of the wall was measured using twelve copper-constantan thermocouples . Three of these thermocouples were embeded at the tank bottom and the remaining nine on the vessel wall at different angular positions and heights. The thermocouples were embeded and firmly cemented into indentations drilled in the wall of the vessel . To prevent leakage, these indentations were drilled in such a manner that they did not completely penetrate the thickness of the wall, but left a 0.5mm thickness of metal over the end of the hole on the inside of the vessel, see Fig. 3.9 . The indentations were arranged at different positions and heights, the first one being 10cm above the top of the vessel and the rest in sequence at 5cm from each other at different angular positions.

Three thermocouples were used to measure the inlet and outlet temperatures of the cooling water in the jacket . The inlet temperature was measured by means of two rigidly mounted thermocouples protruding about 10mm into the pipe just before entery to the jacket. The outlet temperature of the coolant leaving the jacket was measured by a third thermocouple mounted rigidly and protruding about 15mm into the pipe fitting about 10cm away from the exit point .

All temperatures were monitored on a digital recorder. All thermocouples were checked for accuracy and calibrated before plcing them in-situ in the experimental equipment. The thermocouples were calibrated by placing them in a laboratory constant temperature water bath, measuring the temperature of the bath contents with a thermometer graduated in tenths of a degree Centigrade and comparing it with the direct digital thermometer reading. This procedure was repeated several times for different bath temperatures . It was found that the digital thermometer reading was accurate to $\pm 0.1\ ^{o}c$.

3.2.6 Other Instrumentation

The volumetric flow rate of the mains cooling water was measured with a standard rotameter, which was calibrated by the manufacturer in liters/minute of water having a

range of 4 to 40 liters per minute, measured at 20°C . All heat transfer experiments were carried out keeping the coolant flow rate constant at 7 liters/min . The calibration was checked using a direct weighing technique . Details of the calibration procedure together with the calibration chart is given in Appendix (3) .

Current and voltage to the immersion heater were measured using a standard 0 to 10A ammeter and 0 to 240V voltmeter respectively. The electrical immersion heater was connected to the mains via a 0 to 240V variable transformer.

3.2.7 Materials Used and Their Preparation

Water, Silicone Oil, BP lubricating oils, Glycerol and various concentrations of sugar solutions were used to represent Newtonian systems . Various concentrations of aqueous solutions of Sodium Carboxy Methyl Cellulose , commonly known as C.M.C (trade name: Cellefas B.300, plus some B.50 supplied by Imperial Chemical Industries), polyacrylamide (trade name: Magnofloc 351, supplied by Allied Collodes), Carbopol 934 (supplied by Honeywill and Stein Ltd.) and Biozam R (supplied by Hercules Powder Company), and various grades of chocolates(supplied by Rowntree) were usred as non-Newtonian fluids.

The polymer solutions were made by adding the solid polymer powder slowly to warm water and agitating the

contents of the vessel at impeller speed of approximately 2 rps . Care was taken to ensure that the powder did not agglomerate into large relatively slow dissolving lumps.

3.2.8 Physical Properties of Materials Used

(i) Viscosity

Viscometric data of the Newtonian and non-Newtonian fluids were obtained using a Haake Rotovisko which is a variable speed concentric cylinder viscometer. It was observed that most non-Newtonian fluids were closely described by the power-law model for the range of sheat rates covered. Thus,

$$\tau = K \dot{\gamma}^n \qquad \text{----------} \qquad 3.3$$

The rheological parameters K and n were obtained from the flow curve (plot of shear stress, τ , verses shear rate, $\dot{\gamma}$). More details of the characterisation on the non-Newtonian fluids, together with the flow curves and the parameters K and n , are given in Appendix (2). For fluids which did not closely follow the power-law model the average apparent viscosity, μ_A, was calculated from the appropriate τ and $\dot{\gamma}_A$, as proposed by Metzner and Otto (12) .

(ii) Thermal Conductivity

A relative steady-state hot wire technique developed by N.E.L[82] was used to measure thermal conductivity of lubricating oils and some of the less viscous materials. Experimental difficulties were encountered when using this technique to measure themal conductivity of Silicone Oil and some of the more viscous non-Newtonian fluids. A concentric cylinder apparatus was built by the author to measure the thermal conductivity of the more viscous fluids.

The hot-wire technique is based on heating a long cylindrical annulus of the fluid around a central platinum wire . The power dissipated by the wire and its temperature are measured whilst the apparatus is surrounded by an accurately controlled constant temperature bath. The bath temperature was accurate to $\pm 0.005^{o}C$.

The conductivity cell which is shown in Fig. 3.10 consisted of a straight platinum filament of mm diameter and 95mm long, welded at each end to a thicker platinum wire of 0. mm diameter and concentrically sealed in a Pyrex glass tube of about 10mm internal diameter . After passing through the glass the platinum wires were connected to copper wires. As a relative method was used it was not necessary for the fine platinum wire to pass exactly along the central axis of the glass tube,

nor was it necessary to know the exact dimensions of the cell. It was only necessary for the platinum wire to be thin enough to cause its temperature to rise a measurable amount with the low voltage and current used . The cell was suspended in a constant temperature bath which was thermostatically controlled.

To calculate the thermal conductivity of the test fluid it was necessary to know the resistance of the platinum wire to within 0.001Ω and to know the current flowing through it to an accuracy of 0.001 amps.

The resistance of the wire was measured using a Wheatstone bridge circuit as shown in Fig. 3.11 . A mirror galvanometer was used to detect the null point. This type of instrument is sensitive to very small e.m.f's of the order of $1.26\ \mu V$.

The current flow through the platinum wire was obtained by measuring the voltage drop produced across a 1Ω standard resistor placed in series with the platinum wire. The voltage drop was measured on a potentiometer with scales 0 - 20mV and 0 -100mV with accuracies of 0.005mV and 0.025mV respectively .

The variable resistance box had a range of 1.0 to 111.10Ω in steps of 0.001Ω. Power for the circuit

was supplied by a Farnell Stabilised Power Supply giving an ouput of 12 volts . The Farnell unit was connected to the mains power supply via an Advance Voltstat constant voltage transformer which produced an output voltage of 240 volts with an input ranging from 190 - 260 volts.

A water bath fitted with a special ultra-sensitive temperature, fully proportional, controller to operate to within $0.005^{o}C$ was used . The experiments were carried out in a constant temperature room ($\pm$ $1^{o}C$) . Variations in the bath temperature were observed on a mercury in glass thermometer with a range of 20 - 26 ^{o}C graduated to $0.01^{o}C$. Variations in the mercury level were observed through a Cathetometer allowing very small changes to be detected. The absolute value of the temperature of the bath did not enter the calculations, it was not necessary, therfore, to know this. It was important, however, that the temperature of the bath was constant to $0.005^{o}C$ (82).

The test sample was placed in the cell, taking care to remove air bubbles from the arm containing the platinum wire . The cell was placed in the constant temperature bath and left for several hours to come to equilibrium.

The power supply was switched on and the current flow through the cell adjusted by means of the slide resistor

in series with the Farnel Power Supply . The Wheatstone bridge circuit was then balanced using the variable resistor . This was achieved when the galvanometer gave no deflection on the most sensitive scale. When the system had reached equilibrium, indicated by the resistance of the platinum wire remaining constant for several minutes, readings of voltage drop across the standard 1 Ohm resistance and resistance of the variable resistor were taken.

After the readings had been taken the current flow through the cell was increased slightly and the experiment repeated

If q Watts of heat are generated in the platinum wire, a heat balance can be written for the test liquid (82):

$$q = \frac{2\pi L\, k_l\, (T_F - T_i)}{\ln (R_i/R_F)} \qquad \text{--------- 3.4}$$

where

k_l = thermal conductivity of the test liquid(W/m^{o}C)

L = length of wire (m)

T_F = filament temperature (^{o}C)

T_i = temperature of inner glass surface (^{o}C)

R_F = filament radius (m)

R_i = inner radius of glass tube (m)

Similarly if the outer wall of the tube is in a well stirred bath at a constant temperature T_b then:

$$q = \frac{2 \pi L k_g (T_i - T_b)}{\ln (R_o/R_i)} \qquad \text{----------} \quad 3.5$$

where k_g is the thermal conductivity of the glass .

From 3.4:

$$(T_F - T_i) = \frac{q \ln (R_i/R_F)}{2 \pi L k_L} \qquad \text{----------} \quad 3.6$$

From 3.5:

$$(T_i - T_b) = \frac{q \ln (R_o/R_i)}{2 \pi L k_g} \qquad \text{----------} \quad 3.7$$

Adding 3.6 and 3.7:

$$\left(\frac{T_F - T_b}{q}\right) = \left(\frac{\ln (R_i/R_F)}{2 \pi L k_l}\right) + \left(\frac{\ln (R_o/R_i)}{2 \pi L k_g}\right) \qquad \text{------} \quad 3.8$$

Assuming a linear relationship between the resistance of platinum and temperature, the:

$$(T_F - T_b) = \text{Constant } (Y_F - Y_b) \qquad \text{----------} \quad 3.9$$

where

Y_F = resistance at filament temperature (Ω)

Y_b = resistance at bulk temperature (Ω)

also:

$$q = Y_F I^2 \quad \text{----------} \quad 3.10$$

Therefore:

$$\left(\frac{Y_F - Y_b}{Y_F I^2}\right) = \left(\frac{C_1}{k_1}\right) + \left(\frac{C_2}{k_g}\right) \quad \text{---------} \quad 3.11$$

or:

$$m = \left(\frac{C_1}{k_1}\right) + \left(\frac{C_2}{k_g}\right) \quad \text{----------} \quad 3.12$$

and, as the temperature of the bath is constant, m represent the slope of a graph of resistance versus power input.

C_1 and C_2 are given by:

$$C_1 = \left(\frac{1}{2\pi L}\right) \ln (R_i/R_F) \left(\frac{Y_F - Y_b}{T_F - T_b}\right) \quad \text{----} \quad 3.13$$

and

$$C_2 = \left(\frac{1}{2\pi L}\right) \ln (R_o/R_i) \left(\frac{Y_F - Y_b}{T_F - T_b}\right) \quad \text{-----} \quad 3.14$$

The function $\left(\frac{Y_F - Y_b}{T_F - T_b}\right)$ is the temperature coefficient of resiatance for platinum .

The values of the constants C_1 and C_2 could be measured from physical measurements on the cell . However as an absolute method was not required a greater accuracy can be obtained by calculating C_1 and C_2 empirically from experiments on liquids of known thermal conductivity . Provided that the physical dimensions of the cell do not change and the experiments are carried out at approximately the same temperature ($\pm$ 1^{o}C) (82), the results obtained are within 3% of the accepted values .

The experiment was carried out using two liquids of known thermal conductivity (Toluene and Methanol) . A 10 : 1 ratio was used for the fixed ratio of the Wheatstone bridge . When a balance point was reached the resistance of the cell, lead wires and the 1 Ohm resistor was then equal to one tenth the value of the variable resistance . For the balanced Wheatstone bridge circuit:

$$\left(\frac{Y_1}{Y_2}\right) = \left(\frac{Y_3}{Y_4}\right) \qquad \text{----------} \qquad 3.15$$

The bridge was first balanced with the lead wires to the cell connected together to obtain a value for their

resistance . This value was found to be constant over the range of voltage drop and current flow used .

As stated previously the current flow through the cell was obtained by measuring the voltage drop produced across a 1 Ohm standard resistor , and using ;

$$q = Y_F I^2 \qquad \text{----------} \qquad 3.16$$

a graph was plotted of q versus Y_F and was found to be a straight line . The slope of the line was measured.

Then for each liquid:

$$m = \left(\frac{C_1}{kl}\right) + C_2 \qquad \text{----------} \qquad 3.17$$

assuming k_g = constant . Hence C_1 and C_2 could be measured .

The results for various test fluids are given in Appendix (2) .

The steady-state hot wire technique described above could not be used for some of the high viscosity Newtonian fluids. This was basically due to difficulties in introducing these highly viscous materials into the cell.

A concentric cylinder apparatus was,thus, built to measure the thermal conductivity of these materials . The apparatus consisted basically of two water jackets which supplied and removed heat and two identical fluid chambers, see Fig. 3.12 . To reduce convection it was necessary ti use very thin films. The whole apparatus was placed in a draught free area and covered with lagging to minimize heat losses to surrounding.

The experiment consisted of heating one of the fluids by pumping hot water through one jacket and cooling the other fluid by passing cold water through the other jacket. Two constant water baths were used to supply water to the jackets . One of the fluids used was a standard liquid of known thermal conductivity (Silicone Oil) while the other fluid was the liquid under investigation.

Copper-constantan thermocouples were used to measure appropriate temperatures after equilibrium was reached .At equilibrium and assuming heat transfer across the film by conduction only :

$$\left(\frac{Q\,x}{A}\right) = k_l\,(T_1 - T_2) = k_s\,(T_3 - T_4) \quad \text{--------} \quad 3.18$$

where

Q = heat supplied/removed (W)

k_1 = thermal conductivity of test fluid (W/m ^oC)

k_s = thermal conductivity of standard fluid (W/m ^oC)

$(T_1 - T_2)$ = temperature difference across the test liquid (^oC)

$(T_3 - T_4)$ = temperature difference across the standard liquid (^oC)

x = film thickness equal for both fluids (m)

A = heat transfer area equal for both fluids (m^2)

The thermal conductivity of the test liquid is easily calculated from equation 3.18 . The experiment was repeated several times for each fluid and results were accurate to ±5% of the accepted values. The results for various test fluids are given in Appendix (2) .

(iii) Density Measurement

Density of Glycerol, Lubricating oils and some of the less vicous fluids were measured using a standard specific gravity bottle. Density of chocolate was provided by Rowntree (York) . All results are given in Appendix (2).

(iv) Specific Heat

The specific heat of most Newtonian and non-Newtonian fluids was measured in a well insulated electrical calorimeter. The insulation consisted of a small air gap, an

outer vessel,then an 8cm thick expanded polystyrene block. Heating was by means of a copper heating coil, a stirrer with a small mass compared to that of the test fluid was also used . The temperature was measured on a thermometer calibrated to $0.1^{o}C$.

A measured quantity of test fluid was placed in the calorimeter and a measured voltage applied across the heating coil for a measured time . The current flow was switched off and the vessel quickly and vigorously agitated and the temperature rise noted. The applied voltage was adjusted to give a temperature rise of about $5^{o}C$ after 30 seconds . The resistance of the coil was also measured. By using test fluids of known specific heat it was found that an accuracy of $\pm$ 3% could be obtained by this system. The results for various fluids are given in Appendix (2).

3.3 Experimental Procedure

Isothermal power data was obtained by carrying out torque measurements at several impeller speeds . Fluid densities and viscosities were evaluated at the mean temperature of the fluid which was noted before and after each torque measurement.

Heat transfer observations were carried out under steady state conditions using mains cooling water inside the jacket.

Steady-state was achieved when there was no further change in temperature of the bulk fluid or the temperature of the cooling water out of the jacket. Once steady state was reached in the vessel, for particular speed of the impeller, the inlet and outlet temperatures of the coolant, and the coolant flow rate were noted; together with the twelve readings of the tank wall temperatures. Voltage and current input to the immersion heater were also noted for each impeller speed. In addition temperature of the bulk fluid was measured, once the equilibrium had been reached, using the travelling thermocouples . From these data, the value of jacket-side film heat transfer coefficient, h_j, was calculated as shown below.

For heat transfer from the agitated liquid, through the wall of the jacket, to the liquid in the jacket the total rate of heat transfer, Q, is given by:

$$Q = M\, Cp_c\, (T_o - T_i) = V\, I \qquad \text{---------- } 3.19$$

where

M = mass flow rate of the coolant (kg/s)

Cp_c = specific heat of the coolant (J/kg ^oC)

T_o = outlet temperature of the coolant through jacket (^oC)

T_i = inlet temperature of cooling water to jacket (^oC)

V = voltage to the immersion heater (V)

I = current to the immersion heater (A)

Rotational speed, N, of the impeller was obtained using a tachometer which was placed on the impeller shaft. The shaft mounted torque transducer recorder was also noted, thus, input data were obtained.

The rotational speed of the impeller was changed and the above procedure repeated.

In order to prevent degradation of some of the more viscous non-Newtonian matetials the electrical immersion heater was replaced by a hot water heating coil. In these runs, the inlet and outlet temperatures of the hot water as well as its flow rate was recorded in order to check the heat load, Q .

3.4 General Description of Vessel 2

Limited experimental work was also carried out both by the author and others (85,86) in an existing small (0.15m diameter vessel) rig mainly for the purpose of scale-up . The layout and mode of operation of Vessel 2 is similar to that of Vessel 1 , except for small differences in the ancillary equipment. Plate 3.12 show vessel 2 and its ancillary equipment .

3.5 Technical Specification of Equipment

3.5.1 Vessel 2

The vessel was a flat-bottomed, cylindrical tank fabricated

from brass with a mild steel jacket. It had a diameter of 0.15m and a height of 0.195m .

Two short tubes, one at the top and the other one at the bottom of the jacket served as inlet and outlet for the cooling water. Six thermocouples, covering range of heights and angular psitions, placed in the vessel wall were used for measuring the wall temperature. The thermocouples are discussed in details in section 3.5.3 .

A 0.19KW motor with a speed ratio of 10 : 1 was used for driving the impeller. In order to get down to slower speeds an infinitely variable reducer was added which gave rotational speeds from 0 to 2.5 rps.

3.5.2 Agitators

Agitation was provided by a variety of anchor and helical ribbon impellers fabricated from stainless steel and having geometrical configuration as shown in Fig. 3.13 . Also see plates 3.7 and 3.6 .

3.5.3 Instrumentation

Six thermocouples were used to measure the tank wall temperature. They were embeded into the wall in the same manner described for vessel 1 . The six thermocouples were arranged at different angular positions and heights,

the first one being 13mm above the bottom of the vessel and the rest in sequence at 25mm intervals from each other at different angular positions. These thermocouples were calibrated by circulating water at a fixed temperature from the vessel to the jacket and back into the vessel again using a pump. The procedure was carried out at several temperatures in order to get the relation between e.m.f and the temperature. A "Kent" milivoltrecorder was used to record the thermocouple ouputs. The cold junction of the thermocouples was water + ice mixture in a thermoflask.

Coolant flow rates were measured with a standard rotameter which was calibrated in liter/minute of water measured at $20^{o}C$ having a range of 1.0 to 8.0 l/min. The calibration was checked using the method of direct weighing and found to be accurate to $\pm 1\%$.

Power data was obtained for vessel 2 by placing the tank upon an air bearing and measuring the torque on the vessel due to the rotation of the impeller. Full details of this torque measuring device are given elsewhere(22,83) .

3.5.4 Experimental Procedure

The experimental procedure carried out was the same as that employed for vessel 1 . The solutions were characterized using the Haake Rotovisko viscometer . All relevant

physical properties were determined using the same techniques as described for vessel 1.

CHAPTER 4

RESULTS AND DISCUSSION

Isothermal power data for both Newtonian and non-Newtonian fluids will be considered first followed by a discussion of temperature profiles and heat transfer rates. Finally combined power and heat transfer data will be treated. All Figures and Tables are given in Appendix (1).

Experimental data presented in this chapter will be critically compared with published work.

4.1 Isothermal Power Data

Isothermal power data were obtained for both vessel 1 (0.4m diameter tank) and vessel 2 (0.15m diameter tank) using various Newtonian and non-Newtonian fluids and various impellers (see section 3.2.2).

The power number values, P_o, were plotted against the Reynolds number, Re, on logarithmic scale , see Fig. 4.1 and Fig. 4.10 . Data were taken over a Reynolds number range of $1x10^{-3}$ to $1x10^{4}$.

4.1.1 Anchor Impellers

Figure 4.1 show the results of isothermal power data for anchor impellers. A straight line of slope -1 is obtained in each case up to a Reynolds number of about

100 indicating that in this laminar flow region:

$$P_o = K_p (Re)^{-1} \quad \text{----------} \quad 4.1$$

The value of the proportionality constant, K_p, obtained from the graph, is the value of Power number, P_o, at Re=1 . These K_p values are also given in tabulated form in Fig. 4.1 .

The slope of the power curves gradually decreases after Re = 100 and P_o becomes essentially constant beyond a Reynolds number of about 10,000 indicating that this is the turbulent flow region. Thus, in this region, i.e. for $Re > 10,000$:

$$P_o = \text{Constant (A)}$$

Values of the constant A are also tabulated in Fig. 4.1 .

For Reynolds numbers less than about 100, however, a separate line is obtained for each anchor indicating the influence of impeller geometry upon K_p in the laminar region.

In order to study the full effect of all the important geometrical parameters on power in the laminar region, it was decided to combine the data obtained in this work

with data extracted from the literature .

(i) <u>The effect of Clearance between Impeller Blade and Vessel Wall</u>

Uhl and Voznik(3), Nagata (1), Beckner and Smith (21) and a number of other workers (22,2,19,20) have clearly demonstrated the significant effect of clearance between the impeller blade and vessel wall upon the power consumption of anchor impellers. To investigate whether there is any correlation between the Power nimber, P_o, and the clearance between the impeller blade and vessel wall, C, the values of K_p was plotted against the respective dimensionless geometrical parameter C/D_T , see Fig. 4.2 .

Data reported by ten workers have been combined with the results obtained in this work. A total of twenty geometries were used. The ratio of all other geometrical parameters such as h/D, H/D_T, and W/D were the same for all twenty systems except C/D_T . using linear regression analysis the following correlation was obtained:

$$P_o = 83\ (C/D_T)^{-0.314}\ \ (Re)^{-1} \qquad \text{----------4.2}$$

A measure of the accuracy of this correlation is given by the % standard error and the linear correlation coefficient. For this correlation the % standard error was 3.93% and the correlation coefficient was 0.971 . For

100% accuracy the value of correlation coefficient would be unity.

It is, perhaps, worthwhile comparing this correlation with equation 2.47 obtained from a correlation proposed by Calderbank and Moo-Young (20). The failure of the proposed correlation is obviously in the incorrect vlaue as well as wrong sign of C/D_T (the exponent of C/D_T was proposed by these workers to be +0.5) .

Equation 4.2, on the other hand, is in good agreement with those of Kashani (22),equation 2.60, and Beckner and Smith (21), equation 2.59, for Newtonian fluids. But where as equations 2.59 and 2.60 were derived from only a limited amount of data and a short range of C/D_T. Equation 4.2 does not suffer from the same drawbacks as it was obtained from a large number of data and is applicable over a much wider range of C/D_T . The range of C/D_T covered is $0.01 < C/D_T < 0.13$. Most industrial applications is covered by this range of C/D_T . For $C/D_T = 0$, see scraped heat exchangers (79) .

It should also be pointed out that equation 4.2 correlated the non-Newtonian data obtained in this work with the same accuracy. In the case of non-Newtonian fluids, Re is replaced by the non-Newtonian generalized Reynolds, Re_1, obtained using Metzner and Otto method (12) see section 2.1.1 .

(ii) <u>The Effect of Agitator Height, h, on Power</u>

After establishing the effect of C/D_T upon power , a graph of $P_oRe\ (C/D_T)^{0.314}$ was plotted against the dimensionless geometrical parameter h/d combining data from nine published papers with results from this work. The graph is shown in Fig. 4.3 from which the following correlation is obtained using linear regression analysis:

$$P_o = 85\ (C/D_T)^{-0.314}\ (h/D)^{0.476}\ (Re)^{-1} \quad \text{-------} \quad 4.3$$

for the range:

$$0.01 < C/D_T < 0.13$$

$$0.10 < h/D < 1.0$$

$$W/D \simeq 0.1 \ \&\ \ H/D_T \simeq 1.0$$

For this correlation the % standard error is 4.1% and the linear correlation coefficient is 0.994 .

(iii) <u>The Effect of Agitator Width, W, on Power</u>

To establish the influence of agitator width, W, on power consumption of anchor impellers, a graph of $P_oRe(C/D_T)^{0.314}(h/D)^{-0.476}$ was plotted against the respective dimensionless parameter W/D on linear graph paper, see Fig. 4.4 . A total of twenty different geometries from eight other published papers were used and the graph indicates that,

for all engineering purposes, the impeller width, W, has no effect on power . Thus in the range $0.05 < W/D < 0.14$, power may be predicted from equation 4.3 .

Uhl and Voznik (3) using only two impellers differing in width by 30% also suggested that the effect of impeller width on power is negligible . Sterbcek and Tausk (51) explained that this is because in the laminar region shear forces do not act on the agitator surface but on its edges, the drag caused by the arm surface itself being negligible. The main drag is, therefore, concentrated at the edges and the power input is determined more by edge length than by agitator surface.

(iv) <u>The Effect of Liquid Height, H, on Power</u>

To study the effect of liquid height, H, on power consumption of anchor impellers for laminar mixing of both Newtonian and non-Newtonian liquids, a graph of $P_o Re\ (C/D_T)^{0.314}(h/D)^{0.476}$ was plotted against the respective dimensionless parameter (H/D_T) using data from thirty different geometries obtained from ten other published papers . The graph is shown in Fig. 4.5 and indicates that for all practical and engineering purposes the influence of H/D_T, in the range $0.32 < H/D_T < 1.5$, upon power consumption for this type of impeller is negligible.

(v) The Final Correlation for Anchor Impellers

The final correlation proposed in this work using over thirty different geometries obtained from about a dozen published papers , is

$$P_o = 85\ (C/D_T)^{-0.314}\ (h/D)^{0.476}\ \ (Re)^{-1} \quad \text{----- } 4.4$$

for Newtonian fluids and

$$P_o = 85\ (C/D_T)^{-0.314}\ (h/D)^{0.476}\ (Re_1)^{-1} \quad \text{----- } 4.5$$

for non-Newtonian materials. Equations 4.4 and 4.5 are applicable over the range:

$.01 < C/D_T < .133$

$.10 < h/D < 1.00$

$.05 < W/D < 1.4$

$.32 < H/D_T < 1.5$

$.01 < Re < 100$

$.01 < Re_1 < 100$

$.20 < n < 1.00$

Equations 4.4 and 4.5 were used to predict the value of K_p for different geometries . The predicted values of K_p was then plotted against the experimental valuees of K_p reported for the appropriate system under investigation.

Worker	C/D_T	h/D	K_p (exp.)	K_p (pred.)	% error
Uhl (2)	0.009	0.5	252	268	+6
	0.024	"	174	197	+13
	0.049	"	142	158	+11
	0.073	"	126	139	+10
Beckner & Smith (21)	0.0264	0.69	205	223	+9.8
	0.0542	0.73	170	183	+7.6
	0.0751	0.77	157	169	+7.6
	0.1067	0.83	144	157	+9.0
	0.1584	0.96	130	149	+14.6
Kashani (22)	0.056	1.07	190	223	+17
	0.060	1.07	240	218	-9
	0.080	1.17	207	199	-4
	0.143	1.33	189	166	-12
Rieger & Novak (84)	0.05	0.89	180	207	+15
Hoo & Wang (40)	0.05	0.9	215	218	+1.4
Pollard & Kantyka (32)	0.083	0.75	180	162	-10
Ullrich & Schrieber (30)	0.076	0.725	190	160	-16
Nagata (1)	0.05	0.75	190	190	0.0
	0.05	0.5	145	157	8.3
Schilo (29)	0.05	1.0	221	227	+2.6
	0.024	1.0	269	274	+2.6
Foresti & Liu (28)	0.066	1.0	340	200	-41
Reher & Bohm (33)	0.05	0.725	270	193	-28.5
	0.083	0.83	270	170	-37
This work	0.019	1.0	290	295	+1.6
	0.039	"	248	235	-5.5
	0.065	"	206	200	-3
	0.1025	"	180	174	-3.4
	0.033	"	230	248	+7.3
	0.123	"	170	164	-3.7

The graph, shown in Fig. 4.6, indicates that equations 4.4 and 4.5 can predict the reported K_p with a % standard error of 7% . As explained previously in section 2.1.2(i), the inadequacy and defficiencies of the correlation proposed by Forresti and Liu (28) and the approximate nature of the correlation put forward by Reher and Bohm (33) are the main reasons for these correlations to overestimate power by about 40% to 30% respectively, see Table 4.1 .

One interesting point that emerges from this study is that equation 4.4 and 4.5 adequately correlates the data for both flat-bottom and curved-bottom anchors so long as the clearance from the anchor to vessel bottom is equal to the clearance from anchor arms to tank sides.

4.1.1A Shear rate constant, k_s

Fig. 4.7 show plots of average shear rate, $\dot{\gamma}_A$, against impeller speed for all anchors studied. A wide range of non-Newtonian shear-thinning materials were used to study the effect of non-Newtonianness upon the shear rate constant.

These results indicate that for each impeller a linear relationship exist between the average shear rate, $\dot{\gamma}_A$, and the impeller speed, N, regardless of the flow behaviour index, n . The slope of the line drawn through the data is the value of k_s . A linear regression analysis was

applied to these results to obtain the best fit through the data . The results are tabulated below:

D_T	D	C/D_T	k_s
0.4	0.318	0.1025	17.5
"	0.348	0.065	23.5
"	0.369	0.039	25.6
"	0.385	0.019	33.3
0.15	0.115	0.117	14.0
"	0.14	0.033	26.0

Table 4.2

The slope, i.e. k_s , increases with a decease in the clearance between the impeller blade and tank wall . In order to investigate the true nature of this dependency of k_s upon C/D_T, it was decided to combine results obtained in this work with data extracted from published literature .

The value or the correlation for the impeller shear rate constant, k_s, are included in Table (1) whenever possible. The merits and demerits of these correlations and values have already been considered in some details with the appropriate power correlations in the previous section. This part is, however, included to consider further anomalies reported in the literature.

It has been shown conclusively that for anchor impellers, the value of mixer shear rate constant, k_s , is strongly affected by the clearance of the impeller from the vessel wall. Calderbank and Moo-Young (20) noticed this but unfortunately their developed correlation does not reflect the true relationship and tends to overestimate the value of k_s by about 50% when compared with the published data. In their correlation for the impeller shear rate constant, k_s, i.e.

$$k_s = \left[9.5 + \frac{9(D_T/D)^2}{(D_T/D)^2 - 1}\right] \left(\frac{3n + 1}{4n}\right)^{n/1-n} \quad \text{---- 4.6}$$

they claimed that k_s was dependent upon the flow behaviour index, n , as well as on C/D_T . It was, however, demonstrated (20) that for a wide range of n values $0.05 < n < 1.68$, the term involving n in equation 4.6 is about 0.84 $\pm$8.5% and may, thus, be treated as a constant . Reher and Bohm (33) must have also noted this point since their correlation only contains the first term on the right hand side of equation 4.6 .

Schilo (29) studying power consumption of anchor impellers also developed a fully theoretical correlation for k_s . The equation given is of the form

$$k_s = \left[\frac{(4\pi)^{n-1}}{n^n} \quad \frac{(D_T/D)^2 - 0.75}{\left[(D_T/D)^{2/n} - 0.75\right]^n} \right]^{\frac{1}{0.9(n-1)}} \qquad \text{---------- 4.7}$$

which is the theoretical coefficient for shear rate at the surface of a rotating cylinder in a cylindrical vessel containing the power-law fluid . Theoretical correlations such as this are both inconsistent with experimental observations and oversimplification . This equation like the one proposed by Calderbank and Moo-Young (20) appears to overestimate the value of k_s .

Beckner and Smith (21), however, noting the effect of C/D_T upon the value of k_s, correlated their data empirically . These workers also reported a strong dependence of the value of shear rate constant, k_s, upon the value of flow behaviour index, n . Their final correlation is of the form:

$$k_s = a\,(1 - n) \qquad \text{----------} \qquad 4.8$$

where a is a geometrical factor depending on both C/D_T and the type of anchor and given by:

$$a = 37 - 120\,(C/D_T) \qquad \text{for} \quad .02 < C/D_T < 1.6 \qquad \text{----} \quad 4.9$$

for flat-bottom plain impellers and

$$a = 106 - 1454\ (C/D_T) \quad \text{for} \quad 0.02 < C/D_T < 0.05 \qquad \text{---- 4.10}$$

for pitched-bladed anchors. The range of flow behaviour index covered was $0.29 < n < 0.73$.

Nagata (1), Kashani (22), Pollard and Kantyka (32) are among the many people who gave values and correlations for k_s independent of the flow behaviour index, n . Most of these workers also noticed the dependence of the shear rate constant, k_s, on C/D_T but no correlation has been reported since no one worker has tested a wide enough range of C/D_T to propose a general correlation.

It was, thus, decided to combine the available literature with results from present study in order to examine the effect of both the flow behaviour index, n, and C/D_T upon the impeller shear rate constant, k_s .

Fig. 4.8 is a plot of impeller shear rate constant, k_s, against the exponent of power-law fluid, n, for $C/D_T \simeq 0.05$. Apart from the values of k_s obtained from equation 4.8 proposed by Beckner and Smith (21), there do not seem to be any significant dependence of k_s on the value of n .

The effect of C/D_T, on the other hand, is very strong and is demonstrated in Fig. 4.9 which is a plot of k_s against C/D_T using data from about a dozen published papers . The data is well correlated with a relation of the form:

$$k_s = 33 - 172.5\ (C/D_T) \quad \text{----------} \quad 4.11$$

with a correlation coefficient of 0.961 and % mean error of 8.3% .

This equation is similar in form to type of dependence found also by Beckner and Smith (21) but where as their correlation, equation 4.8, was obtained from only a few data, equation 4.11 has been obtained from the maximum number of data possible and is applicable over the widest range of C/D_T .

Table 4.3 compares the reported values of k_s with those predicted by equation 4.11 . The predicted values of k_s agrees to about $\pm 10\%$ with those reported by Nagata (1), Pollard and Kantyka (32) and Kashani (22) . It is interesting to notice that all these people used the method of Metzner and Otto (12) to determine their shear rate constant, k_s . Rieger and Novak (84) used a semi-theoretical approach to confirm the applicabilty of Metzner and Otto's

Worker	C/D_T	n	k_s (exp.)	k_s (pred.)	%error
Pollard & Kantyka(32)	.0834	.35-.78	18	19	+5
Kashani (22)	.056 .06 .08 .143	.2 - .8	21.4 24 17 9.5	23.3 22.6 19.5 9.7	+8 -6 +13 +2
Nagata(1)	.05	.2 - .8	25	24.2	-3
Rieger & Novak(84)	.05	-	16	24.2	+39
Calderbank & Moo-Young(20)	.05	.05-1.87	47	24.2	-49
Gluz & Pavlo.(17)	.066	-	12.6	21.6	+42
Schilo (29)	.05 .025	.5 ..54	28 33	24.2 27.1	-14 -18
This work	.019 .039 .065 .1025 .033 .123	.11-.8	33.3 25.6 23.5 17.5 26.0 14.0	29.7 26.3 21.8 15.3 27.3 11.8	-11 +2.7 -7 -13 +5 -15.7

Table 4.3 Anchor Shear rate constant

technique for the evaluation of power consumption. Although they managed to generally prove this, they proposed a correlation for k_s independent of C/D_T. For anchor impellers they proposed:

$$k_s = n^{\left(\frac{2.21}{n-1}\right)} \qquad \text{----------} \qquad 4.12$$

indicating that k_s is strongly influenced by the flow behaviour index, n. Equation 4.12 gives a value of $k_s = 85$ for $n = 0.2$, and a value of $k_s = 286$ for $n = 0.1$. These values of k_s are about 3 to 11 times the recommended value of about 25 (for $C/D_T = 0.05$) respectively. These high values of k_s may well lead to underestimation of power.

Schilo (29) suggested the theoretical correlation, equation 4.7, for k_s. For $C/D_T = .05$ ($D/D_T = 0.9$), equation 4.7 predicts values of $k_s = 22.4$ for $n = 0.95$, $k_s = 28.4$ for $n = 0.5$ and $k_s = 35$ for $n = 0.2$. As compared with results from this work and other published data, equation 4.7 overestimates k_s by about 40% for $n = 0.2$, by 14% for $n = 0.5$ and predicts a good approximation for k_s for $n = 0.95$ (i.e. 24.4 as compared to experimental value of 25). From this analysis, it is obvious that the more non-Newtonian the fluid, the higher will be the error involved in using equation 4.7 to

predict k_s . Their data for $C/D_T = 0.05$ is also plotted in Fig. 4.8 (solid line) .

Calderbank and Moo-Young (20) also used a correlative equation for the evaluation of k_s which leads to overestimation of k_s , equation 4.6 . This is due to the type of assumptions they made in the derivation of their correlation; such as their use of generalized Reynolds number based on analogy with pipe flow .

The correlative equation given for k_s by Beckner and Smith (21) has already been dealt with in detail in the last section. The important points about this correlation, equation 4.8, are that it reflects the true dependence of k_s upon C/D_T . However, it also appears to indicate a strong dependence of k_s upon the flow behaviour index, 'n , which is contridictory to the findings of other workers (1,22) including this study. This latter point is the main cause for their correlation to fail drastically to predict the k_s value especially as n increases . Their correlation is also plotted in Fig. 4.8 for $C/D_T = .05$ (dotted line) .

It, therefore, appears that whenever the method of Metzner and Otto (12) has been used to evaluate the value of the impeller shear rate constant, k_s, and to

determine the power consumption, the correlations from different workers tend to agree a lot better than when a correlation is developed purely theoretically .

4.1.2 Helical Ribbon Impellers

Fig. 4.10 and Table 4.4 show the results of isothermal power data for all helical ribbon impellers. A straight line of slope -1 is obtained in each case up to a Reynolds number of about 10 (and in some cases up to 100) indicating that in this region, i.e. laminar regime:

$$P_o = K_p \, Re^{-1} \quad \text{----------} \quad 4.13$$

The value of the proportionality constant, K_p, obtained graphically (i.e. $K_p = P_o$ at $Re = 1.0$) are given in Table 4.4 .

The slope of power number-Reynolds number curves gradually decreases after $Re = 10$ and P_o becomes essentially constant beyond a Reynolds number of about 10,000 indicating that in this region the power number is almost independent of Reynolds number . This is the turbulent flow region for which:

$$P_o = \text{Constant (B)} \quad \text{----------} \quad 4.14$$

Line	D_T (mm.)	C/D	P/D	Nb	K_p	B
1	400	0.0682	1	1	160	0.35
2	"	"	"	2	240	0.42
3	"	"	0.5	1	215	0.38
4	"	0.0263	1	1	200	0.53
5	"	"	0.5	1	285	0.46
6	"	0.0405	0.5	1	250	0.33
7	150	0.0556	1	2	280	0.28
8	"	0.104	0.56	1	216	0.38
9	"	0.077	1	1	145	0.41

Table 4.4 Helical Ribbons Isothermal Power Data

Values of the constant B are also given in Table 4.4 . As seen from Fig. 4.11, for $Re \simeq 10$ (in some cases 100), a separate line is obtained for each impeller indicating the influence of impeller geometry upon K_p in the laminar region .

In order to investigate the full effect of all the important geometrical parameters on K_p in the laminar region, it was decided to combine the data obtained in this work with data extracted from the published literature.

(i) Effect of Clearance between Impeller Blade and Vessel Wall, C, and Impeller Pitch, P, on Power

A number of investigators (1,11,22,23,25) have studied the effect of-clearance between impeller blade and vessel wall and impeller pitch upon K_p . A few investigators (1,23,25) have also provided correlations that account for the effect of these parameters, see Table 4.5 . However, as stated previously in section 2.1.1(ii), most of these correlations are based on insufficient data. In many cases there was not a wide enough change in the geometry to enable a reliable correlation to be established (1,40). These points are highlighted when comparing some of these correlations. For example, the exponent of Nb, the number of blades, seems to vary from 0.2 (47) to 1.0 (23), that of clearance between impeller blade and

WORKER	CORRELATION
Carreau & Patterson (25)	$P_o Re^{0.93} = 24\, N_b\, (D / D_T)^{.91}\, (D / L)^{-1.23}$
Zolkanik (4)	$P_o Re = 1000\, (F_H / D^2)^{0.187}$
Reher & Bohn (33)	$P_o Re = 10.5\, (C / D_T)^{-1}$
Bourne & Butler (15)	$P_o Re = 1/\pi^2\, (h / D)^{-1} (D / D_T)^2 \left[4\pi / n\, (D / D_T)^{-2/n} - 1 \right]^{-n}$
Lastovstev (87)	$P_o Re = 2\, (P / D)^{-.7} (W / D)^{.54} N_b^{.6}$
Blasinki & Rzyski (48)	$P_o Re = 34.1\, (C / D)^{-0.53} (P / D)^{-0.63} (W / D)^{1.01} (W / D)^{0.14} (H / D)^{0.45} N_b^{.79}$
Hall & Godfrey (23)	$P_o Re = 66\, N_b\, (C / D)^{-.6} (P / D)^{-.73} (h / D)(W / D)^{.5}$
Nagata (1)	$P_o Re = 37.0\, (C / D)^{-.5} (P / D)^{-.5} N_b^{-.5}$
Brauer & Schmidt-Traub (47)	$P_o Re = 16.9\, N_b^{0.2} (h / D) \left[\left[1 / 1-(D / D_T)^2 \right] + 11.5\, (W / D)(D / D_T) / (P / D) \right]^{.2}$
Kappel (46)	$P_o Re = 60\, (C / D)^{-.3} (P / D)^{-.5} N_b^{.8}$
Kappel & Selbring (45)	$P_o Re = 14\, N_b^{0.9} (h / D) \left[(P / D)^{-2/3} / 1-(D / D_T)^2 \right]$
Bourne et-al (44)	$P_o Re = 134\, (h / D)(P / D)^{-0.3} (C / D)^{-0.3}$

Table 5 Power Data for Ribbons

vessel wall, C/D, between -0.3 (46) to -1.0 (33) while that of impeller pitch, P/D, seems to vary from -0.3 (46) to -2 (45) . The effect of impeller width, W/D, only appears in a few correlations (23,48,87) and the exponent of this parameter seems to vary between 0.14 (48) and 1.0 (47) .

It was, thus, decided to use the published untreated data in its original form, rather than using the published correlations as much as possible.

Using the following conditions:

$W/D = 0.1$, $h/D = 1.0$, $H/D_T = 1.0 \sim 1.02$ and $Nb = 2$

and equation 4.15 developed previously, i.e

$$P_o = D\,(C/D)^{\alpha}\,(P/D)^{\beta}\,Re^{-1} \qquad \text{----------} \qquad 4.15$$

the appropriate power number, P_o, and Reynolds numbers, Re, were calculated and a multiple linear regression analysis performed by a TI 59 programmable calculator to compute the best values of D, α, and β in equation 4.15 . (The programme was written by TI 59 manufacturers and kept on the Applied Statistics Module file as a library programme).

To obtain the correct form of equation 4.15 needed for

the calculator programme, it was made linear by taking logs on both sides of the equation. Thus:

$$\ln (K_p) = \ln(D) + \alpha \ln(C/D) + \beta \ln(P/D) \quad \text{-----} \quad 4.16$$

The natural logarithmic values of the K_p and respective dimensionless geometrical parameter (C/D) and (P/D) were used as the data for the calculator .

A total of sixteen geometries from ten different publications were combined with results from this work to obtain the following correlation:

$$P_o = 107 \ (C/D)^{-0.2774} \ (P/D)^{-0.5332} \ Re^{-1} \quad \text{------} \quad 4.17$$

with a correlation coefficient of 0.925 and a mean % error of 7.3% .

A detailed comparison between the correlation obtained in this work and those published will be made later in this section. It is, however, worthy of note, at this stage, that the exponents of (C/D) and (P/D) in equation 4.17 compares very well with that of Kappel (46), see Table 4.5 ,while the exponent of (P/D) only appears to agree with that of Nagata (1), Table 4.5 .

(ii) Effect of Number of Impeller Blades,Nb, on Power

Having established the influence of C/D and P/D upon K_p , it was then decided to investigate the effect of number of impeller blades, Nb, on K_p . Using the same programme as above and combining the data from this work with over a dozen other published works resulted in the following correlation:

$$P_o = 75\ (C/D)^{-0.2774}\ (P/D)^{-0.5332}\ (Nb)^{0.54}\ Re^{-1} \qquad \text{---------- 4.18}$$

with a correlation coefficient of 0.900 and a mean % error of 9.4% . Equation 4.18 was obtained for the following conditions;

$$W/D = 0.1\ ,\quad h/D = 1.0\ ,\quad \text{and}\quad H/D_T = 1.0 \sim 1.02$$

The natural logarithmic values of the $\dfrac{K_p}{(C/D)^{-0.2774}\ (P/D)^{-0.5332}}$ and Nb were used as the data for the calculator programme .

(iii) Effect of Impeller Width, W, and Impeller Height,h, on Power

The few published papers that account for the effect of impeller width (23,47,48,87) tend to disagree on the extent of its influence upon K_p . For doubling the width of the

width of the impeller, the mixing power increases by about 41% according to Hall and Godfrey (23) . Blasinski and Rzyski (48) predicts an increase of only 10% for the same change in impeller width while the semi-theoretical correlation put forward by Brauer and Schmidt - Traub (47) indicates that for doubling the impeller width, the mixing power increases by 54% .

It was, therefore, decided to use all possible data from the literature and combine them with results from this work in order to investigate the dependence of K_p on impeller width, W, and height, h .

The natural logarithmic values of the $\frac{K_p}{(C/D)^{-.2774}(P/D)^{-.5332}Nb^{.54}}$ andt the respective dimensionless geometrical parameter W/D and h/D were used as the data for the calculator programme which gave:

$$P_o = 150\ (C/D)^{-.2774}\ (P/D)^{-.5332}\ (h/D)(W/D)^{.325}\ Nb^{.54}$$

$$Re^{-1} \quad \text{-------} \quad 4.19$$

for $H/D_T \simeq 1.0 - 1.02$

Equation 4.19 was used to predict K_p for each geometry . This predicted value was then compared with the experimental

value of K_p reported . Table 4.6 shows the results and the % deviation between $K_{p_{predicted}}$ and $K_{p_{experimental}}$.

(iv) Comparison with other Published Correlations

One important point that is indicated from Table 4.6 is that within the range studied, liquid height, H, does not seem to have any significant effect on K_p . Equation 4.19 correlates the data of Bourne and Butler (15) for which H/D_T = 1.3 to -15%, that of Ulbrecht and Schrieber (30) for which $H/D_T \simeq 1.36$ to -6% and the data of Kappel (46) for which H/D_T = 0.99 to +15% . Bourne and Butler (15) have shown that impeller power can vary by as much as 20% depending on its direction of rotation, and since very few investigators give this information about their experiments, it is difficult to obtain general correlations that can predict power to better than $\pm$15% . Apart from the pumping direction of the ribbon, other factors that may influence the power and have not been included in many of the published papers are the clearance of impeller blade from tank bottom, number, shape and size of support bars and size and length of central shaft . It is, therefore, very important to realize that equation 4.19 still correlates 83% of the published data with a % average accuracy of 8.6% with a maximum of $\pm$20% .

AUTHOR	C/D	P/D	W/D	h/D	H/D_T	Nb	K_p (exp.)	K_p (pred.)	% error
Nagata (1)	0.0265	1	0.105	1	1	2	300	292	-3
	"	"	"	"	"	1	207	198	-4
	"	0.5	"	"	"	"	350	237	-22
Gray(7)	0.0295	0.75	0.08	0.96	1.17	2	414	327	-20
Zolkanik (4)	0.01	0.5	0.10	1.0	1.0	1	878	575	-57
	"	1.0	"	"	"	1	710	260	-63
	"	0.5	"	"	"	2	1000	547	-45
	"	1.0	"	"	"	2	808	377	-53
Bourne et-al (44)	0.0625	0.388	0.103	1.19	1.22	2	450	477	+6
	0.025	0.362	0.121	1.11	"	"	620	582	-6
	0.024	0.362	0.113	1.11	"	"	620	570	-8
	0.051	0.391	0.103	1.19	"	"	530	494	-7
	0.015	0.362	0.112	1.11	"	"	720	653	-9
	0.007	0.350	0.110	1.08	"	"	932	798	-14
	0.051	0.570	0.121	1.17	"	"	407	397	-3
	0.0134	0.537	0.113	1.09	"	"	639	540	-15
	0.006	0.516	0.110	1.06	"	"	800	665	-17
	0.0593	0.826	0.124	1.27	"	"	402	339	-16
Hall & Godfrey (23)	0.055	0.517	0.135	1.0	1.0	1	220	257	+12
	0.048	0.495	0.097	1.0	1.02	1	207	228	+10
	0.048	1.0	0.097	0.94	"	2	250	241	-4
	0.0545	1.0	0.098	1.0	"	1	130	143	+10
	0.0495	1.0	0.100	1.0	"	2	246	248	+0.8
Kappel (46)	0.01	0.5	0.1	1.0	1.0	1	334	378	+12
	0.03	"	"	"	"	1	246	377	+13
	0.05	"	"	"	"	1	208	247	+16
	0.01	"	"	"	"	2	591	247	-8
	0.03	"	"	"	"	2	416	547	-3
	0.05	"	"	"	"	2	359	403	-3
	0.01	1	"	"	"	1	242	350	+7
	0.03	1	"	"	"	1	178	260	+8
	0.05	1	"	"	"	1	142	166	+17
	0.01	0.5	"	"	"	2	392	378	-4
	0.03	"	"	"	"	2	300	277	-8
	0.05	"	"	"	"	2	253	242	-4
Hoo & Wang (40)	0.025	0.5	0.095	0.98	1.0	1	290	286	-1.4
	0.025	1.0	"	"	"	1	186	198	+7
	0.025	0.5	"	"	"	2	426	416	-2
	0.025	1.0	"	"	"	2	273	288	+5.5
	0.025	0.7	"	"	"	4	350	455	+30
Kashani (22)	0.032	0.42	0.1	0.85	1.0	1	212	253	+19
Reher & Novak (84)	0.095	1.28	0.114	1.0	1.0	2	130	185	+42
	0.055	1.10	0.103	1.0	1.0	2	232	226	-2.6
Gluz & Pavlo.(17)	0.036	1.75	0.167	1.0	1.0	1	235	227	-3
Jhonson (41)	0.0515	0.772	0.103	1.0	1.19	2	310	276	-11
Den-Hartog (8)	0.0215	0.61	0.091	1.0	1.05	2	609	385	-37
Ullrich & Schrieber (30)	0.0575	1.25	0.087	1.0	1.36	2	237	222	-6
This Work	0.0682	1	0.097	1	1.1	1	160	148	-8
	"	"	"	1	"	2	240	215	-12
	"	0.5	"	1	"	1	215	214	-0.5
	0.0263	1	"	1	"	1	200	193	-4
	"	0.5	"	1	"	1	285	279	-2
	0.0405	"	"	1	"	1	250	247	-1.2
	0.0556	1	0.096	1.02	"	2	280	232	-17
	"	0.56	0.104	1.08	"	1	216	235	+8.8
	0.0769	1.02	0.10	1.02	"	1	145	146	+0.7
	0.1637	0.53	0.106		"	1		167	

Table 4.6 Isothermal Power Data for Helical Ribbons

Equation 4.19, however, underestimates the power for geometries used by Zolkanik (4) by as much as 63% , see Table 4.6 . Zlokanik (4) used flat metal bands to attach the impeller to the shaft. These bands ran vertically downward on the outer edge of the ribbon, bending at a right angles underneath, and then attached to the shaft. It is, therefore,reasonable to expect higher power consumption for these impellers compared to a standard agitator.

The relatively high deviation between K_p(predicted) and K_p (experimental) for the geometry of Hoogendorn and Den-Hartog (8) is difficult to explain since very little information is provided in the paper as regards to torque measuring technique but Kappel (46) pointed out that this relatively high value of K_p (experimental) may well be due to the steady bearing used by these workers to measure torque .

A further interesting point to note about equation 4.19 is that it overestimates the value of K_p for the geometry of Hoo and Wong (40) with Nb = 4.0 . This paper is one of the few papers cited on power consumption of a quadruple helical ribbon impeller . These workers,unfortunately, give no details of the experimental rig, torque measuring techniques or impeller geometries . It is,however, indicated that the quadruple helical ribbon used in their

work was basically a modification of a double helical ribbon. It was in effect two concentric helical ribbons attached to the same support bars with the diameter of the inner ribbon about 43% smaller than the diameter of the outer ribbon (this information was extracted from the drawing of the ribbon cited in the paper (40)). It is, therefore, reasonable to expect a lower power consumption for this geometry compared to an standard ribbon and equation 4.19 seems to support this point .

The effect of impeller height, h/D, is identical with the values given by Hall and Godfrey (23), Kappel and Seibring (45), Brauer and Schmidt-Traub (47), and Blasinski and Rzyski (48) , while the effect of impeller width, W/D, is almost the mean value of the exponents given by Hall and Godfrey(23) and Blasinski and Rzyski (48) .

The exponent of impeller pitch, P/D, agrees very well with that of Nagata (1) and Kappel (46) while it is 27% lower than that proposed by Hall and Godfrey (23) . In other words, the correlation proposed by Hall and Godfrey (23) predicts a 39% decrease in power for doubling the P/D ratio while equation 4.19 estimates a decrease of 31% in power for the same change in pitch, P/D .

The exponent of the ratio C/D is in good agreement

with those proposed by Bourne et-al (44) and Kappel (46). It is, however, 54% lower than that proposed by Hall and Godfrey (23) and 44.5% lower than that put forward by Nagata (1) . The exponent of the number of impeller blades, Nb, on the other hand, is in very good agreement with the value proposed by Nagata (1) while it is 50% lower than that of Hall and Godfrey (23) . It is important to note that the exponent of Nb in the correlation of Hall and Godfrey (23) was based on only two impellers and could be very inaccurate.

4.1.2A Shear rate constant, k_s

Fig. 4.12 shows plots of average shear rate, $\dot{\gamma}_A$, against impeller speed for all helical ribbon impellers studied . A wide range of shear-thinning materials were used to study the effect of non-Newtonian behaviour upon the shear rate constant, k_s . The data indicated that for all practical and enginnering puposes, the shear rate constant, k_s, is independent of flow behaviour index, n . This conclusion was also reached by other workers (1,22,23,11).

Studies conducted by Hall and Godfrey (23) and Nagata (1) confirmed that impeller pitch , P/D, or number of blades, Nb, has no significant influence on the shear rate constant, k_s., see Table 2 . Indeed Nagata (1) obtained a constant value of 30 for k_s regardless of

impeller pitch, P/D, or number of blades, Nb . It is, however, shown conclusively (1,22,23) that the value of the constant, k_s, is greatly influenced by the clearance between the impeller blade and vessel wall, C/D . Graph 4.13 is a plot of the shear rate constant, k_s, against the dimensionless parameter, C/D, on linear graph paper. Within the range $.0263 < C/D < .164$, the data from this work and those extracted from literature may be correlated by a single equation of the form:

$$k_s = 34 - 114\ (C/D) \quad \text{----------} \quad 4.20$$

in the range

$$0.0263 < C/D < .164$$

It is important to realise that equation 4.20 is only applicable within the range of C/D studied, because, as the clearance between the impeller blade and the tank wall increases, it is expected that the value of the impeller shear rate constant, k_s would approach the constant value of about 12 which is the value of k_s for open impellers such as turbines and propellers proposed by Metzner and Otto (12) . It is also worth noting that the majority of ribbons used in industry will have a C/D in the

$$k_s = 4\pi \left[\frac{n \left[1 - (D/D_T)^{2/n} \right]}{1 - (D/D_T)^2} \right]^{\frac{1}{1-n}} \qquad \text{------} \quad 4.21$$

For n = 0.4 and C/D 0.025 , equation 4.21 predicts a value of 16 which is about half the reported value of k_s (1,23,22) . Mitsuishi and Miyairi (24), on the other hand, have proposed a semi-theoretical equation for k_s , based on the analogy with flow between two parallel flat plates, i.e.

$$\dot{\gamma}_A = \left(\frac{\pi}{\sqrt{2}} \right) \left(\frac{D}{D_T - D} \right) N \qquad \text{----------} \quad 4.22$$

i.e.

$$k_s = \left(\frac{\pi}{\sqrt{2}} \right) \left(\frac{D}{D_T - D} \right) \qquad \text{----------} \quad 4.22A$$

giving

$$k_s = 1.1 \ (C/D)^{-1} \qquad \text{----------} \quad 4.22B$$

Equation 4.24 tends to overestimate the value of k_s at very small clearances and uderestimates k_s for large values of C/D, see Fig. 4.13 .

4.2 Temperature Distribution in the Agitated Fluid

The variation in temperature of the agitated fluid under steady state conditions was monitored for a range of Newtonian and non-Newtonian materials and the ability of the various impellers to level out these distributions was observed .

Initial investigations indicated very little angular or radial temperature variations within the bulk of the liquid in the vessel. In other words, at any constant height but different angular and radial positions, the bulk temperature varied only by about $\pm 1\ ^{o}C$. It should be emphasised that " within the bulk of the liquid" , means the distance from the inner side of the impeller blade to the centre of the vessel . There was, however, a large temperature gradient between the wall and the inner side of the impeller blade (cooler near the wall). Thermocouples placed near the wall at different axial positions indicated very little vertical variation in temperature near the wall of the vessel . A typical experimental result is shown in Fig. 4.14 .

The largest temperature gradients within the fluid bulk were observed in the vertical directions as shown by Fig. 4.14 . Fig. 4.15 and 4.16 are typical experimental

results which give the influence of impeller rotational speed(rps) and the fluid properties upon vertical temperature variations in the central region of the large tank (0.4m diameter) . From these graphs, it would appear that as the speed is increased a sharp critical value is reached when uniformity of temperature is obtained . In the case of anchor impellers, this critical speed appears to be about 0.35(rps) regardless of the fluid viscosity or impeller geometry, see Fig. 4.15 . For helical ribbon impellers, however, the critical speed at which uniformity of temperature is obtained seems to decrease with an increase in fluid viscosity . In other words, the effectiveness of the ribbon as a mixer increases as the fluid viscosity increases. This observation has not been reported by any other worker. However, Nagata (1) proposed a lower critical speed of 10 rpm for helical ribbons, regardless of fluid viscosity. He also pointed out that this effective impeller speed may depend on vessel/impeller geometry but gave no correlation .

Assuming that for a close clearance impeller , the critical speed, N_c, is a function of fluid properties and system geometries, it may be written that:

$$N_c = f\ (\varrho, \mu, Cp, k, g, C, P, Nb, \text{other geometrical factors}) \qquad \text{---------- } 4.23$$

Using dimensionless analysis it is possible to show that:

$$\frac{\varrho N_c D^2}{\mu} = f\left[(\mu Cp/k),\ (N^2D/g),\ (C/D),\ (P/D),\ (Nb),\right.$$
$$\left.\text{other dimensionless geometrical factors}\right] \quad \text{---------- 4.24}$$

The dimensionless group, N^2D/g, is called the Froude number. It characterises uneven surfaces which are produced by vortexing . Skelland (19) reports that in agitated systems, Froude effects can be neglected at values of Reynolds number less than about 300 . Since close-clearance impellers generally operate at Reynolds numbers less than this value, the effect of Fr may be ignored.

In order to investigate the nature of the function in equation 4.24, the critical Reynolds number, Re_c, based on the critical speed, N_c, was plotted against Prandtl number ($\mu Cp/k$) for the 0.352m diameter ribbon (P/D = 0.5, Nb = 1.0, C/D = 0.0682) using both Newtonian and non-Newtonian fluids . It should be pointed out that the critical Reynolds number, Re_c, used in this work is defined as the Reynolds number at which the standard deviation of the twelve thermocouple readings in the central region of the tank (bulk temperature) is about 1.00($\pm$10%) ^oC . A standard deviation of 0.8 ^oC was used by Nagata (1) to specify the critical Reynolds

number. This is one of the few papers describing temperature distribution in agitated fluids in vessels. But even this paper does not give much quantitative information on the effect of some of the important geometrical parameters and fluid properties upon temperature variations in the tank.

As seen from graph 4.17, a straight line is obtained on log-log paper. The data was analysed using linear regression which resulted to the following empirical correlation :

$$Re_c = 5.69 \times 10^6 \; Pr^{-1.3} \qquad \text{---------- 4.25}$$

with a mean % error of 20% and a correlation coefficient of 0.921 .

Graphs 4.18, 4.19 and 4.20 show the effect of clearance, C/D, impeller pitch, P/D, and number of impeller blades, Nb, upon the critical Reynolds number, Re_c . The final correlation using linear regression analysis is :

$$Re_c = 1.84 \times 10^8 (P/D)^{0.428} (C/D)^{1.261} (Nb)^{-1.42} \; Pr^{-1.3}$$

---------- 4.26

in the range:

$$0.1 < Re_c < 258$$

$$10^2 < Pr < 10^6$$

$$0.0263 < C/D < 0.068$$

$$0.5 < P/D < 1.0$$

$$Nb = 1,2$$

$$W/D = 0.1$$

$$h/D = 1.0$$

$$H/D_T = 1.05$$

with a mean % error of 16% and a correlation coefficient of 0.831 .

It is apparent from the few data used in this work that impeller geometry has a great influence upon leveling out temperature variations in the tank. The numerical constants of equation 4.26 should, however, be regarded in the light of the relatively few points used in its evaluation.

One important point that emerges from this analysis is that equation 4.26 predicts the critical Reynolds number, Re_c, for non-Newtonian fluids as well as for Newtonian liquids. Another interesting point to notice about equation 4.26 is that it indicates that number of impeller blades, Nb, has a greater influence upon leveling out temperature variations than impeller pitch, P/D . It, therefore,seems

advantageous to use a P/D = 1, and Nb =2, rather than P/D = 0.5, and Nb = 1 since power consumption in both cases is almost the same (see equation 4.19, section 4.1.2), and since the fabrication costs of the two impellers are also very similar.

However, perhaps, the most important point about equation 4.26 is that it indicates critical Reynolds number and hence speed, N_c, increases as the fluid viscosity decreases . For lubricating oil with a viscosity of about 18 poise at room temperature and using the 0.352m diameter ribbon with P/D = 0.5 , Nb = 1.0 , C/D = 0.0685 , the critical Reynolds number, Re_c, was found experimentally to be 180 (N_c=0.45 rps) . For Silicone Oil, on the other hand, with a viscosity of about 1000 poise at room temperature and using the same impeller and under the same experimental conditions, the critical Reynolds number, Re_c, was found to be 0.35 (N_c= .086 rps) . An anchor impeller would give a very similar result for both the lubricating oil and the Silicone Oil, i.e. a critical speed , N_c, of about 0.35 rps in both cases. In practice, of course, one would not use a helical ribbon for a fluid of viscosity as low as that of lubricating oil, but nevertheless, such studies reveal a great deal of useful quantitative information on helical ribbon and anchor impellers .

Following a similar procedure described above, the data for anchor impellers were treated using linear regression analysis which resulted to the following simple relationship between the critical Reynolds number, Re_c, and the Prandtl number, Pr:

$$Re_c = 5x10^5 \, Pr^{-1} \quad \text{----------} \quad 4.27$$

with a correlation coefficient of 0.888 and a % mean error of 10% .

It is interesting to see that the exponent of Prandtl number in equation 4.27 compares well with the value of -0.921 obtained in equation 4.26 for helical ribbon impellers. It is also interesting to notice that equation 4.27 indicates that for anchor impellers, fluid viscosity has no apparent effect upon the ability of the impeller to level out the temperature gradients in the vessel.

Within the range of variables investigated in this work, anchor geometry had very little effect upon leveling out temperature gradients in the tank. It must, of course, be pointed out that, as far as anchor is concerned, the only geometrical variable tested was the clearance between the impeller blade and the vessel wall. More data is required to establish the exact dependence of the critical Reynolds number, Re_c, upon the anchor geometry.

Mitzushina (90) reported a value of 50 as the critical Reynolds number. This worker used scrapers on the blade and it is interesting to notice that the attachment of the scraping blade to the edge of the anchor impeller gave no better results. This agrees well with the present work where no effect of anchor geometry (mainly C/D) upon the critical impeller speed, N_c, was noticed. Uhl (2) and Coyle et-al (6) have also provided qualitative information on temperature variations in the mixing vessel agitated by an anchor but none of these papers give any quantitative information on how these temperature gradients may be used for design of mechanically agitated systems.

Nagata (1) also reported large temperature unevenness in the mixing vessel agitated by an anchor at Reynolds numbers below 100. For helical ribbon impellers, this worker proposed a lower critical speed of 10 rpm regardless of fluid viscosity (no Re_c is provided for helical ribbons). However, he pointed out that this critical impeller speed may depend on vessel/impeller geometry but gave no correlation. The present investigation reveals that the critical impeller speed for helical ribbon impellers not only depends upon system geometry but is also greatly influenced by fluid properties as indicated by equation 4.26 .

4.3 Heat Transfer

To date, most published work on heat transfer in close clearance, mechanically agitated vessels has been done with helical ribbon and anchor impellers . In general terms, it may be said that adequate correlations of the available data exist in the turbulent flow region ($Re > 10$, or 100 according to some workers (8,4,30,31), and that in,the case of helical ribbons, impeller geometry has a negligible effect upon heat transfer (1,6,24,61) . In the laminar region, however, agitator geometry is found to have an important effect which is not well correlated at present .

Research to determine the effect of clearance on heat transfer, particularly in the laminar region, is necessary to optimize economically a small clearance agitated heat exchanger because the impeller power requirement is strongly dependent upon the clearance between the blade tip and the vessel wall as well as on other impeller geometrical factors.

The major aim of this investigation is to study the effect of some of the important geometrical parameters and fluid properties upon heat transfer for a particular class of agitators . Presently available correlations are carefully examined and the most promising used for comparison with the correlations developed in this work .

4.3.1 Helical Ribbons

The heat transfer analysis of this system is arranged so that the experimental heat transfer coefficients could be compared with values calculated in terms of the film theory, natural convection theory, and the conduction theory of Coyle et-al (6) .

(i) Forced Convection Correlations

Values of the jacket-side heat transfer coefficient, h_j, were calculated from the experimental data using the procedure outlined in section 3.3 . Then h_j was combined with the other values to calculate the Nusselt number, Nu, $(h_j D_T/k)$. The values of Nu calculated from the data are plotted against Reynolds number, Re, $(\rho ND^2/\mu)$. in Fig. 4.21 for the 0.352m and 0.135m diameter ribbons with P/D = 0.5, Nb = 1.0, . These curves are separated for each fluid to show the pattern of the data.

The data were treated using linear regression analysis , discussed in the previous section, to obtain the best fit through each set of points . The results are also tabulated in Fig. 4.21 .

As indicated by Fig. 4.21 , the exponent for the Re , for each set of runs, decreases as the Reynolds number decreases . In other words, there is only a slight

improvement in the jacket-side film heat transfer coefficient, h_j, with variation in impeller speed at low Re . h_j is not, however, totally independent of the stirrer speed or viscosity as claimed by Coyle et-al (6) and others (65) . The exponent of Re extracted from Rautenback's data (65) is about 0.16 which agrees well with the present results . It is, therefore surprising when he concludes that there is no relation at all between heat transfer coefficient and impeller speed.

Fig. 4.22 and 4.23 show the effect of Prandtl number, Pr, and viscosity ratio ,(μ_b / μ_w), upon heat transfer coefficient respectively . The exponent of Prandtl number obtained using linear regression analysis was found to be 0.336 while that of the viscosity ratio, μ_b/μ_w, was 0.188 . The exponent of Prandtl number agrees with the published work of most investigators (1,4,89,90,91) who suggest a value of 1/3 (0.333) . The exponent of the viscosity correction term, on the other hand, is very close to the value of 0.2 proposed by Nagata (1) for $1.0 \leqslant Re \leqslant 10^3$. It is, however, about 34% higher than the value of 0.14 reported by Mizushina et-al (90) and Miyairi and Mitsuishi (24) . These workers did not evaluate the exponent of the viscosity ratio experimentally but assumed it to be 0.14 based on heat transfer studies

in tubes by Sieder and Tate (52) . In the light of the present work and that of Nagata (1), this assumption is incorrect, certainly at $Re \lesssim 10^3$. At Reynolds numbers greater than about 10^3, Nagata (1) claims that a better correlation of the data may be obtained by using an exponent of 0.14 rather than 0.2 . The Reynolds number range covered in this work is not sufficient to place much confidence in the data above $Re > 10^3$ and it is, therefore, advisable to use a value of 0.14 for the exponent of the viscosity ratio at Reynolds number greater than 10^3 . It should also be pointed out that in most practical situtions the mixing and heat transfer operation will be carried out at Reynolds numbers less than about 10^3 for helical ribbon type impellers.

Fig. 4.24 shows the effect of impeller geometry on the jacket-side film heat transfer coefficients over the whole range of Reynolds numbers studied in this work . Fig. 4.24 indicates that transition starts at a Reynolds number of about 1.0 and terminates at about 10 . It is, however, interesting to notice that the transition range is much narrower for the larger clearance impellers, i.e. for the impeller with C/D = 0.1637, turbulence seems to start at $Re \simeq 2.0$ (slope of the graph is almost 2/3) while for the ribbon with C/D = 0.0263, turbulence does not start

until $Re \simeq 10$. This is one reason for the present state of confusion in the literature as to when laminar regime terminates and turbulent takes over . Miyairi and Mitsuishi (24) give $Re = 180$ as the lower limit for turbulence . Nagata (1) gives a single correlation for $1.0 \leqslant Re \leqslant 10^3$ while Ishibashi and Yamanaka (91) calim that transition starts at $Re = 50$. It is also important to notice that most published work on heat transfer only extend down to a Reynolds number of about 1.0, but go up to Reynolds numbers of about 10^5 which is rarely used in actual industrial applications. The present work indicates that the laminar regime extends up to Re 1.0 and, thus, there is a distinct lack of information on heat transfer to both Newtonian and non-Newtonian fluids in agitated tanks in the true laminar region .

As Fig. 4.24 demonstrates , above a Reynolds number of about 10, the present data for all impellers could be correlated by a single equation viz:

$$Nu = 0.45\ (Re)^{0.598}\ (Pr)^{0.336}\ (Vis)^{0.188} \quad \text{----- 4.28}$$

with a correlation coefficient of 0.922 and mean % error of 10.6% for the following range:

$$10 < Re < 10^3$$

$$4 \times 10^2 < Pr < 10^6$$

$4x10^{-2} < Vis < 1.0$

$0.0263 < C/D < 0.1637$

$0.5 \quad P/D \quad 1.0$

$Nb = 1,2$

$W/D = 0.1$

$h/d = 1.0$

$H/D_T = 1.0$

Fig. 4.25 is a plot of $(Nu/ Pr^{\alpha} Vis^{\beta})$ against Reynolds number, Re, for most published correlations . The values of α and β together with details of geometry used in each case is given in Table 4 .

The heat transfer coefficient reported by Gluz and Pavlushenko (17) and Miyairi and Mitsuishi (24) are lower while those of Ishibashi and Mizushina (91) are higher than the present results and the points of transition are also different . In the range of Reynolds number 10 - 100, the present results agrees very well with those of Gluz and Pavlushenko (17) and Miyairi and Mitsuishi (91) . For Reynolds numbers above 100, the present results fall in between those of Mizushina (90), Ishibashi and Yamanka (91), Gluz and Pavlushenko (17) and Miyairi and Mitsuishi(24) . The correlation reported by Miyairi and Mitsuishi (24) predicts the lowest heat transfer coefficient for any Reynolds number as indicated

in Fig. 4.25 . This may be explained partly by the fact that their impeller had an exceptionally low W/D value (W/D = 0.053 compared to the normal value of 0.1) . The correlation reported by Nagata (1), on the other hand, gives the highest heat transfer coefficient for any value of Reynolds number . This is patly due to the unusual heating arrangement used by Nagata (1). In his investigation, Nagata used a mixing vessel in which cooling water jackets and steam heated jackets were located side by side at 90^{o} intervals (1) . He pointed out that this arrangement would give higher heat transfer Coeffi-cients than a uniformly heated or cooled vessel mainly because of the entrance region effect from the insulated to heated parts . Nagata (1) also reported one single correlation which is supposed to correlate data in the range $1.0 < Re < 10^{3}$. This is a very wide range of Re and most workers give two to three separate correlations to cover the same range in Reynolds number. The present investigation give two separate correlation in this range of Re.

As indicated in Fig. 4.24 a separate line is obtained for each impeller below a Reynolds number of about 1.0 emphasising the influence of impeller geometry on heat transfer coefficients in the mixing tank .

Figures 4.26 to 4.28 show the effect of impeller geometry on the jacket side film heat transfer coefficients in the region where Re is less than 1.0 . It was found that in this region an exponent of 0·16 for the Reynolds number could adequately correlate the data for all helical ribbon implellers. It should, however, be mentioned that a better fit could be obtained by using a slightly higher exponent for the Reynolds number with the impellers having large clearances.(see Fig. 4.26A, data for C/D = 0.1637, where exponent of 0.25 would give a better fit) . An exponent of 0.16 was used mainly because it gave a much better fit for the small clearance impellers which are often recommended for industrial applications. The data for the large clearance (C/D = 0.1637) impeller is included mainly for comparison and to highlight the fact that most of these correlations are purely empirical and should only be used within the range specified . Extrapolating the correlations could lead lead to gross errors .

Fig. 4.26B is a cross plot of the data from Fig. 4.26A . It shows the effect of impeller clearance, C/D, on heat transfer coefficient . The data is plotted as $(Nu/Pr^{0.336}\ Vis^{0.188})$ against the respective dimensionless parameter, C/D, evaluated at Re = 1.0 . Linear regression analysis of the data gave a slope of -0.452 with a

% mean error of 5% and a correlation coefficient of 0.985 . The only work published to date that accounts for the effect of clearance, C/D, on heat transfer is that of Nagata (1) who, using four double (Nb = 2) helical ribbons with varying clearances,(see Table 4.6), gave an exponent of -0.333 for C/D .

Figures 4.27A and 4.28A indicate the effect of pitch, P/D, and number of blades, Nb, on heat transfer coefficients for the 0.352m and 0.382m and 0.135m diameter helical ribbons . The first point that emerges from Fig. 4.27A is that as far as heat transfer is concerned there seems to be very little difference between the impeller with P/D = 0.5 , Nb = 1 and that with P/D =1, Nb = 2 . These two geometries have the same heat transfer characetristics within the experimental accuracy of the data . This is quite an important point because it was demonstrated in section 4.1.2 , equation 4.19, that the power requirements for these two geometries are also very similar. It was also shown in section 4.2 that the impeller with P/D = 1, Nb = 2 had a greater influence upon levelling out temperature variations in the tank than the impeller with P/D = 0.5 , Nb = 1 . So it, now, appears to be advantagous, having considered both power consumptions and heat transfer characetristics of both systems, to use a bouble helical ribbon with a P/D = 1 rather than a

single helical ribbon with a P/D = 0.5 whenever possible.

Figures 4.27B and 4.28B are plots of $(Nu/Pr^{0.336}\ Vis^{0.188})$ against number of impeller blades, Nb, and the dimensionless parameter, P/D, respectively at Re = 1.0 . A staright line of slope 0.222 for Nb and -0.235 for P/D is obtained . It is not possible to compare these results with any published work as no other worker has provided correlations that accounts for the influence of P/D and Nb on heat transfer coefficient. It should also be emphasised that these results are based on only a limited number of data. They are, however, the only correlations, to date, accounting for changes in impeller geometry.

Combining the data for all the impellers and using linear regression analysis, the following empirical correlation was obtained:

$$Nu = 0.171\ (Re)^{0.16}\ (Pr)^{0.336}\ (Vis)^{0.188}(C/D)^{-0.452}$$
$$(P/D)^{-0.235}\ (Nb)^{0.222} \quad \text{-----} \quad 4.29$$

with a correlation coefficient of 0.960 and a mean % error of 8.7% for the following range:

$$Re \leqslant 1.0$$
$$4x10^{2} < Pr < 10^{6}$$

$4x10^{-2} < Vis < 1.0$

$0.0263 < C/D < 0.1637$

$0.5 < P/D < 1.0$

$Nb = 1,2$

$W/D = 0.1$

$h/D = 1.0$

$H/D_T = 1.0$

Fig. 4.29 is a plot of Nu (experimental) vs. Nu (predicted) by equation 4.29 for some of the impellers studied in this work . A straight line of slope 1 is obtained on linear graph paper indicating that equation 4.29 correlates the data adequately well . However, care must be taken in using equation 4.29, to predict the rate of heat transfer at such low Reynolds numbers, because it says nothing about the temperature distributions that might exist in the tank. Equation 4.26 developed in section 4.2, must be used to check that the system is operating above the critical Re. If the calculated Reynolds number is below this critical value, Re_c, impeller speed should be increased till a Reynolds number above Re_c is obtained. Equation 4.29 may then be used if this operating Reynolds number is below about 1.0 . If the operating Reynolds number is above 10, equation 4.28 should be used to predict the heat transfer coefficient. In the transition region, i.e. $1.0 < Re < 10$, no general equation could be obtained to correlate the data as it is . It is, therefore, best to avoid operating

within this range if at all possible. However, in cases, when the Reynolds number falls within the transition range, a simple estimate of the heat transfer coefficient, h_j, may be obtained by taking the average of the results from the two correlations, i.e. equation 4.28 and 4.29 .

(ii) Heat Transfer based on the Penetration Model

A number of investigators (65,78) have attempted to correlate their data at low Reynolds numbers using the penetration theory which is often applied to turbulent scraped surface heat operations. (79)

The basic correlation based on this model may be written in the following form(79):

$$h_j = \left(\frac{2}{\sqrt{\pi}}\right)\sqrt{k\ Cp\ N\ Nb\varrho} \qquad \text{---------- 4.30}$$

and in dimensionless form as;

$$Nu = 1.13\ (Re)^{\frac{1}{2}}\ (Pr)^{\frac{1}{2}}\ (Nb)^{\frac{1}{2}} \qquad \text{--------- 4.31}$$

Compared to equation 4.29, this equation overestimates the heat transfer coefficient by a few hundred percent and as such is of little value for close clearance impellers (79,65) . It is interesting to see that the exponent of the impeller number of blades is about 56%

higher than that developed in this work, i.e. 0.222, see equation 4.29 .

Rautenback (65), on the other hand, modified the simple penetration theory by allowing for a liquid layer between the wall of the vessel and the tip of the stirrer and, thus, developed an equation which in dimensionless form may be written as:

$$Nu = 0.568\ (Re)^{0.23}\ (Pr)^{0.23}\ (Nb)^{0.23}\ (C/D_T)^{-0.54} \quad \text{--------} \quad 4.32$$

The cited paper, unfortunately, gives no detail of the impeller geometry, but from the photograph provided, it seems that their impeller has a P/D = 0.5, W/D = 0.1, h/D = 1.0 . For this system equation 4.29 developed in this work reduces to:

$$Nu = 0.2\ (Re)^{0.16}\ (Pr)^{0.336}\ (Vis)^{0.188}\ (Nb)^{0.222}\ (C/D)^{-0.452} \quad \text{-----} \quad 4.33$$

It is very interesting to see how well the exponent of the impeller number of blades, Nb, obtained in the present analysis compares with the value reported in equation 4.32

by Rautenback (65) . Ignoring the difference between (C/D) and (C/D_T) since the impeller diameters and tank diameters are very close, the exponent of the dimensionless clearance factor, C/D or C/D_T obtained in the present investigation also agrees within 20% of the value reported by Rautenback (65) . The exponent of Re reported by this worker is about 43% higher than that found here, while the exponent of Prandtl number is about 32% lower than the value found experimentally in the present work . These differences, however, tend to cancell each other out and the overall effect is that equation 4.32 reported by Rautenback (65) was found to correlate the heat transfer data in this work to $\pm$20% for Reynolds numbers below about 1.0 and for impellers with P/D = 0.5, W/D = 0.1, h/D = 1.0, and Nb = 1.0 . This is a reasonable fit for engineering purposes and it, therefore, seems as if for Reynolds numbers below about 1.0, dimensionless analysis and the modified penetration theory yields the same results for the impellers tested .

It must, however, be remembered that equation 4.32 gives no information on the temperature distribution in the core region of the vessel and assumes perfect mixing and hence a uniform bulk temperature . Large

temperature gradients may exist in the tank if the operating Reynolds number is below the critical Reynolds number, Re_c, - developed in section 4.2 .

Finally, it is important to note that equation 4.32 should only be used for the impellers it was derived for i.e. P/D = 0.5, Nb = 1,2 . Fot the system with P/D = 1, Nb = 1, equation 4.32 could not correlate the data as it does not differentiate between this system and that with P/D = 0.5 , Nb = 1.0 .

(iii) Heat Transfer based on Conduction Model

Coyle et-al (6) argue that the heat transfer in the viscous range (Re <10) with close clearance impellers is primarily by a mechanism of conduction through a film whose effective thickness is related mainly to the clearance between the impeller tip and the vessel wall . These workers, using both 0.356m and 0.762m diameter tanks with impellers giving 0.0127m clearance approximated the resistance to heat transfer by a static conduction film equal to 0.00635m, or one-half the clearance, C, or:

$$h_j = \frac{k}{(C/2)} \qquad \text{----------} \qquad 4.33$$

Before using equation 4.33 to predict the heat transfer coefficients obtained experimentally in this work it is important to realise that within the operating speed range of 7 to 50 rpm (0.117 to 0.833 rps) used in their work Coyle et-al (6) reported values for h_j varying from 20 to 32.4 $W/m^2\,^oC$ evidencing a slight effect of agitator speed on heat transfer coefficient at low Reynolds numbers .

. Coyle et-al (6) used a clearance of 0.0127m in both 0.356m and 0.762m diameter vessels with impellers having a P/D = 0.5, Nb = 1.0, h/D = 1.0 (His impeller also had a central screw attached to it). Data from the 0.352m, 0.37m and 0.38m and 0.113m diameter impellers obtained in this work was used to check the conduction theory . In order to keep other variables equal, only data for the geometries with P/D = 0.5, Nb =1 (h/D = 1.05) was used to check equation 4.33 . The results are tabulated below:

D(m)	Speed range (rps)	h_j(Coyle) ($W/m^2\,^oC$)	h_j(experimental) ($W/m^2\,^oC$)
0.352	0.039-0.432	13.2	13.8 - 19.5
0.370	0.039-0.378	21.2	14.0 - 21.8
0.380	0.058-0.198	31.8	24.0 - 26
0.113	0.072-0.379	17.2	14.0 - 25.5

Table 4.7

The above table indicates that the conduction mechanism, at best, is only a crude average of the jacket-side film heat transfer coefficient and does not reflect the change in h_j with impeller speed . Impellers with different geometries to that used by Coyle et-al (6), i.e. P/D = 1, Nb = 1, gave results much worse than those in the above table. It is,therefore, concluded here that the mechanism of heat transfer in the viscous range with close clearance impellers is more complicated than the simple conduction through a film near the vessel wall . Results obtained in this work indicate that in the laminar region the heat transfer coefficient is not only strongly affected by the clearance between impeller blade and vessel wall, but also depends on impeller speed and other geometrical factors such as impeller pitch, and number of blades.

(iv) Heat Transfer by Natural Convection

A number of investigators (35,5) have argued that at low Re, the influence of natural convection heat transfer may be of significance and should be taken into consider-ation. There is, however, no published work on natural convection heat transfer to high viscosity fluids in vessels at Prandtl numbers in the range of practical interest to the present problem. It was, therefore, decided to carry out a few steady-state free convection heat transfer experiments in the large mixing tank in

order to see the influence of natural convection upon the overal heat transfer operation . The experimental procedure and technique was very similar to the forced convection runs described before in section 3.3 with the exception that the impeller was stationary . For each fluid, the heat load, Q, was changed at the end of each run and the experiment repeated several times in order to get a series of values of h_j and the appropriate dimensionless Grashof numbers, Gr, and Prandtl numbers, Pr .

The results for all fluids used are shown in Fig. 4.30 where the data is plotted as Nu(Natural) against(GrPr) on log-log paper . Linear regression analysis resulted to the following equation:

$$Nu_{nat.} = 1.41\ (GrPr)^{1/5} \qquad \text{----------} \quad 4.34$$

The exponent of GrPr is 25% lower than the normal value of $\frac{1}{4}$ reported in the literature for flow on simple surfaces (75,67) . The proportionality constant in equation 4.34, i.e. 1.41 , however, is twice the normal value reported in the literature for flow on simple surfaces, but since its exact value depends on factors such as size and shape, it is difficult to put much emphasis on this discrepancy.

Equation 4.34 should be regarded in the light of the few data from which it was derived. It is, however, very interesting to note that for some of the impellers, it predicts values of the jacket-side film heat transfer coefficient, h_j, which are very close to the experimental values under the same operating conditions. For example, for the 0.352m diameter ribbon with P/D = 0.5, Nb = 1.0, and a heat load of about 520W, pure natural convection experiments and equation 4.34 predicts a value of about 13.8 $W/m^2\ ^oC$ for h_j. In the range of speed from 2.3 to 26 rpm the measured heat transfer coefficients vary from 13.6 to 19.5 $W/m^2\ ^oC$, see table 4.7. The measured experimental values of h_j includes contributions from both natural and forced convection and it is clear, from the above analysis, that the natural convection plays a very significant part in heat transfer at low Reynolds numbers and that the total combined heat transfer coefficient approaches this natural convection value as speed decreases to zero.

However, it was not possible, at this stage, to combine the data for natural and forced convection experiments to get a general correlation that accounts for the influence of both of these mechanisms on the jacket side film heat transfer coefficient. This is mainly due to lack of experimental data and could form part of the

research programme for future work .

Finally, the Grashof number, Gr, used in the above analysis was defined as:

$$Gr = \frac{L^3 \rho^2 g \beta \Delta T}{\mu^2}$$

where most of the terms have their usual definition given before in section 2.2.1, except the term L which is a linear dimension defined arbitarily, in the present work, as the height of the liquid in the tank (which is also equal to vessel diameter = 0.4) . The term ΔT is also defined as the bulk fluid to vessel wall temperature.

4.3.2 Anchor Impellers

Heat transfer data for anchor impellers were treated in the same way descibed in section 4.3.1 for helical ribbons.

Compared to helical ribbons, anchor impellers generally give larger temperature variations in the bulk region of the vessel at any impeller speed and for any fluid. The presence of large temperature gradients that existed in the core region of the tank at low impeller speeds made it very difficult to obtain accurate reproducable heat transfer coefficients and hence from a practical design standpoint, only the data for Re greater than 10 could

be used with any degree of confidence .

Furthermore, some of the data obtained during the experimental runs was later found to lie below the critical Reynolds number, Re_c, necessary to ensure complete mixing and hence uniform bulk fluid temperature. The Prandtl numbers and the viscosity correction range covered for the anchor impellers was, therefore, found to be insufficient to place much confidence in exponents of the Prandtl numbers and viscosity correction term that might result from a general regression analysis of the data.

An exponent of 0.333 for the Prandtl number was reported by Uhl (2) and confirmed by others (1,62) for Newtonian and non-Newtonian liquid heat transfer with anchors at low Reynolds numbers. The correlation proposed by Uhl (2) and given in Table 4 is:

$$Nu = 1.0\ (Re)^{0.5}\ (Pr)^{0.333}\ (Vis)^{0.18} \quad \text{-------} \quad 4.35$$

for

$$30 < Re < 300$$

Most investigators also agree with Uhl (2) on the value of the exponent for the viscosity correction term, i.e. 0.18 (1,62,17,18) . It was, therfore, decided to use

these values as exponents of Prandtl number and the viscosity correction term . Graph 4.31 shows a plot of $(Nu/Pr^{0.333}Vis^{0.18})$ against Reynolds number, Re, for all four anchors used in the 0.4m diameter tank. As seen from this plot above a Reynolds number of about 10 (ensuring that Re_c is also exceeded) a separate line is obtained for each anchor indicating the effect of the clearance between the impeller tip and vessel wall on the jacket side film heat transfer coefficient . Fig. 4.32 is a cross plot of Fig. 4.31 and shows the effect of the respective dimensionless clearance factor, C/D, on the heat transfer coefficient. The final correlation using linear regression is:

$$Nu = 0.1\ (Re)^{0.653}\ (Pr)^{0.333}\ (Vis)^{0.18}\ (C/D)^{-0.363} \qquad \text{---------- 4.36}$$

with a correlation coefficient of 0.992 and % mean error of 6.5% and for the following range of variables:

$$10 < Re < 300$$

$$0.0236 < C/D < 0.143$$

$$0.11 < n < 1.0$$

$$W/D = 0.1$$

$$h/D = 1.0$$

$$H/D_T = 1.02$$

One of the most important points about equation 4.36 is that it indicates a decrease in the rate of heat transfer

with increasing clearance between the vessel wall and the anchor tip within the experimental range tested. This result is in contrary to the findings of Uhl (2) and Uhl and Voznik (3) for anchor agitated Newtonian liquids . These workers reported decrease of the rate of heat transfer to a minimum with increasing clearance between the vessel wall and the anchor and then an increase in the rate of heat transfer with further increase in clearance. They also proposed an optimum value of 0.05 to 0.08 for C/D . Within the range of C/D tested in this work, i.e $0.0236 < C/D < 0.143$, no such trend in the rate of heat transfer could be observed. The rate of heat transfer tended to decrease with increase in the clearance between the tank wall and the anchor tip. Nagata (1), however, gave one single correlation for the same Reynolds number range and reported that the clearance factor, C/D, had no effect on heat transfer rate.

Lahaya (92) recently has proposed a correlation for anchor agitated mixing vessels that takes the following for:

$$Nu = 194.8\ (C/D)^{.057}(W/D)^{-.2}(Re)^{.573}(Pr)^{.33}(Vis)^{.34} \qquad 4.37$$

for

$$.01 < C/D_T < 0.0288$$

$0.14 < W/D < 0.208$

$150 < Re < 2000$

This paper provides very little information on the Pr and the viscosity correction term range . Equation 4.37 is the only correlation that suggests an influence of impeller width on heat transfer coefficient. All impellers used in the present investigation had a W/D of 0.1 and as such no comparable correlation could be provided in this work. The exponent of C/D in equation 4.37, is much lower than that obtained in the present investigation but it does show a monotonous trend as found in the present work.

As seen from equation 4.36 proposed from the analysis of the present results and correlations cited by various workers and summarized in Table 4 , there appears to be little agreement between various investigators on the effect of anchor geometries on heat transfer rate. Most published correlations, however, agree on a value of 0.333 for the exponent of Prandtl number and a value of 0.18 for the exponent of the viscosity correction term . Brown (88) is the only worker who claimed a value of 0.25 for the exponent of Prandtl number . He is also among the few workers who claimed a value of 0.14 for the exponent of the viscosity correction term. But there was not a good

variation in the Viscosity correction term, (μ_b/μ_w) in his work .

The exponent of Reynolds number varies between 0.500 to 0.670 . Fig. 4.33 is a plot of $(Nu/Pr^{1/3}Vis^{0.18})$ against Re for most published works . Fig. 4.34 is a plot of $(Nu/Pr^{0.333}Vis^{0.18}(C/D)^{-0.363})$ aganist Re for some of the published work . This latter graph was plotted to see how well equation 4.36 correlates the published data? It is seen from Fig. 4.32 that the larger anchors used in the present investigation, i.e. C/D = 0.0236, 0.0405 give heat transfer rates that are very close to those of Heinlein and Sandall (62) and Gluz and Pavlushenko (63) , For $10 < Re < 100$. Data obtained in this work only extends up to a Reynolds number of about 200, but it is seen from Fig. 4.33 that extraploting the lines for the two larger anchors to Re above 200 produces results that will lie very close to those of Pollard and Kantyka (32) and Martone and Sandall (62) . The correlation reported by Uhl(2) for C/D = 0.054, line 7 in Fig. 4.33, predicts higher heat transfer coefficients than the present work for any value of Re , see also Fig. 4.34 . Uhl is also the only worker who claimed that the rate of heat transfer decreases to a mininimum with increasing clearance between the vessel wall and the anchor tip and then starts to

increase with further increase in clearance . This phenomena could not be substantiated by any other worker except Heinlein and Sandall (62) . They, however, reported that their results could not be conclusive either, due to the relatively large standard deviations in their correlation constants. Nagata (1) and Pollard and Kantyka (32) could not observe any effect of impeller clearance upon heat transfer rate at all and reported a single correlation for all their impellers . The correlation proposed by Nagata, line 10, predicts the highest heat transfer coefficient for any Reynolds number . However, he pointed out that the variations of liquid temperature are significant at low Re and that the temperature at the same location fluctuated with time in the case of some of the anchors. He, therefore, concluded that the proper temperature difference is difficult to determine and the heat transfer correlation is not satisfactory. Nagata (1), hence, says that his correlation between $10 < Re < 200$ is only approximate. It is important to point out that not many workers have paid full attention to these temperature gradients that exist in the core region of the vessel at low Reynolds numbers, particularly for anchors, and this is one reason for the disagreements among various workers and the existence of so many different correlations for this impeller.

For $Re > 200$, the correlation proposed by Nagata(1) also predicts the highest heat transfer coefficients and this may partly be explained by the unusual heating and cooling arrangement used in their experimental rig. In his investigation Nagata (1) used a mixing vessel in which cooling jackets and steam heated jackets were located side by side at 90^{o} intervals (1) . He pointed out that this arrangement would give higher heat transfer coefficients than a uniformly heated or cooled vessel mainly because of the entrance region effect from the insulated to heated parts.

Furthermore, due to the existence of large temperature gradients in the core region of the vessel at Reynolds numbers below the critical vakue, Re_c, (given by equation 4.27 in section 4.22) it was not possible to obtain heat transfer correlations below Reynolds numbers of about 10 . Such large temperature variations have been reported by Nagata (1), Coyle et-al (6), and others (4,17) and this is one reason why no correlation exists for the rate of heat transfer in anchor agitated systems for Re below about 10 . However, the limited data obtained in the range of Reynolds number between 1.0 and 10 , see Fig. 4.31, indicates that in this range the dependency of the heat transfer coefficient on Re and hence impeller speed decreases rapidly. A very

approximate value of 1.5 for the term ($Nu/Pr^{0.333}Vis^{0.18}$) is obtained from Fig. 4.31 for $1.0 < Re < 10$. For Silicone oil, this gives a value of about 30 $W/m^2\ ^oC$ for the jacket-side film heat transfer coefficient which is still 2.3 times the value predicted using the conduction mechanism proposed by Coyle et-al and discussed in section 4.3.1(iii).

Finally, equation 4.35 has the same drawback as equation 4.29 developed in section 4.3.1(i) for helical ribbons in that it says nothing about the temperature variations that might exist in the tank during the heat transfer operation. Equation 4.27 developed in section 4.2 must be used to check that the system is operating above the critical Re. If the calculated Reynolds number is below this critical value, $\overline{Re_c}$, impeller speed should be increased till a Reynolds number above Re_c is obtained. Equation 4.35 may then be used if this operating Reynolds number is below about 10. Equation 4.35 can safely be extraplotted to Reynolds numbers higher than 300 as it predicts similar heat transfer values to those of Uhl(2) and others (32,62), see Fig. 4.33. As discussed above, equation 4.35 should not be extraplotted to Reynolds numbers below about 10 since it will greatly underestimate the value of the jacket side heat transfer coefficient. Helical ribbon impellers are recommended in this region as they give better uniformity in temperature of the bulk fluid at low Re, see section 4.2.

4.4 Heat Transfer and Associated Power Consumption

Very few investigators have studied combined heat transfer and power consumption of close clearance impellers. It would be useful from a practical standpoint to present correlations based on power consumption in order to find the optimum geometry of the vessel and impeller to give the maximum effects for minimum power consumption. Furthermore, many of viscous liquids exhibit a highly temperature sensitive viscosity and, thus, the power requirement in the laminar and transitional regions will be affected strongly by viscosity variations near the wall.

Askew and Beckmann(58), Calderbank and Moo-Young(93) and Uhl(2) have reported empirical correlations for average heat transfer in terms of power per unit volume. Hiraoka et-al (94), recently, derived a correlation for heat transfer using the power consumption per unit volume from the consideration of the analogies . Also, recently, Samo et-al (95) measured local and mean heat transfer coefficients in mixing vessels and presented heat transfer data in terms of dimensionless power per unit volume. Using dimensional analysis they proposed that:

$$\left(\frac{hD_T}{k}\right) = f\left[\frac{\varepsilon D^4}{\nu^3}\ ,\ \text{Pr, Vis, } \begin{matrix}\text{dimensionless}\\ \text{geometrical factors}\end{matrix}\right] \qquad \text{---------- 4.38}$$

where the only symbols that need explaining are given from the power consumption of the impeller:

$$\varepsilon = \frac{P}{\frac{\pi}{4} D^2 H \rho} \qquad \text{---------- 4.39}$$

and

ν = kinematic viscosity.

Using heat transfer data they obtained the following correlation for turbulent heat transfer coefficient for open impellers:

$$\left(\frac{hD_T}{k}\right) = 0.512 \left(\frac{\varepsilon D^4}{\nu^3}\right)^{23} (Pr^{1/3}) (D/D_T)^{0.52} (W/D)^{0.08}$$

---------- 4.40

The relationship between $(\varepsilon D^4/\nu^3)$ and the conventional Reynolds number, Re ($ND^2/$) is (95)

$$(\varepsilon D^4/\nu^3) = K (\rho ND^2/\mu)^3 (P/\rho N^3 D^5) \qquad \text{---------} \quad 4.41$$

where K contains parameters involving the shape of the apparatus .

Assuming the exponent of the Prandtl number, viscosity correction term and all the other dimensionless geometrical factors are the same as in equation 4.29 obtained in

section 4.3.1(i), for helical ribbons in the range $Re < 1.0$, the data was treated by plotting $\left(\varepsilon D^4/\nu^3\right)$ against

$$\frac{Nu}{Pr^{0.333} Vis^{0.188} (C/D)^{-0.452} (P/D)^{-0.235} (Nb)^{0.222}}$$

shown in Fig. 4.35 for some of the impellers used in this work. The data was analysed using linear regression and the following empirical correlation was obtained:

$$\left(\frac{hD_T}{k}\right) = 0.113 \left(\varepsilon D^4/\nu^3\right)^{0.074} (Pr)^{0.333} (Vis)^{0.188} (C/D)^{-0.452} (P/D)^{-0.235} (Nb)^{0.222} \qquad 4.42$$

with a correlation coefficient of 0.895 and % mean error of 12% .

Equation 4.42 is in effect an alternative form of equation 4.29 obtained in section 4.3.1(i), with the dimensionless group, $\varepsilon D^4/\nu^3$), used in the correlation of the jacket side film heat transfer coefficient rather than Re . In order to obtain the value of $\left(\varepsilon D^4/\nu^3\right)$ for a given Re, the power number P_o is, of course, needed. in the present investigation torque was measured during the heat transfer runs and provided the mean bulk temperature, T_b,

is used to evaluate fluid physical properties such as viscosity and density, the isothermal power curve was found to correlate the power data during heat transfer runs. For any Re, the power number, P_o, tended to lie above the best straight line obtained for the isothermal conditions but the effect remained well within the data scatter .

Therefore, to evaluate $(\varepsilon D^4/\nu^3)$ for a given Re, the power number was obtained from the experimental equation for the particular impeller, i.e.

$$P_o = K_p (Re)^{-1} \quad \text{----------} \quad 4.43$$

where the value of K_p depends on the impeller geometry and given in Table 4.4, section 4.1.2 . Substituting for P_o from equation 4.43 into equation 4.41:

$$(\varepsilon D^4/\nu^3) = K (Re)^3 (K_p Re^{-1}) \quad \text{----------} \quad 4.44$$

i.e.

$$(\varepsilon D^4/\nu^3) \propto Re^2 \quad \text{----------} \quad 4.45$$

But from equation 4.42 :

$$Nu \propto (\varepsilon D^4/\nu^3)^{0.074} \quad \text{----------} \quad 4.46$$

i.e.

$$Nu \propto (Re^2)^{0.074} \qquad \text{----------} \quad 4.47$$

Therefore

$$Nu \propto (Re)^{0.148} \qquad \text{----------} \quad 4.48$$

Therefore equation 4.48 predicts that the Nusselt number should be proportional to Reynolds number raised to the power 0.148 . Equation 4.29 obtained in section 4.3.1(i) has a value of 0.16 for the exponent of Re for the same Reynolds number range.

The limited data obtained in the range $20 < Re < 600$ was treated similarly for all ribbons by plotting $(\varepsilon D^4/\sqrt{}^3)$ against $(Nu/Pr^{0.336}\ Vis^{0.18})$ as shown in Fig. 4.36 . Linear regression analysis yielded the following equation:

$$Nu = 0.596\ (\varepsilon D^4/\sqrt{}^3)^{0.163}\ (Pr)^{0.333}\ (Vis)^{0.18} \qquad \text{----------} \quad 4.49$$

with a correlation coefficient of 0.925 and mean % error of 6.95% . Equation 4.49, however, should be regarded in the light of the few data used in its derivation and should only be used as a guide for design.

The data for anchor impellers was treated in exactly

the same way by plotting $(Nu/Pr^{0.333}_{vis}{}^{0.18}_{(C/D)}{}^{-0.363})$ against $(\varepsilon D^4/\nu^3)$ on log-log paper as shown in Fig. 4.37 . Linear regression analysis gave the following equation:

$$Nu = 0.207\ (\varepsilon D^4/\nu^3)^{0.158}\ (Pr)^{0.333}\ (Vis)^{0.18}\ (C/D)^{-0.363} \quad \text{---------- 4.50}$$

with a correlation coefficient of 0.841 and % mean error of 4.5% and for the following range:

$$20 < Re < 600$$

$$0.0236 < C/D < 0.143$$

$$0.11 < n < 1.0$$

$$W/D = 0.1$$

$$h/D = 1.0$$

$$H/D_T = 1.02$$

The data below Re about 10 could not be treated in the same way, as explained previously in section 4.3.2, due to lack of sufficient data in this region. There was also too much scatter in the limited data obtained in this region to make any generalisation accurate.

Fig. 4.38 is a plot of $(Nu/Pr^{0.333}\ Vis^{0.18})$ against $(\varepsilon D^4/\nu^3)$ for the helical ribbons, equation 4.49, and

for the 0.382m diameter anchor impeller, equation 4.50, for the Reynolds number in the range $20 < Re < 600$. It is interesting to note from Fig. 4.38 that within the practical range of C/D, i.e. $0.05 < C/D < 0.08$, the anchor impellers are about as satisfactory as the helical ribbons for heat transfer operations (in the Re range $20 < Re < 600$). Therefore, generally it is not the power input required but other considerations such as the cost of the impeller and the range in which an impeller is effective, in for example leveling out temperature variations in the bulk region of the tank, which would determine the choice of an impeller for the application of heat transfer to jackets. Uhl (2) comparing anchors with open impellers such as turbines and propellers arrived at a similar conclusion. However, he plotted the horse power, P, against $(Nu/Pr^{0.333} Vis^{0.18})$ and obtained a separate line for each fluid. His results, therefore, could not be used for design purposes.

CHAPTER 5

CONCLUSIONS AND RECOMMENDATIONS

Isothermal power input data, temperature profiles, heat transfer and combined power input and heat transfer rates were measured for a series of ribbon and anchor impellers in a 0.4m and a 0.15m diameter jacketed vessel. Several viscous Newtonian and non-Newtonian liquids were used. The results obtained were correlated in dimensionless form to permit comparison between fluids and to assist in comparing with previously published correlations.

5.1 Isothermal Power Data

The isothermal power data obtained in this work were combined with data extracted from literature and using linear regression analysis the following empirical correlations were obtained:

$$P_o = 85\ (C/D_T)^{-0.314}(h/D)^{0.476}\ Re^{-1} \qquad \text{-------5.1}$$

for anchors and for the following range of variables;

$0.01 < Re < 100$

$0.01 < C/D < 0.133$

$0.1 < h/D < 1.0$

$0.05 < W/D < 1.4$

$0.32 < H/D_T < 1.5$

and

$$P_o = 150\ (C/D)^{-0.2774}(P/D)^{-0.5332}(h/D)(W/D)^{0.325}$$

$$(Nb)^{0.54}\ Re^{-1} \qquad \text{----- 5.2}$$

for helical ribbons in the range

$0.001 < Re < 100$

$0.006 < C/D < 0.1637$

$0.35 < P/D < 1.75$

$0.08 < W/D < 0.167$

$0.85 < h/D < 1.27$

$1.0 < H/D_T < 1.36$

$1.0 < Nb < 4.0$

Equations 5.1 and 5.2 were found to predict the power requirements in this study as well as most of the published work with an accuracy of $\pm$7% and $\pm$8.6% respectively(these are %mean errors).

The present study also confirms the applicability of Metzner and Otto(12) technique to obtain the impeller shear rate constants, k_s, for non-Newtonian fluids. However, the value of the impeller shear rate constant, k_s, was found to depend strongly on the clearance between impeller blade and vessel wall. For helical ribbon impellers,other geometrical parameters such as pitch or number of blades were found to have a negligible effect on the value of k_s.

The values of the impeller shear rate constant, k_s, was also found to be essentially independent of fluid reheological properties.

The results obtained in this work were combined with extracted data from the literature and the following correlations were obtained using regression analysis:

$$k_s = 33 - 172.5\ (C/D_T) \quad \text{----------} \quad 5.3$$

for anchor impellers

and

$$k_s = 34 - 114\ (C/D) \quad \text{----------} \quad 5.4$$

for ribbons.

Equations 5.3 and 5.4 predicted the values of the impeller shear rate constant, k_s, obtained in this work and most of those extracted from the literature with an average accuracy of $\pm$ 8.3% and 9.4% respectively.

5.2 Temperature Profiles.

Measurements of temperature profiles in the tank at low Reynolds numbers led to correlations for the evaluations of critical Reynolds numbers, Re_c, for both helical ribbon

and anchor impellers. It was observed that below this critical Reynolds number, Re_c, large temperature gradients existed in the core region of the tank regardless of impeller type.

For helical ribbons, impeller geometry was found to have a significant influence on the ability of the agitator to level out these temperature variations, see Fig. 4.16 . Analysis of the limited data obtained in this work resulted in the following correlations for ribbon impellers:

$$Re_c = 1.84 \times 10^{8} (P/D)^{0.428} (C/D)^{1.261} (Nb)^{-1.42} \; Pr^{-1.3} \qquad \text{---------- 5.5}$$

for the following range of variables;

$0.1 < Re_c < 250$

$10^2 < Pr < 10^6$

$0.0263 < C/D < 0.068$

$0.5 < P/D < 1.0$

$Nb = 1,2$

$W/D = 0.1$

$h/D = 1.0$

$H/D_T = 1.05$

For anchor impellers, experimental data revealed that anchor geometry had little effect on the critical Reynolds number, Re_c, but it must be emphasised that only the effect of clearance between impeller tip and vessel wall was tested. Analysis of the limited data obtained in this work resulted in a correlation of the form:

$$Re_c = 5 \times 10^5 \, Pr^{-1} \quad \text{----------} \quad 5.6$$

Both equations 5.5 and 5.6 are based on only a limited data and the values of the constants in these equations should be regarded in this light. However, they are the only correlations published to date that give some indication on the general ablity of close-clearance impellers to level out temperature gradients at low Reynolds numbers. They give some indication on the critical Reynolds numbers below which a particular impeller should not be operated.

5.3 Heat Transfer Data

The experimental heat transfer data for both Newtonian and non-Newtonian fluids measured in the 0.4m diameter and the 0.15m diameter vessel were combined with the results extracted from the literature which resulted to the following equations:

(i) $10 < Re < 10^3$

$$Nu = 0.45\ (Re)^{0.598}(Pr)^{0.336}(Vis)^{0.188} \quad \text{---- 5.7}$$

(ii) $Re < 1.0$

$$Nu = 0.171\ (Re)^{0.16}(Pr)^{0.336}(Vis)^{0.188}(C/D)^{-0.452}$$

$$(P/D)^{-0.235}(Nb)^{0.222} \quad \text{----- 5.8}$$

for helical ribbons and

$$Nu = 0.1\ (Re)^{0.653}(Pr)^{0.333}(Vis)^{0.18}(C/D)^{-0.363}$$

$$\text{---------- 5.9}$$

for anchor.

Full details of the variables covered are given in Chapter 4.

Heat transfer data obtained in this study was critically compared with published work. From a practical design standpoint, equations 5.7 to 5.9 are the only correlations which one can use with any degree of confidence.

Equation 5.7 indicates that in the range of Reynolds number, $10 < Re < 10^3$, impeller geometry has little effect on heat transfer, while for $Re < 1.0$, equation 5.8 shows that agitator geometry has a marked effect on the rate of heat transfer through the jacket. Notice that equation

5.8 was derived for W/D = 0.1, and H/D_T= 1.0 and if there is any influence of impeller width, W, or liquid height, H, on heat transfer rates, equation 5.8 does not reflect this. It should, therefore,be used ribbons having W/D = 0.1 and H/D_T = 1.0

5.4 Heat Transfer and Associated Power Data

Power input measurements were carried out during some of the heat transfer runs. Results indicated that provided the mean bulk temperature, T_b, is used to evaluate fluid physical properties such as viscosity and density, the isothermal power curve was found to correlate the power data during heat transfer runs. For any Re the power number, P_o, tended to lie above the best straight line obtained for the isothermal conditions but the effect remained well within the experimental scatter.

The heat transfer data and its associated power inputs were treated and the following empirical correlations were obtained:

(a) helical ribbons;

(i) $10 < Re < 10^3$

$$(hD_T/k) = 0.596\ (\varepsilon D^4/\nu^3)^{0.163}(Pr)^{0.333}(Vis)^{0.18} \qquad \text{---------} \quad 5.10$$

(ii) Re 1.0

$$(hD_T/k) = 0.113\ (\varepsilon D^4/\nu^3)^{0.074}(Pr)^{0.333}(Vis)^{0.188}$$
$$(C/D)^{-0.452}(P/D)^{-0.235}(Nb)^{0.222}$$

---------- 5.11

(b) anchor impellers

$$(hD_T/k) = 0.207\ (\varepsilon D^4/\nu^3)^{0.158}(Pr)^{0.333}(Vis)^{0.18}$$
$$(C/D)^{-0.363}$$ ---------- 5.12

The main point about equations 5.10 to 5.12 is that they offer an easy comparison between different types of impellers. This is important since in any design, it is advantagous to obtain the optimum geometry of the vessel and impeller to give the maximum effect for minimum power consumption.

Equation 5.10 for helical ribbons was plotted against equation 5.12 for a typical anchor (C/D =0.0268), see Fig. 4.38. The results indicated that within the practical range of C/D , i.e. $0.05 < C/D < 0.08$, the anchor impellers are about as satisfactory,at the same power input,as the helical ribbons for heat transfer operations(in the Re range $20 < Re < 600$) . Therefore , generally it is not the

power input required but other considerations such as the cost of the impeller and the range in which an impeller is effective, in for example leveling out temperature variations in the bulk region of the tank, which would determine the choice of an impeller for the application of heat transfer to jackets.

5.5 Recommendations

As a result of this study the following recommendations for future research programmes are made:

(i) The values of the constants in equations 5.5 and 5.6, developed for the evaluation of the critical Reynolds numbers, should be regarded in the light of relatively few data used in their derivation. Extensive work should be carried out with a number of both viscous Newtonian and non-Newtonian fluids with widely different physical and thermal properties, to confirm the values of the constants in equations 5.5 and 5.6. Additional work is also needed for both helical ribbons and anchors in order to confirm the dependency of the critical Reynolds number, Re_c, on impeller geometry.

(ii) Additional work is needed in the true laminar region (Re < 1.0) to determine the proper correlating method. In particular, extensive tests should be carried out to establish the influence and the contribution of natural convection to heat transfer at low Reynolds numbers. Tests should be conducted with a number of viscous Newtonian and non-Newtonian materials to establish the controlling parameters in both natural and forced convection regions. Suggestions have been made in this work with regard to these controlling parameters but much more data is needed to confirm these.

NOTATION

A = Inside/Outside area of the vessel(m^2).

also = Constant in equation 2.4

a = Constant given by equations 2.22 & 2.23 .

B = Constant in equation 2.16 and given by equations 2.18 & 2.19 .

C = Clearance between impeller tip and vessel wall (m) .

C_p = Liquid specific heat (J/kg ^oC) .

C_1, C_2 = Constants in equation 3.17

D = Impeller diameter (m)

D_T = Vessel diameter (m)

f = function in equations 2.2 & 2.83 .

g =Acceleration due to gravity (m/s^2) .

h = Impeller height (m) .

H = Liquid height in the tank (m) .

h_j = Jacket-side film heat transfer coefficient (W/m^2 ^oC) .

h_c = Coolant-liquid film heat transfer coefficient (W/m^2 ^oC) .

I = Current (A) .

k, k_1 = Liquid thermal conductivity (W/m ^oC) .

k_g = Thermal conductivity of glass in equation 3.4 (W/m ^oC) .

k_s = Impeller shear rate constant .

K_p = Constant in equation 2.4 .

K = Consistancy index (kg/m s^{2-n}) .

L = Length of wire in equation 3.4 (m)

M = Coolant liquid flow rate (kg/s) .

n = Flow behaviour index for power law fluids .

N, N_c = Impeller speed (rps) .

Nb = Impeller number of blades .

P = Power input (W) .

Q = Rate of thermal energy flow across a surface (W) .

R_i = Inner radius of glass tube (m) in equation 3.4 .

R_F = Filament radius (m) in equation 3.4

R_o = Outer radius of glass tube (m) in equation 3.4 .

T = Torque on impeller shaft (Nm) .

T_F = Filament temperature (^oC) , equation 3.4 .

T_i = Temperature of inner glass surface (^oC) , equation 3.4

T_b = Bulk fluid temperature in the tank (^oC).

T_w = Vessel wall temperature (^oC) .

U = Overall heat transfer coefficient ($W/m^2\ ^oC$) .

V = Voltage (V) .

W = Impeller Width (m) .

x = Vessel wall thickness (m) .

Y_b = Resistance at bulk temperature (^oC) in equation 3.4 (Ω)

Y_F = Resistance at filament temperature (^oC) in equation 3.4 : (Ω) .

Greek letters

β = Coefficient of thermal expansion ($/^{o}C$) .

$\dot{\gamma}$, du/dy = Shear rate (s^{-1})

μ_A = Average apparent viscosity (kg/ms) .

μ_b = Viscosity at bulk temperature (kg/ms) .

μ_p = Plastic viscosity (kg/ms) .

μ_w = Viscosity at vessel wall temperature (kg/ms) .

ρ = Liquid density (kg/m^3) .

τ = Shear stress ($dyne/cm^2$) .

τ_y = Yield stress ($dyne/cm^2$) .

ν = Kinematic viscosity

ε = Power input/ Vessel volume [$P/(\pi/4)\ D^2H\rho$].

Dimensionless Groups

Re = Reynolds number $(\rho ND^2/\mu)$.

Re_c = Critical Reynolds number $(\rho N_c D^2/\mu)$.

Fr = Froude number (N^2D/g) .

P_o = Power number $(P/\rho N^3D^5)$.

Nu = Nusselt number $(h_j D_T/k)$.

Pr = Prandtl number $(Cp\,\mu/k)$.

Gr = Grashof number $(g\ D^3\ \beta\ \Delta T\ \rho^2/\mu^2)$.

Vis. = Viscosity ratio (μ_b/μ_w) .

$(\varepsilon D^4/\nu^3)$ = Power input per unit volume .

BIBLIOGRAPHY

1.. Nagata, "Mixing: Principles and applications", 1975 (John Wiley & Sns).

2. Uhl, V.W., "Heat Transfer to Viscous Materials in Jacketed Agitated Kettles", Chem. Engng. Progress, Symposium Series, Vol. 51, No.17, 1955, pp. 93-108 .

3. Uhl, V.W. and Voznick, H.P., "The Anchor Agitator", Chem. Engng. Progress, Vol.56, No.3, March 1960, pp. 72-77 .

4. Zlokarnik, M. "Heat tansfer at the inside wall of a stirred tank when cooling and heating in the range of Reynolds numbers from 0.5 to 10^5", Chemie Ingenieur Technik, Vol.41, No.22, 1969, pp. 1195-1202 .

5. Camurdan, M.C., "Laminar Heat Transfer in Agitated Vessels", M.Sc. Dissertation, University of Bradford, 1976 .

6. Coyle, C.K., Hirschland, H.E., Michel, B.J., and Oldshue, J.Y., "Heat Transfer to Jackets with Close Clearance Impellers in Viscous Materials", Can. J. Chem Engng., Vol. 48, 1970, pp. 275 .

7. Gray, J.B.,"Batch Mixing of Viscous Liquids", Chem. Engng. Prog., Vol. 59, No. 3, March. 1963, pp. 55-59 .

8. Hoogendoorn, C.J. and Den Hartog, A.P.," Model studies on mixers in the viscous flow region", Chem. Engng. Sci., Vol. 22, 1967, pp. 1689-1699 .

9. Edwards, M.F., and Wilkinson , W.L., "Heat Transfer in Agitated Vessels" Part I - Newtonian Fluids, The Chemical Engineer, Aug. 1972, pp. 310-329 .

10 i b.i d , Part II Non-Newtonian Fluids, The Chemical Engineer, Sept. 1972, pp.328-335

11. Kappel, M. "Development and application of a method for measuring the mixture quality of miscible liquids", III. Application of the new method for highly viscous Newtonian liquids, Inter. Chem. Engng., Vol. 19, No. 4, Oct. 1979, pp. 571-590 .

12. Metzner, A.B., and Otto, R.E., A.I. Chem. Engng. J., Vol. 3, No. 3, 1957 .

13. Magnusson, K., IVA, Vol. 23, No. 2, 1952, pp. 86 - 99 (Sweden) .

14. Peters, D.C. and Smith, J.M., Can. J. Chem. Eng., Vol. 47, 1969, pp. 268 .

15. Bourne,J.R. and Butler, H. "Power Consumption of Helical Ribbon Impellers in viscous Liquids", Trans. Instn. Chem. Engrs., Vol. 47, 1969, pp. T263-270 .

16. Birds, R.B., Stewart, W.E. and Lightfoot, E.N. "Transport Phenomena", 1960 (Hohn Wiley & Sons, Inc.) .

17. Gluz, M.D., and Pavlushenko, I.S., "Experimental Investigation of Heat Transfer during Stirring of Non-Newtonian Liquids," Journal of Applied Chemistry, USSR, Vol. 39, 1966, pp. 2323-2330 .

18. Hagedorn, D., and Salamone, J.J., "Batch Heat Transfer Coefficients for Pseudoplastic Fluids in Agitated Vessels," I & E C Process Design & Development, Vol. 6, No. 4, Oct. 1967, pp. 469-475 .

19. Skelland, A.H.P., "Non-Newtonian Flow and Heat Transfer", 1967, (New York: John Wiley & Sons Inc.) .

20. Calderbank, P.H. and Moo-Young, M.B., "The Power Characteristics of Agitators for the Mixing of Newtonian and Non-Newtonian Fluids ", Trans. Instn. Chem. Engrs, Vol. 39, 1961, pp. 337-347 .

21. Beckner, J.L. and Smith, J.M., "Anchor-Agitated Systems: Power input with Newtonian and Non-Newtonian Pseudoplastic fluids", Trans, Instn Chem. Engrs., Vol. 44, 1966, pp. T224-236 .

22. Kashani, M.M., "Mixing of Thixotropic Liquids", M.Sc. thesis, Bradford University, Aug. 1975 .

23. Hall, K.R. and Godfrey, J.C., "Power Consumption by Helical Ribbon Impellers", Trans. Instn. Chem. Engrs., Vol. 48, 1970, pp. T201-208 .

24. Mitsuishi, N. and Miyairi, Y.,"Heat Transfer to Non-Newtonian Fluids in An Agitated Vessel", J. Chem. Engng. Japan , Vol. 6, No. 5, 1973. pp. 415-420 .

25. Carreau, P.J., Patterson, W.I., and Yap. C.Y., "Mixing with Helical Ribbon Agitators", AIChE Journal, Vol. 25, No. 3, May 1979, pp. 508-521 .

26. Mitsuishi,N. and Hirai, N. " Power Requirements in the Agitation of Non-Newtonian Fluids", J. Chem. Engng, Japan, Vol. 2, No. 2 , 1969, pp.217-224 .

27. Kelkar, J.V., Mashelkar, R.A., and Ulbrecht, J., "On the Rotational Viscoelastic Flows Around Simple Bodies and Agitators", Trans. Instn Chem. Engrs., Vol. 5, No. 4, Oct. 1972, pp.343-352 .

28. Foresti, R. and Liu, T.,"Agitation of Non-Newtonian Liquids", Industrial & Eng. Chemistry, Vol. 51, No. 7, July 1959, pp.860-864 .

29. Schilo, D., Chemie Ing. Techn., Vol. 41, No. 5+6, 1969, pp.253- 259 (German)

30. Ullrich, H., and Schreiber, H. , Chemie Ing, Techn., Vol. 39, No. 5/6, 1967, pp. 218 -224 (German)

31. Chavan, V.V., and Ulbrecht, J. "Power correlation for helical ribbon impellers in inelastic non-Newtonian fluids", Chem. Eng. Journal, Vol. 3, 1972, pp.308-311 .

32. Pollard, J. and Kantyka, T.A., "Heat Transfer to Agitated non-Newtonian Fluids", Trans. Instn Chem. Engrs., Vol. 47, 1969, pp. T21 -26 .

33. Reher, E.O. and Bohm, R., Chem. Techn., Vol. 22, No. 3, March 1970, pp. 136-140 (German) .

34. Penney, W.R. and Bell, K.J., "Close Clearance Agitators", 1 Power Requirements, Indust. & Eng. Chem., Vol. 59, No. 4, 1967, pp. 40-54 .

35. ib.id 2 Heat Transfer Coefficients, Indust. & Eng. Chem., Vol. 59, No. 4, April 1967, pp. 47-54

36. Nagata, S. et-al, "Mixing of highly viscous non-Newtonian liquids", Intn. Chem. Engng., Vol 12, No.1 Jan. 1972, pp. 175-182

37. Nagata, S. et-al, "Power Consumption of Mixing Impellers in Pseudoplastic Liquids", J. Chem. Eng. Japan, Vol. 4, No. 1, 1971, pp. 72-76 .

38. Nagata, S. et-al, "Power consumption of Mixing Impellers in Bingham Plastic Liquids", J. Chem. Eng. Japan, Vol. 3, No. 2, 1970, pp. 237-243 .

39. Penney, W.R.and Bell, K.J. " Heat Transfer in a thermal processor agitated with a fixed clearance, thin, flat blade", Chem. Engng., Progress Symposium Series, Vol. 65, No. 92, pp. 1-11 .

40. Ho, F.C., and Kwong, A., " A Guide to Designing Special Agitators ", Chem. Eng. July 1973, pp. 94-104 .

41. Johnson, R.T.,"Batch Mixing of Viscous Liquids", I & E C Process Design & Dev., Vol. 6, No. 3, July 1967, pp. 340-345 .

42. Bourne, J.R., and Butler, H., "An Analysis of the Flow produced by Helical Ribbon Impellers", Trans. Instn Chem. Engrs., Vol. 47, 1969, pp. T11-T17 .

43. Chavan, V.V., And Ulbrecht, J.,"Power Correlation for Close Clearance Helical Impellers in Non-Newtonian Liquids", I & E C Process Des. & Develop., Vol. 12, No. 4, 1973, pp. 472 .

44. Bourne, J.R., Knoepfli, W., and Riesen, R., "Batch and Continous Blending of Newtonian Fluids using Helical Ribbon Impellers", BHRA, 3rd European Conference on Mixing, York, England, April 1979.

45. Kappel, M., and Seibring, Verfahrenstechnik, Vol. 4, 1970, pp. 10 (German) .

46. Kappel, M. et-al , Chemie Ing. Techn., Vol 47, No. 23, 1975, pp. 953-963 (German) .

47. Brauer, H., and Schmidt-Traub, H., Chemie. Eng. Techn., Vol. 44, No. 21, 1972, pp. 1237-1240 (German) .

48. Blasinski, H., and Rzyski, E.,"Power requirements of helical ribbon impellers", The Chem. Engng. J., Vol. 19, 1980, pp. 157-160 .

49. Holland, F.A. and Chapman, F.S.,"Liquid Mixing and Processing in Stirred Tanks", 1966 (New York: Reinhold Publications Inc.) .

50. Sterbacek, Z. and Tausk, P. "Mixing in the Chemical Industry", 1965, (Oxford: Pergamon Press) .

51 E.E.U.A. "Agitator Selection and Design", 1963, (London: Constable & Co.) .

52. Sieder, E.N., and Tate, G.E. " Heat Transfer and Pressure Drop of Liquids in Tubes", Indust. & Eng. Chem., Vol. 28, No. 12,1936, pp.1429-1434 .

53. Chilton, H. and Drew, B., "Heat Transfer Coefficients in Agitated Vessels", Indust. & Eng. Chem., Vol. 36, No. 6, June 1944, pp. 510-516 .

54. Kapustin, A.S., International Chemical Engineering, Vol. 3, 1963, pp. 514.

55. Pursell, H.P., M.Sc. Thesis, 1954, Newark College of Engineering, New Jersey.

56. Akse, H., Beek, W.J., Van Berkel, F.C.A., and DeGraauw, J., Chem. Engng. Sci., Vol. 22, 1967, pp. 135 .

57. Gordon, M., M.Sc. Thesis, 1941, University of Minnesota, Minneapolis .

58. Askew, W.S. and Beckmann, R.B., Ind. Engng. Chem., Proc. Des. & Dev., Vol. 4, 1965, pp. 311 .

59. Oldshue, J.Y. and Gretton, A.T., "helical coil heat transfer in mixing vessels", Chem. Engng. Progress, Vol. 50, No. 12, Dec. 1954, pp. 615-621 .

60. Research Results, Ind. & Eng. Chemistry, Vol. 54, 1962, pp. 100 .

61. Uhl, V.W. and Gray, J.B. "Mixing: Theory and Practice", 1966, Vol. 1 (New York: Academic Press Inc.) .

62. Heinlein, H.W. and Sandall, O.C. "Low Reynolds Number Heat Transfer to Non-Newtonian Fluids in Anchor-Agitated Vessels", Ind. Eng. Chem. Process Des. & Develop., Vol. 11, No. 4, 1972, pp. 490-495 .

63. Gluz, M.D., and Pavlushenko, I.S. " Dimensionless Equations for Heat Transfer Processes During Mixing of Non-Newtonian Liquids", Journal of Applied Chemistry, USSR, Vol. 39, No. 10, Oct.1966, pp.2288-2295 .

64. Uhl, V.W. "Mechanically Aided Heat Transfer To Viscous Materials", American Soc. Mech. Engrs., Winter annual meeting, Dec. 1970, pp. 109-117 .

65. Rautenbach, R. and Bollenrath, F.M. " Heat Transfer in Stirred Vessels to High-Viscosity Newtonian and non-Newtonian Substances", Germ. Chem. Eng., Vol. 2. 1979, pp. 18-24 .

66. Hiraoka, S. and Ito, R. "On the Relation of Power input and Transport Phenomena at the Wall of Agitated Vessels", J. Chem. Eng. Japan., Vol. 6, No. 5, 1973, pp. 464-467 .

67. Fujii, T. and Uehara, H.,"Laminar Natural Convection Heat Transfer from the Outer Surface of a Vertical Wall", Int. J. Heat & Mass Transfer, Vol.13, 1970, pp. 607-615 .

68. Tien, C., "Laminar Natural Convection Heat Transfer from Vertical - Plate to Power-law Fluid", Appl. Sci. Res., vol. 17, pp. 233-248 .

69. Fand, R.M., and Morris, M. and Lum, M.," Natural convection heat transfer from horizontal cylinders to air, water and Silicone oils for Rayleigh numbers between $3x10^2$ and $2x10^7$", Int. J. Heat & Mass Transfer, Vol. 20, 1977, pp. 1173-1184 .

70. Bell, S.A. and Hudson, J.L. " An experimental study of centrifugally driven free convection in a rectangular cavity", Int. J. Heat & Mass Transfer, Vol. 18, 1975, pp. 1415-1423 .

71. Soehngen, E.E. " Experimental studies on Heat Transfer at very High Prandtl Numbers", paper presented at the III All Union Conference on Heat and Mass Transfer, Minsk, USSR, 1968.

72. Tien, C., Reilly, I.G. and Adelman, M., "Experimental study of natural convective heat transfer from a vertical plate in a non-Newtonian fluid", The Can. J. Chem. Engng., Aug. 1965, pp. 157-160 .

73. Churchill, S.W. and Chu, H.H.S. " Correlating equations for laminar and turbulent free convection from a vertical plate", Int. J. Heat & Mass Transfer, Vol. 18, 1975, pp. 1323-1329 .

74. LeFevre, E.J. and Ede, E.J. "Laminar free convection from the Outer Surface of a Vertical Circular Cylinder," Brit. Dept. of Sci. Ind. Res. Paper 114, 1956 .

75. Acrivos, A. "On the combined effect of forced and free convection heat transfer in laminar boundary flows", Chem. Engng. Sci., Vol. 21, 1966, pp. 343-352 .

76. Lorenz, H., Z. Tech. Phys., No. 9, 1934 (German) .

77. Gryzagoridis, J. "Combined free and forced convection from an isothermal vertiwal plate", Int. J.H eat & Mass Transfer, Vol. 18, 1975, pp. 911-916.

78. Uhl, V.W. "Mechanically Aided Heat Transfer in High Viscosity Mixing", Chem. Engng. Progress Symposium series, Vol. 65, No.92, pp. 12-19 .

79. Harriott, P. " Heat Transfer in Scraped-Surface Exchangers", Chem. Engng. Progress Symposium Series, Vol. 55, No. 29, pp. 137-139..

80. Cummings, G.H and West, A.S. " Heat Transfer Data for Kettles with Jackets and Coils", Indust. & Engng. Chem., Vol. 42, No. 11, 1950, pp. 2303-2313 .

81. Brooks, G. and Su, G.J. , Chem. Engng. Progress, Vol. 55, 1959 , pp. 54.

82. Irving, J.B., Jamieson, D.T., and Paget, D.S "The thermal conductivity of . fluids", Trans. Instn Chem. Engrs., Vol. 51, 1973, pp. 10 .

83. Edwards, M.F.,Godfrey, J.C. and Kashani, M.M " Power requirement for the mixing of Thixotropic liquids", J. of Non-Newtonian Fluid Mechanics, Vol. 1, 1976, pp. 309-322 .

84. Rieger, F. and Novak, V. " Power consumption of Agitators in Highly viscous Non-Newtonian Liquids", Trans. Instn Chem. Engrs., Vol. 51, 1973, pp. 105 -111 .

85. Ghenai, S.E. , "Laminar Heat Transfer", M.Sc. Thesis, 1980, University of Bradford .

86. Wang, H.Z.,"Heat transfer in Tanks at Low Re", To be published, Bradford University.

87. Lastovtsev, A.M, and Gorodnicheva, E.I. "Calculating power consumption for mixing high viscosity Newtonian liquids with blade mixers", Khimicheskoe i Neftyanoe Mashinostroenie, No. 6, June 1970, pp. 8 (USSR) .

88. Brown, Trans. Instn. Chem. Engrs., Vol. 25, 1947, pp. 181 .

89. Gluz, M.O & Pavlushenko, I.S., Zh. Prikl. Khim., Vol. 40, 1967, pp. 1485 (USSR).

90. Mitzushina, T.R. et-al, Kagaku Kogaku, 34, 1970, pp. 1205 (Japan) .

91. Ishibashi, K. and Yamanaka, A., " Heat transfer in Agitated Vessels with Special Types of Impellers", J. Chem. Eng. Japan, vol. 12, No. 3, 1979, pp. 230-236 .

92. Lahaye, Ph., Int. Symposium on Mixing, Faculte Polytechnique De Mons, 1978 (French) .

93. Calderbank, P.H. and Moo-Young, M.B. , Chem. Engng. Sci., Vol. 28, 1961, pp. 39 .

94. Hiraoka, S. and Ito, R., J. Chem. Engng. Japan, Vol. 6, 1973, pp. 464 .

95. Sano, Y. et-al, " Correlation of Heat Transfer Coefficient at the Wall of Mixing Vessel", J. Chem. Engng. Japan, Vol. 13, No. 2, 1980, pp. 147-150 .

96. Reiner, M. "Deformation and flow", 1949, (London: H.K. Lewis & Co.) .

97. Wilkinson, W.L. "Non-Newtonian Fluids", London/ Oxford/New York/Paris, 1960 .

98. Perry, R.H. and Chilton, C.H. "Chemical Engineers' Handbook", 5th Edition, McGraw-Hill .

99. Tanka, et-al, Kagaku Kogaku, Vol. 5, No. 87, 1966 (also see Ref. 9) .

100. Sandall - Patel , Ind. Engng. Chem. Process Des. & Dev., Vol. 9, No. 1, 1970, pp.139 .

101. Muller, A.B., and Otto, R.E., AIChE J., Vol. 3, No. 3, 1957, pp. 3 .

102. Chattopadhyay, S. "Mixing of Newtonian and Non- Newtonian Fluids", M.Sc. Thesis, Bradford University, 1977.

103. Ammoie - Foumanie, S. " Mixing in Agitated Vessels", 3rd year report, University of Bradford, 1975 .

APPENDIX 1(i)

Tables relating to Chapter 2

Table 1 Power Data for Anchors

D_T	D	D/D_T	H/D_T	h/D	W/D	C/D_T	Re used	Re range	Kp	A	k_s	φ_p	Materials used	Comments	Reference
30,5	25,41	.833	1	.75	.083	.0834	$\frac{ND^2\rho}{\mu_a}$	.1 - 20	180	-1	18 FOR Re=50 $32N^{2,75}$ FOR Re=50	$\frac{P}{\rho N^3 D^5}$	WATER, GLYCEROL / WATER SOLUTION CHALK/WATER SLURRY, CMC SOLUTION	POWER LAW RELATION USED .35 = n = .78	63
12,6 .042	11,20 .037 .035 .030	.889 .881 .833 .714	1 1 1 1	1,06 1,07 1,17 1,33	.067 .1 .107 .125	.056 .06 .08 .143	$\frac{N^{2-n}D^2\rho}{K}(Ks)^{1-n}$	.1 - 10	190 95	-1 -1	21,5 24 17 9,5	$\frac{P}{\rho N^3 D^5}$ $\frac{P}{\rho N^3 D^5}\left(\frac{C}{Dt}\right)^{1/3}$	B.P OILS, GLYCEROL, SUGAR SOL. 2,5%-3%-3,5% CMC SOL .23%-.25%-.3% CARBOPOL SOL 2,5%-3,5% LAPONITE SALAD CREAM TOMATO KETCHUP YOGURT, PAINT	.145 = K = 4,51 PROCEDURE GIVEN FOR CALCULATION OF POWER FOR THIXOTROPIC FLUIDS .2 = n = .8 5.8 = k = 60 $Nm^{-2}s^n$ 1,1 = μ_a = 11,8 NSm^{-2}	22
12,7 12,7	11,9 11,9	.937 .937	1 1	1,06	.109 .109	.03	$\frac{N^{2-n}D^2\rho}{K}(Ks)^{1-n}$	1,5-28 15-20	230 290	-1 -1	16 25	$\frac{P}{\rho N^3 D^5}$	30%, 85% GLYCEROL, LUB OILS, 2% CMC SOLUTION	POWER LAW RELATION USED CONICAL BOTTOM VESSEL + ANCHOR	102
12.6 12.6	12,1 12,1	.96 .96	1 1	.952 .952	.087 .087	.02	$\frac{N^{2-n}D^2\rho}{K}(Ks)^{1-n}$	1,8 - 10	310 335	-1 -1	NOT REPORTED 42.8	$\frac{P}{\rho N^3 D^5}$	GLYCEROL, B P OILS, 2% CMC, CHOCOLATE MELT	PLAIN FLAT BOTTOM ANCHOR ANCHOR WITH CONICAL BOTTOM IN A CYLINDRICAL CONICAL VESSEL POWER LAW RELATION USED	103
40 30 20		.90 .90 .90 .95 .95 .5	NOT REPORTED	.75 .50 .25 .95 .95 .5	.1 .1 .1 .1 .1 .1	.05	$\frac{ND^2\rho}{\mu_a}$ $\frac{ND^2\rho}{\mu_p}$	.2 - 20 .2 - 20	190 150 68 200	-1 -1 -1 -1	25 25	$\frac{P}{\rho N^3 D^5}$ $\left(\frac{P}{\rho N^3 D^5}\right)-4.8\left(\frac{\tau_y}{\rho N^2 D^2}\right)$	.3%-6,2% CMC SOLUTIONS 10-15% AQUEOUS SOLUTION OF PAA 10-15% TOLVENE SOLUTION OF PAA KAOLIN $CACO_3$ TIO_2 $MgCO_3$ SOLUTION IN WATER	METZER-OTTO TECHNIQUE APPLIED TO NON NEWTONIAN FLUIDS POWER LAW RELATION USED .27 = n = 1 .01 = K = 690 POWER LAW RELATION COULD NOT FIT PAA VISCOMETRIC DATA BINGHAM PLASTIC FLUIDS	36 37 38
		.935	1,26				$\frac{N^2D^2\rho}{\tau_o}$	-27 27 - 510 -22 22 450	248 97,8 221 92,5	-1 -,72 -1 ,72	—	$\frac{P}{\rho N^3 D^5}$	BINGHAM PLASTIC FLUIDS USED	$\frac{Y}{d}$ = .03 $\frac{Y}{d}$ = .11	
10 14,76	9 13,3	.901	NOT GIVEN	.89 .89	.133 .19	.05 .05	$\frac{N^{2-n}D^2\rho}{K}$	.01 - 10	180	-1	16 (±.92) or $n^{2,21/n-1}$ 19,87 (±1,08) or $n^{2,34/n-1}$	$\frac{P}{KN^{n+1}D^3}$	CMS SOL, POLYACRYLAMIDE SOLUTIONS. CMS AND CORN SYRUP SOLUTION	POWER LAW RELATION USED .31 = n = .97 .5 = K = 60 $Kgm^{-1}s^{n-2}$ ϕ_p PLOTTED AGAINST (1-n) WITH INTERCEPT=k_p AND SLOPE=K_s AN m=-1 WAS ASSUMED	84
	UHL + VOZNICK GEOMETRY					.009 .00256 .0054 .0065 .011 .022 .0465	$\frac{ND^2\rho}{\mu}$	2 - 20 30 - 600	550 350 250 170 240 230 170	-1 -1 -1 -1 -1	—	$\frac{Pg}{\rho N^3 D^4 L}$	DATA FROM UHL + VOZNICK CYLINDER OILS	RECORRELATION OF UHL AND VOZNICK DATA ONLY USING A MODIFIED ϕ_p CLAIMED TO GIVE BETTER SCALE-UP	34
24			1		.083	.0167	$\frac{ND^2\rho}{\mu}$	100 - 600	200	.375	—	$\frac{P}{\rho N^3 D^5}$	WATER, WATER/GLYCERINE WATER, MOLASSES, OIL	ONLY NEWTONIAN FLUIDS TESTED 1 = μ = 500p	101

Table 1 cont....

D_T	D	$\frac{D}{D_T}$	$\frac{H}{D_T}$	$\frac{h}{D}$	$\frac{W}{D}$	$\frac{C}{D_T}$	Re USED	RANG OF Re	Kp	A	K_s	ϕp	MATERIAL USED	COMMENTS	WORKERS
30	260	.87	1	NOT GIVEN	.08	.0666	$\frac{N^{2-n} D^2 \rho}{K} (4\bar{\lambda})^{1-n}$	2 – 20 360 – 3.10^5	198 3,5	-1 -.02	$4\bar{\lambda}$ 12,6	$\frac{P}{\rho N^3 D^5}$	WATER, OILS, Na SALTS OF CMC, 70% SUSPENSIONS OF KCL IN A POLYESTER	POWER-LAW ASSUMED .6 ≤ n ≤ 1	63
29	27,9	.96	NOT REPORTED	.477		.019	$\frac{N^{2-n} D^2 \rho}{K} (\frac{H}{h})^n (\frac{D}{D+D_t})$	.001 – 10	160	-1		$\frac{Pg}{\rho N^3 D^5} (A^{1-n})$ A = 50	D.C. 200 SILICONE OIL, 10% CMC SOLUTION 5% POLYISOBUTYLENE 77% CATALPO CLAY n = .34, 5 2 - 1 - 1,6	POWER-LAW RELATION ASSUMED .34 ≤ n ≤ 1,63 19 ≤ k ≤ 816 CORRELATION FAILED FOR DILATENT FLUIDS	28
25	24,55	.982	;51	.5	.098	.009	$\frac{N D^2 \rho}{\mu}$	.2 – 20	252	-1		$\frac{P}{\rho N^3 D^5}$	CYLINDER OIL	ONLY ONE TEST FLUID USED (NEWTONIAN) ALSO BAFFLE WIDTH WAS FOUND TO HAVE NO EFFECT ON POWER	2
	23,8	,952				.024			187	-1					
	22,55	.902				.049			150	-1					
	21,35	.854				.073			126	-1					
60	58,68	,978	1,22	,89	,085	.011		20 – 600	217	-.75					
	57,48	,558			.1276	.021			195	-.75					
	54,84	,914				.043			144	-.75					
NOT	GIVEN	,9	1	,9	1	.05	$\frac{N D^2 \rho}{\mu}$	100	215	-.955			ONLY NEWTONIAN FLUIDS WERE TESTED	PLAIN ANCHOR ANCHOR WITH BAFFLES ($\frac{W}{D}B$ = .1) ANCHOR WITH SCRAPERS ANCHOR WITH SMALL SCRAPERS AND BAFFLES	40
		,9	1	,9	1	.05			245	-.955					
		1	1,2	1	.14	-		2 – 60	203	-1					
		1	1	1	14	-		1 2000	245	-.638					
29,9	21,71	.948	,32	,69	.115	.0264	$\frac{N^{2-n} D^2 \rho}{K} [a(1-n)]^{1-n}$	.3 – 90	82	-.93	$a(1-n)^{1-n}$	$\frac{P}{\rho N^3 D^5} (\frac{C}{D_t})^{1/4}$	SILICONE OILS, LUB. OILS, GOLDEN SYRUP 7,16%, 9,46% + 10% CMC POLYMERISED LINSEED OIL SOLUTION OF POLYBUTADIENE IN ETHYLBENZENE ACCURACY +70% – 30% FORNON-NEWTONIAN ±20% NEWTONIAN	FLAT BLADED ANCHOR $a = 37 - 120 (\frac{C}{D})$ FOR .68 ≤ D/D_t ≤ .96 PITCH BLADED ANCHOR FOR $a = 106 - 1454 (\frac{C}{D_t})$ .9 ≤ D/D_t ≤ .96 POWER LAW RELATION USED .266 ≤ n ≤ .765 100 ≤ K ≤ 2475 ($9cm^{-1} S^{n-2}$)	21
	20,44	,953	18,83	,73	,122	.0542									
	19,48	,851	1,18	,77	,125	.0751									
	18,04	,737	1,5	,83	,139	.1067									
	15,65	,583	1,46	,96	,159	.1584									
22,9	22,11	,956	1	,678	PITCH	.0177									
	20,82	,909	1	,720	BLADED	.0454									
	19,31	,843	1	,777		.0764									
	17,96	,784	1	,935		.1078									
	16,62	,726	1	,903		.1372									
10	9,5	,95	1		,1	.025	$\frac{N^{2-n} D^2 \rho}{K}$	,1 – 15	1	-.9	$\left[\frac{(4\bar{\lambda})^{n-1}}{n^n} \frac{(\frac{D_t}{D})^2 - .75}{[(\frac{D_t}{D})^n - .75]}\right]^{\frac{1}{n-1}}$	$\frac{(\frac{P}{\rho N^3 D^5}) [(\frac{D_t}{D}) - .75]^n}{2\lambda^2 (\frac{4\bar{\lambda}}{n})^n (\frac{h}{D}) (\frac{D_t}{D})^2}$	NON NEWTONIAN SHEAR THINNING FLUIDS USED	POWER LAW RELATION USED .3 ≤ n ≤ 1	29
	5	,5	1		1	.25									
17,64	17,04	,955	,72	1,15	,067	,033	$\frac{N^{2-n} D^2 \rho}{K} (B^{1-n}) \times (\frac{4n}{3n+1})^n$	,2 – 50	15,9	-1	$B^{1-n} (\frac{4n}{3n+1})^n$	$\frac{P}{(\rho N^3 D^5)} \left[\frac{8Le + De}{2De}\right]^{-1} (\frac{Dt}{D} - 1)^5$	3,5%-4%-4,5%-5% CMC SOL 55% CLAY SOLUTION 79% KAOLIN + PAINT	$Le = h - \frac{W}{2}$, $De = D - W$ POWER LAW RELATION USED .2 ≤ n ≤ .84 69 ≤ K ≤ 980 ($\frac{dyn\ s^n}{cm^2}$)	20
	7,49	,42	1	1,13	,074	,29									
8,6	7,28	,847	1,5	,725	,068	,0755	$\frac{N D^2 \rho}{\mu_a}$	,1 – 20	125	-1	NOT GIVEN	$\frac{P}{\rho N^3 D^5}$	NON-NEWTONIAN FLUIDS USED	AVERAGE APPARENT VISCOSITY WAS USED k&n WERE NOT DETERMINED	30
				1,65					90						
10,7	9,64	,901	1	,775	,078	,05	$\frac{N D^2 \rho}{\mu_a}$	,013 – 100	270	-1	$9,5 + \frac{9(\frac{D_t}{D})^2}{(\frac{D_t}{D})^2 - 1}$	$\frac{P}{\rho N^3 D^5}$		AVERAGE APPARENT VISCOSITY CONCEPT USED	33
	8,91	,833		,84	,09	,0836									

D_T	D	D/D_T	H/D_T	h/D	W/D	P/D	N_b	C/D	R_e used	range of R_e	Kp	m	k_s	Φ_p	materials used	comments	workers
19 29		.98		1	1	.50	1 2		$\frac{ND^2\rho}{\mu}$		1000	1	——	$\frac{P}{\rho N^3D^5}\left(\frac{F_w}{D^2}\right)^{-0.187}$	ONLY NEWTONIAN FLUIDS USED	F_w = IMPELLER SURFACE AREA	4
8.6	7.998	0.93	1.53	1.35	.0875	1.25	2	0376	$\frac{ND^2\rho}{\mu_a}$	0.1–50 50–2200	237 90	1 0.73	——	$\frac{P}{\rho N^3D^5}$	NEWTONIAN AND NON-NEWTONIAN FLUINS USED	AVERAGE APPARENT VISCOSITY CONCEPT USED k&n WERE NOT DETERMINED	30
24 180	23.04	0.96	1.05	0.915	.0905	0.61	2	.021	$\frac{ND^2\rho}{\mu}$	.1–100	620	1	——	$\frac{P}{\rho N^3D^5}$	WATER, WATER/GLYCERINE WATER/MOLASSES, OIL	ONLY NEWTONIAN FLUIDS TESTED $1<\mu<500p$	8
22.86	21.60	.945	1.33	.941	.118	.753	2	.0292	$\frac{ND^2\rho}{\mu}$	1–3	420	+1	——	$\frac{P}{\rho N^3D^5}$	CORN SYRUP ONLY NEWTONIAN FLUIDS USED	FLAT BOTTOM VESSEL ONLY TWO READINGS WERE TAKEN	7
10.16	9.205	.906	NOT GIVEN	.966	.1036	.773	2	.0519		.04–10	300	1	——		CORN SYRUP SOLUTIONS QUADROL/WATER MIXTURES	ONLY NEWTONIAN FLUIDS TESTED $1000<M<40{,}000$ CENTI-POISE	41
26.17		.889	1.22	1.06	.108	.345	2		$\frac{N^{2-n}D^2\rho}{K}$	.003–100	–	1	$4\bar{\Lambda}\left\{\frac{n\left[1-\left(\frac{D}{D_t}\frac{2}{h}\right)^n\right]}{1-\left(\frac{D}{D_t}\right)^2}\right.$	$\left(\frac{P}{\rho N^3D^5}\right)\left[\frac{1}{\bar{\Lambda}^2}\left(\frac{h}{D}\right)^{-1}\left(\frac{D}{D_t}\right)^2\right]$	ONLY TWO NON NEWTONIAN FLUIDS USED TO TEST THE CORRELATION 3% CMC IN WATER CELACOL IN WATER ALSO SUGAR SOL AND GLYCEROL/WATER SOLUTION AND MIXTURES OF CCl_4 IN SEXTOL PMTHALATE	ONLY TWIN IMPELLER USED TO TEST THE CORRELATION ALSO FLOW BEHAVIOUR INDEX WAS ALMOST CONSTANT ANALYTICAL CORRELATION BASED ON POWER CONSUMPTION FOR POWER LAW FLUID BETWEEN TWO CONCENTRIC ROTATING CYLINDERS	15
28.02		.952	1.22	1.06	.108	.345	2										
28.3		.952	1.22	1.06	.108	.345	2										
28.83		.931	1.22	1.06	.108	.345	2										
87.22		.954	1.22	1.06	.104	.345	2							$\left[\frac{4\bar{\Lambda}}{n\left[\left(\frac{D}{D}\right)^{2n}-1\right]}\right]^{-n}$			
30	28.5	.95	1	1	.1	1	1	.0263	$\frac{ND^2\rho}{\mu_a}$	2–30	210	1	30	$\frac{P}{\rho N^3D^5}$	WATER, GLYCEROL, CMC SOLUTIONS (0.3–6.2%) PVA SOLUTIONS IN WATER PVA SOLUTIONS IN TOLUENE (3–3.5%)	AVERAGE APPARENT VISCOSITY CONCEPT USED $27<n<1$ $.01<K<690$ POWER LAW RELATION DID NOT FIT PVA DATA $100<M_a<300$ p	1
30	28.5	.95	1	1	.1	.5	1	.0263			350	1					
30	28.5	.95	1	1	.1	1	2	.0263			340	1					
20 & 30	28.5	.95	1	1	.1						52.5			$\left(\frac{P}{\rho N^3D^5}\right)\left(\frac{D_t-D}{D}\right)^5\left(\frac{1}{N_b}\right)^5$			
														$\left(\frac{P}{D}\right)^5$			
30	28.5	.95	1	.95	.1	1	2		$\frac{ND^2\rho}{\mu_p}$	$10-10^5$	—	1		$\frac{\left(\frac{P}{\rho N^3D^5}\right)-6.13\left(\frac{\tau_y}{\rho N^2D^2}\right)}{320\div 15\left(\frac{\tau_y\rho D2}{\mu^2}\right)^{1/3}}$	BINGHAM PLASTIC FLUIDS USED KAOLIN $CACO_3$ TIO_2 AND $MgCO_3$ SOLUTIONS IN WATER	$10^5<\frac{\tau_y\rho D^2}{\mu^2}<10^8$	
30	29.99	.933	1	NOT GIVEN	.167	.57	2	.359	$\frac{N^{2-n}D^2\rho}{K(4\bar{\Lambda})^{1-n}}$	2–80 120–1600	235 77	1 -.73	$4\bar{\Lambda}$	$\frac{P}{\rho N^3D^5}$	WATER, OILS Na SALTS OF CMC 70% SUSPENSION OF KCl IN A POLYMER	POWER LAW RELATION ASSUMED $6.5<n<1$	17
21	19.921	.901	1	1.1	.103	1.1	2	.0549	$\frac{ND^2\rho}{\mu_a}$	.04 50 50–100	130 32	1 -.7	11	$\frac{P}{\rho N^3D^5}$	NEWTONIAN AND SHEAR THINNING FLUIDS TESTED	AVERAG APPARENT VISCOSITY CONCEPT USED	33
		.84		1.28	.114	1.28											
NOT GIVEN		.93	1.8	1.2	.09	1.24	1	.0376	$\frac{ND^2\rho}{\mu}$	<10	240	1	——	$\frac{P}{\rho N^3D^5}$	NEWTONIAN FLUIDS TESTED		101

WORKER	CORRELATION
Carreau & Patterson (25)	$P_o Re^{0.93} = 24\ N_b\ (D / D_T)^{.91}\ (D / L)^{-1.23}$
Zolkanik (4)	$P_o Re = 1000\ (F_w / D^2)^{0.187}$
Reher & Bohn (33)	$P_o Re = 10.5\ (C / D_T)^{-1}$
Bourne & Butler (15)	$P_o Re = 1/\pi^2\ (h / D)^{-1} (D / D_T)^2 \left[4\pi / n\ (D / D_T)^{-2/n} - 1 \right]^{-n}$
Lastovetev (87)	$P_o Re = 2\ (P / D)^{-.7} (W / D)^{.54} N_b^{.6}$
Blasinki & Rzyski (48)	$P_o Re = 34.1\ (C / D)^{-0.53} (P / D)^{-0.63} (W / D)^{1.01} (N / D)^{0.14} (H / D)^{0.45} N_b^{.79}$
Hall & Godfrey (23)	$P_o Re = 66\ N_b\ (C / D)^{-.6} (P / D)^{-.73} (h / D)(W / D)^{.5}$
Nagata (1)	$P_o Re = 37.0\ (C / D)^{-.5} (P / D)^{-.5} N_b^{.5}$
Brauer & Schmidt-Traub (47)	$P_o Re = 16.9\ N_b^{0.2} (h / D) \left[1 / 1-(D / D_T)^2 \right] + 11.5\ (W / D)(D / D_T) / (P / D)^2$
Kappel (46)	$P_o Re = 60\ (C / D)^{-.3} (P / D)^{-.5} N_b^{.8}$
Kappel & Selbring (45)	$P_o Re = 14\ N_b^{0.9} (h / D) \left[(P / D)^{-2/3} / 1-(D / D_T)^2 \right]$
Bourne et-al (44)	$P_o Re = 134\ (h / D)(P / D)^{-0.3} (C / D)^{-0.3}$

Table 3 Power Data for Ribbons

Table 4 Heat Transfer for Ribbons & Anchors

IMPELLER						TANK					CONSTANTS IN 2.86						
IMPELLER TYPE	D	h/D P/D	W/D	C/D_T	SPEED RANGE (rps)	D	Z/D_T	TYPE BOTTOM	MAT.		Re	A.	a	b	C	FLUIDS / COMMENTS	INVESTIGATOR
SCREW	.18	.5	.4	.33	.494—3.4	.3	1	DISHED	STEEL	C+H	4—92	.479	.45	.33	.18	WATER, SPINDLE & COMPRESSED OIL, AQU. SOLN. OF SODIUM SALT IN CMC, AND SUSPENSION OF KCl IN POLYESTER	Gluz & Pavlushenko (17)
ANCHOR	.26		.08	.08	.473—3.49	.3	1	DISHED	STEEL	C+H	8—30	.636	.5	.33	.18		
SCREW IN DRAUGHT TUBE	.18	.5	.4	.15	.494—3.4	.3	1	DISHED	STEEL	C+H	4—47	.912	.33	.33	.55		
RIBBON	.28		.18	.04	.204—2.896	.3	1	DISHED	STEEL	C+H	$8—10^5$	.633	.5	.33	.18		
RIBBON	.24 .264 .28 .284 .290		.12 .108 .102 .10 .098	.125 .068 .036 .028 .017		.3	1	DISHED	STEEL	C+H	.1 - Rec Rec= $\frac{39T}{T-D}$ 8—D—.97	1.75	1/3	1/3	.2	$Nu = 1.75\ Re^{1/3} Pr^{1/3} Vis^{-2} \left\{\frac{T-D}{D}\right\}^{-1/3}$ MILLET GELLY, WATER, CMC SOLN, PVA SOLN, GLYCERIN & SILICONE OIL.	Nagata (1)
ANCHOR	.24 .265 .275 .285		.12 .108 .102 .10	.125 .068 .036 .028		.3	1	DISHED	STEEL	C+H	50—500	1.5	1/2	1/3	.2		
ANCHOR	.56		.09	.05	.866—1.05	.61	1	DISHED	STEEL	C+H	10—300	1	1/2	.33	.18	BODIED LINSEED OIL & CYLINDER OIL	Uhl (2)
ANCHOR	.179 .167 .150 .131	.92	.107 .114 .127 .145	.0129 .046 .091 .143		.184	1	FLAT		C+H	12—300	.691 .531 .546 .631	.5	.33	.18	AQU. CARBOPOLL SOLN. AND PRECIPITATED CHALK IN WATER	Heinlein & Sandall (62)
ANCHOR	.14	.96	.1	.04	.06—.3	.150	1	FLAT		C+H	.94—7	.86	.42	.46	.62	BP OIL AND SYRUP SOLUTION	Camurdan (5)
ANCHOR				.01 .02 .03 .05		.4				C+H	.5—100	.358 FOR COOLING & .242 FOR HEATING	1	.5	.02 .08 .14 .14	$Nu = .358 (Re)(Pr)^{.3} + 4000 (Vi)^{c}$ NEWTONIAN FLUID WITH WIDELY VARYING VIS. TEMP. RELATIONSHIPS SUCH AS SILICON OILS & PETROLEUM CUTS	Zelkanik (4)
FLAT BLADE				.0688 .028 .00715							7—200	.55 .645 1	.27 .3 .3	.33 .33 .33	.18 .18 .18		Penny & Bell (35)
DOUBLE HELICAL RIBBON	.28	.5	.1	.033		.3		FLAT			1—100	4.2	.33	.33	.2	NON-NEWTONIAN PSEUDOPLASTIC FLUIDS	Nagata (1)
ANCHOR	1.26 1.47	0.88, 0.76	0.06, 0.05	.03, .017		1.52		DISHED			5×10^3-4×10^4	0.45	0.66	0.25	0.14		BROWN (89)
ANCHOR											$\frac{300.5}{3\times10^4}$	0.4	.66	.33	.14	NON-NEWTONIAN POWER LAW	TANAKA (99)
ANCHOR	.18	1	.1	.009		0.183	1	FLAT			$\frac{320}{9\times10^4}$	.315	.66	.33	0.12	NON NEWTONIAN POWER LAW	Sendil Patel (100)

Table 2 cont.....

D_T	D	D/D_T	H/D_T	h/D	W/D	P/D	Nb	C/D	Re used	Re range	Kp	A	k_s	φ_p	Materials used	Comments	Reference
4.12 28.2 28.2 28.2 55		.898 .912 .912 .902 .91	1.02	1.01 .992 .996 1.01 1	.135 .971 .0971 .0981 .1	.517 .495 1 1 1	1 1 2 1 2	.575 .0485 .0539 .05	$\frac{ND^2\rho}{\mu_a}$	.1 — 10	66	1 1 1 1 1	26.6 26.6 23.9 AVERAGE VALUE OF 27 RECOMMENDED	$\left(\frac{P}{\rho N^3 D^5}\right)\left(\frac{P}{D}\right)^{.73}\left(\frac{1}{N_b}\right)\left(\frac{N}{D}\right)^{.5}$	AQUEOUS SOLUTIONS OF CORN SYRUP AND AQUEOUS SOLUTIONS OF CELACOL (1%-5% W/W)	60 μ 460P AVERAGE APPRENT VISCOSITY CONCEPT WAS USED- POWER-LAW RELATION COULD NOT APPLY ELASTIC ANOMOLIES WERE IGNORED- NOT A GOOD VARIATION IN GEOMETRY	23
		.95 .95 .95 .95 .95	1 1 1 1 1	.98 .98 .98 .98 .95	.095 .095 .095 .095 .08	.5 1 .5 1 .7	1 1 2 2 4	.025 .025 .025 .025 .025	$\frac{ND^2\rho}{\mu}$	— 20 — 20 — 20 — 20 — 20	290 186 426 273 350	1 1 1 1 1		$\frac{Pg}{\rho N^3 D^5}$	ONLY NEWTONIAN DATA WERE TESTED	ACCURACY = ±25%	40
GEOMETRICAL SET UP OF NAGNTA, GRAY, BOURNE, BUTLER, HALL . GODFREY, HOOGENDORN AND DEN HARTOG, BOHM, ULBRICH SCHREIBER ZLOKARNIK & JHONSON REHER									$\frac{N^{2-n}D^2\rho}{K}$	— 10	2.49	1		$\frac{P}{\rho N^3 D^5}\left\{\bar{\lambda}a\frac{D_E}{D}\lambda^2\left[\frac{4\bar{\lambda}}{n(\lambda^{2n}-1)}\right]^n\right\}^{-1}$	2%, 2.5% CMC SOL. 2% 3% CELACOL GOLDEN SYRUP (95%) 25% GLYCERINE 2%, 3% NATROSOL 1%, 2%2.5%, PAA	a IS DIMENSIONLESS SURFACE AREA $= \bar{\lambda}\left(\frac{h}{D}\right)\left(\frac{W}{D}\right)/P_0$ $\frac{D_E}{D} = \frac{D_t}{D} - \frac{Z\,(W/D)}{\left\{\frac{D_t}{D}-(1-2\frac{W}{D})\right\}}{\left(\frac{D_t}{D}\right)-1}$ $\lambda = \frac{D_t}{D_E}$ DATA FROM LITERATURE TESTED FOR Ks ACCURACY CLAIMED 12.7% — 41%	31
6.30	6	.952	1.25	.98	.1	.39	2	.0252	$\frac{ND^2\rho}{\mu}$	— 10	522	1		$\frac{P}{\rho N^3 D^5}$	ONLY NEWTONIAN FLUIDS TESTED		45
10	9.6	.952		1	.1	1	2	.0208	$\frac{N^{2-n}D^2\rho}{K}$	— 10	300	1	36.7	$\frac{P}{KN^{n-1}D^3}$	CMC SOL, PAA SOLUTIONS CMC AND CORN SYRUP SOLUTIONS POLYISOBUTYLENE IN DECALINE (VISCO-ELASTIC)	POWER-LAW RELATION USED .31 — n — .97 .5 — K — 60 $Kgm^{-1}S^{n-2}$ ϕ_p PLOTTED vs (1-n) WITH INTERCEPT = Kp AND SLOPE = Ks AN n = -1 WAS ASSUMED Ks VALUE IS CLAIMED TO BE VALID FOR VISCOELASTIC FLUIDS	84
12.55	11.8	.94		.85		.42	1	.032	$\frac{ND^2\rho}{\mu_a}$	.5 — 40	212		30 (±4.21)	$\frac{P}{\rho N^3 D^5}$	LUB. OIL, GLYCEROL, GLUCOSE SYRUP 15-35% CMC IN WATER .25-.45% CARBOPOL IN WATER .23% CARBOPOL IN 75% GLYCEROL TOMATO KERCHUP, SALAD CREAM YOGHURT NONDRIP PAINT 2-4% LAPONITE IN WATER	AVERAGE APPARENT VISCOSITY CONCEPT USED. PROCEDURE DEVELOPED TO ESTIMATE POWER FOR THIXO TROPIC FLUIDS APPLICABILITY OF AVERAGE SHEAR RATE CONCEPT TO THIXOTROPIC FLUIDS WAS ESTABLISHED	22
HOOGENDORN AND DEN HARTOG AND GRAY GEOMETRY									$\frac{ND^2\rho}{\mu_a}$	1-100 1-3	580 470	1 1		$\frac{Pg}{\rho N^3 D^4 L}$	NEWTONIAN DATA ONLY	RECORRELATION OF LIMITED DATA FROM OTHER WORKERS. NO EXPERIMETAL WORK WAS CARRIED OUT L = LENGTH OR HEIGHT OR LIQUID BEING AGITATED	34

APPENDIX 1(ii)

Figures relating to Chapter 3

Fig. 3.1 Laminar Mixing and Heat Transfer in Agitated Vessels

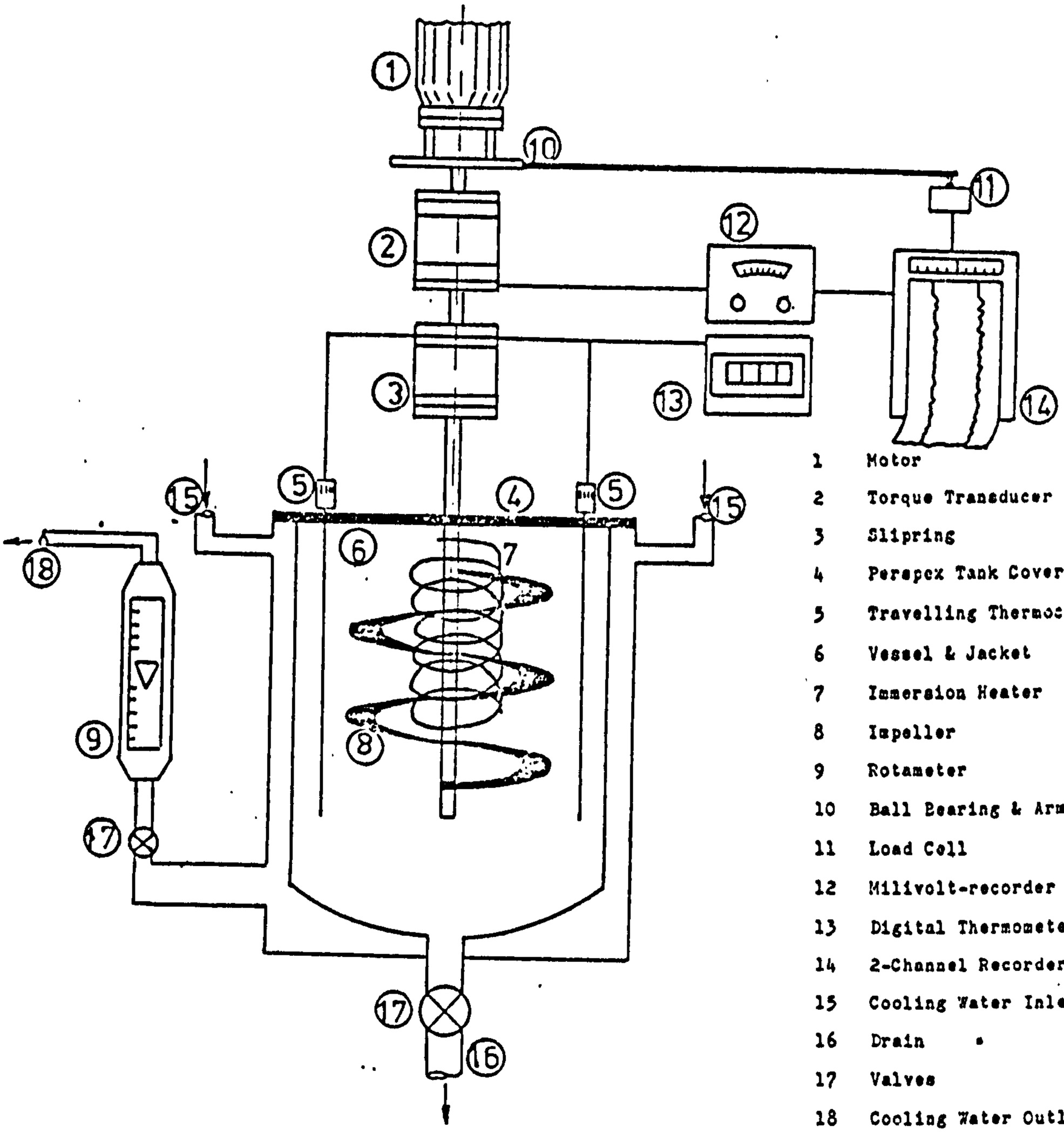

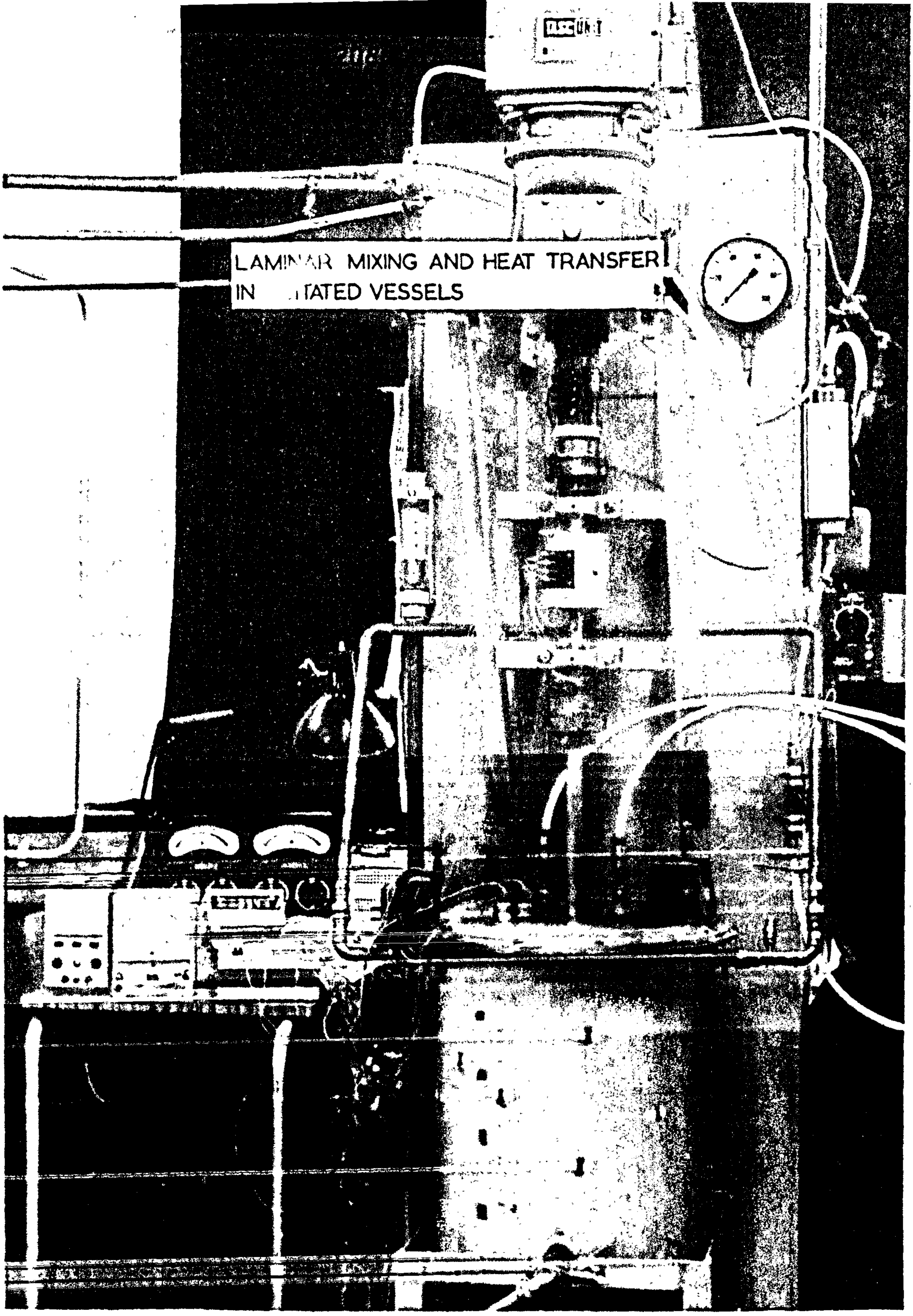

Plate 3,2 Vessel 1 & Ancillary equipment

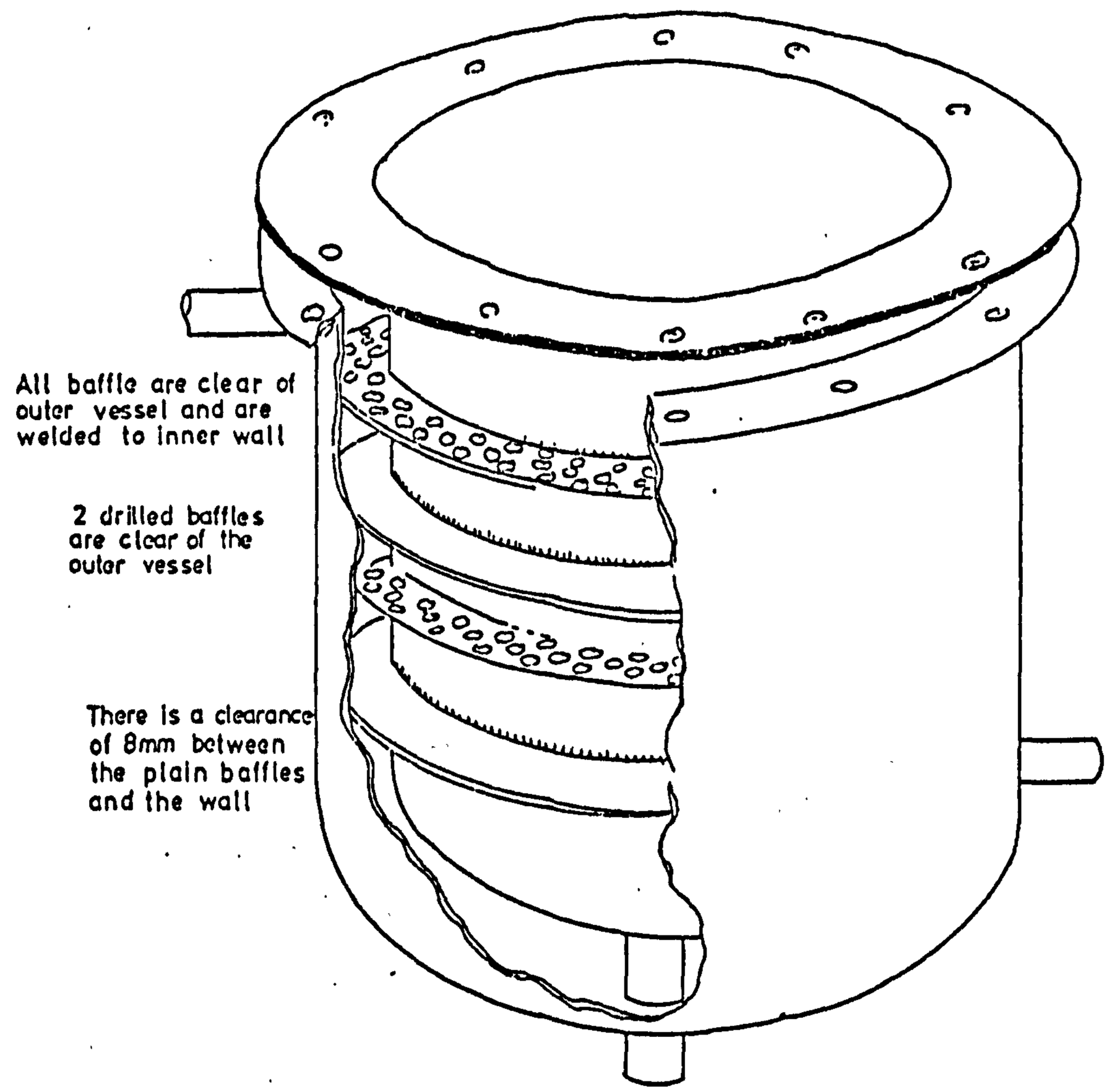

Fig. 3,3 Vessel and Baffled Jacket

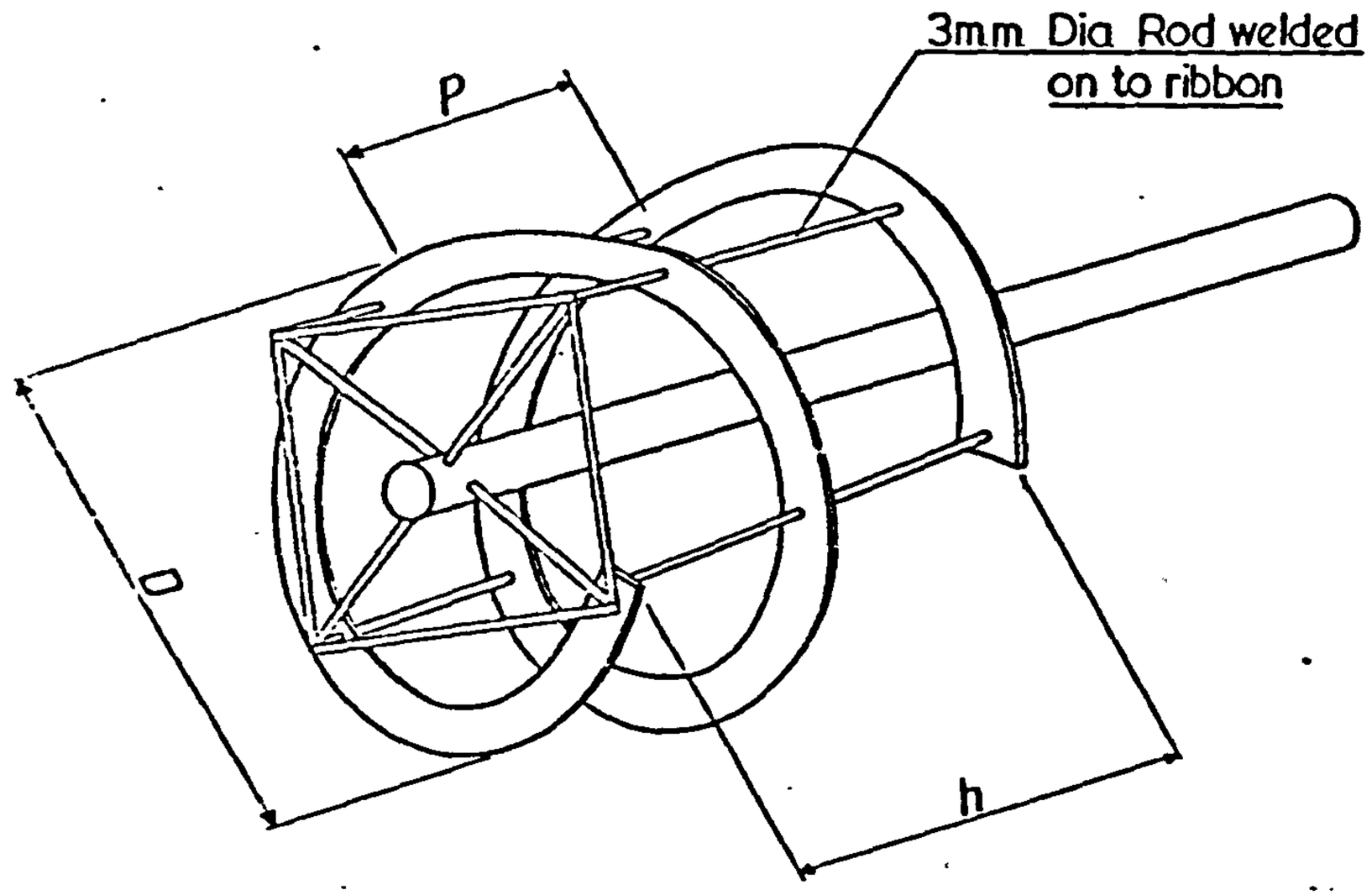

Fig 3.4 Helical Ribbon Impeller

No	D_T	D	W	P	P/D	W/D	C/D	Nb	h/D	H/D_T
1	400	352	34	352	1	.097	.0682	1	1.0	1.1
2	"	"	"	"	"	"	"	2	"	"
3	"	"	"	176	0.5	"	"	1	"	"
4	"	380	37	380	1	"	.0263	1	"	"
5	"	"	"	190	0.5	"	"	"	"	"
6	"	370	36	185	"	"	.0405	1	"	"
7	150	135	13	135	1	"	.0556	2	1.02	"
8	"	"	14	75	.56	.104	"	1	1.08	1.08
9	"	130	13	133	1.02	.100	.0769	1	1.02	"
10	"	113	12	60	.531	.106	.1637	1	"	"

All measurements are in mm.

Fig. 3,5 Anchor Impeller

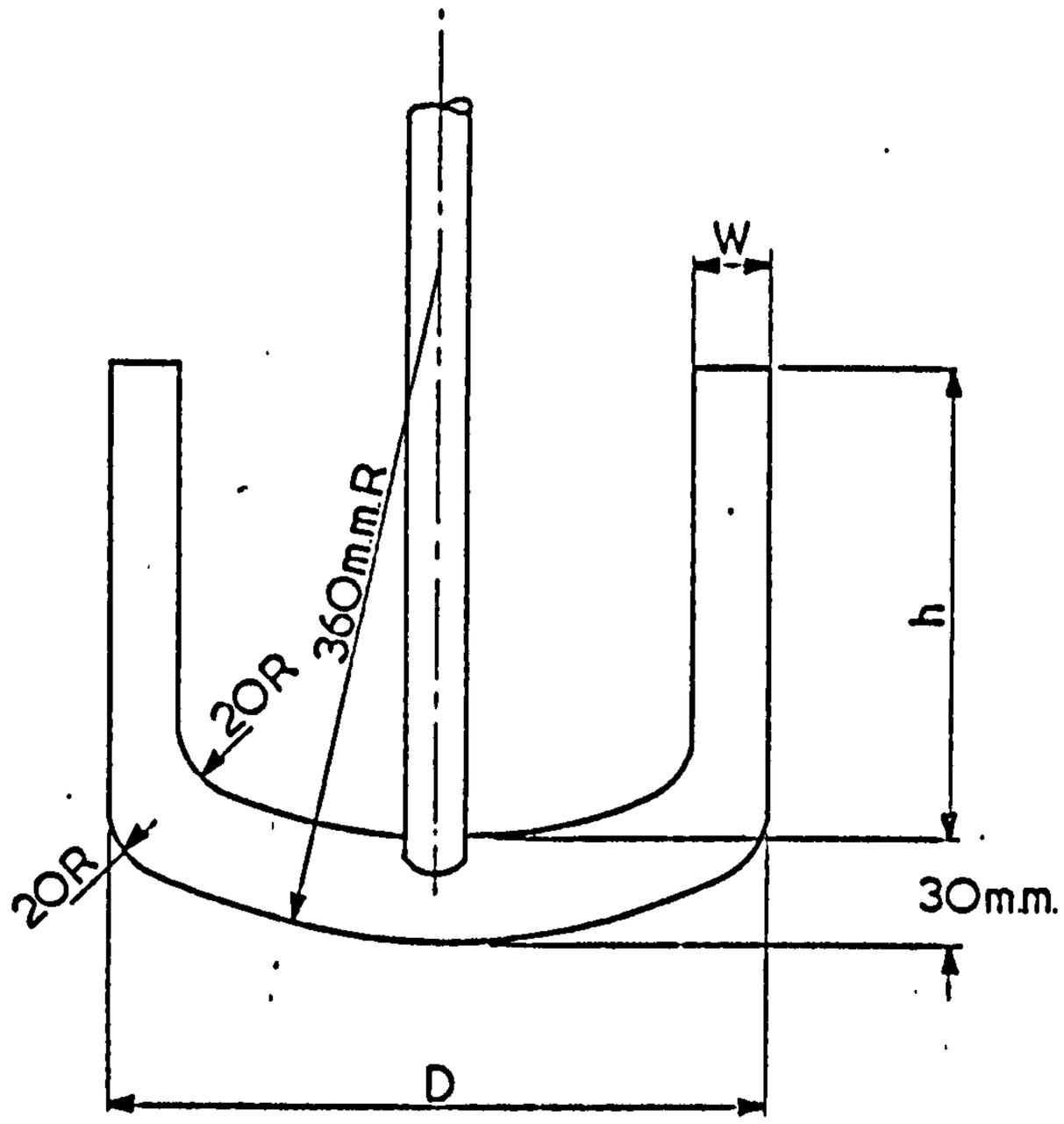

No	D_T	D	W/D	h/D	H/D_T	C/D
1	400	318	0.1	1.0	1.08	0.129
2	"	248	"	"	"	0.075
3	"	369	"	"	"	0.042
4	"	382	"	"	"	0.024
5	150	140	"	"	1.05	0.036
6	"	113	"	"	"	0.164

All measurements in mm.

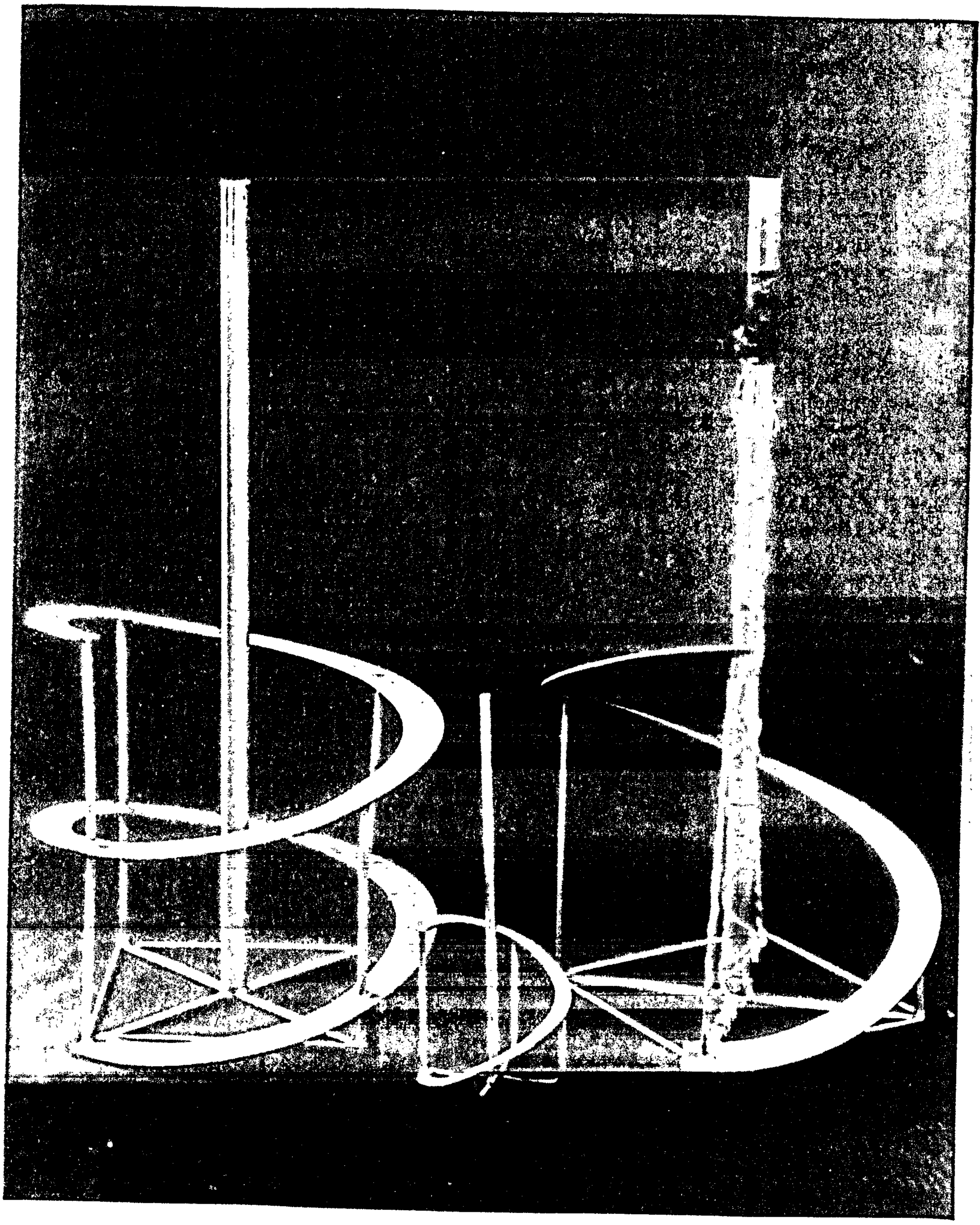

Plate 3,6 Helical Ribbons

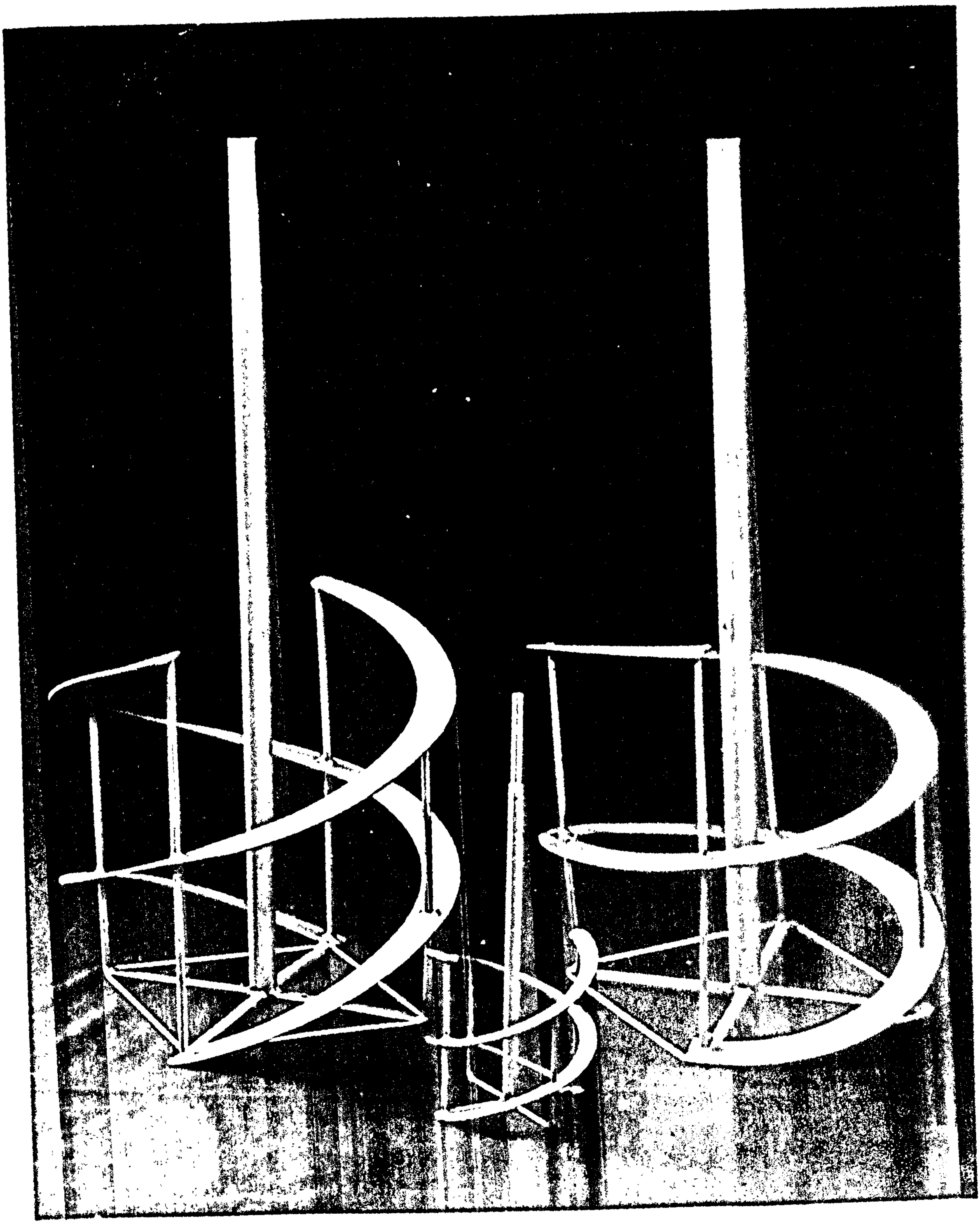

Plate 3,6 Helical Ribbons

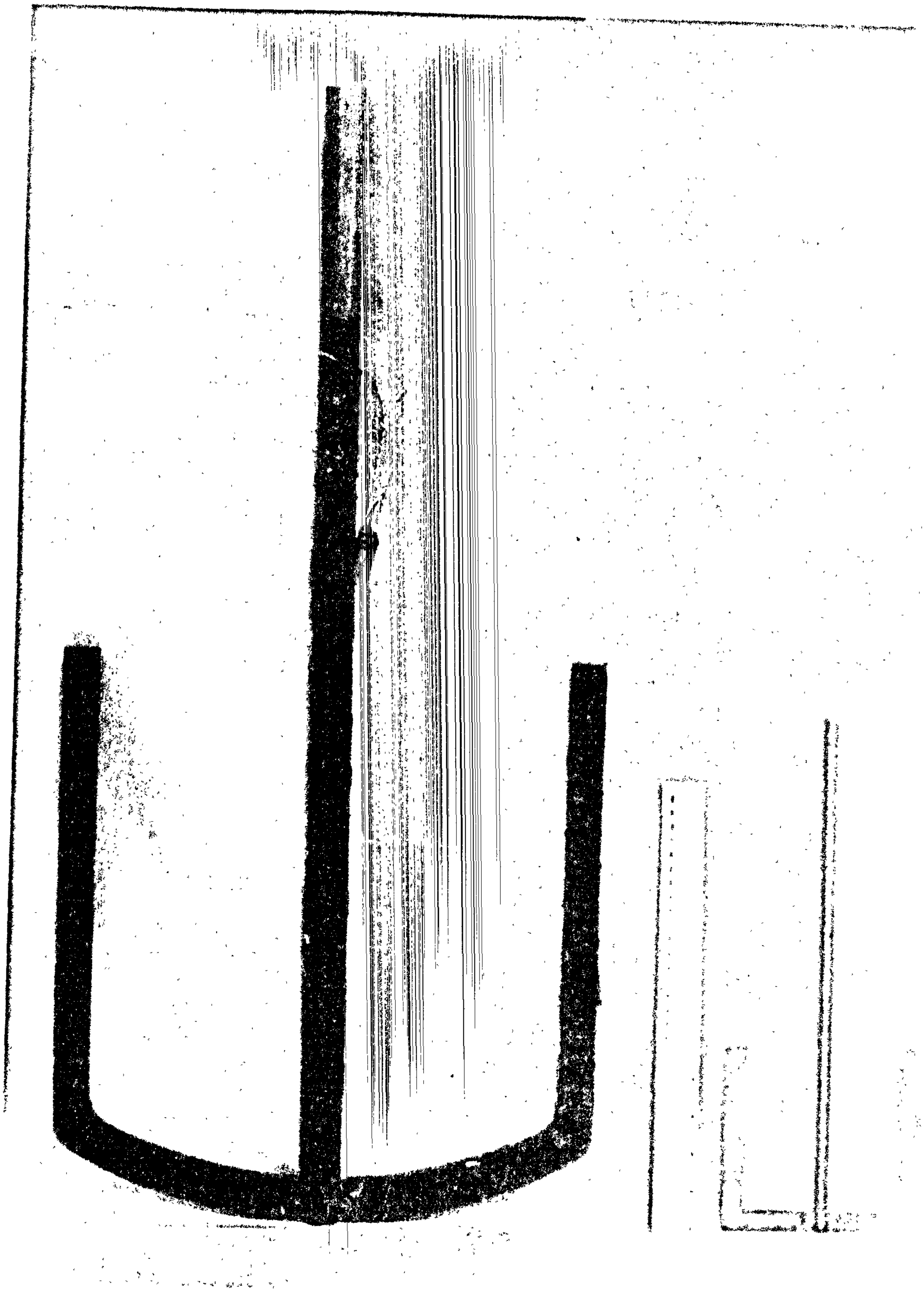

Plate 3,7 ANCHOR IMPELLERS

Plate 3,8 Tank cover & Thermocouples

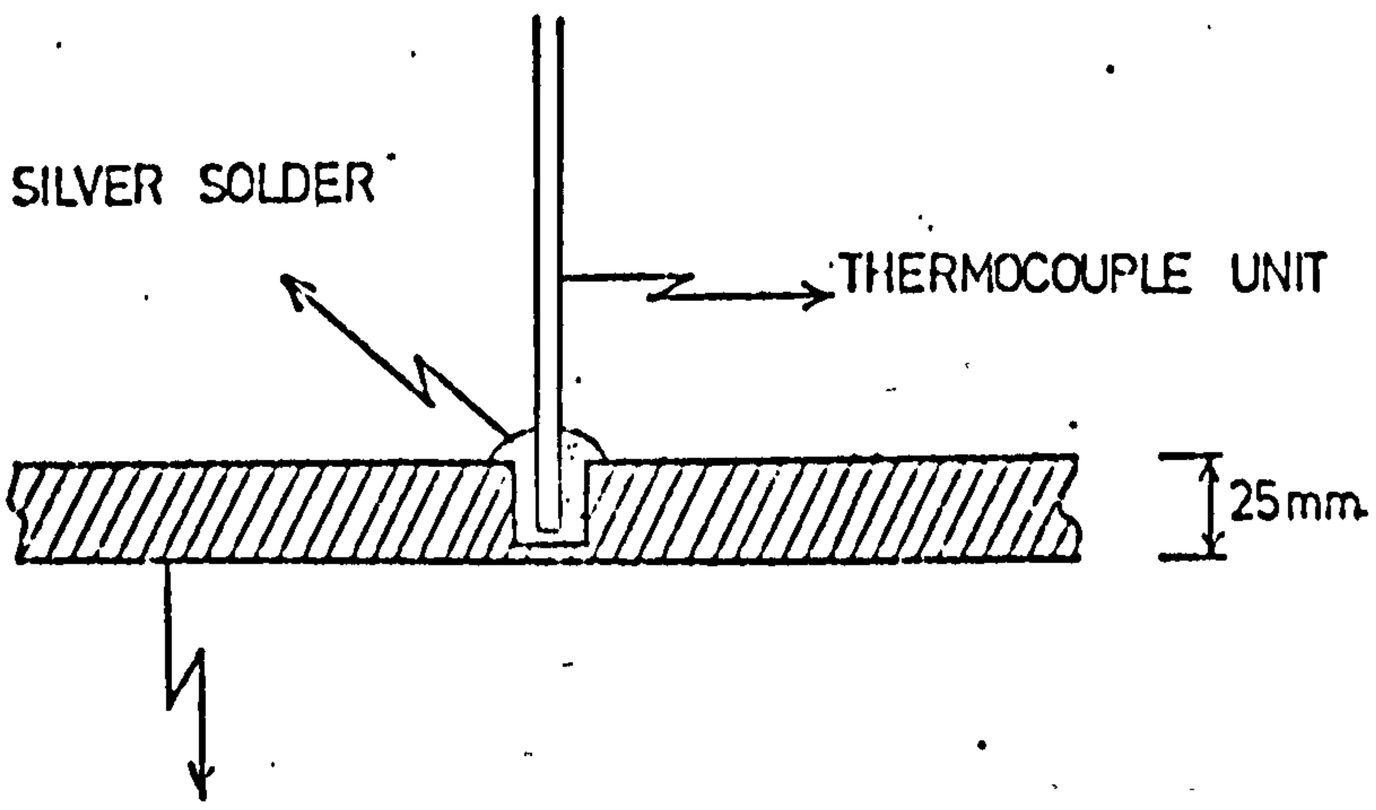

Fig. 3,9 Thermocouple Position

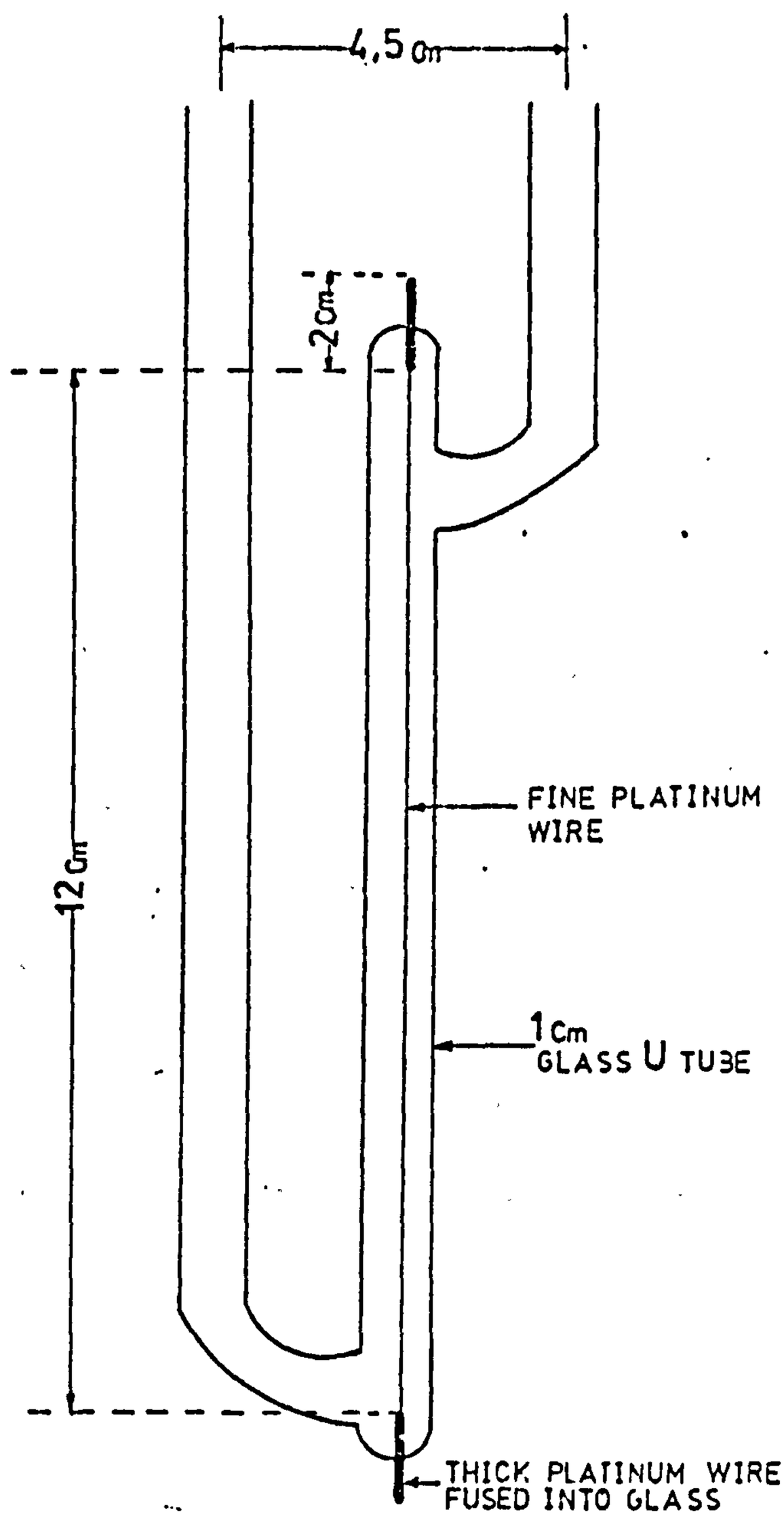

Fig 3,10 Thermal Coductivity Cell

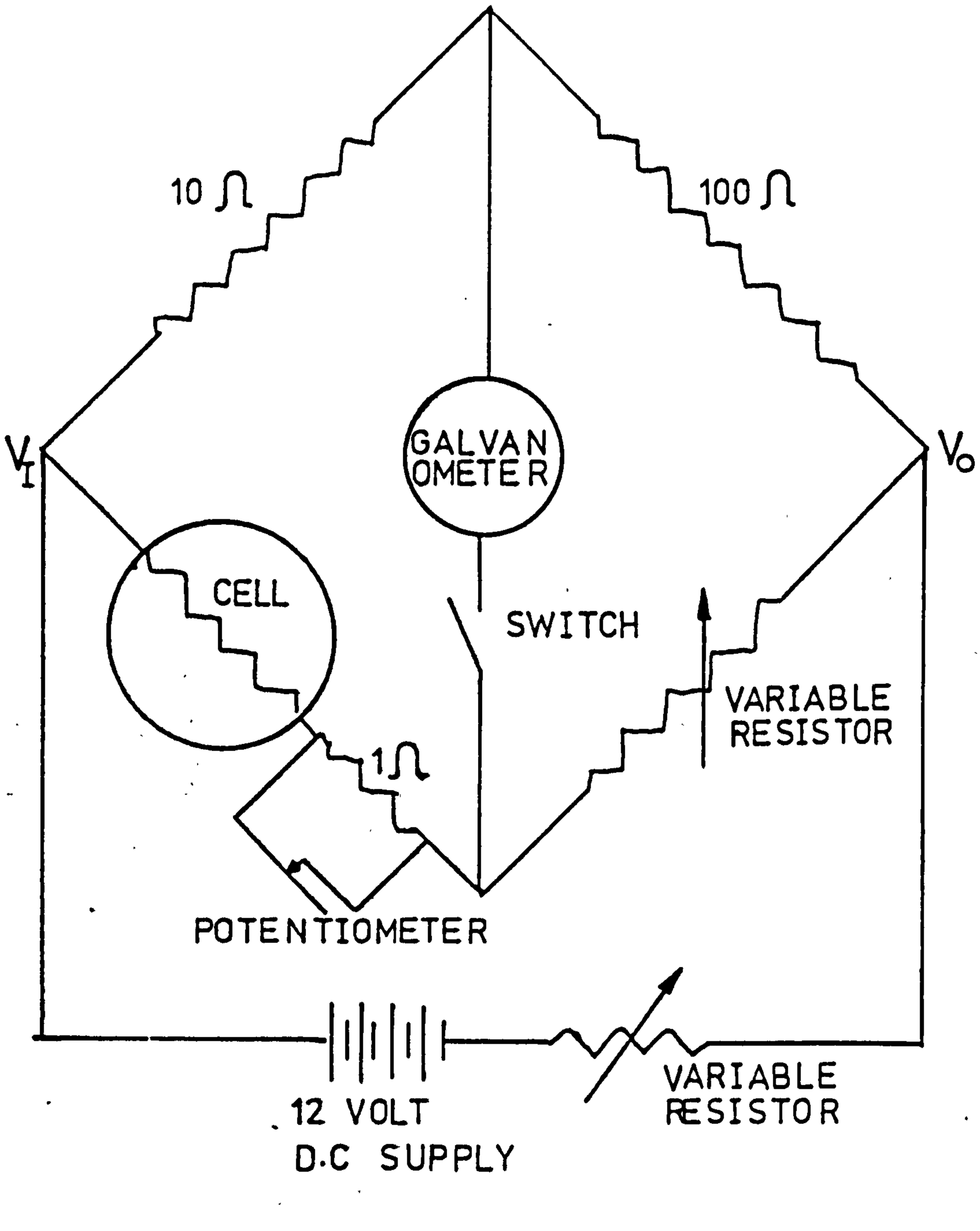

Fig. 3,11 Wheatstone Bridge Circuit

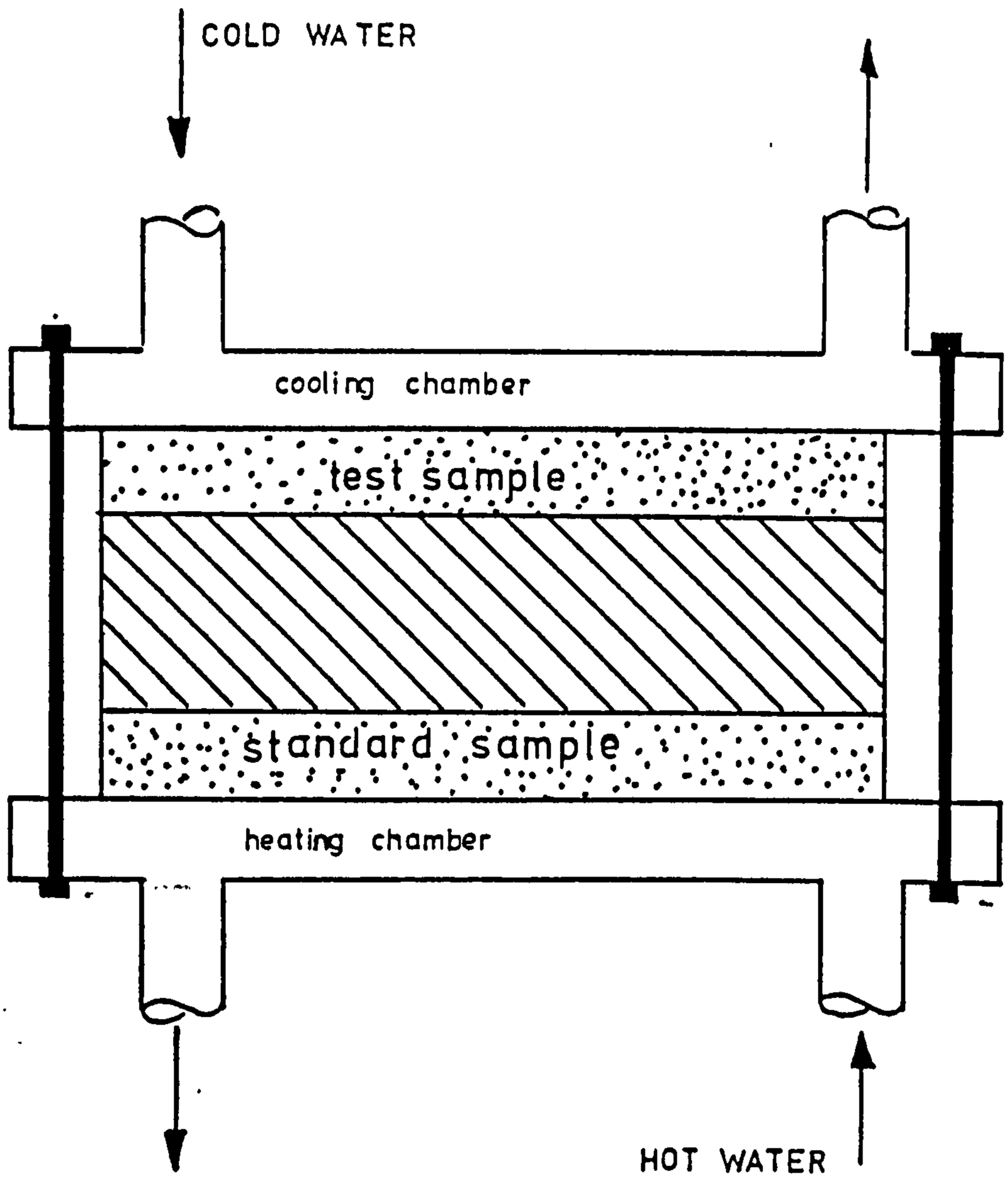

Fig. 3,12 Thermal Coductivity Apparatus

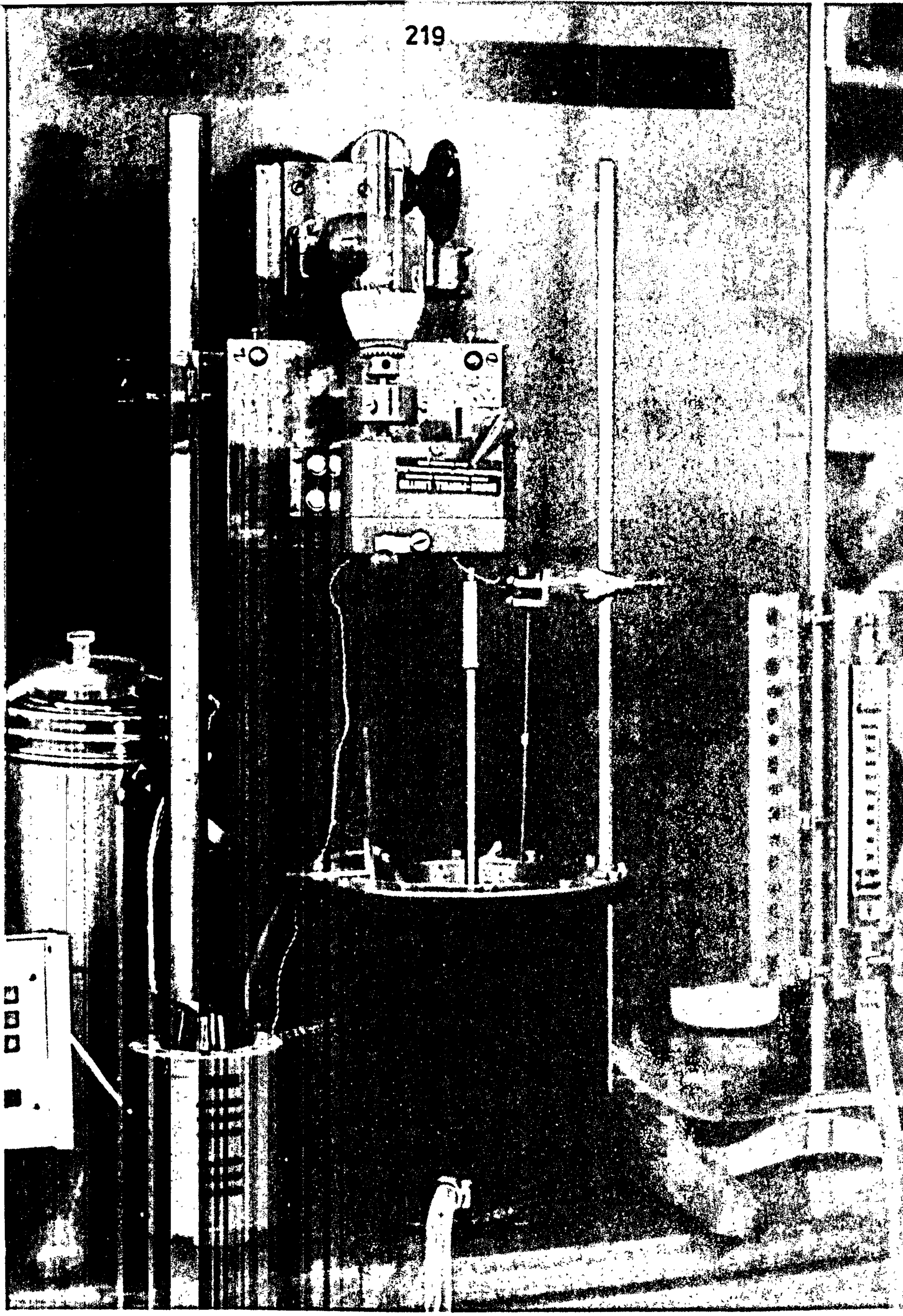

Plate 3,12 Vessel 2 & ancillary equipment

APPENDIX 1(iii)

Figures - Experimental Results relating

to Chapter 4

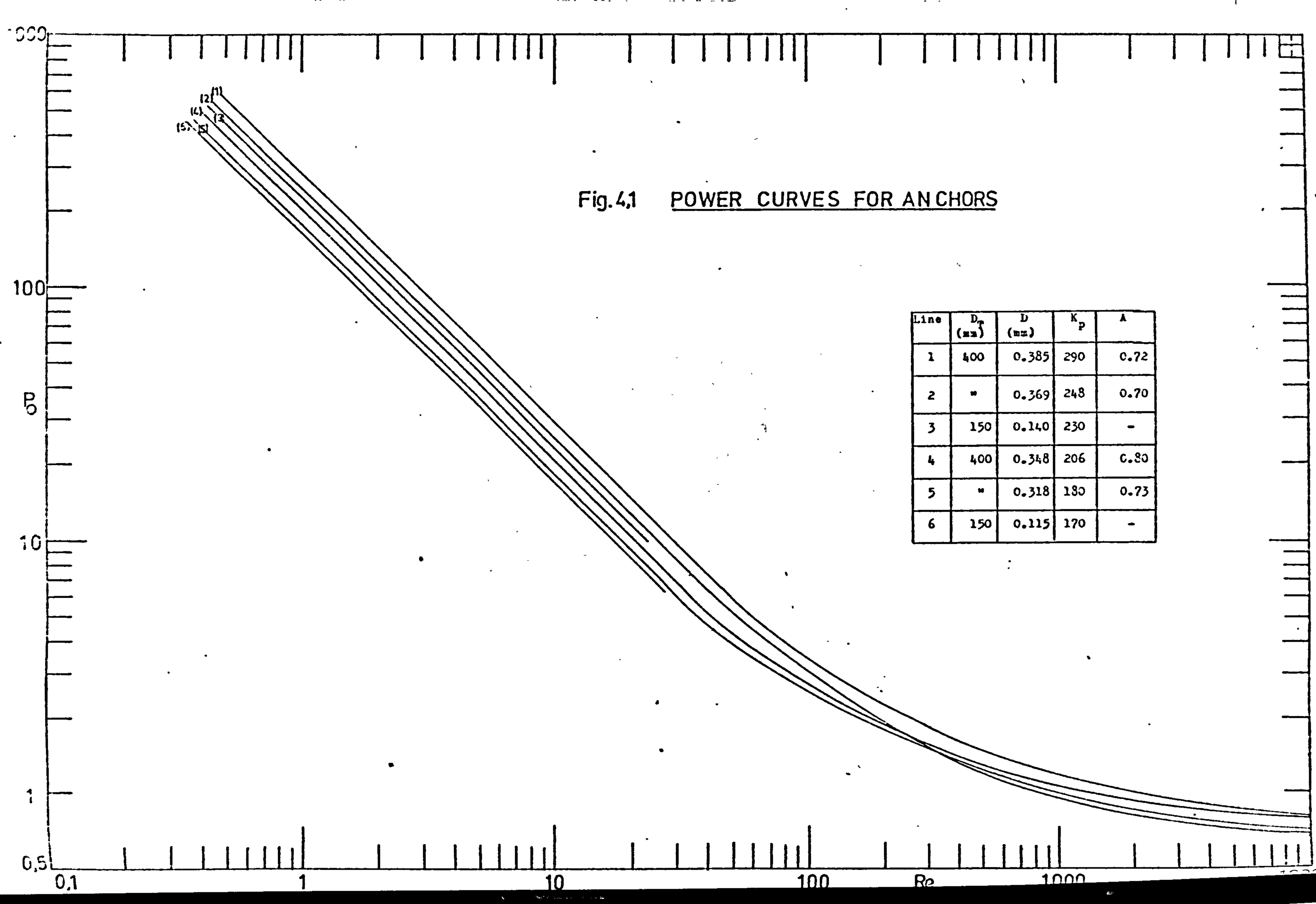

Fig. 4,1 POWER CURVES FOR ANCHORS

Line	D_T (mm)	D (mm)	K_P	A
1	400	0.385	290	0.72
2	"	0.369	248	0.70
3	150	0.140	230	-
4	400	0.348	206	0.80
5	"	0.318	180	0.73
6	150	0.115	170	-

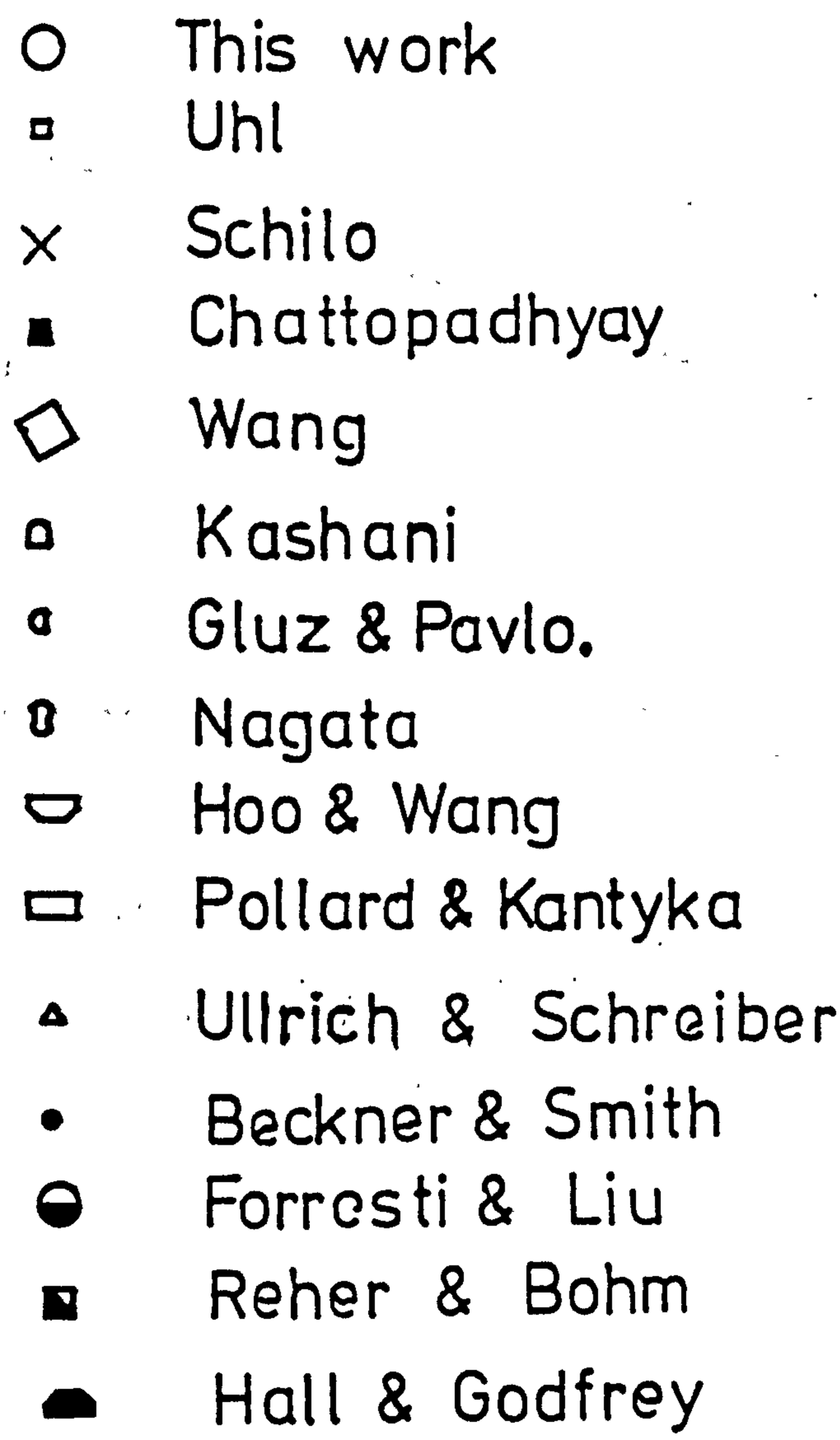
This work
Uhl
Schilo
Chattopadhyay
Wang
Kashani
Gluz & Pavlo.
Nagata
Hoo & Wang
Pollard & Kantyka
Ullrich & Schreiber
Beckner & Smith
Forresti & Liu
Reher & Bohm
Hall & Godfrey

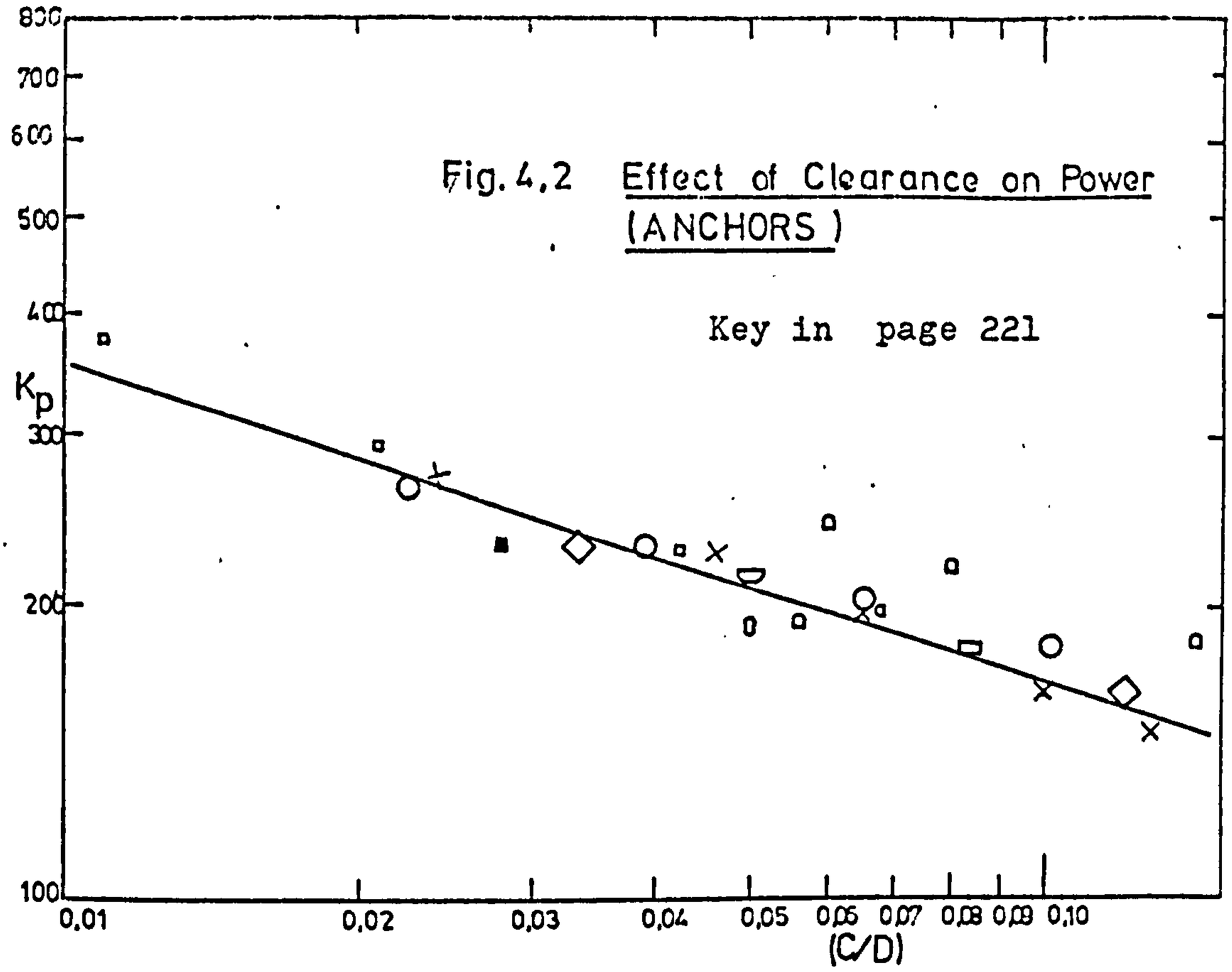

Fig. 4.2 Effect of Clearance on Power (ANCHORS)

Key in page 221

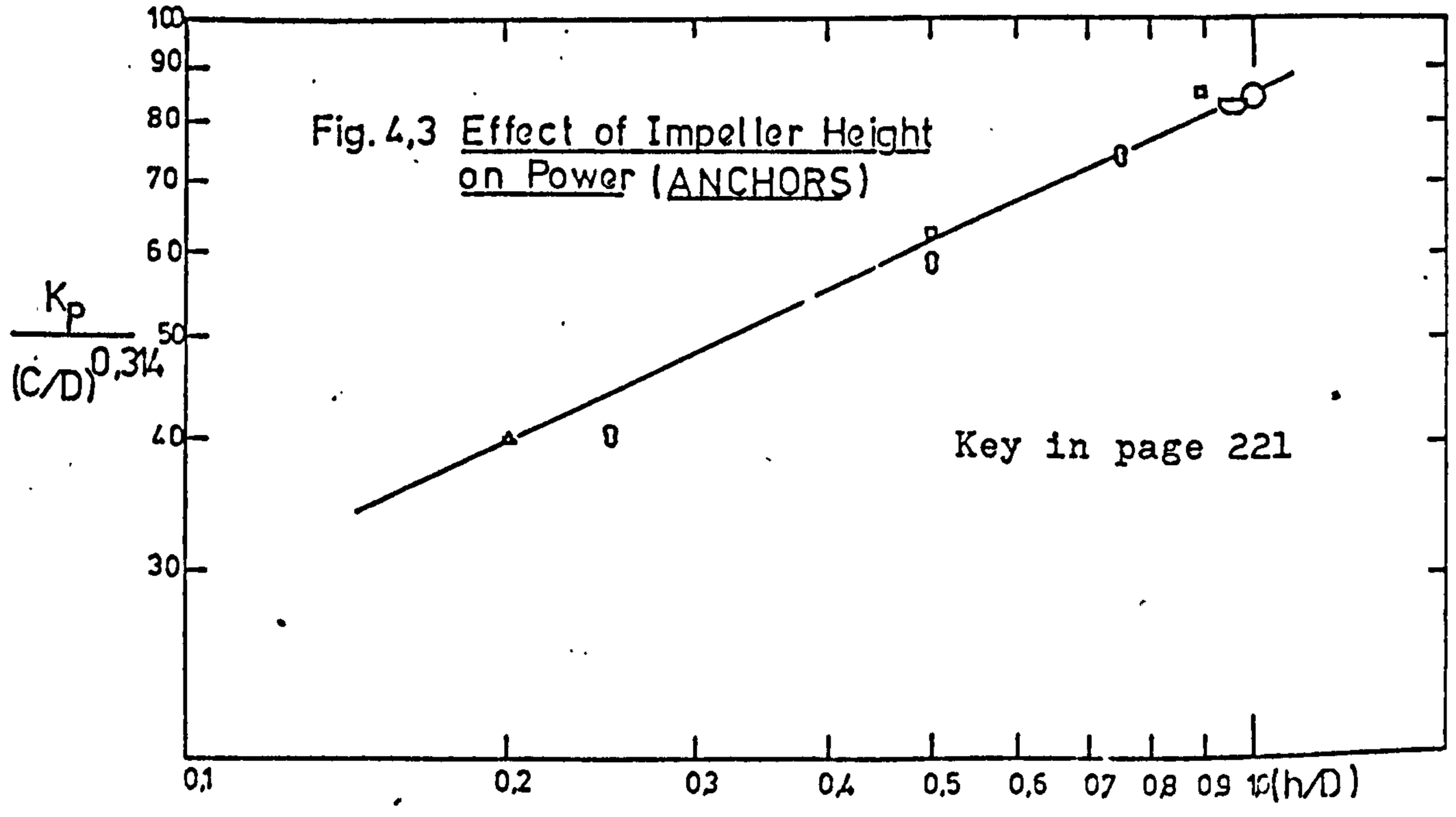

Fig. 4,3 Effect of Impeller Height on Power (ANCHORS)

Key in page 221

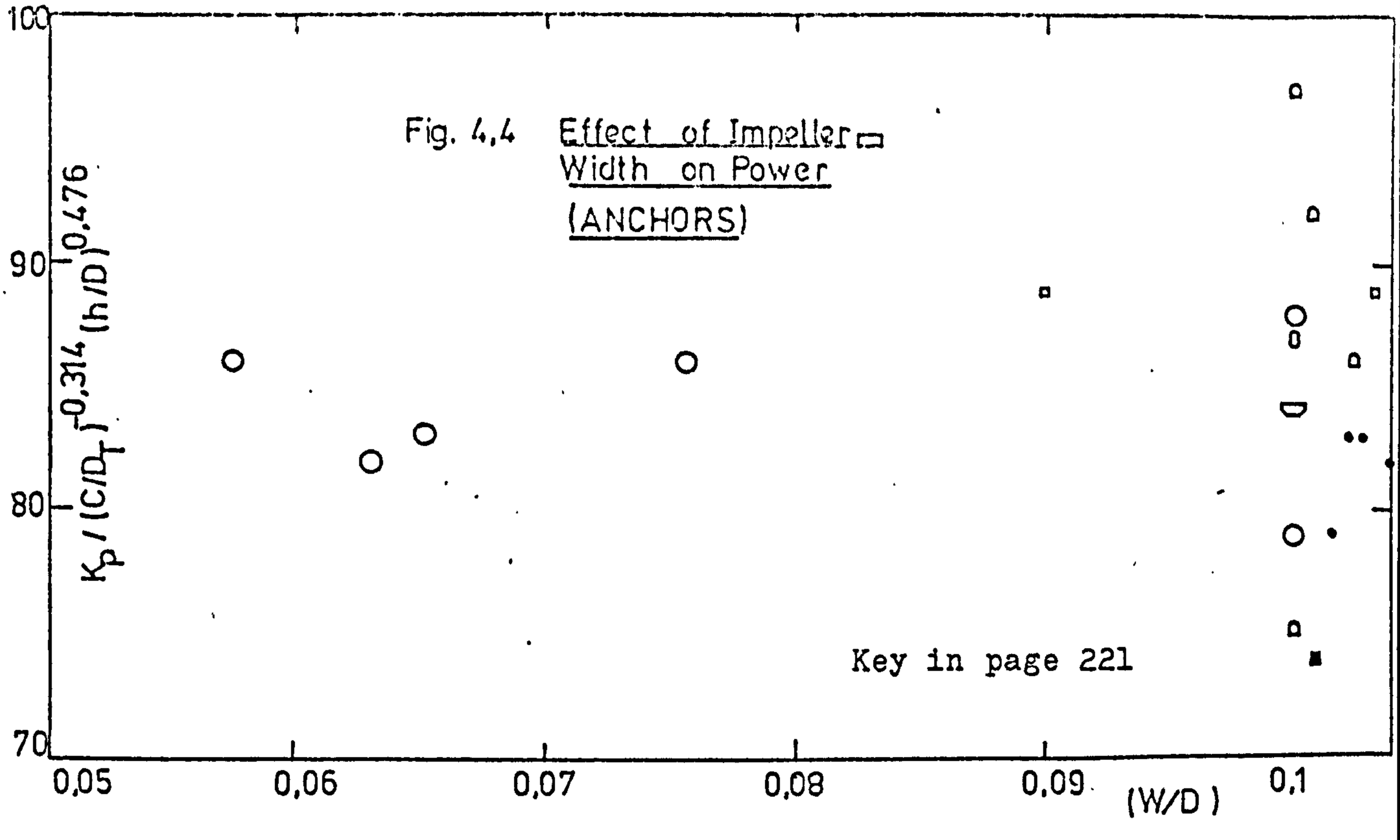

Fig. 4,4 Effect of Impeller Width on Power (ANCHORS)

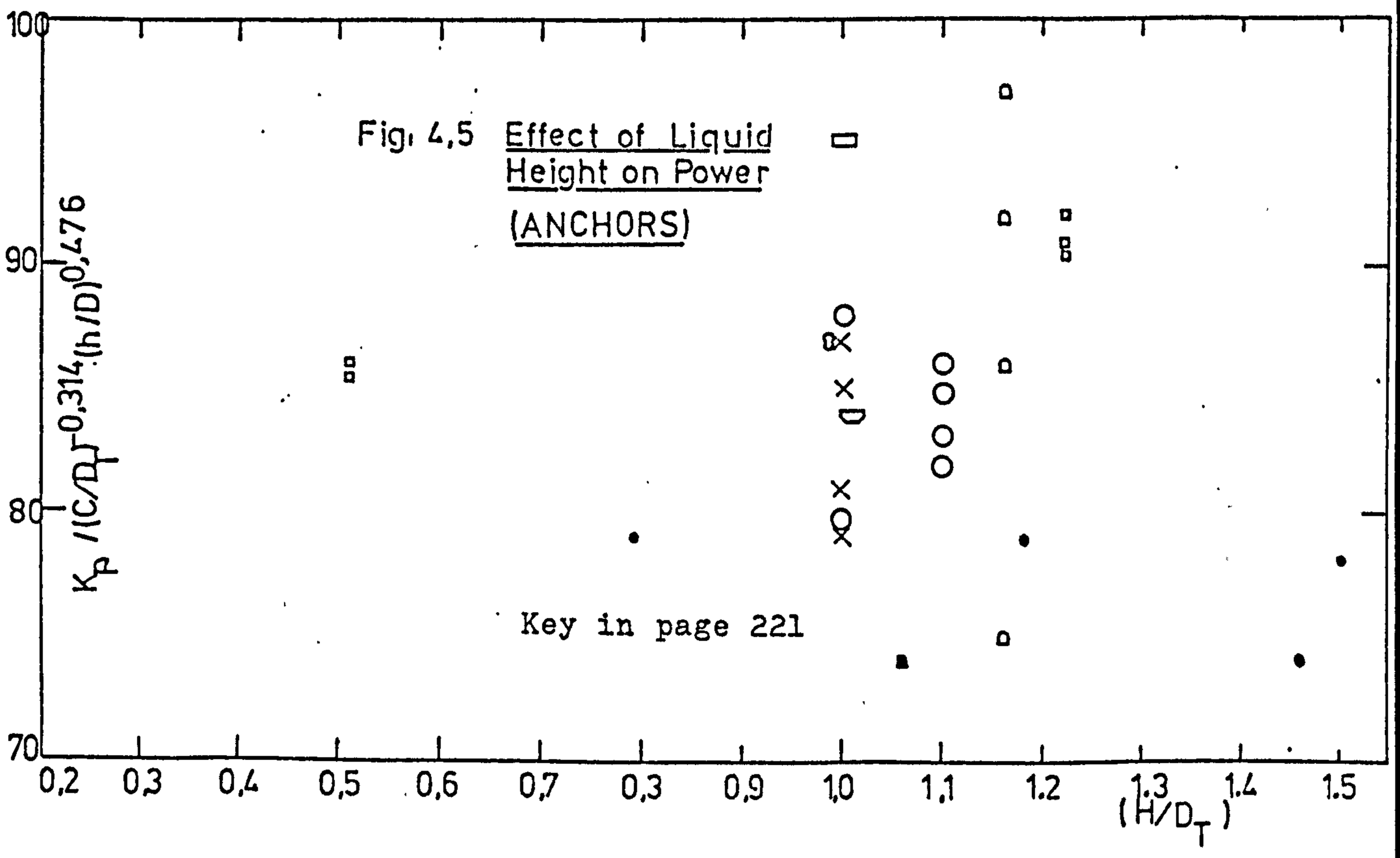

Fig. 4,5 Effect of Liquid Height on Power (ANCHORS)

Fig. 4,6 K_p(predicted)-K_p(experimental)
(ANCHORS)

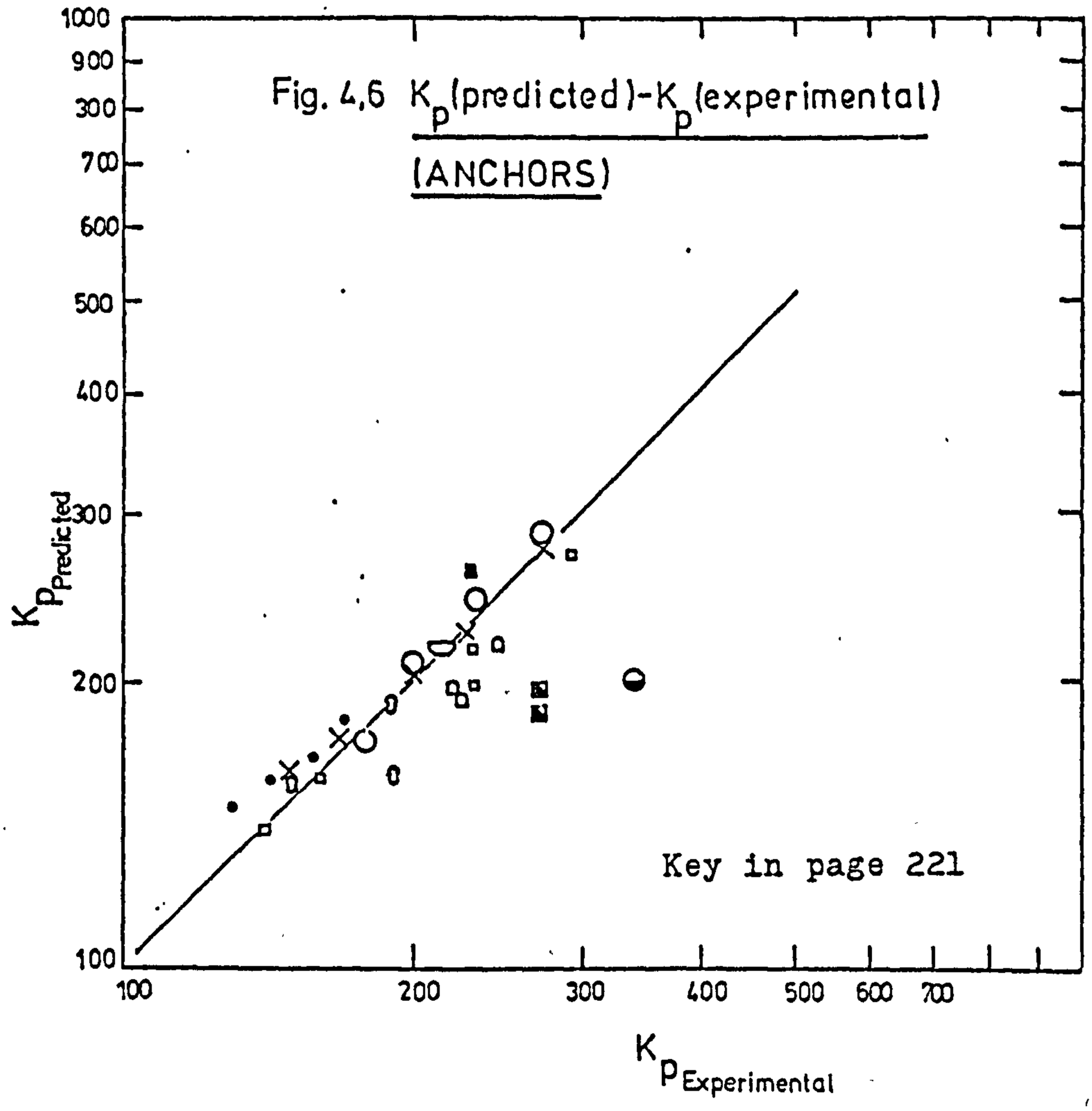

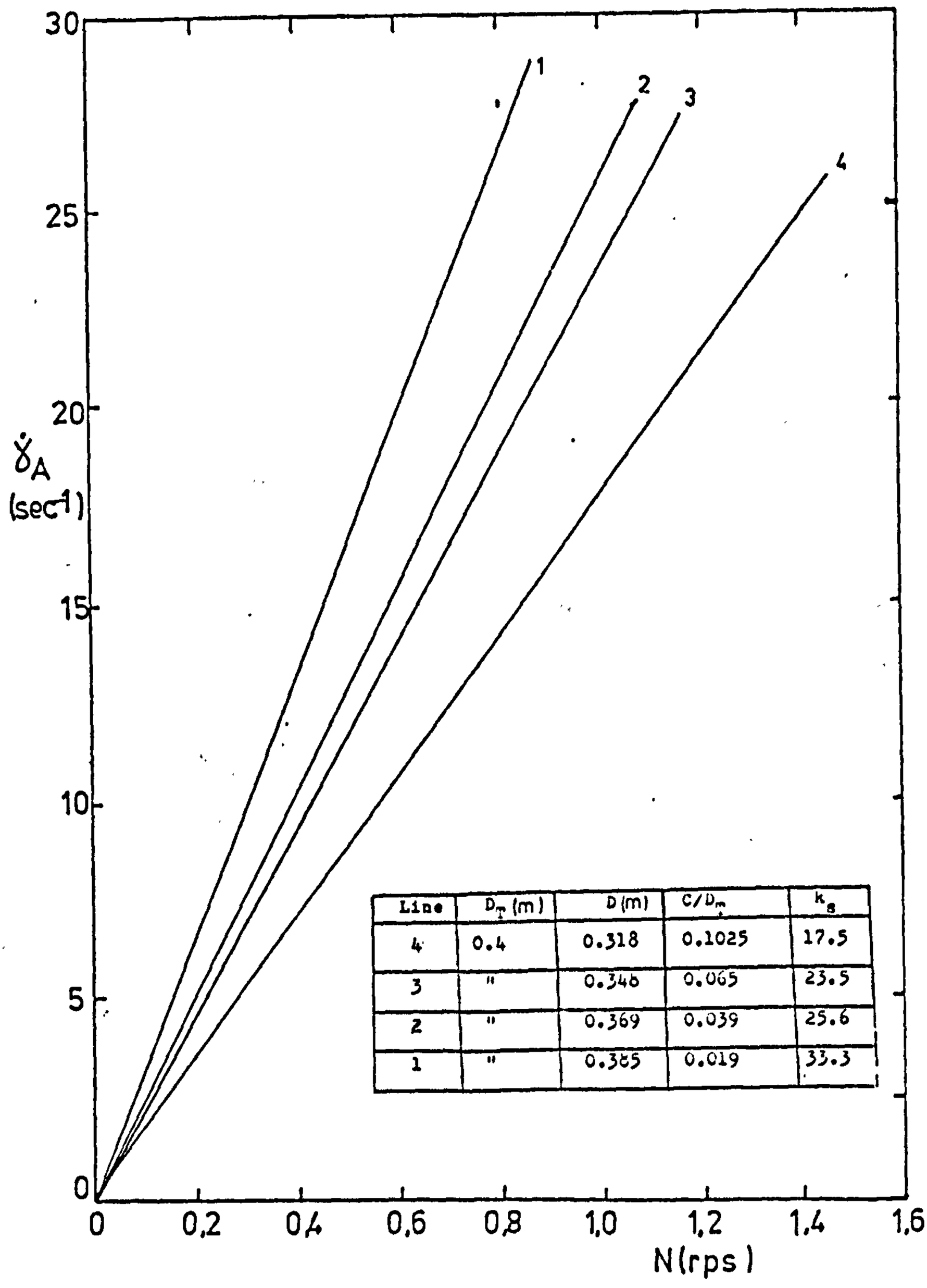

Line	D_T (m)	D (m)	C/D_T	k_s
4	0.4	0.318	0.1025	17.5
3	"	0.346	0.065	23.5
2	"	0.369	0.039	25.6
1	"	0.385	0.019	33.3

Fig. 4.7 Average Shear rate $\dot{\gamma}_A$ vs. Impeller Speed, N (ANCHORS)

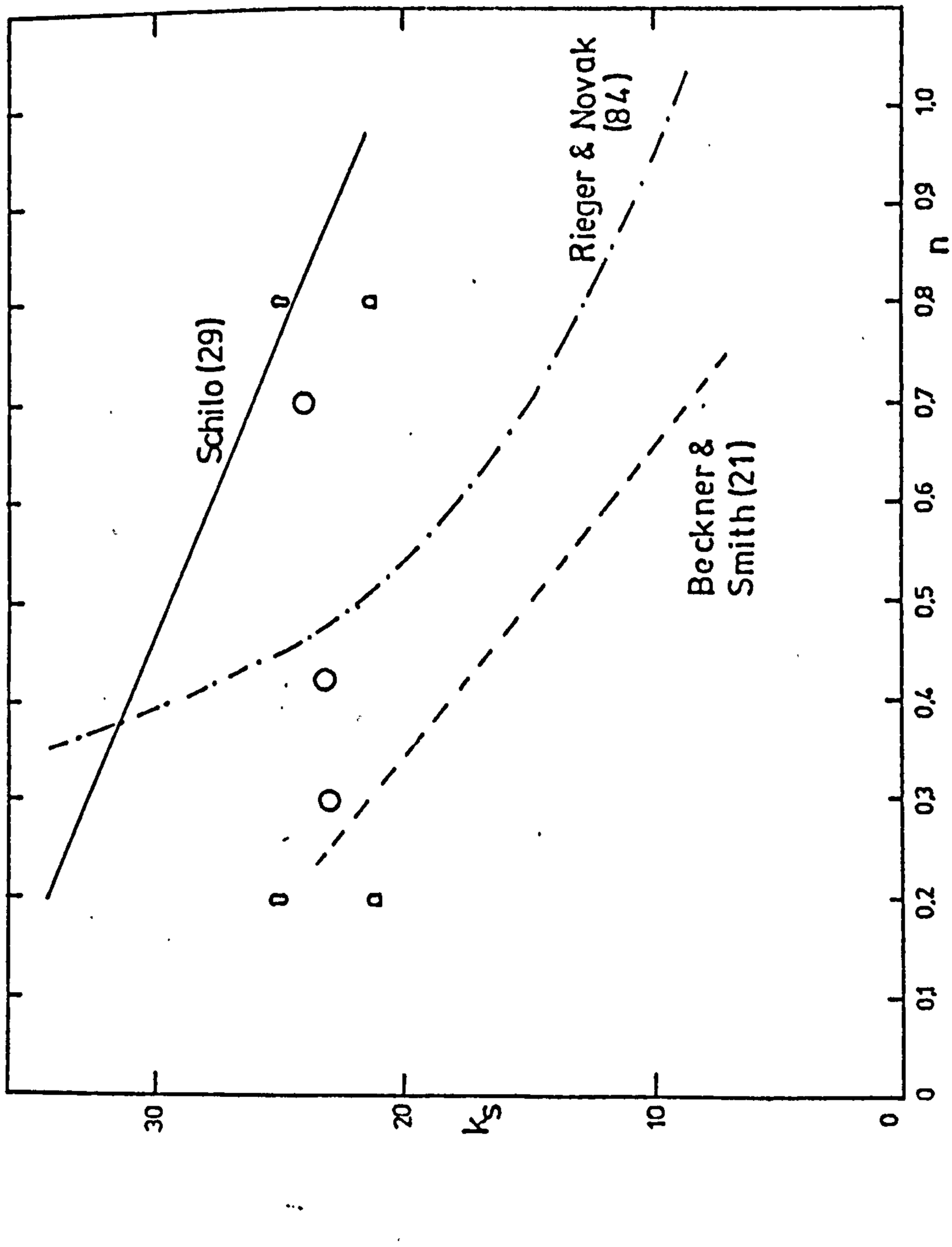

Fig. 4,8 Shear rate constant, K_S, vs. Flow index, n, for $C/D_T = 0,05$ (ANCHORS)

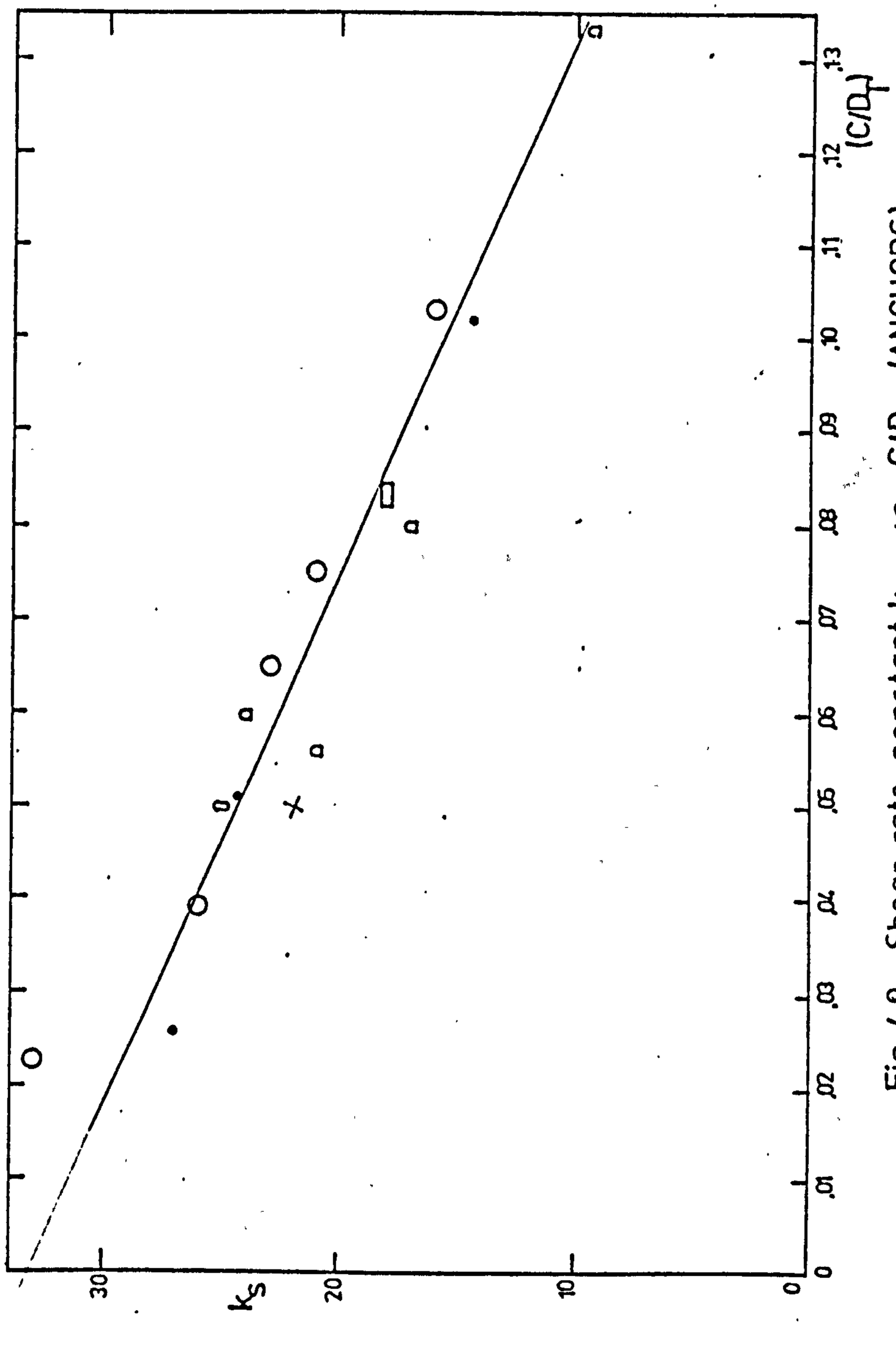

Fig. 4.9 Shear rate constant, K_s, vs C/D_T (ANCHORS)

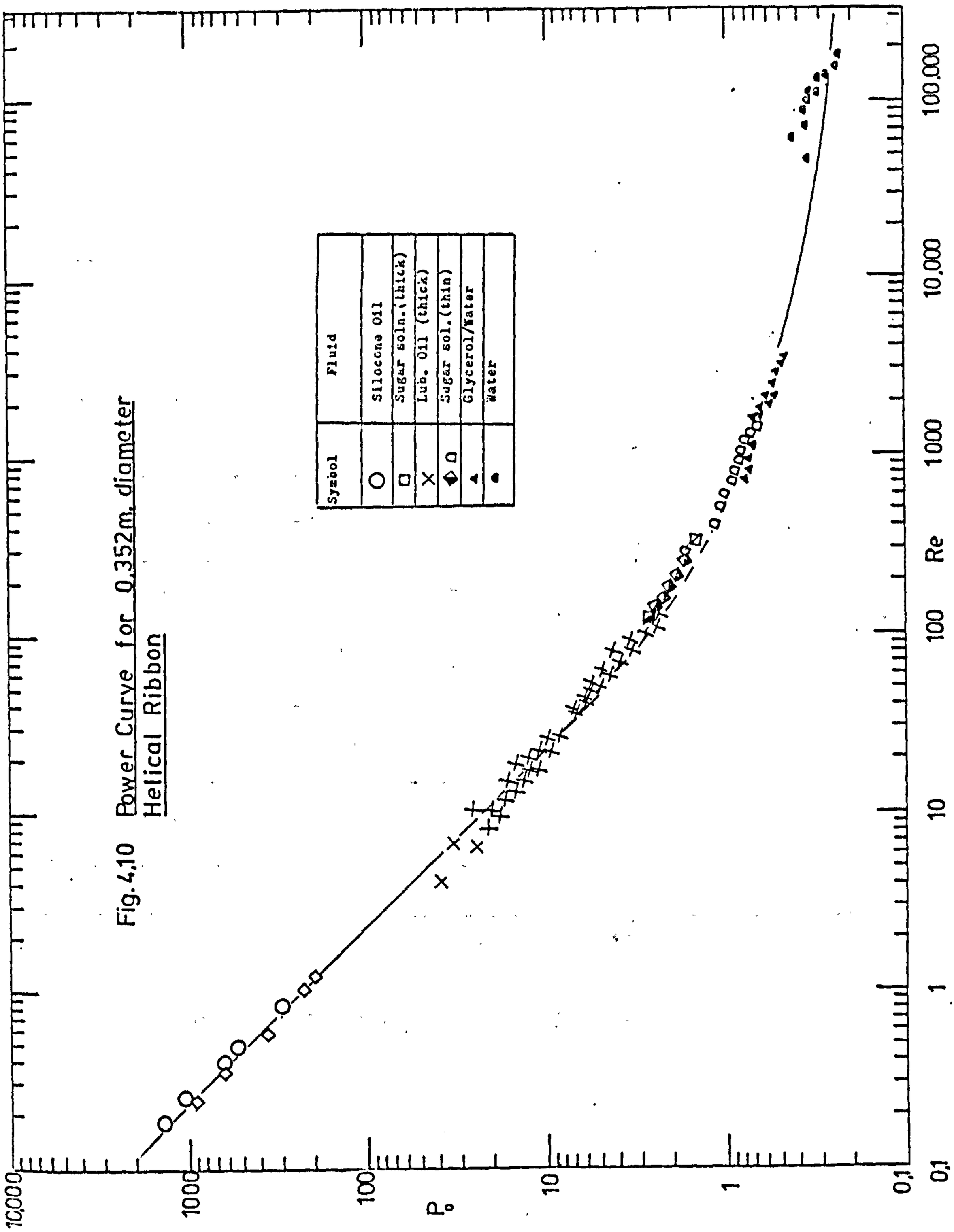

Fig. 4,10 Power Curve for 0.352m. diameter Helical Ribbon

Fig. 4.10 Power Curve for 0.352m. diameter Helical Ribbon

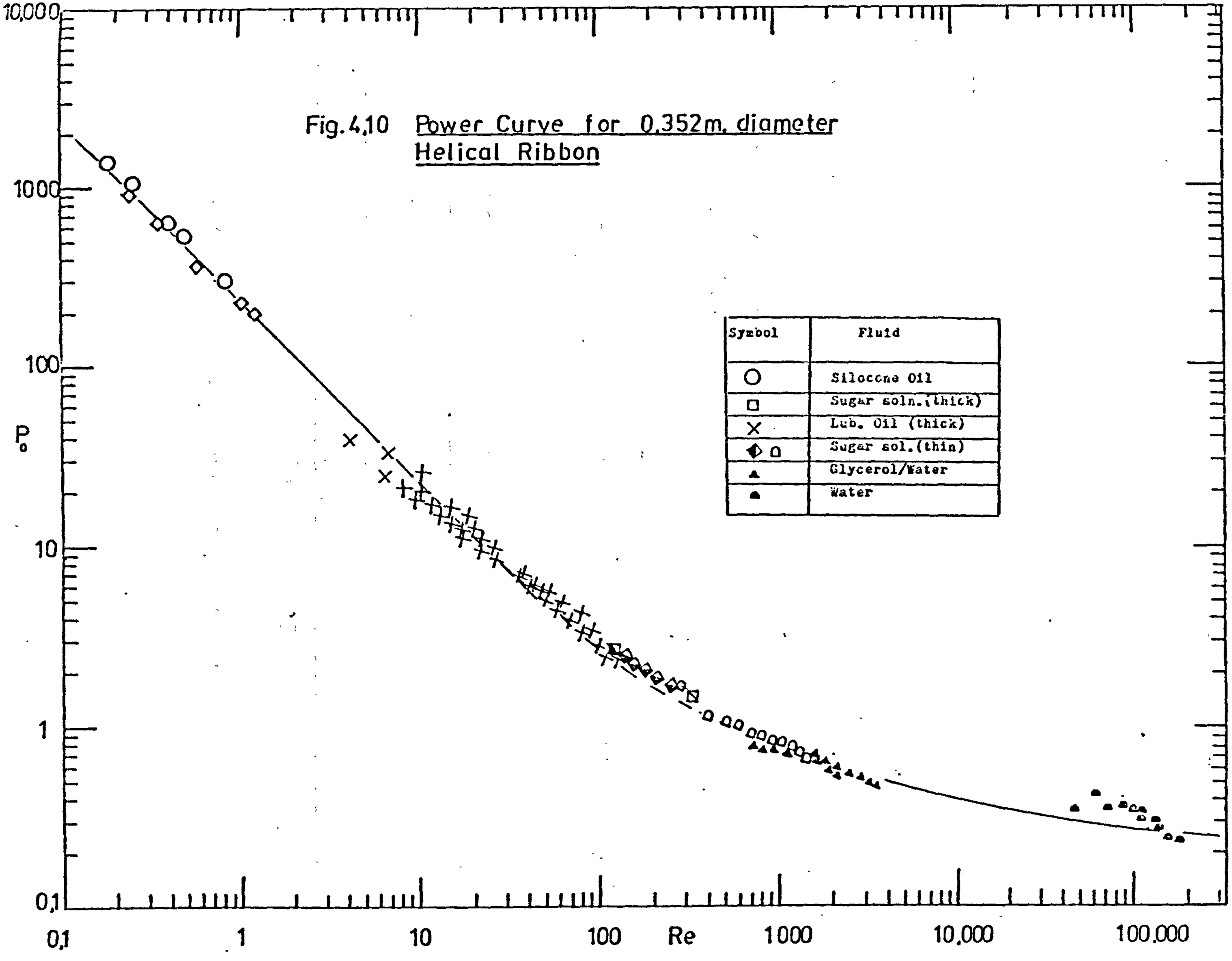

Symbol	Fluid
O	Silocone Oil
□	Sugar soln.(thick)
×	Lub. Oil (thick)
◆ ◻	Sugar sol.(thin)
▲	Glycerol/Water
●	Water

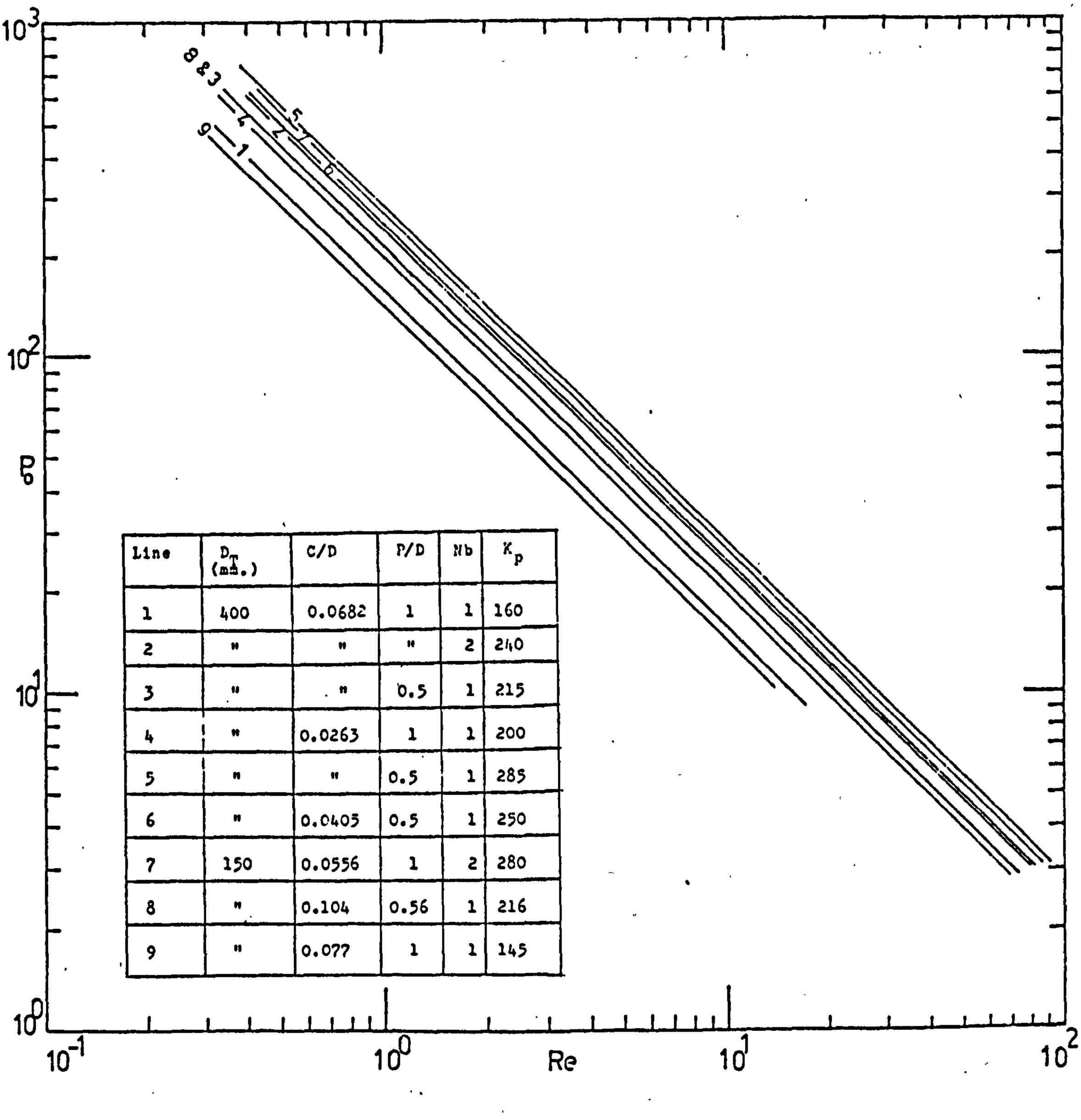

Line	D_T (mm.)	C/D	P/D	Nb	K_p
1	400	0.0682	1	1	160
2	"	"	"	2	240
3	"	"	0.5	1	215
4	"	0.0263	1	1	200
5	"	"	0.5	1	285
6	"	0.0405	0.5	1	250
7	150	0.0556	1	2	280
8	"	0.104	0.56	1	216
9	"	0.077	1	1	145

Fig. 4.11 POWER CURVES FOR RIBBONS

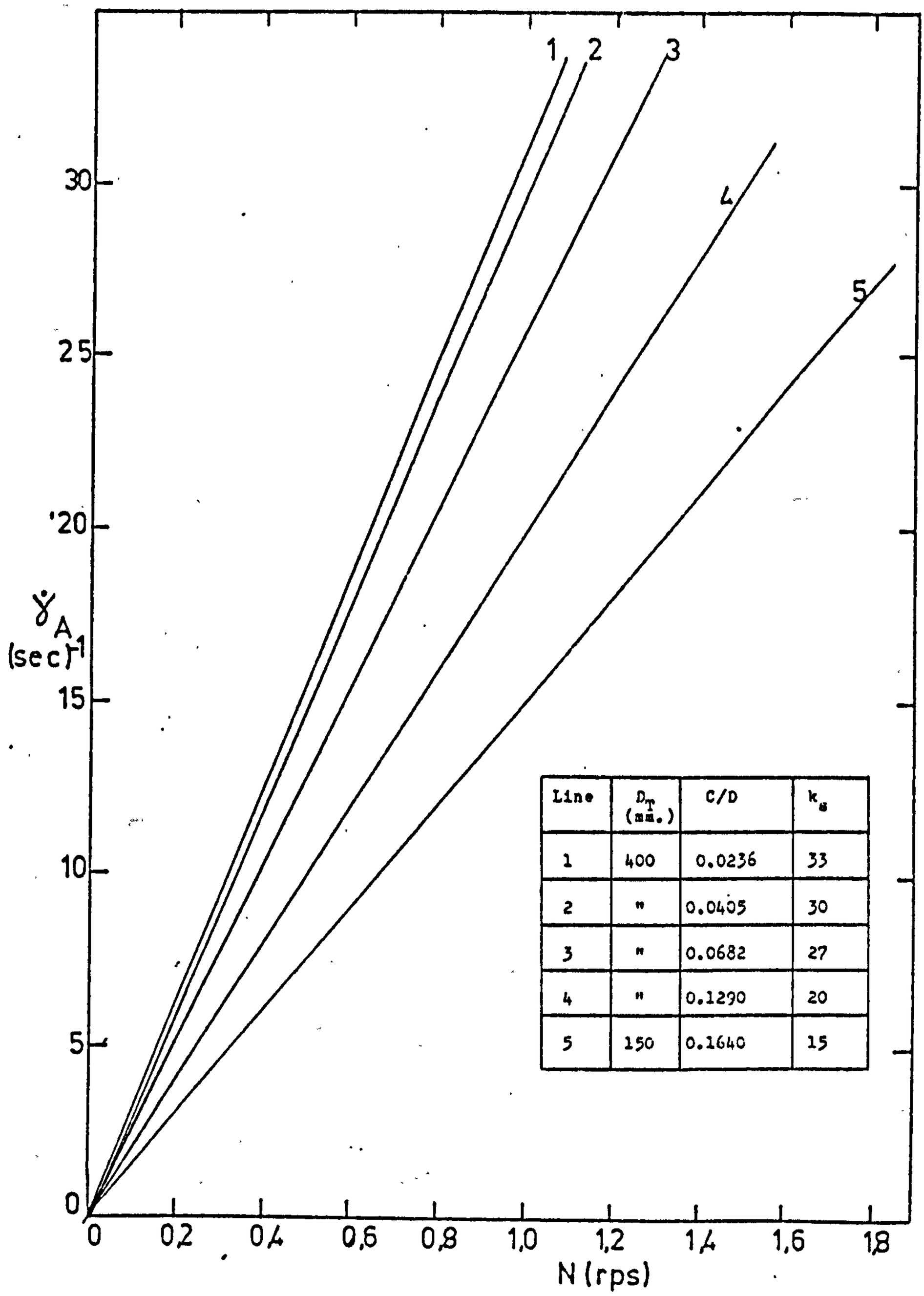

Line	D_T (mm.)	C/D	k_s
1	400	0.0236	33
2	"	0.0405	30
3	"	0.0682	27
4	"	0.1290	20
5	150	0.1640	15

Fig 4.12 Average Shear rate, $\dot{\gamma}_A$, vs. Impeller Speed, N (RIBBONS)

Fig. 4.13 Shear rate constant k_s vs. C/D (RIBBONS)

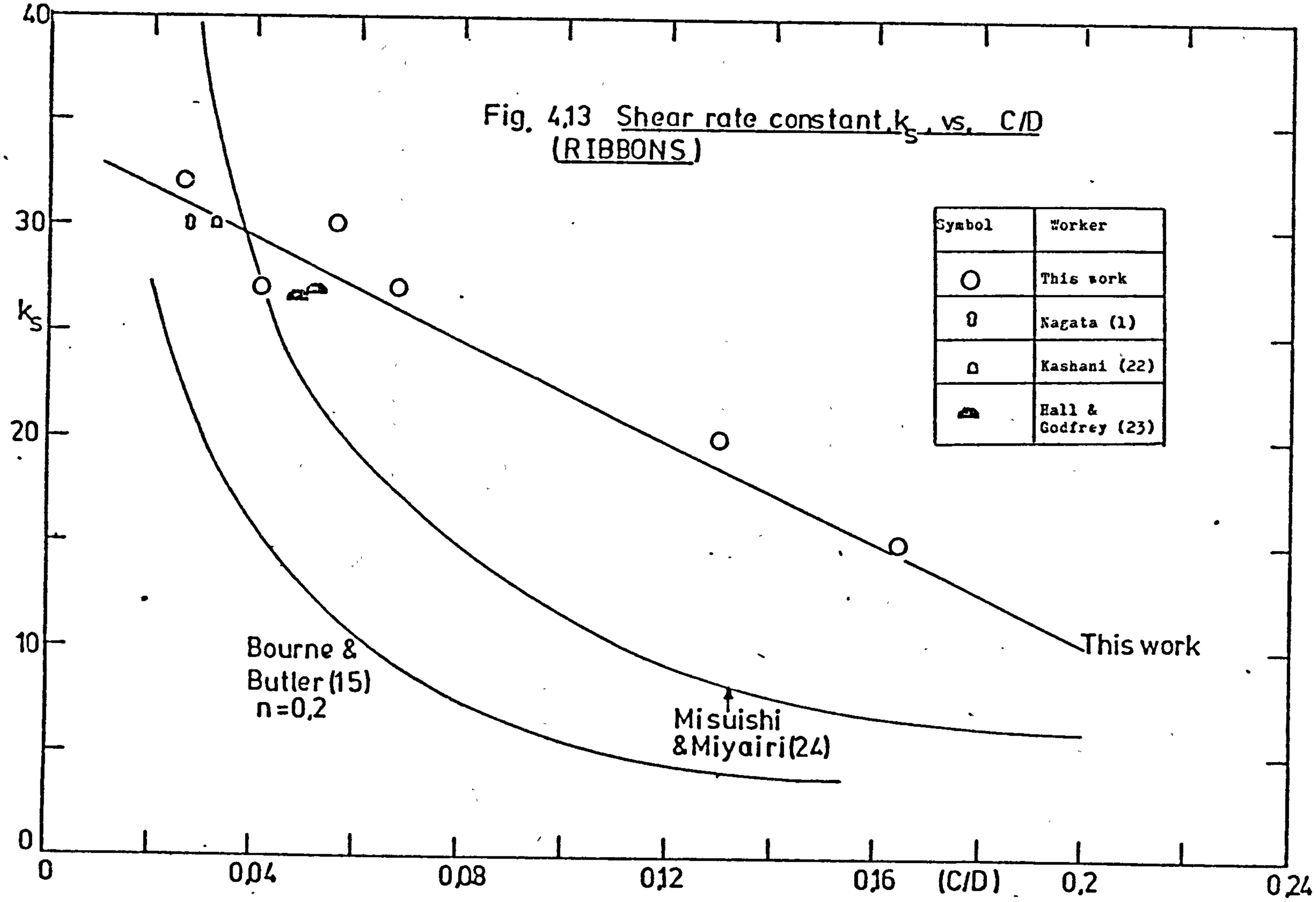

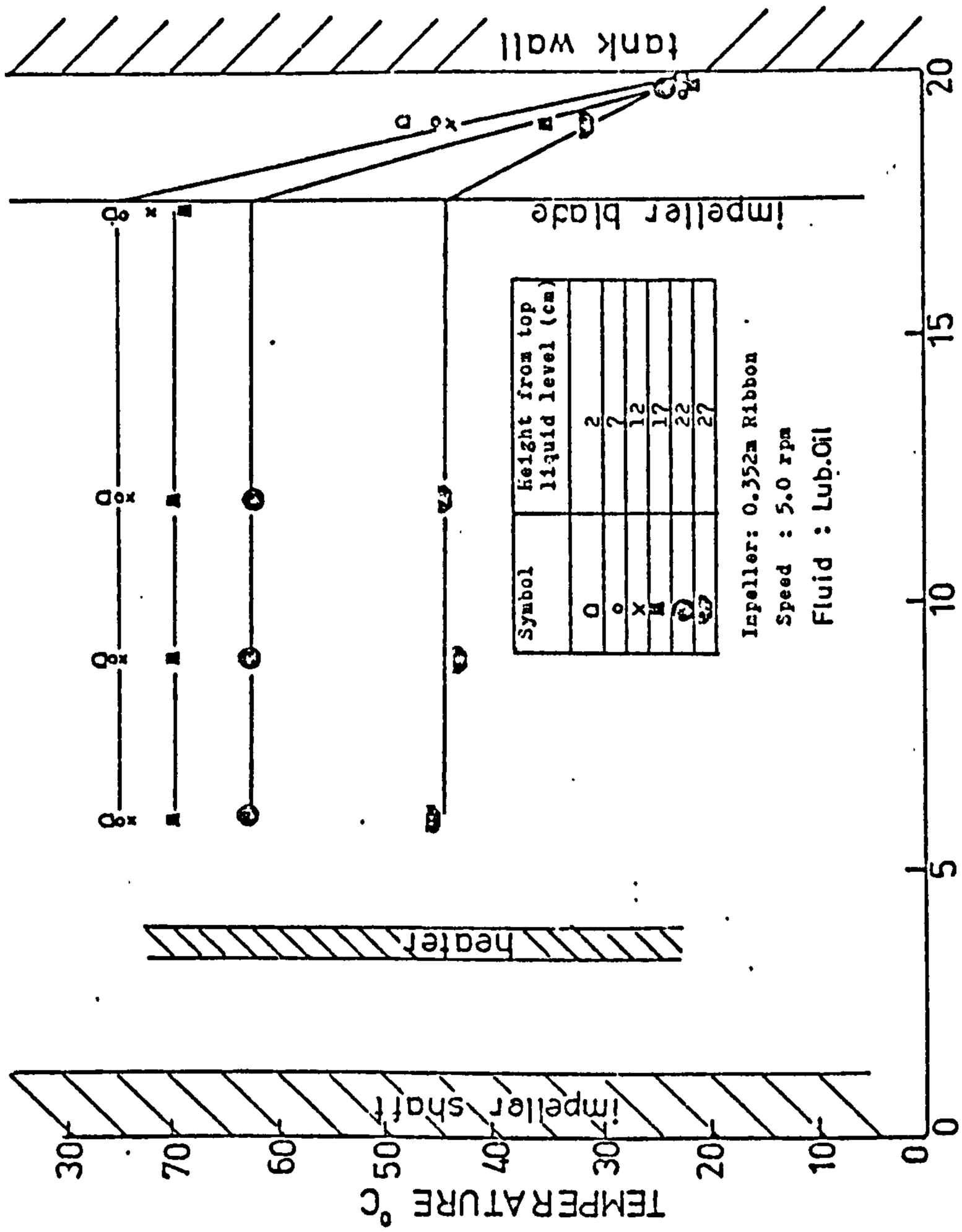

Fig. 4,14 Temperature Distribution in the 0.4m Diameter Vessel

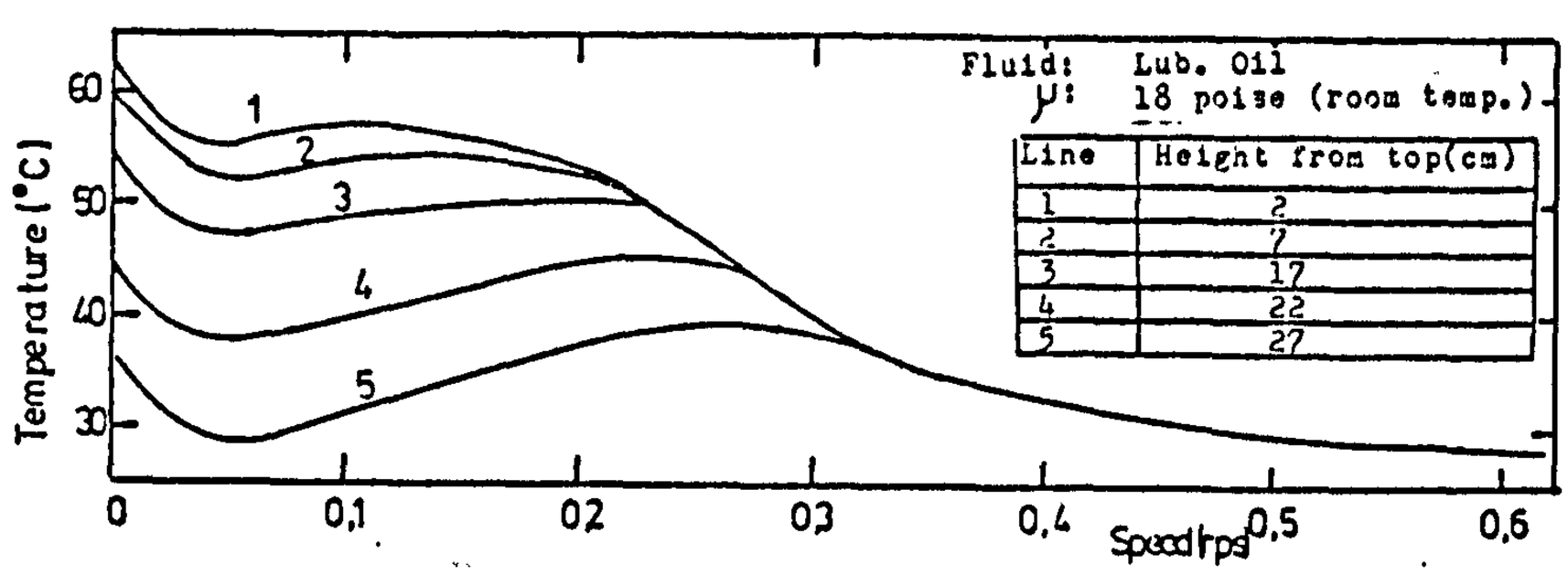

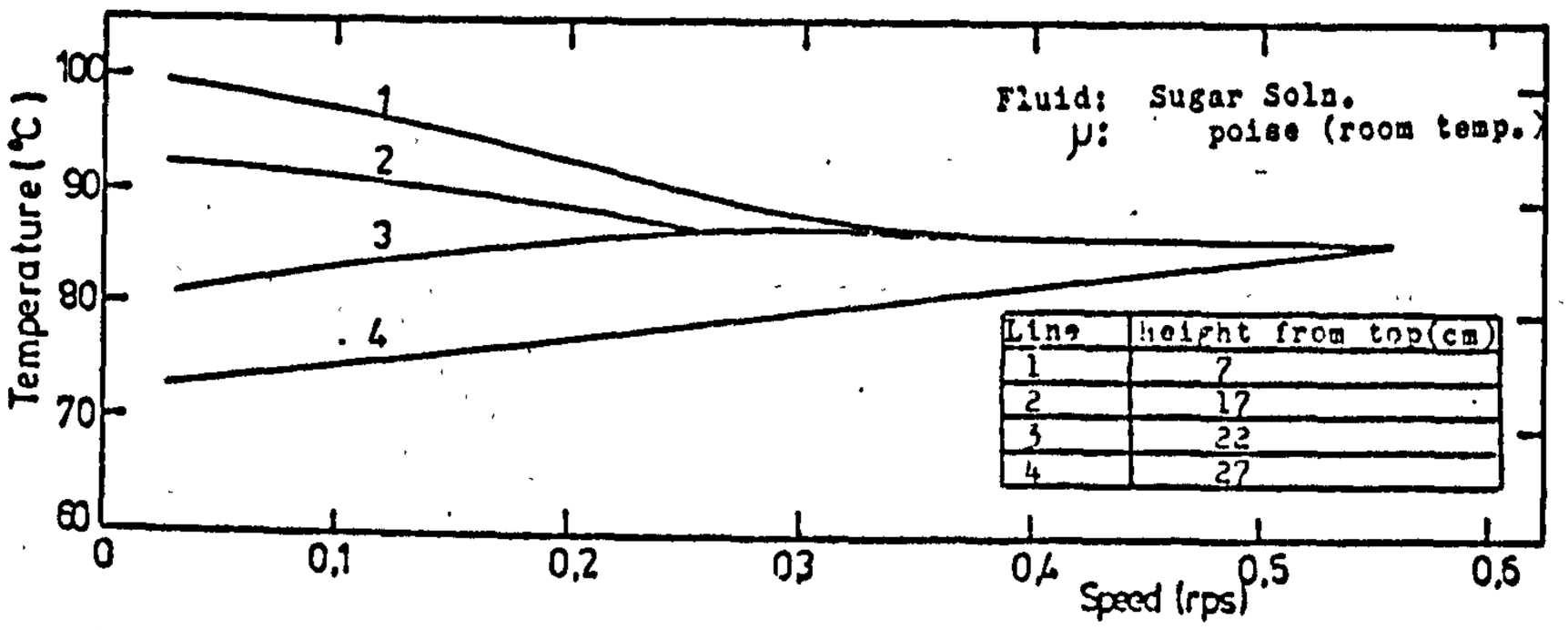

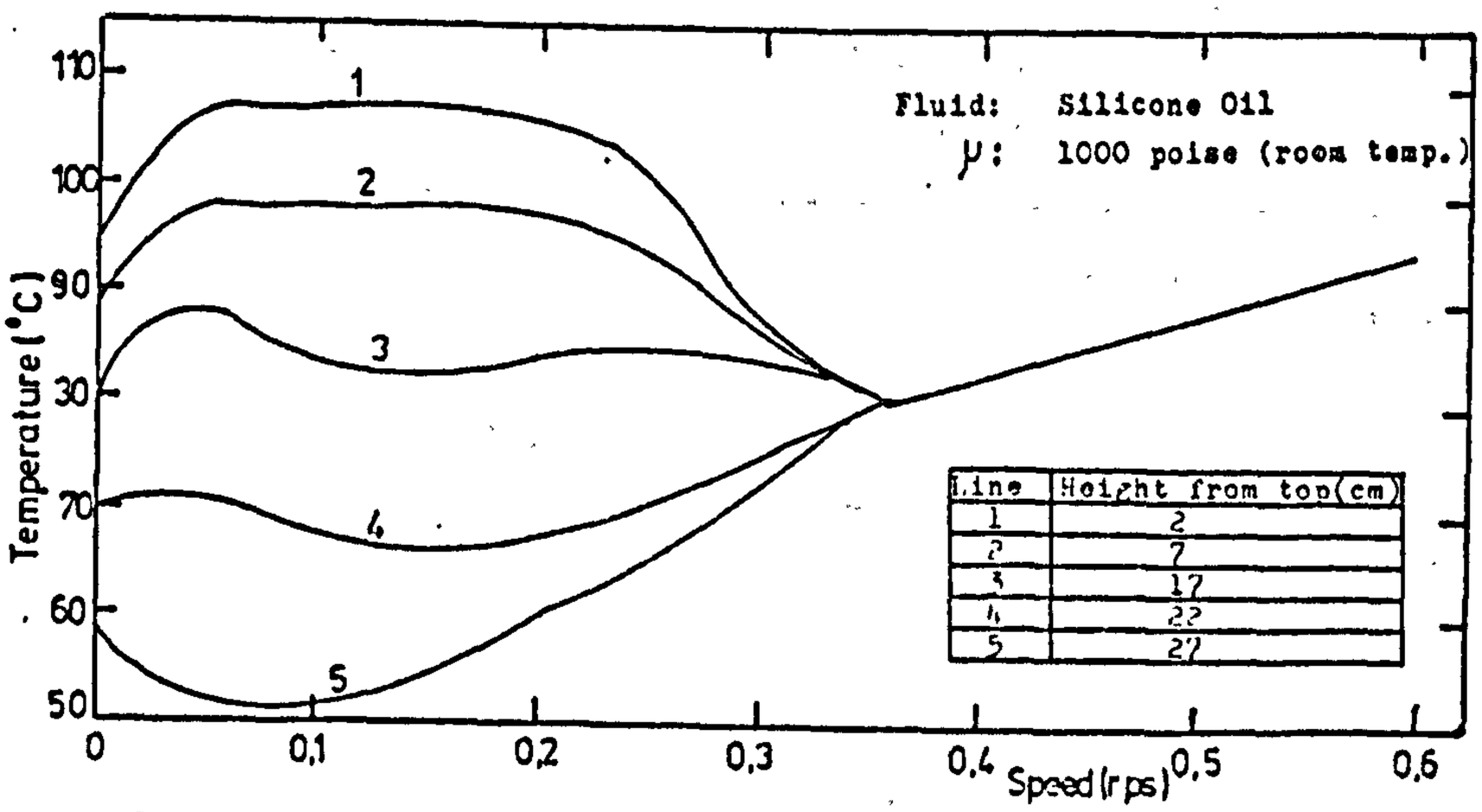

Fig 4,15

Temperature Variation in the 0,4m Vessel for the 0,548m Diameter Anchor

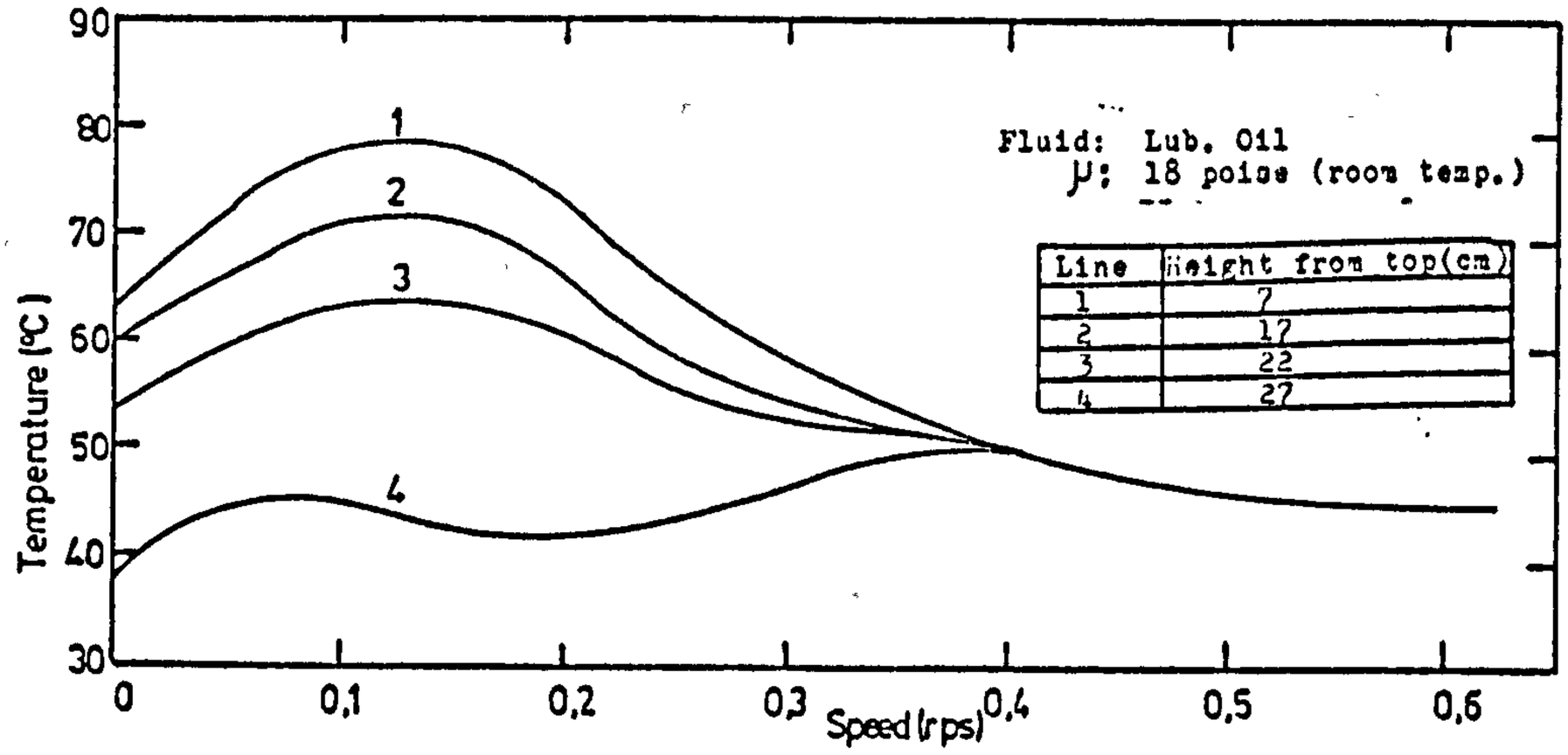

Fig 4,16 Temperature Variation in the 0,4m Vessel for the 0,352m Diameter Ribbon

Fig. 4.17

Critical Reynolds Number vs. Prandtl Number fot the 0.352m Diameter Helical Ribbon

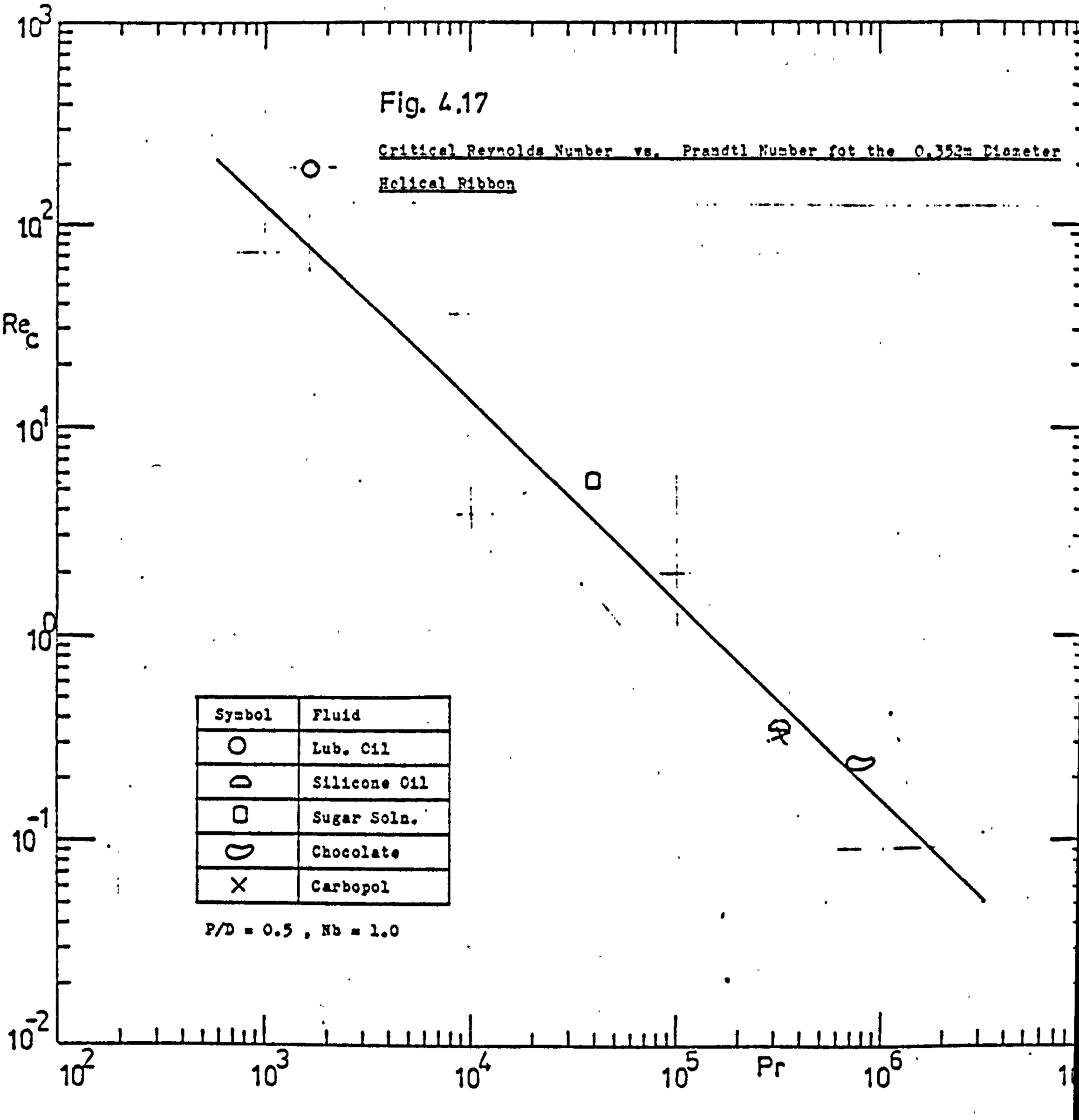

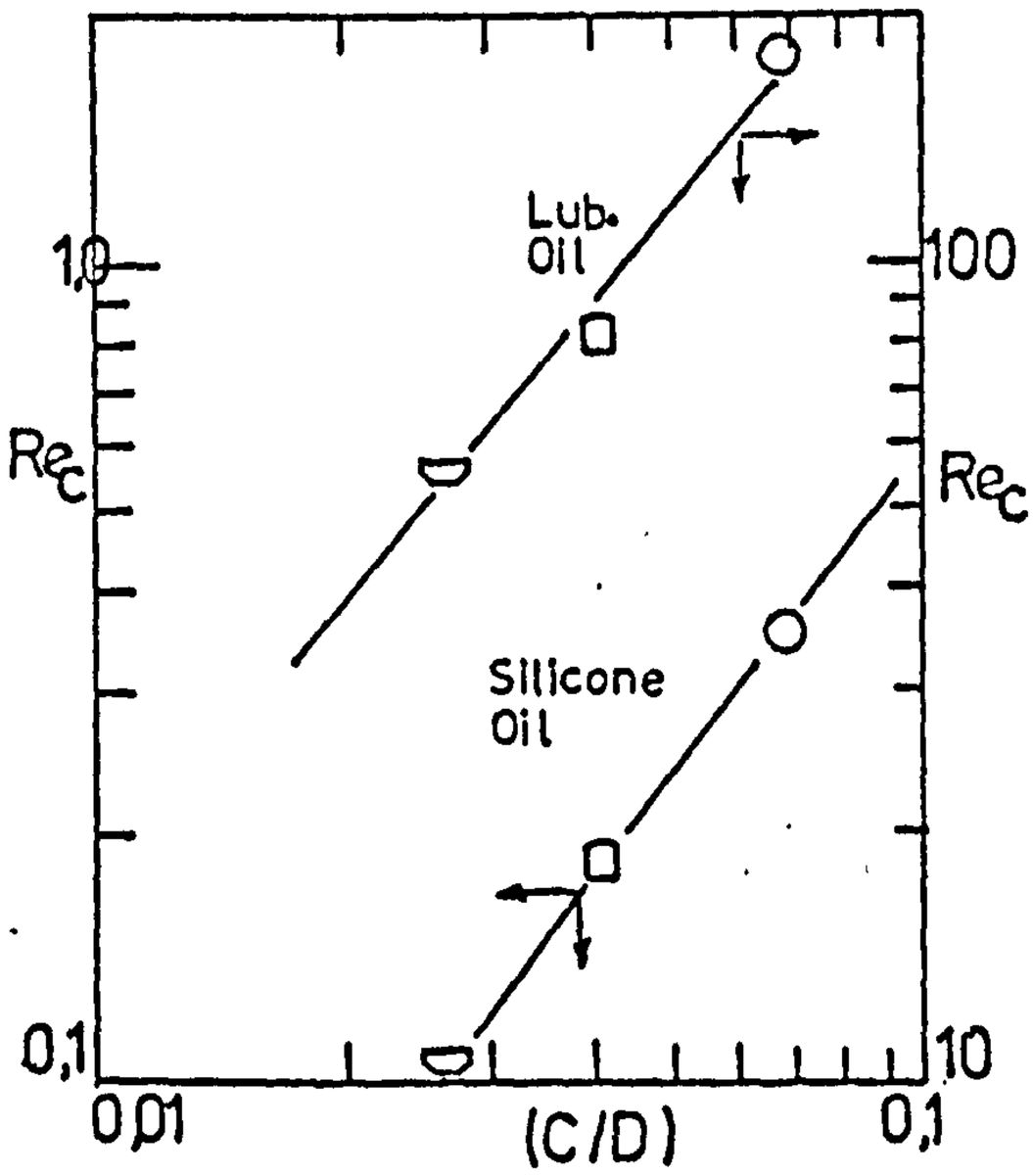

Fig. 4,18

Effect of Clearance, C/D, on Critical Reynolds Number, Re_c, for Helical Ribbon Impellers.

Symbol	D(m)	C/D
○	0.352	0.0682
□	0.370	0.0405
⌓	0.380	0.0285

Fig. 4,19 Effect of Impeller Pitch, on Re_c for Ribbons.

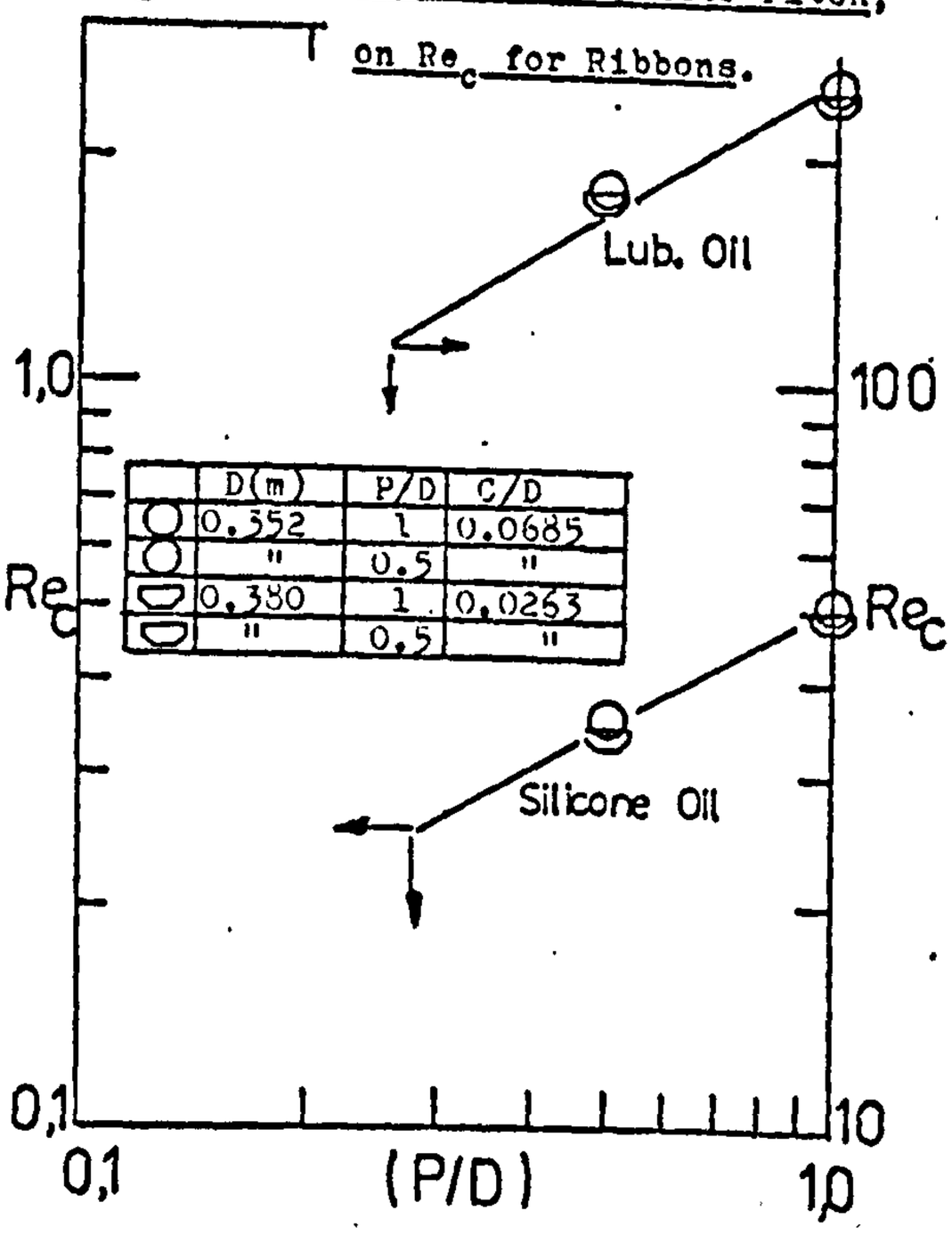

	D(m)	P/D	C/D
○	0,352	1	0,0685
○	"	0,5	"
⌓	0,380	1	0,0263
⌓	"	0,5	"

Fig. 4,20 Effect of Number of Blades, on Re_c for Ribbons.

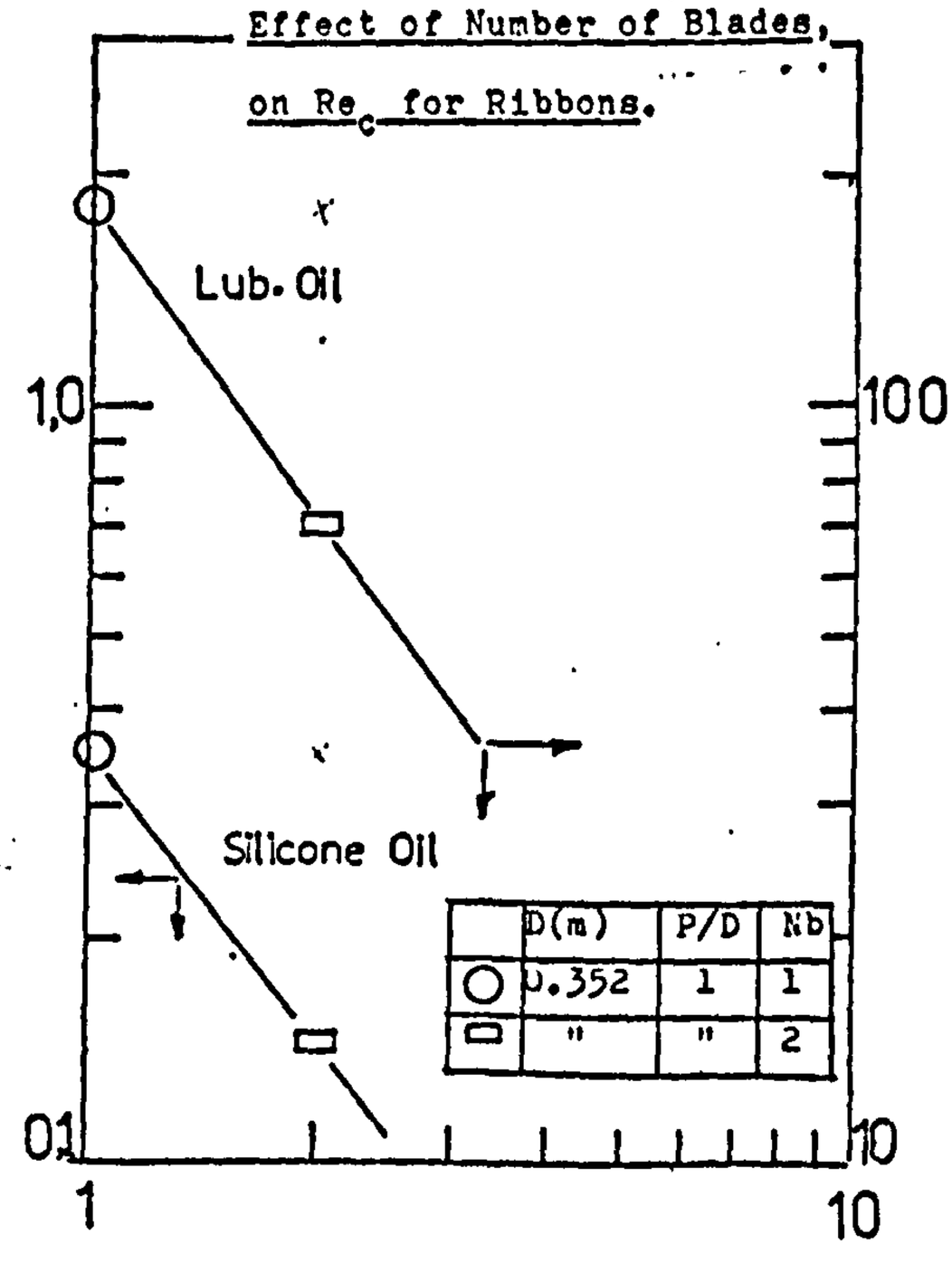

	D(m)	P/D	Nb
○	0.352	1	1
□	"	"	2

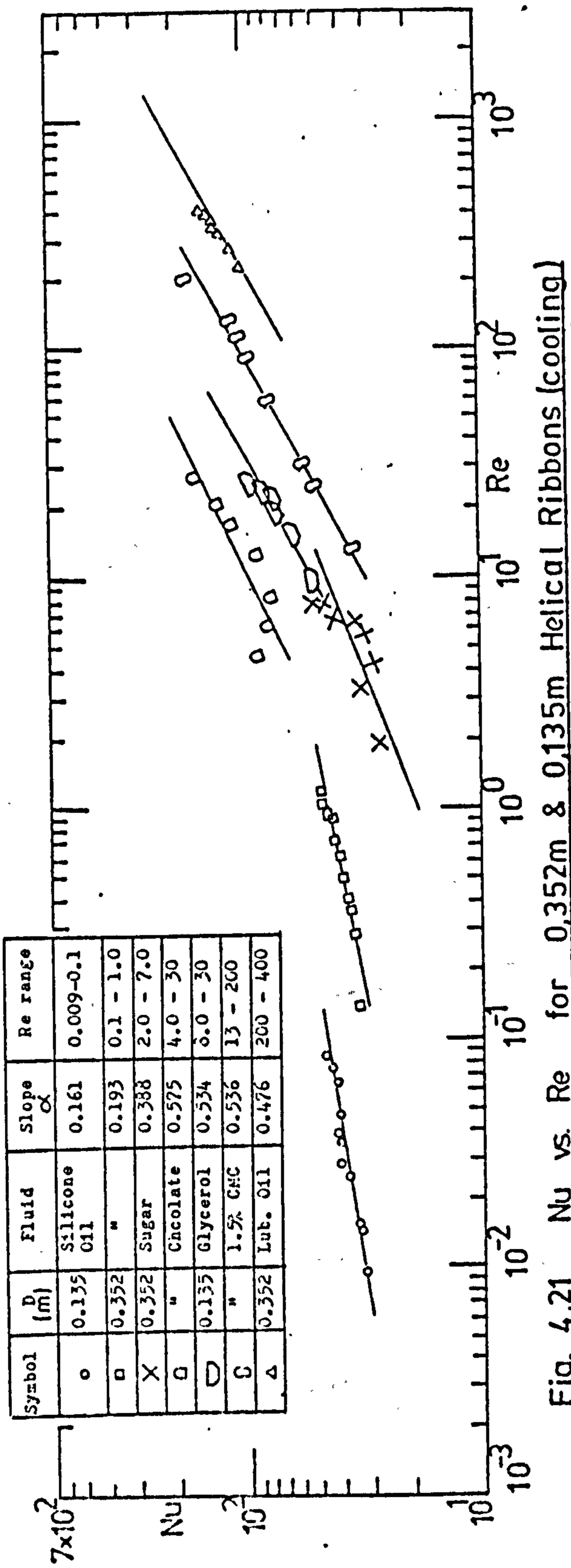
Nu vs. Re for 0,352m & 0,135m Helical Ribbons (cooling)
Nu
Re
7×10^2
10^2
10^1
10^0
10^-1
10^-2
10^-3
10^3
Symbol	D (m)	Fluid	Slope α	Re range
o	0.135	Silicone Oil	0.161	0.009-0.1
□	0.352	"	0.193	0.1 - 1.0
X	0.352	Sugar	0.388	2.0 - 7.0
◇	"	Chcolate	0.575	4.0 - 30
D	0.135	Glycerol	0.534	5.0 - 30
C	"	1.5% CMC	0.536	13 - 200
Δ	0.352	Lub. Oil	0.476	200 - 400

Fig. 4,21

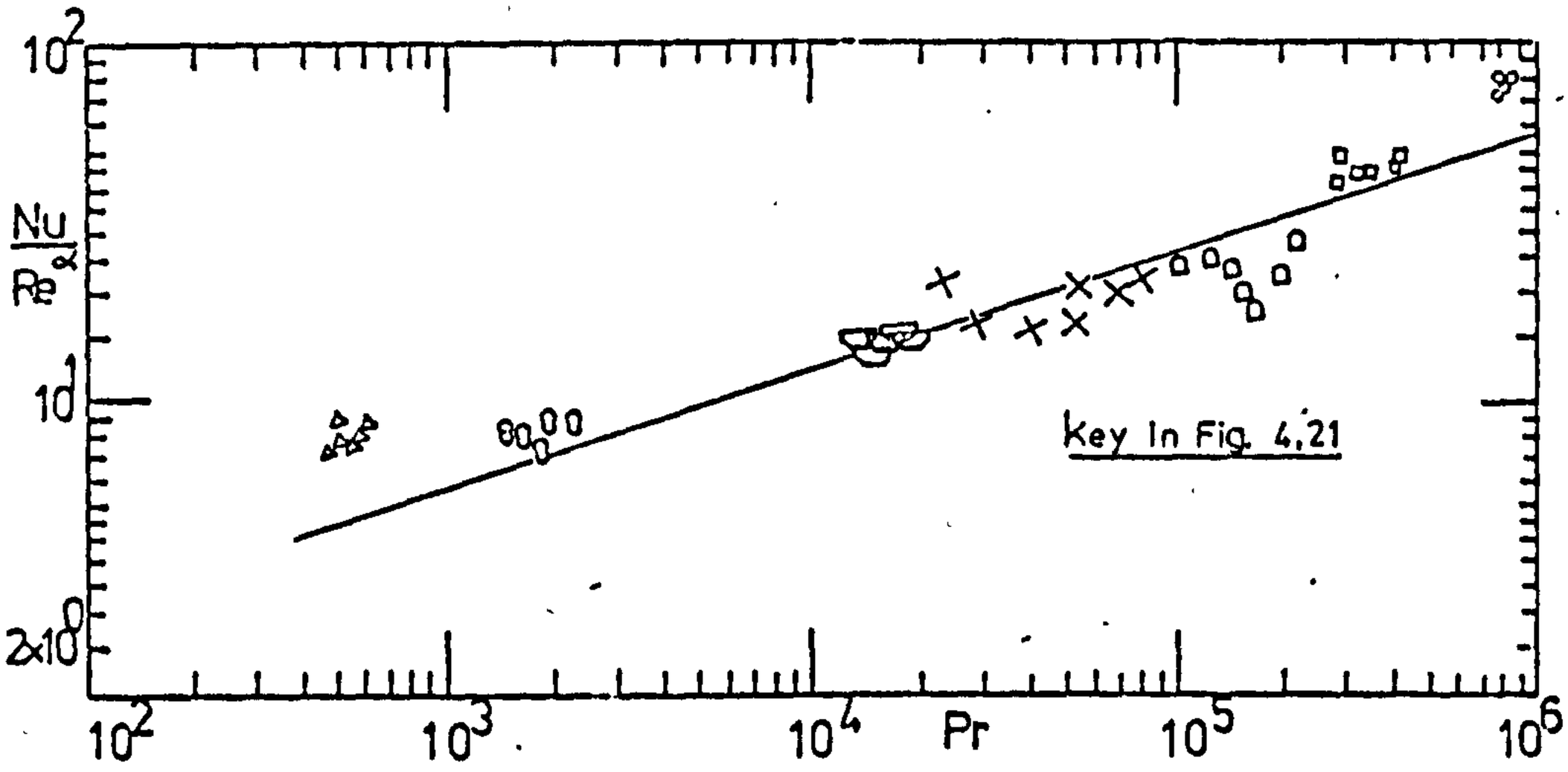

Fig. 4,22 Pr correlation for 0,352m & 0,135m diameter Helical Ribbons

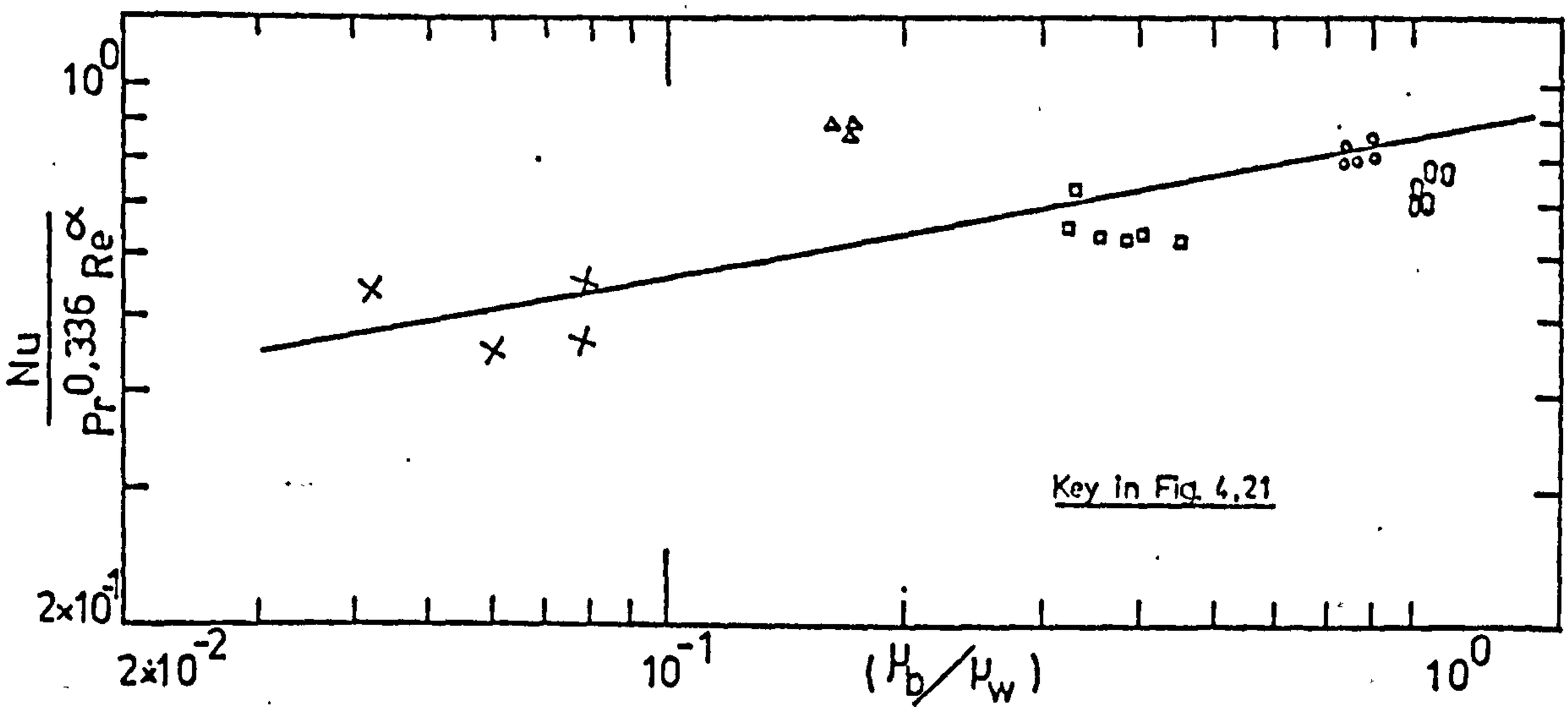

Fig. 4,23 Viscosity ratio correlation for 0,352m & 0,135m Helical Ribbons

Fig. 4,24 HEAT TRANSFER CORRELATION FOR HELICAL RIBBONS

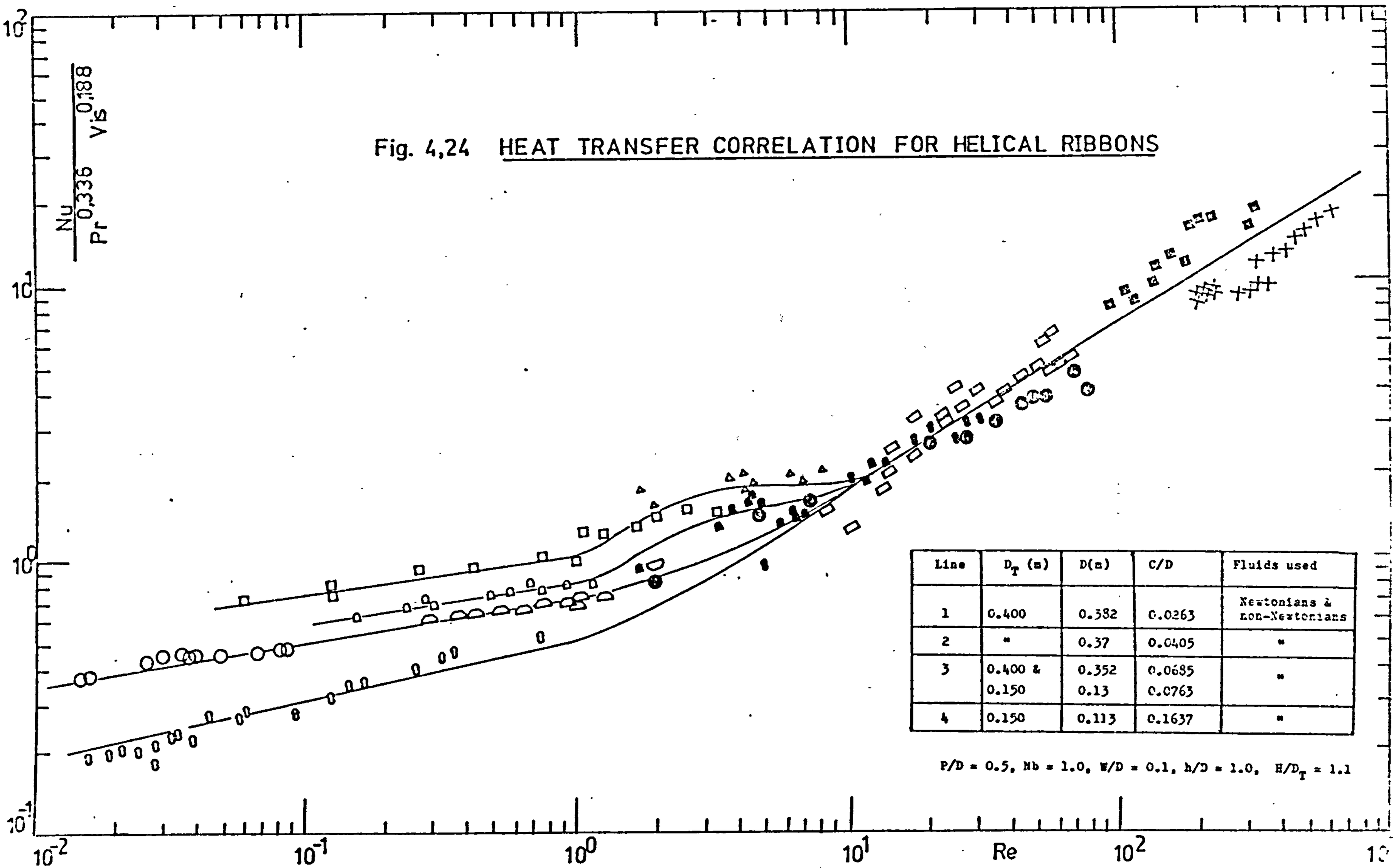

Line	D_T (m)	D(m)	C/D	Fluids used
1	0.400	0.382	0.0263	Newtonians & non-Newtonians
2	"	0.37	0.0405	"
3	0.400 & 0.150	0.352 0.13	0.0685 0.0763	"
4	0.150	0.113	0.1637	"

P/D = 0.5, Nb = 1.0, W/D = 0.1, h/D = 1.0, H/D_T = 1.1

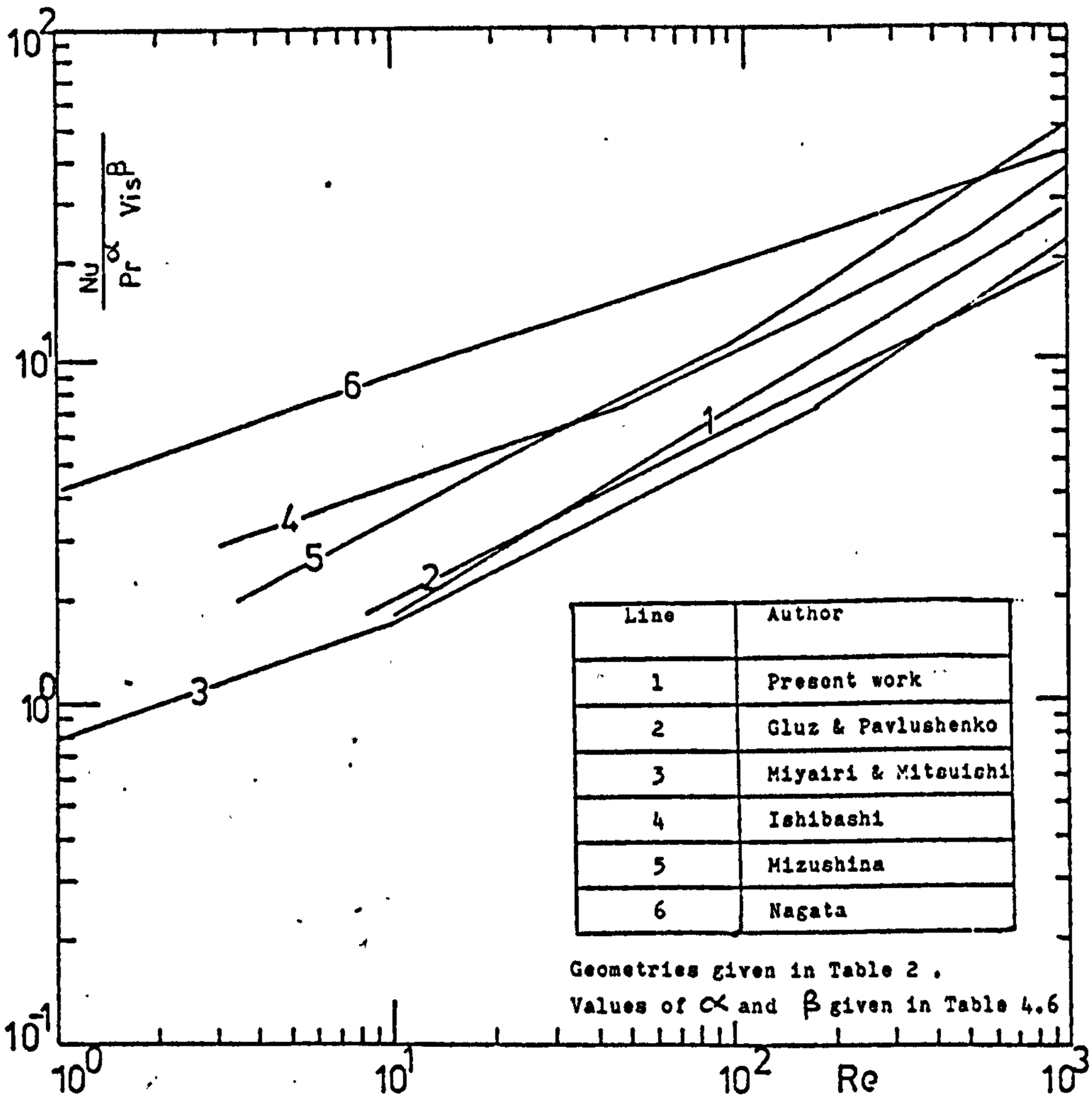

Fig. 4,25 Heat transfer correlation for helical ribbon impellers by several authors.

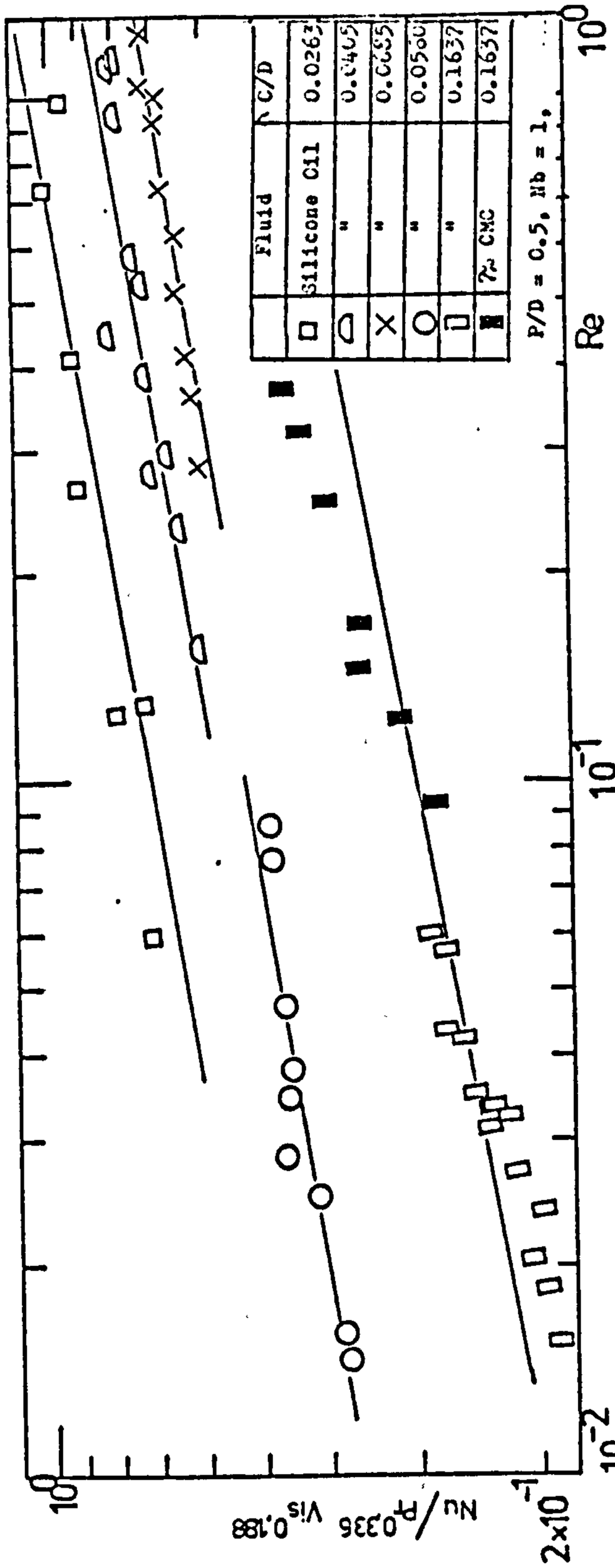

Fig. 26A Effect of Clearance on Heat Transfer Coefficient in the Laminar Region for Anchor Impellers.

Fig 4,26B Effect of Clearance on Heat Transfer Coefficient in the Laminar Region for Helical Ribbon Impellers. Data evaluated at Re= 1.0

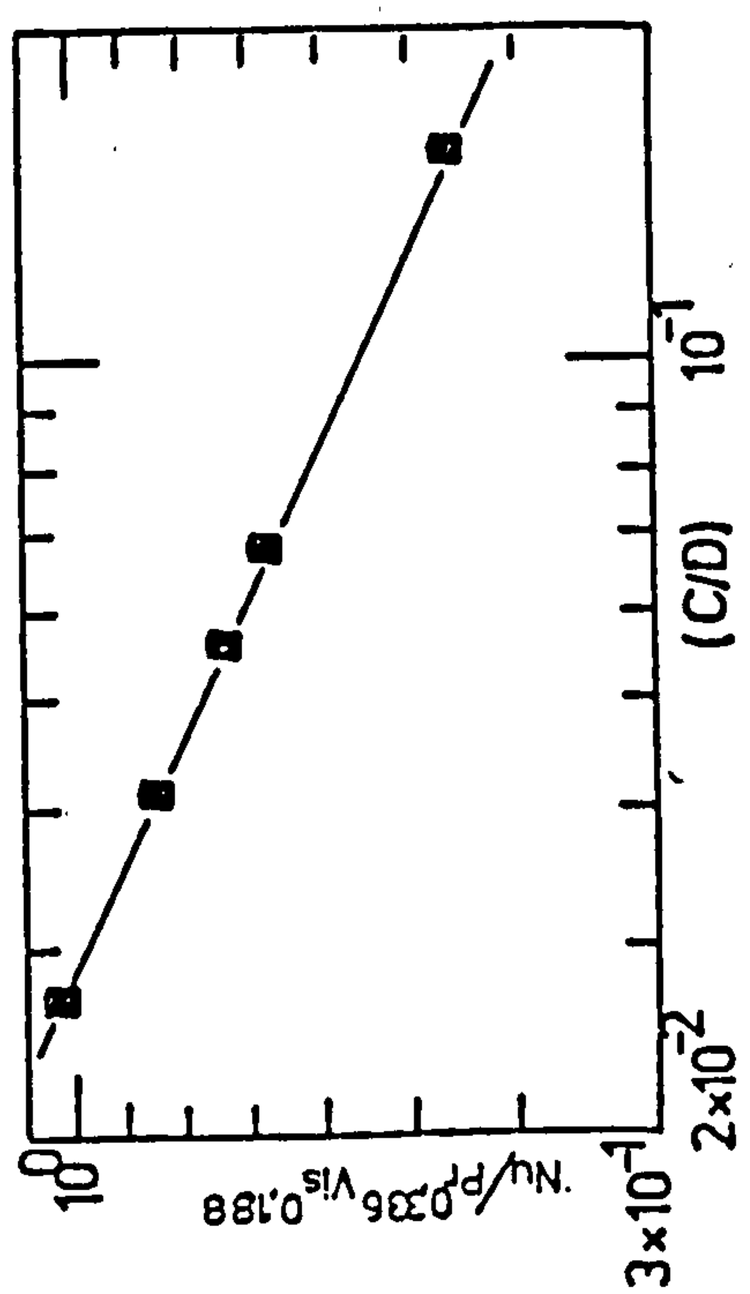

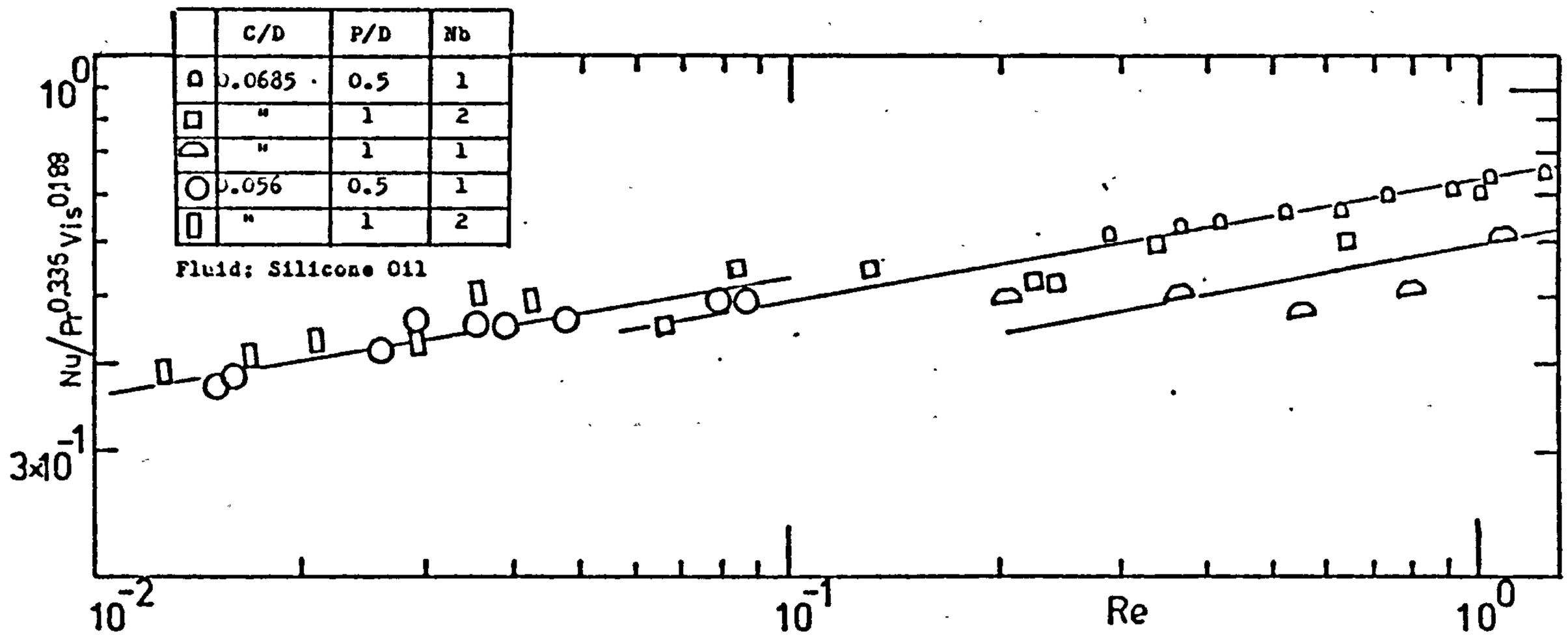

Fig. 27A Effect of Impeller Pitch, P/D, and Impeller Number of Blades, Nb, on Heat Transfer Correlation in the Laminar Region for 0,352m Diameter Ribbon

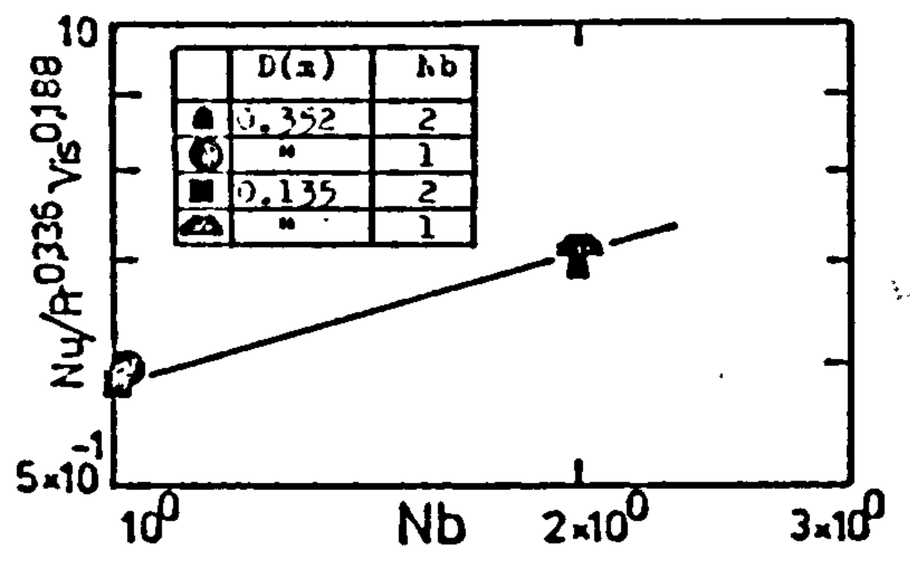

Fig 4,27B

Effect of Number of Blades, Nb, on Heat Tranefer Coefficient in Laminar Region for 0,352m Ribbon Data evaluated at Re = 1,0

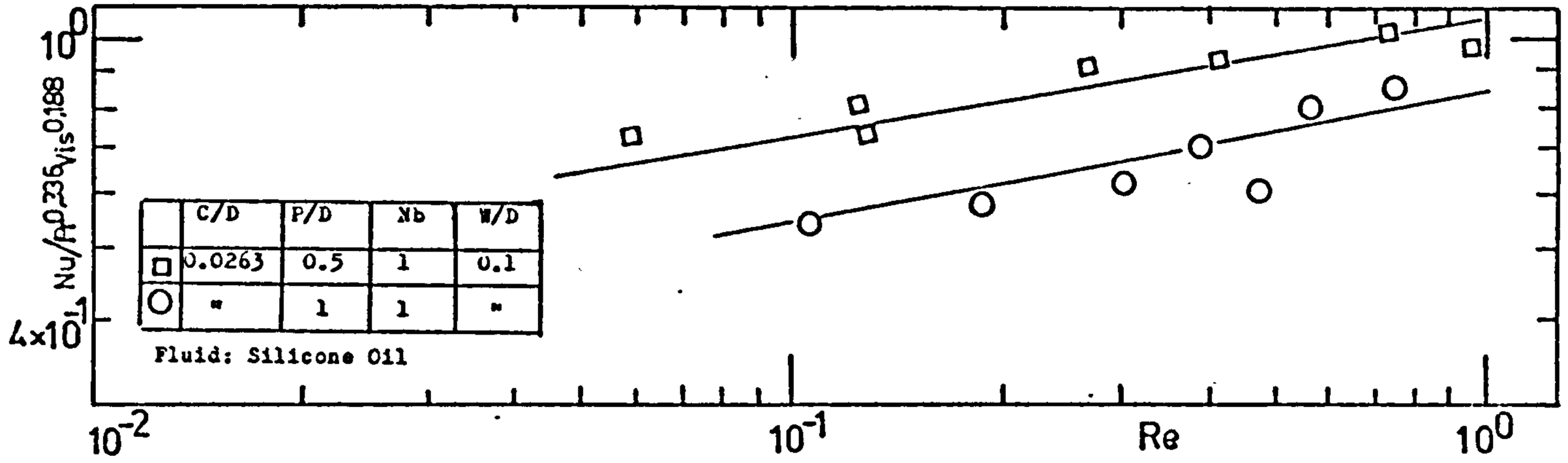

Fig. 28A Effect of Impeller Pitch, P/D, on Heat Transfer Correlation in the Laminar Region for 0.382m Diameter Helical Ribbon.

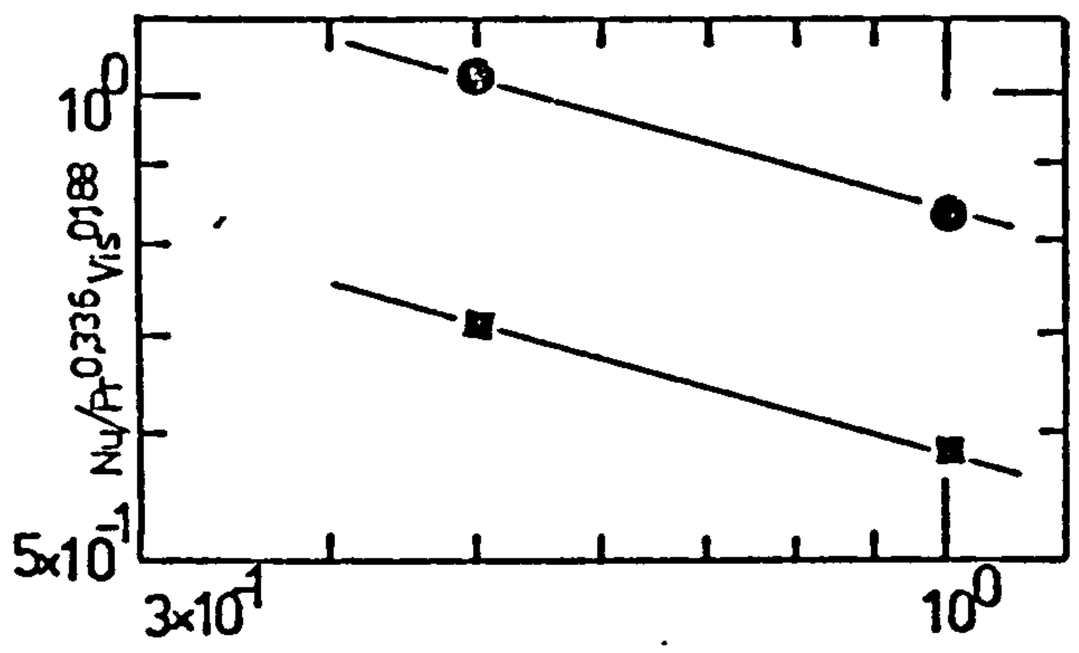

Fig 4,28 B

Effect of Impeller Pitch, P/D, on Heat Transfer Coefficent in the Laminar Region for 0.352m Ribbon Data evaluated at Re = 1,0

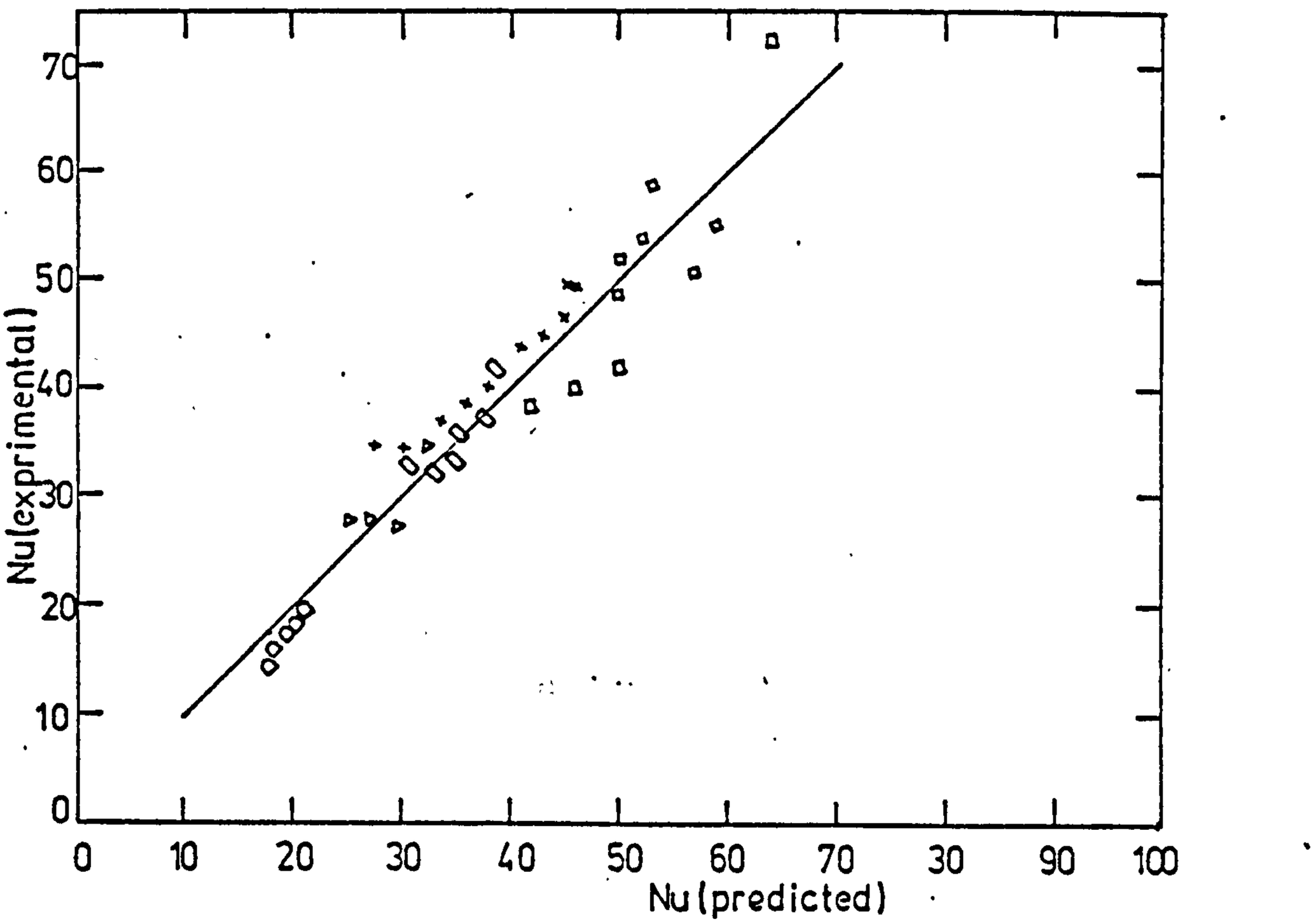

Fig 4,29 Experimental Nu against Predicted Nu for Some Helical Ribbon Impellers in the Laminar Region

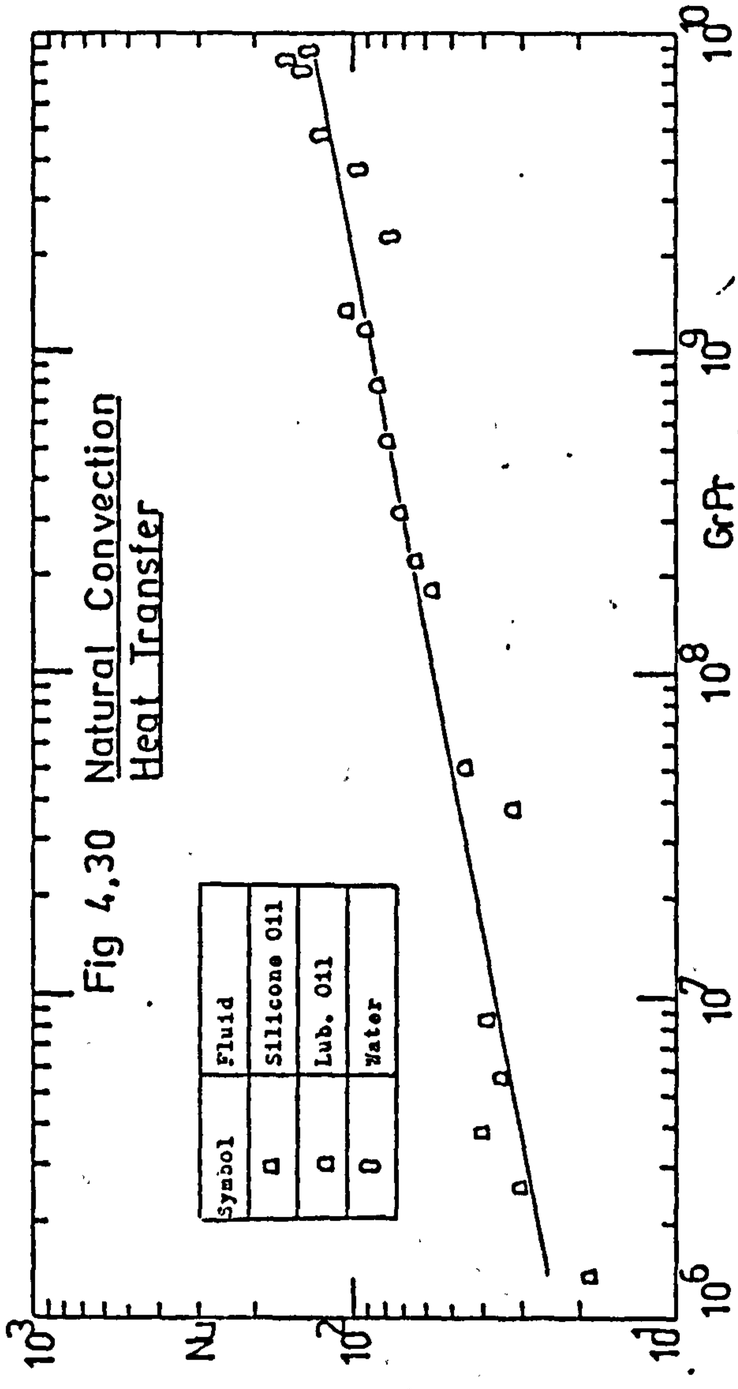

Fig 4.30 Natural Convection Heat Transfer

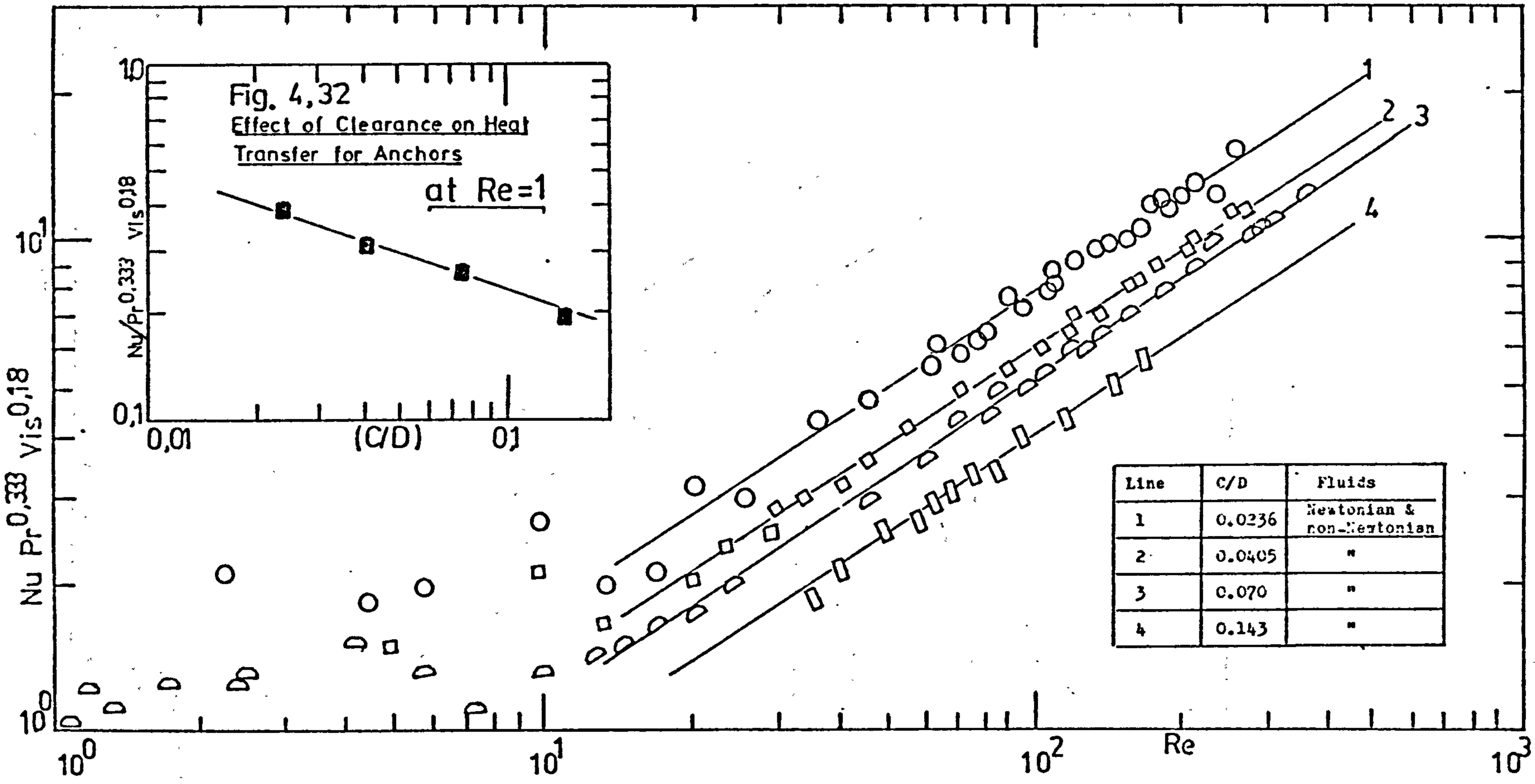

Fig 4,31 Heat Transfer for Anchors

Line	C/D	Worker
1 - 4	0.0236 - 0.143	This work
5	0.011 - 0.143	Heilein & Sandall
6	0.0769	Gluz & Pavlushenko
7	0.054	Uhl
8	0.055 - 0.125	Pollard & Kantyka
9	0.008	Martone & Sandall
10	0.0263	Nagata

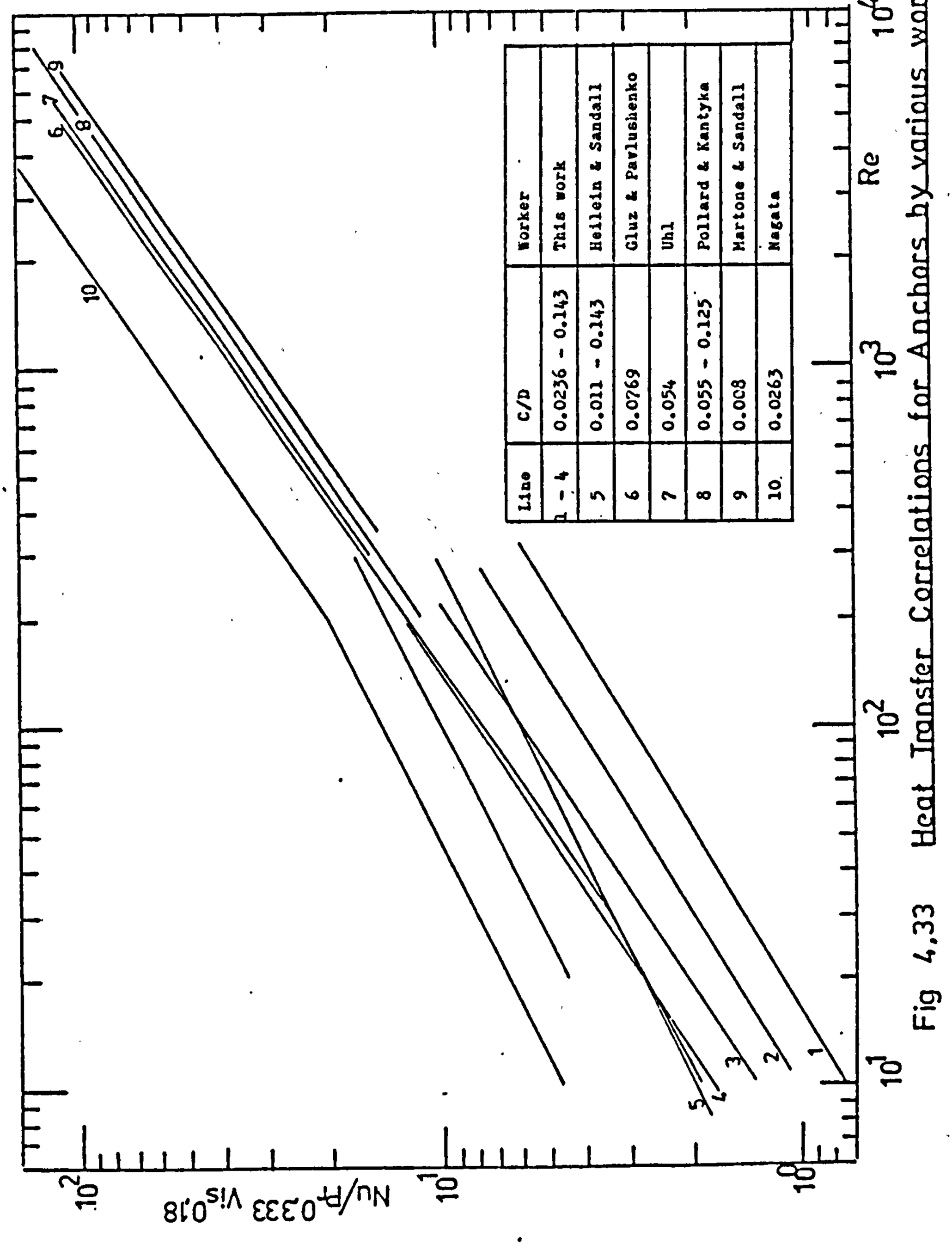

Fig 4,33 Heat Transfer Correlations for Anchors by various workers

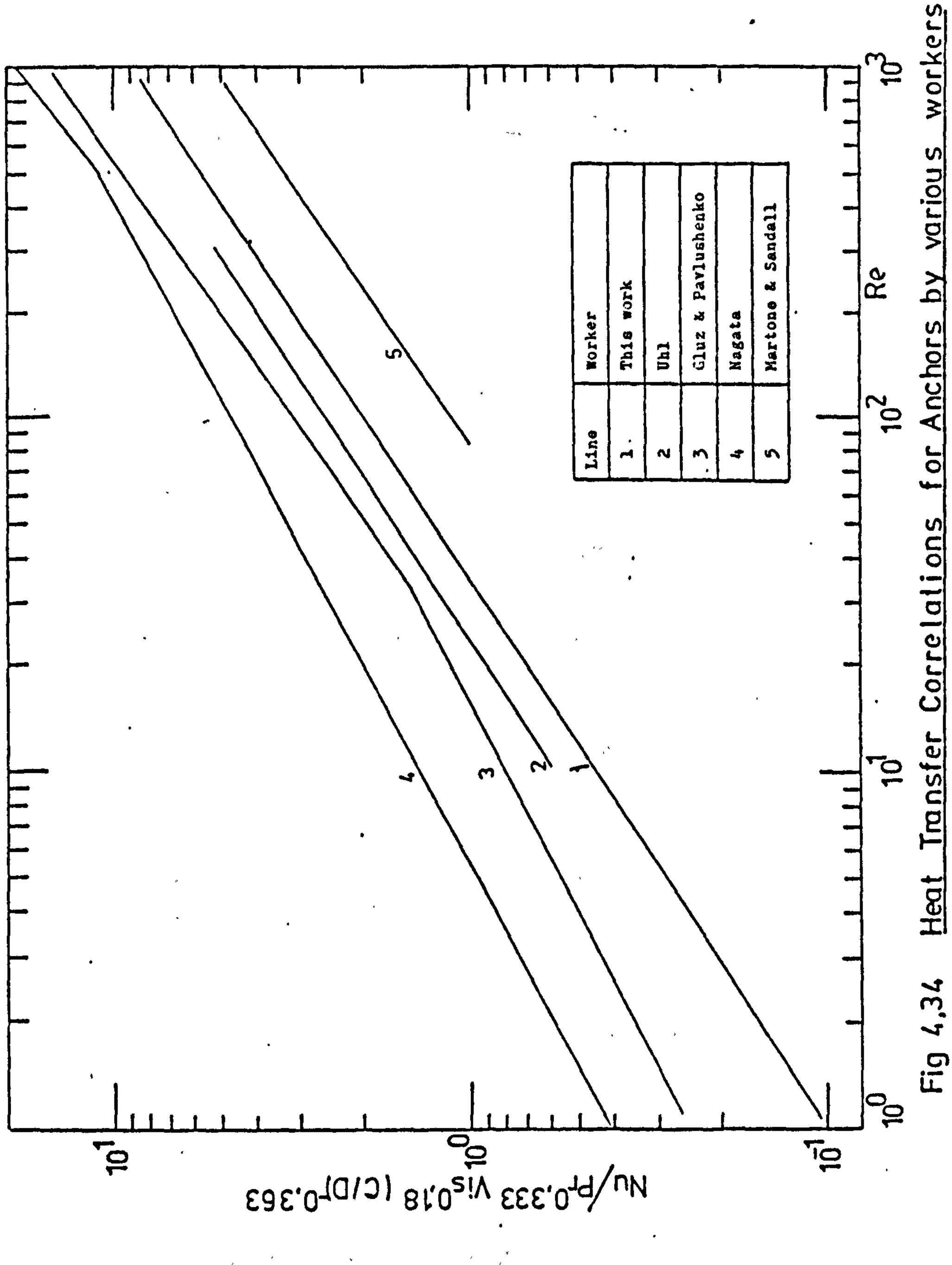

Fig 4,34 Heat Transfer Correlations for Anchors by various workers

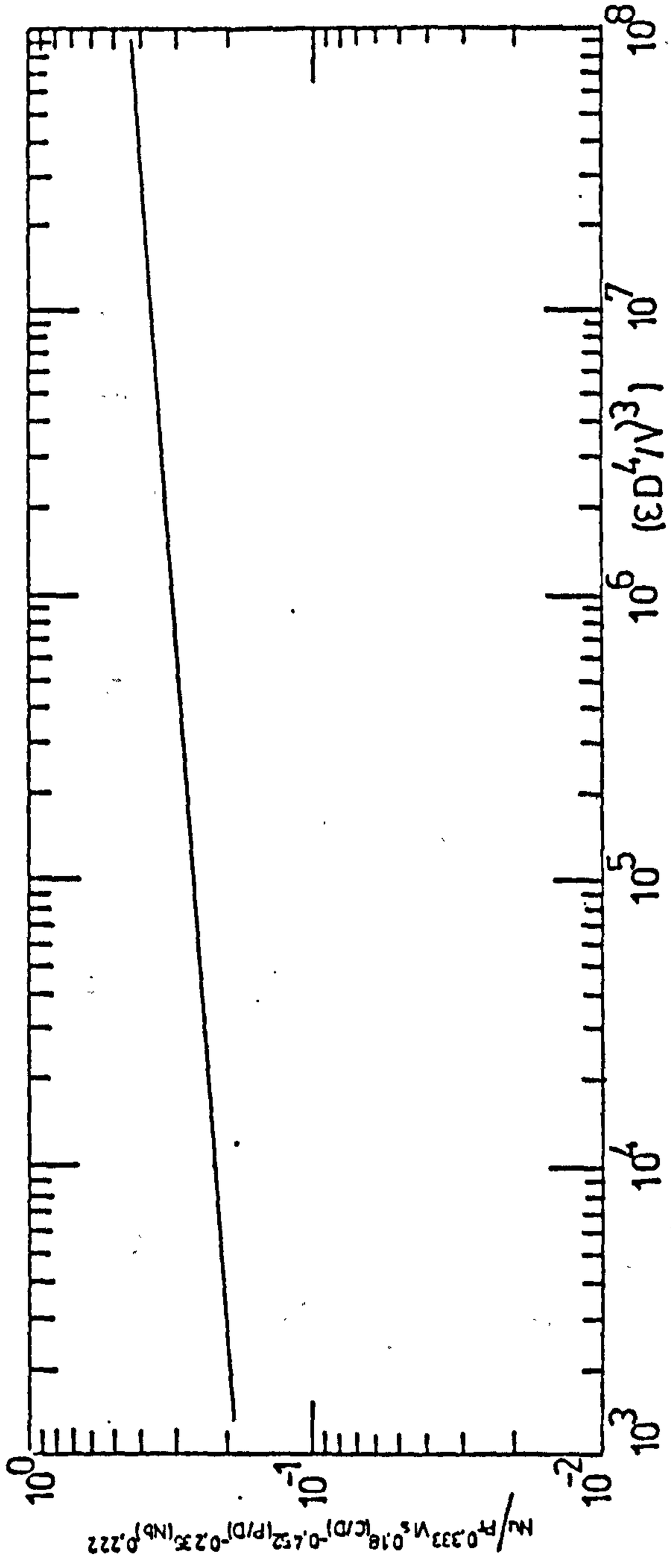

Fig 4,35 Dimensionless Power input vs. Heat Transfer for Ribbons in Laminar Region.

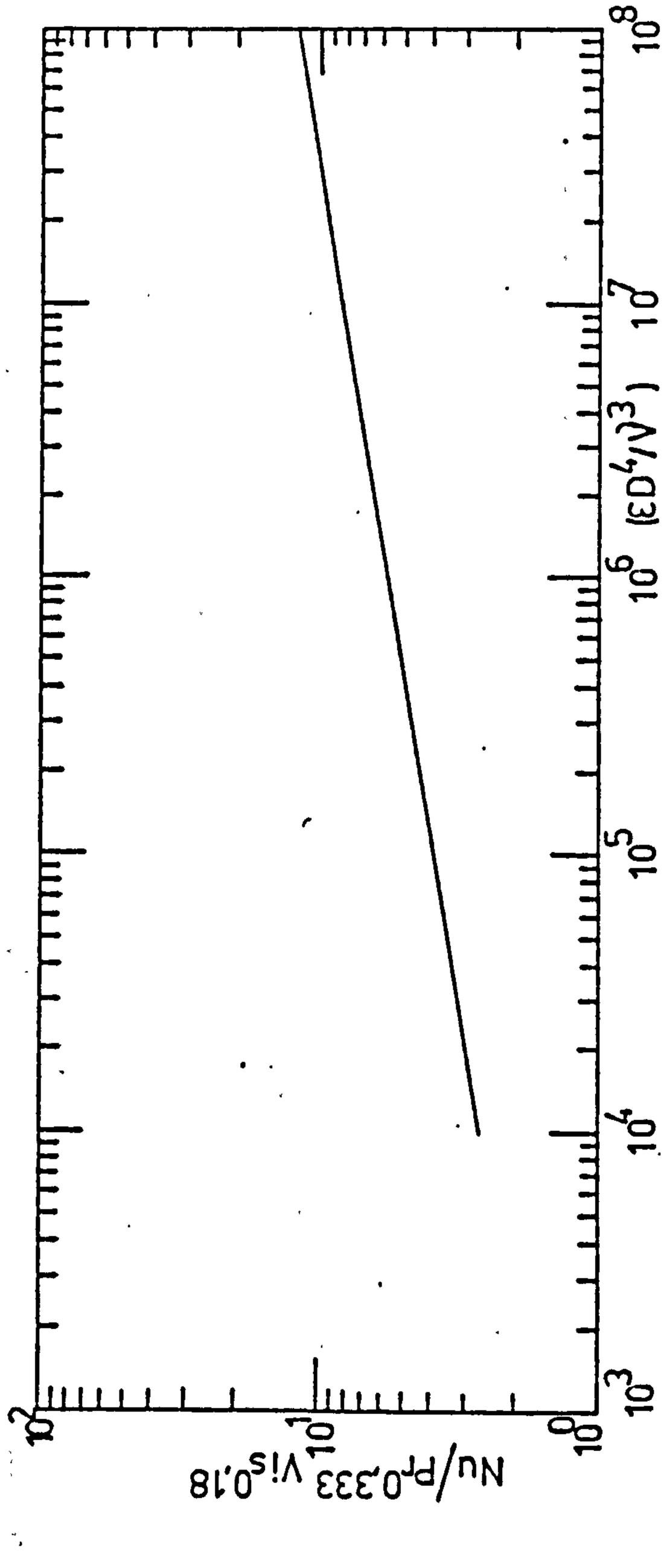

Fig 4,36 Dimensionless Power input vs Heat Transfer for Helical Ribbons in Turbulent region.

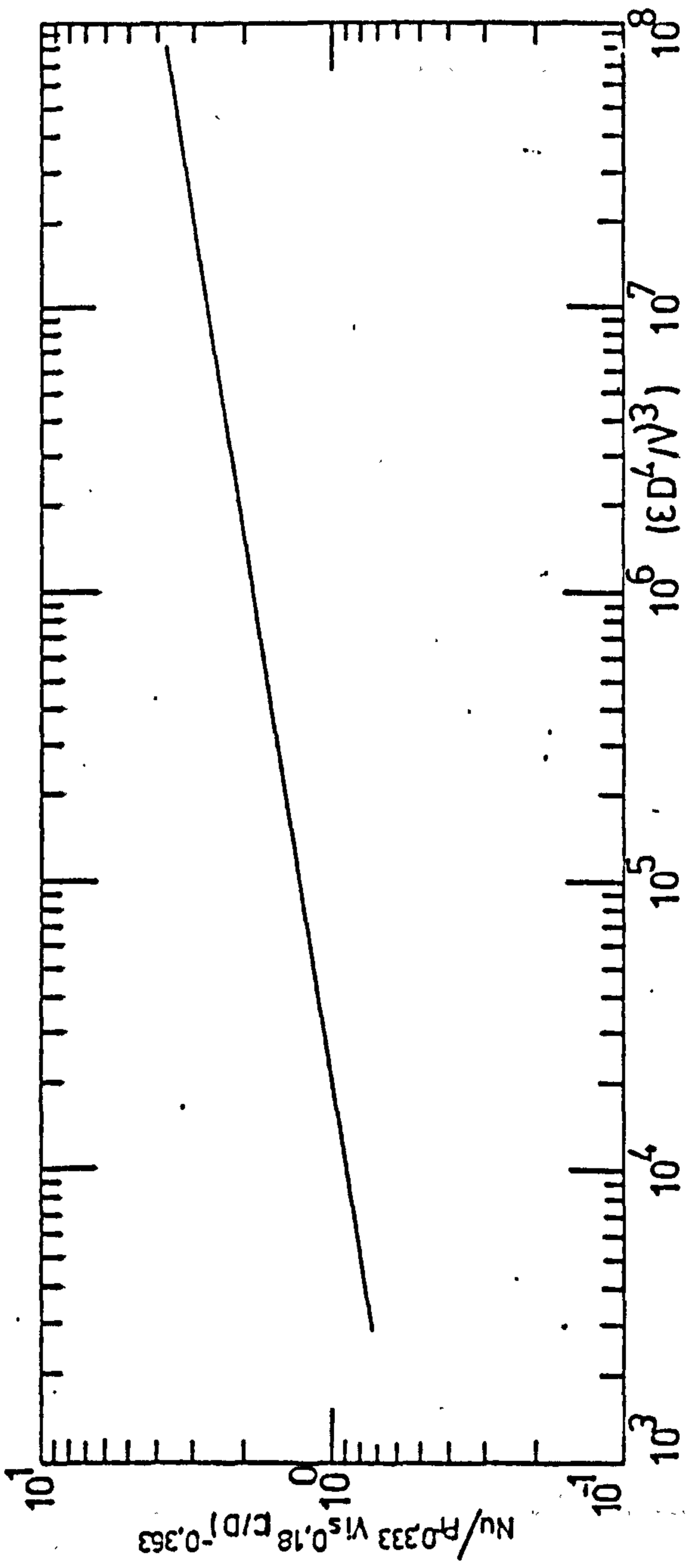

Fig. 4,37 Dimensionless Power input vs. Heat Transfer for Anchors in Turbulent region.

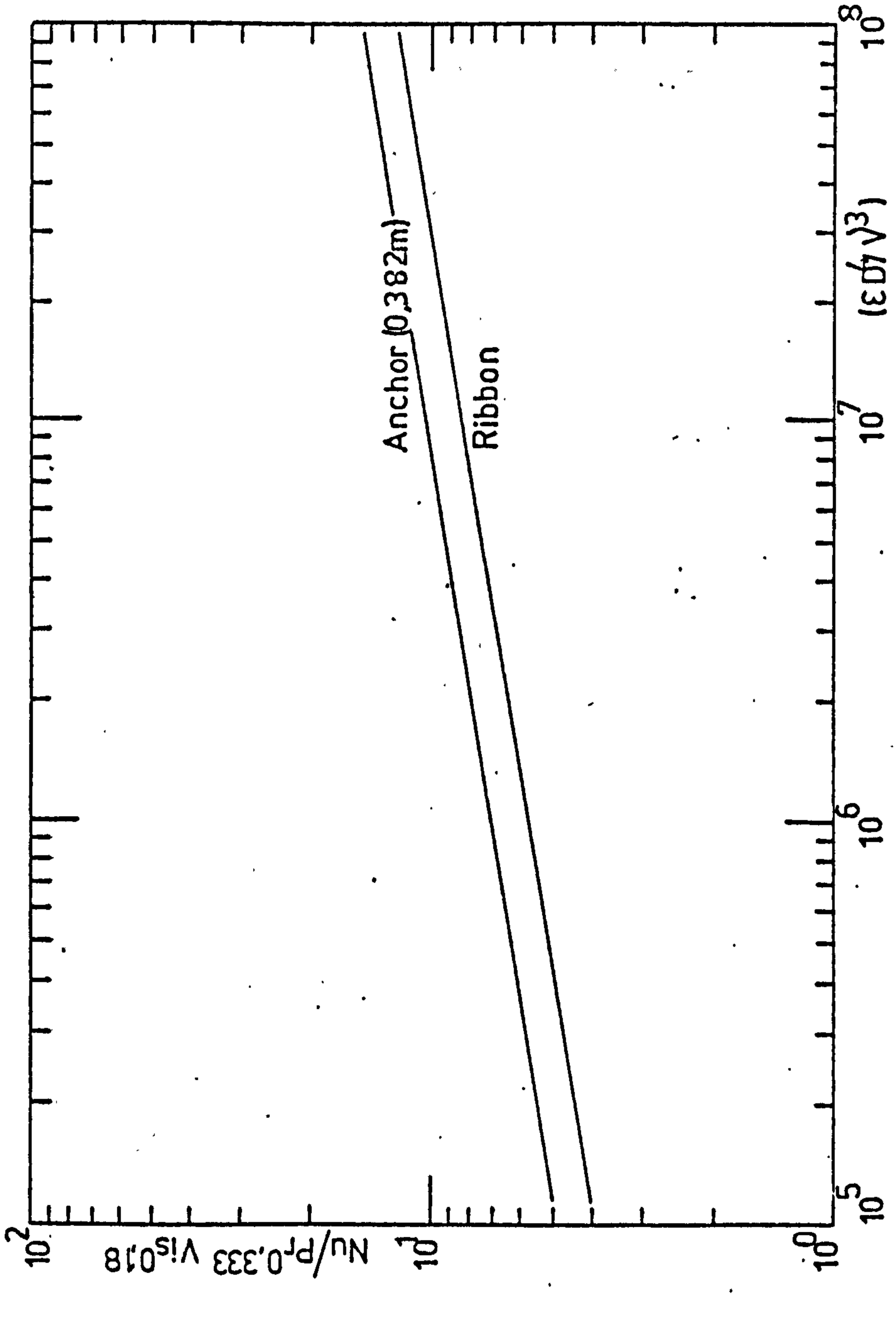

Fig 4,38 Dimensionless Power input vs. Heat Transfer for the Anchor and Ribbon Impellers

APPENDIX 1(iii)

TABLE A 1.1

Tank Diameter: 0.4m P/D = 0.5 , Nb = 1.0

Impeller: Ribbon D = 0.352m Temp. = 22 ^{o}C

Material: Silicone Oil μ = 98 Nsm^{-2} ρ = 985 kgm^{-3}

N(rps)	T(Nm)	P_o	Re
0.028	4.12	6200	0.035
0.038	5.65	4617	0.047
0.055	8.06	3145	0.069
0.068	10.0	2553	0.085
0.099	14.6	1763	0.123
0.116	17.1	1498	0.145
0.132	19.5	1323	0.164
0.15	22.0	1160	0.187

TABLE A1.2

Tank Diameter: 0.4m P/D =0.5 , Nb = 1.0

Impeller: Ribbon D = 0. 352m Temp. = 25 ^{o}C

Material: Sugar μ = 28.9 Nsm^{-2} ρ = 1381 kgm^{-3}

N(rps)	T(Nm)	P_o	Re
0.046	1.94	771	0.28
0.070	3.00	514	0.42
0.110	4.70	327	0.66
0.140	5.98	257	0.84
0.170	7.28	212	1.02
0.220	9.55	166	1.30
0.290	12.39	124	1.74
0.300	12.80	120	1.80
0.390	17.00	94	2.30
0.450	19.3	80	2.70
0.520	22.5	70	3.10
0.570	24.7	64	3.40
0.680	29.1	53	4.10
0.760	32.3	47	4.60
0.860	36.9	42	5.20
0.920	39.2	39	5.50
1.000	42.8	36	6.00

TABLE A 1.3

Tank Diameter: 0.4m P/D = 0.5 , Nb = 1.0

Impeller: Ribbon D = 0. 352m Temp. = 20 ^{o}C

Material: Lub. Oil μ = 1.8 Nsm^{-2} ρ = 893 kgm^{-3}

N(rps)	T(Nm)	P_o	Re
0.07	0.2	53	4.3
0.16	0.5	25	9.8
0.32	1.01	12.8	19.7
0.43	1.34	9.4	26.4
0.45	1.75	7.4	27.7
0.61	1.96	7	37.5
0.67	2.19	6.5	41.2
0.74	2.47	6.0	45.5
0.81	2.73	5.6	49.8
0.86	2.9	5.2	52.9
1.01	3.47	4.5	62.1
1.13	3.97	4.1	69.5
1.27	4.55	3.7	78.1
1.41	5.23	3.5	86.7
1.47	5.51	3.5	90.4
1.52	5.69	3.3	93.4

TABLE A1.4

Tank Diameter: 0.4m P/D = 0.5 , Nb = 1.0

Impeller: Ribbon D = 0.352 m Temp. = 22 ^{o}C

Material:Glycerol μ = 0.07 Nsm^{-2} ρ = 1218 kgm^{-3}

N(rps)	T(Nm)	P_o	Re
0.35	0.1	0.78	755
0.46	0.17	0.76	992
0.61	0.27	0.7	1315
0.75	0.41	0.7	1617
0.85	0.49	0.65	1833
0.97	0.59	0.6	2091
1.05	0.68	0.59	2264
1.16	0.76	0.54	2500
1.27	0.89	0.53	2738
1.37	1.02	0.52	2954
1.50	1.14	0.49	3234
1.62	1.26	0.46	3493

TABLE A1.5

Tank Diameter: 0.4m P/D = 0.5 , Nb = 1.0

Impeller: Ribbon D = 0.352 m Temp. = 22 ^{o}C

Material: Water $\mu = 1x10^{-3}$ Nsm^{-2} $\varrho = 1000$ kgm^{-3}

N(rps)	T(Nm)	P_o	Re
0.154	0.02	0.98	19081
0.66	0.13	0.35	81777
0.84	0.20	0.33	104080
0.99	0.23	0.29	122665
0.37	0.04	0.34	45845
0.47	0.08	0.42	58235
0.56	0.09	0.34	69386
0.75	0.16	0.33	92928
0.84	0.19	0.31	104079
0.93	0.22	0.3	115231
1.05	0.24	0.26	130099

TABLE A 1.6

Tank Diameter: 0.4m P/D = 0.5 , Nb = 1.0

Impeller: Ribbon D = 0.352 m Temp. = 33 °C

Material: Chocolate μ = Nsm^{-2} ρ = 1280 kgm^{-3}

N(rps)	T(Nm)	P_o	Re	μ_A	$\dot{\gamma}_A$	k_s
0.062	3.6	866	0.231	42.5	1.7	28
0.131	4.0	212	0.944	22.0	3.7	28
0.208	5.0	105	1.90	17.4	8.4	27
0.309	7.3	69	2.90	17.0	8.7	28
0.409	8.1	44	4.50	14.5	11.5	28
0.502	8.9	32	6.22	12.8	14.6	29
0.579	9.6	26	7.65	12.0	16.2	28
0.749	11.7	19	10.6	11.2	21.0	28

TABLE A 1.7

Tank Diameter: 0.4m P/D = 0.5 , Nb = 1.0

Impeller: Ribbon D = 0.352 m Temp. = 25 ^{o}C

Material: 3% Carbopol μ = Nsm^{-2} ρ = 1000 kgm^{-3}

N(rps)	T(Nm)	P_o	Re	μ_A	$\dot{\gamma}_A$	k_s
0.099	7.4	878	0.246	50.0	2.67	27
0.183	8.4	292	0.742	30.6	4.94	27
0.253	9.2	167	1.290	24.3	6.58	26
0.362	9.4	83	2.610	17.2	10.1	28
0.411	9.9	68	3.190	16.0	11.1	27
0.525	10.2	43	4.970	13.1	14.2	27
0.638	11.6	33	6.600	12.0	16.0	25
0.711	11.3	26	8.320	10.6	18.5	26
0.821	12.2	21	10.40	9.8	20.5	25

TABLE A 1.8

Tank Diameter: 0.4m P/D = 1.0 , Nb = 2

Impeller: Ribbon D = 0.352 m Temp. = 41 ^{o}C

Material: Silicone Oil μ = 70 Nsm^{-2} ϱ = 968 kgm^{-3}

N(rps)	T(Nm)	P_o	Re
0.031	3.6	4528	0.053
0.058	6.7	2400	0.100
0.093	11.0	1510	0.159
0.12	13.7	1141	0.210
0.143	16.4	960	0.250
0.154	18.0	910	0.264
0.163	19.0	857	0.280
0.170	19.8	824	0.291
0.181	21.1	774	0.310
0.190	22.0	729	0.330

TABLE A 1.9

Tank Diameter: 0.4m P/D = 1.0 , Nb = 2

Impeller: Ribbon D = 0.352 m Temp. = 25 ^{o}C

Material: Sugar μ = 30 Nsm^{-2} ρ = 1390 kgm^{-3}

N(rps)	T(Nm)	P_o	Re
0.041	2.1	1043	0.235
0.078	4.0	547	0.448
0.145	7.4	295	0.832
0.196	10.0	218	1.125
0.201	10.3	213	1.150
0.267	13.6	160	1.530
0.311	15.9	137	1.790
0.432	22.1	99	2.480
0.518	26.6	83	2.970
0.611	31.3	70	3.510

TABLE A 1.10

Tank Diameter: 0.4m P/D = 1.0 , Nb = 2

Impeller: Ribbon D = 0.352 m Temp. = 20 ^{o}C

Material: Lub. Oil μ = 1.8 Nsm^{-2} ρ = 893 kgm^{-3}

N(rps)	T(Nm)	P_o	Re
0.222	0.651	17.2	13.7
0.386	1.13	9.9	23.7
0.432	1.26	8.8	26.6
0.490	1.44	7.8	30.1
0.531	1.60	7.2	32.6
0.586	1.71	6.5	36.1
0.635	1.86	6.0	39.0
0.721	2.20	5.5	44.3
0.911	2.74	4.3	56.0
1.06	3.19	3.7	65.0
1.35	4.06	2.9	83.0
1.70	6.22	2.8	105.0

TABLE A 1.11

Tank Diameter: 0.4m P/D = 1.0 , Nb = 2

Impeller: Ribbon D = 0.352 m Temp. = 22 °C

Material: Water/ Glycerol μ = 0.07 Nsm^{-2} ρ = 1218 kgm^{-3}

N(rps)	T(Nm)	P_o	Re
0.43	0.173	0.89	927
0.61	0.285	0.73	1315
0.69	0.335	0.67	1488
0.75	0.378	0.64	1617
0.83	0.434	0.6	1789
1.01	0.570	0.53	2178
1.20	0.73	0.48	2587

TABLE A 1.12

Tank Diameter: 0.4m P/D = 1.0 , Nb = 2

Impeller: Ribbon D = 0.352 m Temp. = 22 ^{o}C

Material: Water $\mu = 1 \times 10^{-3}$ Nsm^{-2} $\rho = 1000$ kgm^{-3}

N(rps)	T(Nm)	P_o	Re
0.35	0.042	0.4	43336
0.43	0.06	0.38	53279
0.56	0.121	0.45	69386
0.59	0.13	0.42	73103
0.63	0.14	0.41	78060

TABLE A 1.13

Tank Diameter: 0.4m P/D = 1.0 , Nb = 2.

Impeller: Ribbon D = 0.352 m Temp. = 33 ^{o}C

Material: Chocolate μ = . Nsm^{-2} ρ = 1280 kgm^{-3}

N(rps)	T(Nm)	P_o	Re	μ_A	$\dot{\gamma}_A$	k_s
0.048	4.05	1597	0.149	51.3	1.25	26
0.063	4.60	1049	0.227	44.2	1.64	26
0.091	5.30	582	0.409	35.4	2.46	27
0.131	6.23	330	0.721	28.9	3.54	27
0.142	6.48	292	0.815	27.7	3.83	27
0.165	6.80	227	1.05	25.0	4.62	28
0.189	7.54	192	1.24	24.2	4.91	26
0.246	8.32	125	1.91	20.5	6.64	27
0.311	9.50	89	2.69	18.4	8.09	26
0.521	11.9	40	6.00	13.8	13.6	26
0.662	13.0	27	8.70	12.1	17.2	26
0.713	14.0	25	9.50	11.9	17.8	25
0.813	14.5	20	11.7	11.1	20.3	25

TABLE A 1.14

Tank Diameter: 0.4m P/D = 1.0 , Nb = 2

Impeller: Ribbon D = 0.352m Temp. = 34 °C

Material: Biozam R μ = Nsm^{-2} ρ = 1000 kgm^{-3}

N(rps)	T(Nm)	P_o	Re	μ_A	γ_A	k_s
0.043	6.94	4364	0.055	96.5	1.16	27
0.081	7.74	1371	0.175	57.3	2.19	27
0.121	8.31	660	0.363	41.3	3.27	27
0.139	8.79	529	0.454	38.0	3.61	26
0.146	9.17	500	0.48	37.7	3.65	25
0.182	8.97	315	0.762	29.6	4.91	27
0.211	9.50	248	0.970	27.1	5.49	26
0.278	10.3	155	1.550	22.2	6.95	25
0.381	10.9	87	2.750	17.2	9.50	25
0.501	11.4	53	4.540	13.7	12.5	25
0.586	12.1	41	5.810	12.5	14.1	24
0.690	12.3	30	8.150	10.5	17.3	25

TABLE A 1.15

Tank Diameter: 0.4m P/D = 1.0 , Nb = 1.0

Impeller: Ribbon D = 0. 352m Temp. = 22 °C

Material: Silicone μ = 98 Nsm^{-2} ρ = 985 kgm^{-3}
Oil

N(rps)	T(Nm)	P_o	Re
0.028	3.13	4714	0.035
0.041	4.61	3236	0.051
0.079	8.90	1683	0.098
0.110	12.3	1204	0.137
0.136	15.2	982	0.168
0.165	18.5	800	0.206

TABLE A 1.16

Tank Diameter: 0.4m P/D = 1.0 , Nb = 1.0

Impeller: Ribbon D = 0.352m Temp. = 25 ^{o}C

Material: Sugar μ = 30 Nsm^{-2} ρ = 1390 kgm^{-3}

N(rps)	T(Nm)	P_o	Re
0.043	1.43	648	0.247
0.085	2.83	328	0.488
0.143	4.79	196	0.821
0.193	6.44	146	1.10
0.310	10.30	90	1.78
0.390	13.00	72	2.24
0.431	14.40	65	2.47
0.561	18.80	50	3.22
0.683	23.00	41	3.92
0.726	24.20	38	4.17
0.829	28.00	34	4.76

TABLE A 1.17

Tank Diameter: 0.4m P/D = 1.0 , Nb = 1.0

Impeller: Ribbon D = 0. 352m Temp. =20 ^{o}C

Material: Lub. Oil μ = 1.8 Nsm^{-2} ϱ = 893 kgm^{-3}

N(rps)	T(Nm)	P_o	Re
0.218	0.438	12.0	13.4
0.433	0.864	6.00	26.6
0.682	1.360	3.80	41.9
0.821	1.660	3.20	50.5
0.943	1.910	2.80	58.0
1.08	2.150	2.40	66.4
1.19	2.390	2.20	73.2
1.30	2.600	2.00	80.0
1.45	2.910	1.80	89.1
1.53	3.060	1.70	94.1
1.65	3.350	1.60	101.4
1.73	3:540	1.50	106.3

TABLE A 1.18

Tank Diameter: 0.4m P/D = 1.0 , Nb = 1.0

Impeller: Ribbon D = 0.352 m Temp. = 22 °C

Material: Water $\mu = 1 \times 10^{-3}$ Nsm^{-2} $\rho = 1000$ kgm^{-3}

N(rps)	T(Nm)	P_o	Re
0.35	0.046	0.36	43366
0.43	0.068	0.35	53279
0.62	0.153	0.38	76821

TABLE A 1.19

Tank Diameter: 0.4m P/D = 1.0 , Nb = 1.0

Impeller: Ribbon D = 0.352 m Temp. = 33 °C

Material: Chocolate μ = Nsm^{-2} ϱ = 1000 kgm^{-3}

N(rps)	T(Nm)	P_o	Re	μ_A	$\dot{\gamma}_A$	k_s
0.056	2.87	833	0.192	46.2	1.51	27
0.089	3.54	406	0.394	35.8	2.40	27
0.143	4.39	195	0.822	27.6	3.86	27
0.176	4.71	138	1.160	24.1	4.93	28
0.201	5.02	113	1.420	22.4	5.63	28
0.253	5.63	80	1.990	20.2	6.83	27
0.336	6.58	53	3.030	17.6	8.74	26
0.394	7.00	41	3.880	16.1	10.2	26
0.432	7.60	37	4.360	15.7	10.8	25
0.510	7.73	27	5.900	13.7	13.8	27
0.582	8.38	22.5	7.100	13.0	15.1	26
0.670	8.81	17.8	9.010	11.8	18.1	27
0.701	9.35	17.3	9.270	12.0	17.5	25
0.803	9.93	14.0	11.50	11.1	20.1	25

TABLE A 1.20

Tank Diameter: 0.4m P/D = 1.0 , Nb = 1.0

Impeller: Ribbon D = 0.352 m Temp. = 25 ^{o}C

Material: 3% Carbopol μ = Nsm^{-2} ρ = 1000 kgm^{-3}

N(rps)	T(Nm)	P_o	Re	μ_A	$\dot{\gamma}_A$	k_s
0.201	6.32	182	0.878	28.4	5.43	27
0.340	7.06	71	2.27	18.6	9.18	27
0.382	7.15	57	2.79	17.0	10.3	27
0.629	8.20	24	6.67	11.7	16.4	26
0.683	7.90	19.7	8.14	10.4	19.1	28
0.780	8.10	.5.4	10.4	9.3	21.8	28
0.849	8.50	13.7	11.7	9.0	22.9	27
0.911	8.80	12.3	13.0	8.7	23.7	26
1.1	9.20	8.8	18.2	7.5	28.6	26
1.18	9.60	8.0	20.0	7.3	29.5	25

TABLE A 1.21

Tank Diameter: 0.4m P/D = 0.5 , Nb = 1.0

Impeller: Ribbon D = 0.370 m Temp. = 20 ^{o}C

Material: Silicone Oil μ = 100 Nsm^{-2} ρ = 985 kgm^{-3}

N(rps)	T(Nm)	P_o	Re
0.031	8.16	7694	0.042
0.050	11.9	4313	0.069
0.058	14.5	3905	0.079
0.066	16.7	3474	0.090
0.077	18.7	2858	0.105
0.088	20.4	2387	0.121
0.097	23.8	2292	0.133
0.116	27.2	1831	0.169
0.147	34.0	1425	0.201
0.178	40.1	1147	0.244
0.201	44.2	991	0.275
0.305	66.3	646	0.418
0.340	73.8	578	0.466
0.370	76.5	507	0.507

TABLE A 1.22

Tank Diameter: 0.4m P/D = 0.5 , Nb = 1.0

Impeller: Ribbon D = 0.370 m Temp. = 22 ^{o}C

Material: Lub. Oil μ = 1.8 Nsm^{-2} ρ = 893 kgm^{-3}

N(rps)	T(Nm)	P_o	Re
0.062	0.22	58	4.2
0.097	0.34	37	6.6
0.154	0.56	24	10.5
0.180	0.67	21	12.2
0.330	1.39	13	22.4
0.420	1.71	9.8	28.5
0.590	2.51	7.3	40.0
0.690	3.00	6.4	47.0
0.760	3.30	5.8	52.0
0.890	3.98	5.1	60.0
1.01	4.53	4.5	69.0
1.11	5.10	4.2	75.4
1.24	5.61	3.7	84.0
1.37	6.29	3.4	93.0
1.58	7.38	3.0	107
1.62	7.76	3.0	110

TABLE A 1.23

Tank Diameter: 0.4m P/D = 0.5 , Nb = 1.0

Impeller: Ribbon D = 0. 370m Temp. = 22 ^{o}C

Material: Water/ Glycerol μ = 0.07 Nsm^{-2} ρ = 1218 kgm^{-3}

N(rps)	T(Nm)	P_o	Re
0.38	0.20	1.01	905
0.56	0.34	0.81	1334
0.63	0.44	0.83	1500
0.79	0.61	0.73	1882
0.92	0.79	0.69	2192
1.04	0.92	0.63	2477
1.10	1.07	0.66	2620
1.24	1.28	0.62	2954
1.35	1.52	0.62	3216
1.44	1.56	0.56	3430

TABLE A1.24

Tank Diameter: 0.4m P/D = 0.5 , Nb = 1.0

Impeller: Ribbon D = 0.370 m Temp. = 33 °C

Material: Chocolate μ = Nsm^{-2} ϱ = 1280 kgm^{-3}

N(rps)	T(Nm)	P_o	Re	μ_A	$\dot{\gamma}_A$	k_s
0.07	5.5	781	0.32	39.0	2.00	29
0.14	7.1	255	0.98	25.0	4.34	31
0.20	8.6	152	1.65	21.2	5.80	29
0.32	10.3	71	3.51	16.0	9.60	30
0.43	12.0	46	5.42	13.9	12.9	30
0.51	12.8	35	7.20	12.5	15.1	30
0.60	13.7	27	9.30	11.3	18.0	30
0.67	14.6	23	10.9	10.8	20.4	30

TABLE A 1.25

Tank Diameter: 0.4m P/D = 0.5 , Nb = 1.0

Impeller: Ribbon D = 0.370 m Temp. = 25 °C

Material: 3% Carbopol μ = Nsm^{-2} ρ = 1000 kgm^{-3}

N(rps)	T(Nm)	P_o	Re	μ_A	γ_A	k_s
0.077	8.92	1362	0.187	56.3	2.31	30
0.110	9.31	697	0.366	41.2	3.41	31
0.143	10.1	445	0.571	34.3	4.29	30
0.200	11.0	250	1.02	26.9	5.80	29
0.310	11.1	105	2.43	17.5	9.92	32
0.394	12.3	72.0	3.55	15.2	11.8	30
0.425	12.5	63.0	4.07	14.3	12.8	30
0.533	13.1	42.0	6.13	11.9	16.0	30
0.590	13.7	35.7	7.15	11.3	17.1	29
0.650	14.0	30.0	8.56	10.4	19.0	29
0.820	14.9	20.0	12.7	8.9	23.0	28
0.910	15.0	16.4	15.6	8.0	26.4	29
1.17	16.2	11.0	23.9	6.7	32.8	28

TABLE A 1.26

Tank Diameter: 0.4m P/D=1.0 , Nb = 1.0

Impeller: Ribbon D = 0.380 m Temp. = 22 ^{o}C

Material: Silicone Oil μ = 98 Nsm^{-2} ρ = 985 kgm^{-3}

N(rps)	T(Nm)	P_o	Re
0.028	4.75	4880	0.041
0.035	5.97	3922	0.051
0.056	9.62	2469	0.081
0.078	13.4	1770	0.113
o.115	19.7	1198	0.167
o.120	20.6	1150	0.174
0.131	22.4	1053	0.190
0.136	23.3	1015	0.197

TABLE A1.27

Tank Diameter: 0.4m P/D = 1.0 , Nb = 1.0

Impeller: Ribbon D = 0.380 m Temp. = 19 ^{o}C

Material: Lub. Oil μ = 1.8 Nsm^{-2} ρ = 893 kgm^{-3}

N(rps)	T(Nm)	P_o	Re
0.18	0.584	16.0	12.9
0.25	0.774	11.0	17.9
0.36	1.17	8.0	25.8
0.42	1.35	6.8	30.1
0.49	1.62	6.0	35.1
0.54	1.74	5.3	38.7
0.68	2.20	4.2	48.7
0.74	2.41	3.9	53.0
0.82	2.73	3.6	58.7
0.99	3.20	2.9	71.0
1.12	3.81	2.7	80.2
1.43	5.99	2.6	102.4
1.70	7.81	2.4	122.0

TABLE A 1.28

Tank Diameter: 0.4m P/D = 1.0 , Nb = 1.0

Impeller: Ribbon D = 0.380 m Temp. = 22 °C

Material: Water/ Glycerol μ = 0.07 Nsm^{-2} ρ = 1218 kgm^{-3}

N(rps)	T(Nm)	P_o	Re
0.320	0.173	1.1	804
0.381	0.223	1.0	957
0.421	0.259	0.95	1058
0.560	0.385	0.80	1407
0.601	0.433	0.78	1510
0.676	0.512	0.73	1698
0.732	0.560	0.68	1839
0.821	0.673	0.65	2063
0.901	0.748	0.60	2264
1.100	1.02	0.55	2764
1.200	1.11	0.50	3015

TABLE A 1.30

Tank Diameter: 0.4m P/D = 1.0 , Nb = 1.0

Impellcr: Ribbon D = 0. 38 m Temp. = 25 ^{o}C

Material: 3% Carbopol μ = Nsm^{-2} ϱ = 1000 kgm^{-3}

N(rps)	T(Nm)	P_o	Re	μ_A	$\dot{\gamma}_A$	k_s
0.032	6.19	4791	0.043	108	1.02	32
0.049	6.56	2168	0.095	74.7	1.62	33
0.063	6.92	1383	0.149	61.2	2.08	33
0.082	7.50	884	0.233	50.9	2.62	32
0.101	7.80	606	0.340	43.0	3.23	32
0.123	7.86	412	0.500	35.8	4.06	33
0.135	8.46	368	0.560	34.9	4.19	31
0.142	8.60	338	0.610	33.6	4.40	31
0.150	8.85	312	0.660	33.0	4.50	30

TABLE A 1.31

Tank Diameter: 0.4m P/D = 1.0 , Nb = 1.0

Impeller: Ribbon D = 0. 38 m Temp. = 34 °C

Material: Biozam R μ = Nsm^{-2} ρ = 1000 kgm^{-3}

N(rps)	T(Nm)	P_o	Re	μ_A	γ_A	k_s
0.031	5.91	4878	0.041	110	0.99	32
0.045	6.15	2410	0.083	78.6	1.49	33
0.063	6.59	1316	0.152	59.8	2.08	33
0.092	7.04	660	0.303	43.8	3.04	33
0.121	7.60	411	0.487	35.9	3.87	32
0.136	7.60	324	0.618	31.8	4.49	33
0.147	8.04	295	0.679	31.4	4.56	31
0.210	8.62	155	1.29	23.5	6.51	31
0.263	8.72	100	2.00	19.0	8.42	32
0.382	9.02	49	4.06	13.6	12.6	33
0.492	10.4	34	5.92	12.0	14.8	30
0.583	10.3	24	8.34	10.1	18.1	31
0.672	10.8	19	10.4	9.3	20.2	30

TABLE A1.32

Tank Diameter: 0.4m P/D = 0.5 ., Nb = 1.0

Impeller: Ribbon D = 0.380 m Temp. = 22 °C

Material: Silicone Oil μ = 98 Nsm^{-2} ρ = 985 kgm^{-3}

N(rps)	T(Nm)	P_o	Re
0.031	7.96	6665	0.045
0.039	9.94	5254	0.057
0.05	12.76	4110	0.073
0.066	16.91	3125	0.096
0.077	19.73	2679	0.112
0.093	23.90	2222	0.135
0.110	28.18	1875	0.160
0.130	33.30	1588	0.189
0.150	38.45	1376	0.218

TABLE A1.33

Tank Diameter: 0.4m P/D = 0.5 , Nb = 1.0

Impeller: Ribbon D = 0.380 m Temp. = 19 ^{o}C

Material: Lub. Oil μ = 1.8 Nsm^{-2} ϱ = 893 kgm^{-3}

N(rps)	T(Nm)	P_o	Re
0.23	1.03	17.2	16.5
0.34	1.52	11.7	24.4
0.46	2.05	8.6	33.0
0.53	2.37	7.5	38.0
0.68	3.02	5.8	48.7
0.77	3.54	5.3	55.2
0.81	3.62	4.9	58.0
0.88	4.01	4.6	63.0
0.98	4.43	4.1	70.2
1.04	4.63	3.8	74.5
1.65	7.36	2.4	118
1.83	8.30	2.2	131

TABLE A 1.34

Tank Diameter: 0.4m P/D = 0.5 , Nb = 1.0

Impeller: Ribbon D = 0.380 m Temp. = 22 °C

Material: Water/ Glycerol μ = 0.07 Nsm^{-2} ρ = 1218 kgm^{-3}

N(rps)	T(Nm)	P_o	Re
0.43	0.45	1.6	1080
0.55	0.74	1.4	1382
0.68	0.92	1.3	1709
0.74	0.93	1.1	1859
0.83	1.16	1.1	2085
0.92	1.37	1.05	2312
1.08	1.61	0.90	2714

TABLE A 1.35

Tank Diameter: 0.4m P/D = 0.5, Nb = 1.0

Impeller: Ribbon D = 0.380 m Temp. = 33 ^{o}C

Material: Chocolate μ = Nsm^{-2} ρ = 1280 kgm^{-3}

N(rps)	T(Nm)	P_o	Re	μ_A	$\dot{\gamma}_A$	k_s
0.082	6.95	640	0.45	34.1	2.62	32
0.13	8.46	310	0.93	26.0	4.29	33
0.21	10.61	149	1.94	20.0	6.93	33
0.26	11.35	104	2.75	17.5	8.84	34
0.37	13.26	60	4.82	14.2	13.0	35
0.43	14.33	48	6.00	13.3	14.6	34
0.48	15.25	41	7.00	12.7	15.8	33
0.54	16.00	34	8.40	11.9	17.8	33
0.68	17.91	24	12.0	10.5	22.4	33
0.79	19.14	19	15.2	9.60	26.1	33
0.94	21.40	15	19.5	8.90	30.1	32
1.21	23.63	10	28.7	7.80	38.7	32
1.32	24.47	9	33.0	7.40	42.2	32

TABLE A 1.36

Tank Diameter: 0.4m P/D = 0.5 , Nb= 1

Impeller: Ribbon D = 0.380 m Temp. = 25 °C

Material: 4% CMC μ = Nsm^{-2} ϱ = 1000 kgm^{-3}

N(rps)	T(Nm)	P_o	Re	μ_A	γ_A	k_s
0.056	9.42	2383	0.12	67.8	1.79	32
0.076	10.4	1430	0.20	55.7	2.51	33
0.095	11.2	986	0.29	48.1	3.23	34
0.140	13.1	530	0.54	37.8	4.90	35
0.146	13.5	502	0.57	36.9	5.11	35
0.152	14.4	493	0.58	38.0	4.86	32
0.200	16.4	325	0.88	33.0	6.20	31
0.248	17.6	227	1.26	28.4	8.00	32
0.290	18.5	174	1.64	25.6	9.57	33
0.321	19.4	149	1.92	24.2	10.6	33
0.410	21.4	101	2.82	21.0	13.5	33
0.486	23.5	79	3.64	19.3	15.6	32
0.583	25.3	59	4.84	17.4	18.7	32
0.637	26.1	51	5.58	16.5	20.4	32
0.701	27.3	44	6.45	15.7	22.2	32

TABLE A 1.37

Tank Diameter: 0.4m

Impeller: Anchor D = 0.318 m Temp. = 25 °C

Material: Silicone Oil μ = 98 Nsm^{-2} ρ = 985 kgm^{-3}

N(rps)	T(Nm)	P_o	Re
0.040	3.6	4390	0.041
0.062	5.6	2859	0.063
0.075	6.8	2364	0.076
0.085	7.7	2080	0.086
0.120	10.8	1470	0.122
0.170	15.3	1035	0.173
0.190	17.3	928	0.193
0.250	22.6	709	0.254
0.280	25.2	630	0.285

TABLE A 1.38

Tank Diameter: 0.4m

Impeller: Anchor D = 0.318 m Temp. = 25 °C

Material: Sugar μ = 30 Nsm^{-2} ρ = 1390 kgm^{-3}

N(rps)	T(Nm)	P_o	Re
0.043	1.39	1048	0.20
0.062	1.80	652	0.295
0.073	2.21	577	0.340
0.097	2.69	398	0.460
0.143	3.74	254	0.670
0.181	5.24	222	0.850
0.330	9.01	115	1.550
0.380	10.20	99	1.780
0.460	12.57	83	2.160
0.570	15.64	67	2.670
0.630	17.10	60	2.950
0.714	19.20	53	3.350

TABLE A 1.39

Tank Diameter: 0.4m

Impeller: Anchor D = 0.318 m Temp. = 19 ^{o}C

Material: Lub. Oil μ = 1.8 Nsm^{-2} ϱ = 893 kgm^{-3}

N(rps)	T(Nm)	P_o	Re
0.216	0.442	21	10.8
0.398	0.816	11	20.0
0.452	0.952	10	23.0
0.525	1.12	8.7	26.0
0.595	1.29	7.7	30.0
0.660	1.46	7.4	33.0
0.764	1.67	6.3	38.0
0.834	1.84	5.8	42.0
1.04	2.31	4.5	52.0
1.10	2.48	4.5	55.0
1.19	2.72	4.1	60.0
1.26	2.89	3.9	63.0
1.32	3.06	3.9	66.0
1.44	3.37	3.5	72.0
1.48	3.50	3.5	74.0
1.50	3.60	3.5	75.0

TABLE A 1.40

Tank Diameter: 0.4m

Impeller: Anchor D = 0.318 m Temp. = 22 ^{o}C

Material: Water $\mu = 1 \times 10^{-3}$ Nsm^{-2} $\rho = 1000$ kgm^{-3}

N(rps)	T(Nm)	P_o	Re
0.16	0.013	0.95	16.180
0.30	0.042	0.90	30,337
0.40	0.07	0.85	40,450
0.55	0.13	0.80	55,618

TABLE A 1.40

Tank Diameter: 0.4m

Impeller: Anchor D = 0.318 m Temp. = 25°C

Material: 3% Carbopol μ = Nsm^{-2} ϱ = 1000 kgm^{-3}

N(rps)	T(Nm)	P_o	Re	μ_A	$\dot{\gamma}_A$	k_s
0.166	7.60	1088	0.17	69.0	1.80	16
0.209	8.40	370	0.50	42.2	3.40	16
0.363	8.90	130	1.42	26.0	6.40	18
0.405	8.80	103	1.80	23.0	7.40	18
0.579	9.50	54.4	3.40	17.4	10.5	18
0.687	9.80	40.0	4.60	15.2	12.0	18
0.764	9.00	33.0	5.60	14.0	13.4	18
1.02	10.5	19.5	9.50	11.0	18.0	18
1.17	11.4	16.0	11.60	10.2	20.7	18
1.26	11.9	14.50	12.80	10.0	20.6	16
1.41	12.7	12.30	15.00	9.5	22.5	16
1.54	13.8	11.20	16.50	9.5	22.5	15

TABLE A 1.41

Tank Diameter: 0.4m

Impeller: Anchor D = 0.318m Temp. = 20 °C

Material: 4% CMC μ = Nsm^{-2} ρ = 1000 kgm^{-3}

N(rps)	T(Nm)	P_o	Re	μ_A	γ_A	k_s
0.062	5.82	2923	0.0633	99.0	1.02	17
0.082	6.76	1941	0.0953	87.0	1.36	17
0.093	7.33	1637	0.113	83.0	1.54	17
0.135	8.69	920	0.201	68.0	2.43	18
0.200	11.0	530	0.349	58.0	3.52	18
0.380	16.2	217	0.854	45.0	6.46	17
0.430	17.8	186	0.997	43.6	6.90	16
0.540	19.3	128	1.44	37.6	9.60	18
0.620	20.3	102	1.81	34.7	11.7	18
0.70	22.3	88	2.11	33.6	12.6	18
0.79	24.9	77	2.41	33.2	13.0	17

TABLE A 1.42

Tank Diameter: 0.4m

Impeller: Anchor D = 0.318 m Temp. = 44 °C

Material: Chocolate μ = Nsm^{-2} ϱ = 1280 kgm^{-3}

N(rps)	T(Nm)	P_o	Re	μ_A	$\dot{\gamma}_A$	k_s
0.085	3.93	821	0.233	47.3	1.45	17
0.200	5.52	208	0.880	29.4	3.44	17
0.320	6.93	102	1.800	23.0	5.40	17
0.430	7.60	62	2.960	18.8	7.74	18
0.540	8.51	44	4.160	16.8	9.50	18
0.660	9.24	32	5.730	14.9	11.8	18
0.800	10.61	25	7.300	14.2	13.0	16
0.890	11.03	21	8.700	13.2	14.7	17
1.030	11.30	16	11.30	11.8	18.0	18
1.140	11.55	13.4	13.70	10.8	21.4	19
1.250	12.12	11.7	15.60	10.4	22.5	18
1.370	13.70	11.0	16.90	10.5	22.3	16
1.50	13.60	9.1	20.20	9.6	26.3	18

TABLE A 1.43

Tank Diameter: 0.4m

Impeller: Anchor D = 0.348 m Temp. = 22 ^{o}C

Material: Silicone Oil = 98 Nsm^{-2} = 985 kgm^{-3}

N(rps)	T(Nm)	P_o	Re
0.036	4.71	4546	0.044
0.058	7.77	2887	0.071
0.069	8.98	2357	0.084
0.078	10.04	2063	0.095
0.085	11.45	1981	0.104
0.11	14.45	1493	0.134
0.18	23.56	909	0.219
0.26	34.12	631	0.317
0.29	39.43	586	0.353

TABLE A 1.44

Tank Diameter: 0.4m

Impeller: Anchor D = 0.348 m Temp. = 20 °C

Material: Glycerol = 0.17 Nsm^{-2} = 1278 kgm^{-3}

N(rps)	T(Nm)	P_o	Re
0.14	0.06	2.80	127.5
0.32	0.17	1.60	291
0.44	0.23	1.12	400
0.54	0.34	1.12	492
0.62	0.45	1.12	565
0.76	0.66	1.10	692
0.83	0.79	1.10	756
0.93	0.99	1.10	847
1.02	1.05	0.97	1929
1.10	1.17	0.93	1001
1.17	1.32	0.93	1065
1.26	1.52	0.92	1147

TABLE A 1.45

Tank Diameter: 0.4m

Impeller: Anchor D = 0.348 m Temp. =20 ^{o}C

Material: Lub. Oil = 1.6 Nsm^{-2} = 872 kgm^{-3}

N(rps)	T(Nm)	P_o	Re
0.08	0.17	37.6	5.30
0.11	0.24	27.7	7.30
0.14	0.31	21.7	9.24
0.18	0.38	16.6	11.90
0.22	0.52	15.1	14.50
0.28	0.60	10.8	18.50
0.35	0.75	8.6	23.10
0.38	0.81	7.9	25.10
0.45	0.98	6.8	29.70
0.54	1.28	6.2	35.60
0.59	1.43	5.8	38.90
0.67	1.66	5.2	44.20
0.76	2.01	4.9	50.20
0.82	2.34	4.6	54.10
0.86	2.36	4.5	56.80
0.99	2.92	4.2	65.30

TABLE A 1.46

Tank Diameter: 0.4m

Impeller: Anchor D = 0.348 m Temp. = 25 ^{o}C

Material: Sugar = 30 Nsm^{-2} = 1390 kgm^{-3}

N(rps)	T(Nm)	P_o	Re
0.031	1.12	1033	0.174
0.046	1.56	653	0.260
0.054	1.80	546	0.310
0.06	2.14	526	0.340
0.073	2.6	432	0.410
0.120	4.2	259	0.673
0.130	4.9	257	0.732
0.154	5.5	206	0.861
0.174	6.22	182	0.980
0.282	10.3	115	1.58
0.344	12.4	93	1.94
0.390	14.0	82	2.20
0.460	16.6	70	2.60
0.55	20.2	60	3.10
0.64	24.4	53	3.54
0.77	28.1	42	4.37
0.83	30.1	39	4.72
0.88	32.2	37	4.96
1.02	37.4	32	5.78

TABLE A 1.47

Tank Diameter: 0.4m

Impeller: Anchor D = 0.348 m Temp. = 25 ^{o}C

Material: Water = $1x10^{-3}$ Nsm^{-2} = 1000 kgm^{-3}

N(rps)	T(Nm)	P_o	Re
0.18	0.024	0.90	21,799
0.35	0.085	0.85	42,386
0.46	0.138	0.80	55,708
0.58	0.232	0.85	70,240

TABLE A 1.48

Tank Diameter: 0.4m

Impeller: Anchor D = 0.348 m Temp. =24 ^{o}C

Material: Biozam R = Nsm^{-2} = 1000 kgm^{-3}

N(rps)	T(Nm)	P_o	Re_1	A	A	k_s
0.065	6.8	1980	0.101	78.0	1.63	25
0.078	7.1	1429	0.140	67.5	1.91	24.5
0.130	7.6	550	0.364	43.2	3.12	24
0.220	7.5	190	1.050	25.4	5.61	25.5
0.290	7.6	111	1.810	19.4	7.54	26
0.340	8.2	87	2.290	18.0	8.16	24
0.380	8.6	73	2.730	16.9	8.74	23
0.450	8.6	52	3.840	14.2	10.62	23.6
0.520	8.6	39	5.160	12.2	12.48	24
0.660	9.6	27	7.470	10.7	14.52	22
0.730	9.2	21	9.410	9.4	16.79	23
0.850	8.6	15	13.73	7.5	21.25	25
0.980	9.1	12	17.200	6.9	23.52	24
1.050	9.8	11	18.430	6.9	23.10	22
1.200	9.9	8.5	23.440	6.2	26.40	22

TABLE A 1.49

Tank Diameter: 0.4m

Impeller: Anchor D = 0.348 m Temp. = 25 °C

Material: 3% Carbopol = Nsm^{-2} = 1000 kgm^{-3}

N(rps)	T(Nm)	P_o	Re	A	A
0.085	7.6	1290	0.155	66.5	1.96
0.093	7.8	1111	0.18	62.8	2.08
0.135	8.2	556	0.36	45.3	3.18
0.209	8.9	250	0.80	31.6	4.90
0.378	9.4	81	2.5	18.5	9.50
0.432	9.8	65	3.1	17.0	10.80
0.540	10.5	45	4.5	14.5	13.00
0.618	10.3	33	6.0	12.6	15.70
0.695	10.5	27	7.5	11.2	17.60
0.791	11.3	22	9.0	10.6	19.00
0.888	11.5	18	11.0	9.8	21.00
1.160	13.3	12	16.5	8.5	24.50
1.250	14.1	11	18.0	8.4	25.00
1.34	15.0	10	19.5	8.3	25.50
1.42	15.6	9.5	21.0	8.2	26.00
1.52	16.3	9	23.0	8.0	27.00

TABLE A 1.50

Tank Diameter: 0.4m

Impeller: Anchor D = 0.348 m Temp. = 40 ^{o}C

Material: Chocolate = Nsm^{-2} = 1280 kgm^{-3}

N(rps)	T(Nm)	P_o	Re	A	A	k_s
0.075	4.44	758	0.264	44.0	1.65	22
0.125	5.44	334	0.598	32.4	2.88	23
0.250	7.83	121	1.66	23.3	5.25	21
0.370	8.50	60	3.35	17.1	9.26	25
0.460	9.57	44	4.60	15.5	11.04	24
0.550	10.85	35	5.80	14.7	12.10	22
0.620	11.47	29	6.96	13.8	13.64	22
0.730	13.03	25	8.51	13.3	14.60	20
0.850	14.20	19	10.63	12.4	16.66	20
1.05	14.60	13	15.80	10.3	23.10	22
1.21	16.60	11	18.39	10.2	23.60	20
1.36	16.74	9	22.90	9.2	28.56	21
1.50	18.50	8	25.30	9.2	28.50	19

TABLE A 1.51

Tank Diameter: 0.4m

Impeller:Anchor D = 0.369 m Temp. = 25 °C

Material: Silicone Oil μ = 98 Nsm^{-2} ρ = 985 kgm^{-3}

N(rps)	T(Nm)	P_o	Re
0.04	7.60	4418	0.055
0.089	16.7	1967	0.122
0.16	29.5	1073	0.219

TABLE A 1.52

Tank Diameter: 0.4m

Impeller: Anchor D = 0.369 m Temp. = 25 °C

Material: Sugar μ = 29 Nsm^{-2} ρ = 1390 kgm^{-3}

N(rps)	T(Nm)	P_o	Re
0.043	2.19	783	0.280
0.066	3.47	527	0.427
0.100	4.83	319	0.659
0.120	5.36	246	0.781
0.140	7.30	246	0.915
0.160	7.55	195	1.050
0.170	8.26	189	1.110
0.210	10.68	160	1.340
0.290	14.00	110	1.950
0.310	15.27	105	2.070
0.350	18.00	97	2.320
0.410	21.87	86	2.680
0.544	27.80	62	3.540
0.640	32.85	53	4.150

TABLE A 1.53

Tank Diameter: 0.4m

Impeller: Anchor D = 0.369 m Temp. = 23 °C

Material: Lub. Oil μ = 1.8 Nsm^{-2} ρ = 893 kgm^{-3}

N(rps)	T(Nm)	P_o	Re
0.037	0.17	128	2.5
0.087	0.32	43	6.0
0.14	0.48	26	9.5
0.18	0.61	20	12
0.34	1.20	10	23
0.36	1.50	12	24
0.44	1.60	8	30
0.53	2.00	7	36
0.59	2.30	7	36
0.65	2.50	6	40
0.71	2.90	6	44
0.80	3.41	5.5	48
0.92	3.92	4.7	54
1.02	4.40	4.3	62
1.10	4.91	4.2	69
1.15	5.11	4	74
1.19	5.30	3.8	78
1.23	5.54	3.8	80

TABLE A 1.54

Tank Diameter: 0.4m

Impeller: Anchor D = 0.369m Temp. = 24 °C

Material: Glycerol μ = 0.17 Nsm^{-2} ρ = 1278 kgm^{-3}

N(rps)	T(Nm)	P_o	Re
0.150	0.09	2.80	154
0.181	0.11	2.40	184
0.230	0.16	2.10	235
0.280	0.22	2.00	287
0.331	0.29	1.90	338
0.390	0.26	1.20	399
0.420	0.27	1.10	430
0.470	0.31	1.00	481
0.530	0.39	1.00	543
0.620	0.48	0.90	635
0.750	0.71	0.91	768
0.810	0.78	0.85	829
0.930	1.02	0.85	952
1.05	1.23	0.80	1075
1.20	1.61	0.80	1228

TABLE A 1.55

Tank Diameter: 0.4m

Impeller: Anchor D = 0.369 m Temp. = 25 °C

Material: Water $\mu = 1 \times 10^{-3}$ Nsm^{-2} $\rho = 1000$ kgm^{-3}

N(rps)	T(Nm)	P_o	Re
0.16	0.024	0.85	21,786
0.25	0.061	0.7	34,040
0.29	0.08	0.75	39,487
0.35	0.11	0.75	47,656
0.43	0.16	0.7	58,549
0.55	0.28	0.7	74,889
0.63	0.35	0.8	85,781

TABLE A1.56

Tank Diameter: 0.4m

Impeller: Anchor D = 0.369 m Temp. = 40 °C

Material: Chocolate μ = Nsm^{-2} ρ = 1280 kgm^{-3}

N(rps)	T(Nm)	P_o	Re	μ_A	γ_A	k_s
0.07	5.17	753	0.312	39.1	1:96	28
0.13	7.04	299	0.787	28.8	3.38	26
0.18	8.00	178	1.318	23.8	4.77	27
0.22	8.7	129	1.817	21.1	5.94	27
0.28	9.84	90	2.600	18.8	7.28	26
0.34	11.00	68	3.45	17.2	8.50	25
0.42	11.6	47	5.02	14.6	11.3	27
0.48	12.5	39	6.02	13.9	12.5	26
0.53	13.3	34	7.00	13.2	13.8	26
0.59	13.6	28	8.30	12.4	15.3	26
0.62	13.4	25	9.30	11.6	17.1	28
0.68	14.6	23	10.4	11.4	17.9	26
0.74	15.0	20	12.0	10.8	19.7	27
0.85	16.8	17	14.1	10.5	20.4	24
0.93	17.4	14	16.4	9.9	22.8	24
1.05	17.8	12	20.3	9.0	27.3	26
1.15	18.8	10	23.0	8.7	28.8	25

TABLE A 1.57

Tank Diameter: 0.4m

Impeller: Anchor D = 0.369 m Temp. = 24 °C

Material: Biozam R μ = Nsm^{-2} ϱ = 1000 kgm^{-3}

N(rps)	T(Nm)	P_o	Re	μ_A	$\dot{\gamma}_A$	k_s
0.063	8.58	1983	0.116	74.0	1.73	28
0.089	8.42	975	0.236	51.4	2.58	29
0.15	8.95	365	0.630	32.4	4.28	29
0.23	9.80	170	1.356	23.1	6.21	27
0.28	10.0	117	1.975	19.3	7.56	27
0.32	10.2	91	2.520	17.3	8.54	27
0.37	10.3	69	3.34	15.1	9.92	27
0.41	10.3	56	4.08	13.7	11.1	27
0.48	10.8	43	5.36	12.2	12.5	26
0.53	11.0	36	6.44	11.2	13.8	26
0.64	11.2	25	9.27	9.4	16.6	26
0.75	11.3	19	12.45	8.2	19.4	26
0.82	12.5	17	13.78	8.1	19.7	24
0.95	12.1	12	18.75	6.9	23.3	25
1.02	12.0	10.6	21.7	6.4	25.5	25

TABLE A 1.58

Tank Diameter: 0.4m

Impeller: Anchor D = 0.369 m Temp. = 25 °C

Material: 3% Carbopol μ = Nsm^{-2} ϱ = 1000 kgm^{-3}

N(rps)	T(Nm)	P_o	Re	μ_A	$\dot{\gamma}_A$	k_s
0.07	10.0	1880	0.125	76.0	1.62	23
0.154	11.3	435	0.540	39.0	3.80	25
0.174	11.8	356	0.660	36.0	4.25	24
0.371	13.0	87	2.70	19.0	9.40	25
0.410	13.0	71	3.30	17.0	10.8	26
0.432	13.2	65	3.60	16.4	11.0	25
0.602	13.3	34	7.00	12.0	16.6	28
0.652	13.6	29	8.00	11.0	18.0	28
0.795	14.7	21.4	11.0	9.8	21.0	26
0.834	14.9	19.6	12.0	9.4	22.5	27
0.903	15.5	17.4	13.5	9.1	23.2	26
1.01	16.4	14.7	16.0	8.6	24.8	24
1.11	17.2	12.8	18.4	8.2	26.0	23
1.27	18.8	11.0	22.0	7.9	27.0	21
1.34	19.3	9.8	24.0	7.6	29.0	22

TABLE A 1.59

Tank Diameter: 0.4m

Impeller: Anchor D = 0.382 m Temp. = 22 °C

Material: Silicone Oil = 98 Nsm^{-2} = 985 kgm^{-3}

N(rps)	T(Nm)	P_o	Re
0.032	7.5	5745	0.047
0.078	18.71	2412	0.114
0.100	24.29	1905	0.147
0.160	38.91	1192	0.235

TABLE A1.60

Tank Diameter: 0.4m

Impeller: Anchor D = 0.382 m Temp. = 26 °C

Material: Sugar = 25.6 Nsm^{-2} = 1390 kgm^{-3}

N(rps)	T(Nm)	P_o	Re
0.031	2.28	1319	0.246
0.05	3.4	756	0.396
0.073	5.9	615	0.573
0.112	8.94	396	0.873
0.027	1.63	1245	0.218
0.039	2.5	914	0.30
0.05	3.3	734	0.396
0.081	5.2	441	0.633
0.104	6.9	355	0.818
0.14	9.1	258	1.091
0.16	11.2	244	1.255
0.19	13.4	207	1.500
0.22	15.6	179	1.773
0.24	19.8	192	1.901
0.34	24.0	116	2.727
0.38	27.3	95	3.000
0.42	29.7	94	3.273

TABLE A 1.61

Tank Diameter: 0.4m

Impeller: Anchor D = 0.382 m Temp. = 20 °C

Material: Lub. Oil = 1.8 Nsm^{-2} = 893 kgm^{-3}

N(rps)	T(Nm)	P_o	Re
0.043	0.204	94.0	3.1
0.143	0.612	26.0	10.0
0.181	0.780	21.0	13.0
0.210	0.850	16.0	15.0
0.280	1.160	13.0	20.0
0.400	1.700	9.4	29.0
0.440	1.940	9.0	32.0
0.460	2.040	8.0	33.0
0.550	2.550	7.5	40.0
0.580	2.690	7.0	42.0
0.614	2.890	7.0	45.0
0.660	3.200	6.4	48.0
0.750	3.670	5.7	54.0
0.800	4.100	5.6	58.0
0.860	4.400	5.2	62.0
0.900	4.690	5.0	65.0
1.02	5.440	4.5	74.0

TABLE A 1.62

Tank Diameter: 0.4m

Impeller: Anchor D = 0.382 m Temp. =25 ^{o}C

Material: Glycerol = 0.07 Nsm^{-2} = 1218 kgm^{-3}

N(rps)	T(Nm)	P_o	Re
0.26	0.183	1.72	660
0.35	0.282	1.46	889
0.71	0.819	1.03	1803
0.83	0.924	0.85	2107
1.04	1.433	0.84	2641
1.18	1.757	0.80	2996
1.25	1.996	0.81	3174

TABLE A 1.63

Tank Diameter: 0.4m

Impeller: Anchor D = 0.382 m Temp. = 25 ^{o}C

Material: Water $= 1 \times 10^{-3}$ Nsm^{-2} $= 1000$ kgm^{-3}

N(rps)	T(Nm)	P_o	Re
0.31	0.100	0.80	45,236
0.42	0.185	0.81	61,288
0.56	0.317	0.78	81,717
0.63	0.386	0.75	91,932
0.72	0.504	0.75	105,065

TABLE A 1.64

Tank Diameter: 0.4m

Impeller: Anchor D = 0.382 m Temp. = 25 °C

Material: 4% CMC μ = Nsm^{-2} ϱ = 1000 kgm^{-3}

N(rps)	T(Nm)	P_o	Re	μ_A	γ_A	k_s
0.058	10.9	2500	0.114	74.0	2:04	35
0.093	14.1	1261	0.226	60.0	3.26	35
0.100	14.8	1140	0.250	58.5	3.48	35
0.135	17.5	742	0.384	51.4	4.71	35
0.189	21.2	457	0.622	44.4	6.62	35
0.212	22.7	390	0.730	42.4	7.34	35
0.401	33.3	160	1.780	32.9	13.31	33
0.448	35.6	137	2.080	31.4	14.78	33

TABLE A 1.65

Tank Diameter: 0.4m

Impeller: Anchor D = 0. 382m Temp. = 24 ^{o}C

Material: Biozam R μ = Nsm^{-2} ϱ = 1000 kgm^{-3}

N(rps)	T(Nm)	P_o	Re	μ_A	$\dot{\gamma}_A$	k_s
0.0772	11.58	1500	0.190	59.4	2.2	29
0.170	10.9	291	0.980	25.4	5.6	33
0.135	9.9	419	0.680	28.9	4.9	36
0.178	11.24	274	1.040	25.0	5.7	32
0.201	10.83	207	1.400	21.2	6.8	34
0.212	11.12	191	1.500	21.0	7.0	33
0.293	11.45	103	2.780	15.4	9.7	33
0.347	11.31	73	3.930	12.9	11.8	34
0.394	11.46	57	5.000	11.5	13.4	34
0.417	11.17	50	5.744	10.6	14.6	35
0.533	11.15	30	9.410	8.3	19.2	36
0.618	12.17	25	11.57	7.8	20.4	33
0.656	11.93	21	13.30	7.2	22.3	34
0.695	12.14	19	14.71	6.9	23.6	34
0.795	12.44	15	18.72	6.2	26.2	33
0.842	12.58	14	20.84	5.9	27.8	33
0.899	12.77	12	23.44	5.6	29.7	33
1.07	13.05	9	32.55	4.8	35.3	33

TABLE A 1.66

Tank Diameter: 0.4m

Impeller: Anchor D = 0.382 m Temp. = 40 °C

Material: Chocolate μ = Nsm^{-2} ρ = 1280 kgm^{-3}

N(rps)	T(Nm)	P_o	Re	μ_A	$\dot{\gamma}_A$	k_s
0.043	4.98	2080	0.13	46	1.51	35
0.089	7.13	695	0.410	32	2.94	33
0.141	8.60	334	0.85	24	4.8	34
0.192	10.22	214	1.33	21	6.2	32
0.233	10.34	147	1.93	18	8.4	36
0.285	11.89	113	2.52	16.5	9.5	33
0.337	12.35	84	3.40	14.5	11.8	34
0.381	13.54	72	4.90	14	12.6	35
0.432	14.10	58	6.10	13	14.7	34
0.490	14.62	47	6.80	12	17.2	33
0.532	15.40	42	7.80	11.4	18.3	32
0.589	16.40	37	8.53	11	19.4	33
0.631	17.22	33	10.0	11	20.2	32
0.690	17.63	29	10.40	10	22.8	32
0.721	18.45	27	11.14	10	22.7	33
0.748	18.55	26	12.60	10	23.9	34
0.810	18.86	22	15.10	9.2	26.7	33
0.890	19.40	19	15.46	8.6	30.3	34

TABLE A 1.67

Tank Diameter: 0.15m P/D = 0.56 , Nb = 1.0

Impeller: Ribbon D = 0.135 m Temp. = ^{o}C

Material: Silicone Oil μ = 98 Nsm^{-2} ρ = 985 kgm^{-3}

N(rps)	T(Nm)	P_o	Re
0.035	0.336	39063	.0064
0.054	0.518	25253	.0099
0.081	0.779	16890	.0148
0.093	0.894	14706	.0170
0.112	1.075	12195	.0205
0.16	1.535	8532	.0293
0.21	2.010	6494	.0385
0.29	2.780	4708	.0531
0.34	3.260	4013	.0623
0.38	3.650	3592	.0696

TABLE A1.68

Tank Diameter: 0.15m P/D = .56 , Nb = 1.0

Impeller: Ribbon D = 0.135 m Temp. =20 ^{o}C

Material: Lub. Oil μ = 1.8 Nsm^{-2} ρ = 893 kgm^{-3}

N(rps)	T(Nm)	P_o	Re
0.360	0.064	77	3.26
0.450	0.079	61	4.07
0.730	0.129	38	6.60
0.950	0.167	29	8.60
1.310	0.230	21	11.9
1.630	0.288	17	14.7
1.780	0.303	15	16.1
1.930	0.332	14	17.5
2.600	0.474	11	23.5
3.500	0.624	8	31.6

TABLE A 1.69

Tank Diameter: 0.15m P/D = .56 , Nb = 1.0

Impeller: Ribbon D = 0.135 m Temp. = 24 ^{o}C

Material: 4% CMC μ = Nsm^{-2} ρ = 1000 kgm^{-3}

N(rps)	T(Nm)	P_o	Re	μ_A	γ_A	k_s
0.042	0.379	30120	0.0083	92.4	1.05	25
0.069	0.467	13736	0.0182	69.1	1.73	25
0.093	0.515	8333	0.030	57.0	2.42	26
0.135	0.602	4630	0.054	46.0	3.51	26
0.295	0.839	1351	0.185	29.0	7.67	26
0.386	0.923	868	0.288	24.4	10.4	27
0.532	1.03	510	0.490	19.8	14.9	28
0.736	1.24	321	0.780	17.2	19.1	26
1.210	1.60	153	1.630	13.5	29.0	24
1.400	1.67	119	2.100	12.1	35.0	25

TABLE A 1.70

Tank Diameter: 0.15m P/D = .56 , Nb = 1.0

Impellcr: Ribbon D = 0.135 m Temp. = 33 ^{o}C

Material: Chocolate μ = Nsm^{-2} ϱ = 1280 kgm^{-3}

N(rps)	T(Nm)	P_o	Re	μ_A	$\dot{\gamma}_A$	k_s
.032	0.199	21379	0.0116	64.2	0.83	26
.058	0.261	8494	0.0292	46.3	1.51	26
.073	0.294	6050	0.041	41.6	1.83	25
.095	0.330	4000	0.062	36.0	2.38	25
0.132	0.387	2431	0.102	30.1	3.30	25
0.186	0.461	1459	0.170	25.5	4.46	24
0.193	0.458	1348	0.184	24.4	4.83	25
0.265	0.519	809	0.307	20.1	6.89	26
0.339	0.587	559	0.444	17.8	8.48	25
0.432	0.671	394	0.629	16.0	10.4	24
0.501	0.720	314	0.789	14.8	12.0	24

TABLE A 1.71

Tank Diameter: 0.15m P/D = 1.0 , Nb= 2

Impeller: Ribbon D = 0. 135m Temp. = ^{o}C

Material: Silicone Oil = 98 Nsm^{-2} = 985 kgm^{-3}

N(rps)	T(Nm)	P_o	Re
.052	.564	29790	.0095
.073	.788	21119	.0134
.121	1.307	12748	.0222
.163	1.757	9433	.0300
.193	2.092	7861	.0360
.286	3.116	5442	.0520
.321	3.460	4797	.0590

TABLE A 1.72

Tank Diameter: 0.15m P/D = 1.0 , Nb = 2

Impeller: Ribbon D = 0.135 m Temp. = 20 ^{o}C

Material: Lub. Oil = 1.8 Nsm^{-2} = 893 kgm^{-3}

N(rps)	T(Nm)	P_o	Re
.682	.134	45.1	6.17
.731	.143	42.1	6.61
.921	.181	33.4	8.33
1.130	.222	27.3	10.2
1.27	.249	24.2	11.5
1.69	.331	18.2	15.3
1.90	.373	16.2	17.2
1.96	.385	15.7	17.7
2.58	.509	12.0	23.3
3.51	.691	8.8	31.7

TABLE A 1.73

Tank Diameter: 0.15m P/D = .5 , Nb = 1.0

Impeller: Ribbon D = 0.113 m Temp. = 20 °C

Material: Silicone Oil μ = 98 Nsm^{-2} ρ = 1280 kgm^{-3}

N(rps)	T(Nm)	P_o	Re
0.032	0.114	38537	0.0041
0.041	0.146	30038	0.00526
0.081	0.284	15340	0.103
0.140	0.497	8778	0.018
0.190	0.676	6475	0.0244
0.223	0.794	5525	0.0286
0.293	1.040	4202	0.0376
0.336	1.200	3666	0.0431

TABLE A 1.74

Tank Diameter: 0.15m P/D = .5 , Nb = 1.0

Impeller: Riibon D = 0.113 m Temp. = 19 °C

Material: Lub. Oil μ = 1.8 Nsm^{-2} ϱ = 893 kgm^{-3}

N(rps)	T(Nm)	P_o	Re
0.228	0.015	113	1.44
0.432	0.029	60	2.74
0.693	0.047	37	4.39
0.895	0.061	29	5.67
1.210	0.084	22	7.67
1.360	0.092	19	8.62
1.480	0.103	18	9.38
1.730	0.118	15	11.0
2.100	0.139	12	13.3
2.680	0.188	10	17.0
3.210	0.216	8	20.3

TABLE A 1.75

Tank Diameter: 0.15m P/D = .5 , Nb = 1.0

Impeller: Ribbon D = 0.113 m Temp. = 20 ^{o}C

Material: Glycerol = 1.2 Nsm^{-2} = 1250 kgm^{-3}

N(rps)	T(Nm)	P_o	Re
0.585	0.026	20.6	7.78
0.913	0.04	13.2	12.2
1.29	0.057	9.3	17.2
1.68	0.075	7.2	22.4
1.86	0.084	6.6	24.7
2.24	0.10	5.4	29.8
3.14	0.14	3.8	41.8
3.43	0.15	3.4	45.6
3.79	0.17	3.2	50.4
4.46	0.20	2.8	59.3

TABLE A 1.76

Tank Diameter: 0.15m P/D = .5 , Nb = 1.0

Impeller: Ribbon D = 0.113 m Temp. = 25 °C

Material: 4% CMC μ = Nsm^{-2} ρ = 1000 kgm^{-3}

N(rps)	T(Nm)	P_o	Re	μ_A	$\dot{\gamma}_A$	k_s
.055	.218	24585	.00663	106	.83	15
.073	.245	15673	.0104	90	1.09	15
.099	.282	9819	.0166	76	1.48	15
.132	.306	5993	.0272	62	2.11	16
.162	.320	4158	.0392	53	2.75	17
.195	.372	3340	.0488	51	2.93	15
.268	.421	2000	.0815	42	4.02	15
.321	.456	1509	.108	38	4.82	15
.431	.544	1000	.162	34	6.04	14
.501	.583	792	.206	31	7.01	14
.632	.632	540	.299	27	8.85	14

TABLE A 1.77

Tank Diameter: 0.15m P/D = .5 , Nb = 1.0

Impeller: Ribbon D = 0.113 m Temp. = 25 °C

Material: 3% Carbopol μ = Nsm^{-2} ρ = 1000 kgm^{-3}

N(rps)	T(Nm)	P_o	Re	μ_A	$\dot{\gamma}_A$	k_s
0.052	0.274	34615	.00468	142	.73	14
0.078	0.299	16753	.00967	103	1.09	14
0.099	0.280	9759	.01660	76.3	1.58	16
0.132	0.312	6113	.0265	63.6	1.98	15
0.156	0.323	4525	.0358	55.7	2.34	15
0.183	0.333	3389	.0478	48.9	2.75	15
0.221	0.346	2418	.0670	42.1	3.32	15
0.263	0.402	1983	.0817	41.1	3.42	13
0.333	0.396	1218	.1330	32.1	4.66	14
0.418	0.393	768	.2110	25.3	6.27	15

TABLE A 1.78

Tank Diameter: 0.4m 0.15m

Impeller: Anchor D = 0.14 m Temp. = 20 °C

Material: Silicone Oil = 98 Nsm^{-2} = 985 kgm^{-3}

N(rps)	T(Nm)	P_o	Re
.062	.672	20738	.0122
.083	.896	15423	.0164
.099	1.07	12970	.0195
.113	1.342	12463	.0203
.116	1.250	11050	.0229
.130	1.41	9870	.0256
.165	1.77	7890	.0321
.181	1.96	7100	.0357
.200	2.17	6420	.0394

TABLE A 1.79

Tank Diameter: 0.4m 0.15m

Impeller: Anchor D = 0.14 m Temp. =23 ^{o}C

Material: Glycerol = Nsm^{-2} = kgm^{-3}

N(rps)	T(Nm)	P_o	Re
.421	.0512	27	9.4
.716	.088	16	16.0
1.08	.125	10	24.1
1.45	.171	7.6	32.3
1.83	.222	6.2	41.1
2.32	.276	4.8	51.7
2.95	.363	3.9	65.7
3.34	.406	3.4	74.4
3.86	.462	2.9	86.0
4.62	.548	2.4	103

TABLE A 1.80

Tank Diameter: 0.4m

Impeller: Ribbon D =0.352 , P/D =0.5 , Nb=1.0

Fluid	T_b	N_c	Re_c	Pr
Silicone Oil	85	.086	.35	3×10^5
Sugar	50	.250	5.5	3.3×10^4
Lub. Oil	50	.450		2.9×10^3
Chocolate	45	.073	.25	8×10^5
Carbopol	60	.080	.340	2.8×10^5

TABLE A 1.81

Tank Diameter: 0.4m

Impeller: Ribbon P/D =0.5 , Nb = 1.0

D	C/D	Silicone Oil	Lub. Oil
		Re_c	Re_c
.352	.0682	.35	180
.370	.0405	.183	80
.380	.0263	.105	56

TABLE A1.82

Tank Diameter: 0.4m

Impeller: Ribbon D= 0.352m C/D = 0.0682 , Nb =1.0

P/D	Silicone Oil	Lub. Oil
	Re_c	Re_c
0.5	0.35	180
1.0	0.50	246

TABLE A 1.83

Tank Diameter: 0.4m

Impeller: Ribbon P/D =0.5 , C/D = 0.0685

Nb	Silicone Oil	Lub. Oil
	Re_c	Re_c
1	0.35	180
2	0.142	70

TABLE A 1.84

Tank Diameter : 0.4m

Impeller: Ribbon D =0.352 m P/D = 1 Nb = 2

Material: Silicone Oil

N (r/s)	T_b (°C)	T_w (°C)	Re	Pr	Q (W)	h $\left(\frac{W}{m^2\ °C}\right)$	Nu	$(\varepsilon D^4/\nu^3)$
.020	95.5	28.5	.083	3×10^5	480	11.9	30	5.56
.028	56.6	22.7	.066	5 "	269	13.1	33	3.20
.054	59.1	22.3	.130	5 "	342	15.0	39	11.8
.069	60.0	23.3	.140	5 "	293	13.2	33	24.3
.099	59.4	23.9	.239	5 "	318	15.0	37	41.9
.139	57.8	23.9	.355	5 "	342	17.0	42	82.8
.151	101	27.7	.644	3 "	562	12.7	32	332
.293	91.6	29.9	1.22	6 "	635	17.0	43	1145
.378	88.7	31.4	1.60	3 "	684	19.7	50	1873
.425	87.7	32.0	1.80	3 "	733	21.7	55	2356
.463	86.0	31.5	1.80	3 "	709	21.5	54	2498
.540	83.0	31.5	1.96	3 "	611	19.5	49	3024
.633	83.9	33.6	2.37	3 "	733	24.0	61	4535
.703	84.7	33.0	2.60	3 "	782	25.0	63	6074

TABLE A 1.85

Tank Diameter : 0.4m

Impeller: Ribbon D =0.352 m P/D =1 Nb = 2

Material: Chocolate

N (r/s)	T_b (°C)	T_w (°C)	Re	Pr x10^5	Q (W)	h ($\frac{W}{m^2\ °C}$)	Nu	$(\varepsilon D^4/\nu^3)$
.579	55	41	13.7	1.5	489	57.7	109	1.23×10^4
.610	47	35	11.5	1.8	391	54.3	103	0.75 "
.695	55	41	18.2	1.3	538	65.4	124	1.79 "
.834	54	42	23.4	1.2	587	79.8	151	2.42 "
.926	54	42	27.5	1.2	636	86.2	163	2.96 "
1.04	54	42	33.0	.92	636	87.6	166	3.81 "
1.16	55	43	40.2	1.0	636	87.6	166	5.17 "
1.26	55	44	44.2	.98	684	105	199	5.54 "
1.40	55	43	52.0	.93	733	108	205	6.98 "
1.50	54	43	58.4	.89	684	104	197	7.98 "
1.64	55	43	68.7	.82	831	115	217	10.3 "

TABLE A 1.86

Tank Diameter : 0.4m

Impeller: Ribbon D = 0.352 m P/D = .5 Nb = 1.0

Material: Silicone Oil

N (r/s)	T_b (°C)	T_w (°C)	Re	Pr	Q (W)	h $\left(\frac{W}{m^2\ °C}\right)$	Nu	$(\varepsilon D^4/\nu^3)$
.073	85.5	25.0	.283	3×10^5	514	13.6	34.2	21.0
.104	80.0	24.0	.361	3 "	519	14.8	37.2	33.5
.127	77.0	24.0	.417	3 "	510	15.4	38.7	44.5
.162	75.0	24.0	.511	4 "	510	16.0	40.3	66.4
.201	74.0	24.0	.626	4 "	510	16.3	41.0	100
.245	72.0	24.5	.735	4 "	519	17.5	44	136
.317	69.0	23.0	.907	4 "	519	18.0	45.3	241
.363	67.0	23.0	.992	4 "	510	18.6	46.8	247
.386	67.0	24.0	1.06	4 "	533	19.8	49.8	277
.432	67.6	25.0	1.21	4 "	519	19.5	49.1	363

TABLE A 1.87

Tank Diameter : 0.4m

Impeller: Ribbon D =0.352 m P/D =.5 Nb = 1.0

Material: Sugar

N (r/s)	T_b (°C)	T_w (°C)	Re	Pr x10^4	Q (W)	h ($\frac{W}{m^2\ °C}$)	Nu	$(\varepsilon D^4/\nu^3)$
.035	65	33	1.90	2.3	527	26.3	28.1	-
.097	64	34	4.25	2.8	"	28.1	30.0	-
.185	61	33	5.67	4.0	"	30.0	32.0	-
.140	58	32	3.30	5.2	"	32.0	34.0	-
.282	58	34	6.65	5.2	"	35.0	37.0	-
.363	55	34	6.68	6.7	"	40.0	42.7	-
.444	54	35	6.81	8.0	"	43.0	46.0	-
.529	53	35	7.79	8.0	"	45.6	48.6	-
.639	51	35	7.84	10	"	49.6	53.0	-

TABLE A 1.88

Tank Diameter : 0.4m

Impeller:Ribbon D =0.352 m P/D = .5 Nb = 1

Material: Lub. Oil

N (r/s)	T_b (°C)	T_w (°C)	Re	Pr x10^2	Q (W)	h ($\frac{W}{m^2\ °C}$)	Nu	$(\varepsilon D^4/\nu^2)$
.703	42.0	22.0	229	5.0	537	43	119	3.42×10^7
.818	42.5	22.0	275	4.8	537	42	116	5.37 "
.957	41.7	23.0	311	5.0	527	44	123	7.32 "
1.04	41.8	23.0	338	5.0	537	46	127	8.97 "
1.17	41.0	23.0	359	5.3	529	48	131	10.4 "
1.31	40.0	23.5	381	5.6	529	53	146	11.9 "
1.48	39.0	24.0	398	6.0	535	57	157	13.4 "

TABLE A 1.89

Tank Diameter : 0.4m

Impeller: Ribbon D =0.352 m P/D = 1 Nb = 1.0

Material: Silicone Oil

N (r/s)	T_b (°C)	T_w (°C)	Re	Pr	Q (W)	h $\left(\frac{W}{m^2\ °C}\right)$	Nu	$(\varepsilon D^4/\nu^3)$
.054	83.8	26.1	.203	$3x10^5$	391	10.5	28.5	22.6
.097	83.9	25.8	.362	"	391	11.0	28.0	71.8
.145	84.2	24.5	.544	"	391	10.8	27.0	163
.212	84.6	24.4	.795	"	464	12.7	32.1	349
.290	82.4	27.3	1.09	"	464	14.0	35.0	646
.367	79.3	25.8	1.26	"	464	14.3	36.0	865
.429	78.2	26.7	1.43	"	953	30.1	77.0	1112
.564	78.0	28.0	1.87	"	538	17.8	44.7	1928
.649	78.8	28.8	2.16	"	611	20.2	51.0	2554
.726	78.4	28.8	2.42	"	634	21.2	53.2	3169

TABLE A 1.90

Tank Diameter : 0.4m

Impeller: Ribbon D =0.352 m P/D =1 Nb = 1

Material: Chocolate

N (r/s)	T_b (°C)	T_w (°C)	Re	Pr x10^5	Q (W)	h $(\frac{W}{m^2\ °C})$	Nu	$(\varepsilon D^4/\nu^3)$
.058	42.3	34.1	.260	7.85	147	20.3	38.4	
.116	42.6	34.1	.750	5.4	189	26.3	49.8	
.193	46.9	37.3	1.94	3.4	210	29.0	55.0	
.317	49.8	38.1	4.64	2.4	335	47.3	89.5	
.417	50.0	38.9	7.10	2.1	335	46.9	88.7	
.525	51.3	39.8	10.14	1.8	377	54.1	102	
.633	52.0	40.7	14.35	1.5	419	67.4	128	
.757	53.7	41.7	20.1	1.3	461	63.5	120	
.903	54.6	42.6	27.3	1.1	461	63.5	120	
1.05	55.9	43.9	35.6	1.1	503	69.3	131	
1.20	56.1	44.5	43.7	.95	543	78.0	148	
1.31	55.1	43.5	48.7	.93	545	83.6	158	
1.43	54.3	42.5	55.5	.89	587	82.2	156	
1.50	52.8	41.0	54.9	.94	712	99.7	189	
1.79	54.0	43.2	78.9	.78	691	106	201	
1.89	53.0	41.5	78.3	.83	733	105	199	

TABLE A1.91

Tank Diameter : 0.4m

Impeller: Ribbon D =0. 37 m P/D = 0.5 Nb = 1.0

Material: Silicone Oil

N (r/s)	T_b (^oC)	T_w (^oC)	Re	Pr	Q (W)	h $\left(\frac{W}{m^2\ ^oC}\right)$	Nu	$(\varepsilon D^4/\nu^3)$
0.04	82.4	24	.154	$3x10^5$	510	14.0	35	7.73
0.06	78.6	24.5	.234	3 "	"	15.6	39	17.4
0.09	75.1	24.5	.296	4 "	"	16.7	42	28.3
0.12	71.6	25.4	.272	4 "	"	18.3	46	73.4
0.16	67.6	24.6	.488	4 "	"	19.6	49	74.6
0.19	65.7	25.0	.57	4 "	"	2.7	52	101
0.24	60.7	25.0	.664	5 "	"	23.6	59	135
0.18	66.3	25.0	.527	4 "	"	20.4	51	86.3
0.31	64.5	25.0	.916	4	"	21.3	54	259
0.38	64.6	26.0	1.12	4	"	21.8	55	386

TABLE A 1.92

Tank Diameter : 0.4m

Impeller: Ribbon D =0.37 m P/D =.5 Nb = 1

Material: Sugar

N (r/s)	T_b (°C)	T_w (°C)	Re	Pr $x10^4$	Q (W)	h $\left(\frac{W}{m^2\ °C}\right)$	Nu	$(\varepsilon D^4/\nu^3)$
.062	53	19.8	.900	9.6	558	27.2	29	
.108	45	18.7	1.04	1.4	522	28.5	30	
.151	47	19.4	1.33	1.6	516	29.9	32	
.205	46	19.2	1.67	1.7	502	30.0	32	
.295	47	20.0	2.59	1.6	537	31.2	33	
.378	48	20.7	3.66	1.4	543	31.8	34	
.448	48	20.0	4.04	1.6	516	30.0	32	
.456	49	20.9	4.41	1.4	516	30.0	32	
.641	50	20.5	6.85	1.3	537	29.0	31	
.718	52	19.9	10.4	.96	554	27.6	29	

TABLE A 1.93

Tank Diameter : 0.4m

Impeller: Ribbon D =0.37 m P/D =1 Nb = 1

Material: Lub. Oil

N (r/s)	T_b (°C)	T_w (°C)	Re	Pr x10^3	Q (W)	h $\left(\frac{W}{m^2\ °C}\right)$	Nu	$(\varepsilon D^4/\nu^3)$
.328	49	22	194	3.0	546	32.6	90	2.5x10^7
.386	47	22	199	3.5	534	35.3	97	2.6 "
.455	45	23	200	4.1	543	40.8	113	2.7 "
.564	43	23	216	4.7	522	43.1	119	3.2 "
.649	42	24	233	5.0	516	47.4	131	3.8 "
.749	41	24	193	6.9	522	52.0	144	2.4 "
.834	40	24	210	7.1	543	56.1	155	3.0 "

TABLE A 1.94

Tank Diameter : 0.4m

Impeller: Ribbon D =0.37 m P/D = .5 Nb = 1

Material: Chocolate

N (r/s)	T_b (°C)	T_w (°C)	Re	Pr x10^5	Q (W)	h $\left(\frac{W}{m^2\ °C}\right)$	Nu	$(\varepsilon D^4/\nu^3)$
.093	42.1	32.2	.770	4.6	244	41	77.6	
.224	48.5	36.1	3.03	2.8	489	65	123	
.417	50.6	36.6	7.94	2.1	416	49	93	
.548	51.0	37.5	12.1	1.7	489	60	113	
.625	51.0	38.7	14.9	1.6	489	66	125	
.695	50.0	38.4	17.5	1.5	489	70	132	
.780	49.9	38.3	21.0	1.4	513	73	138	
.872	52.0	40.5	25.0	1.3	489	70	132	
.926	52.0	41.6	27.3	1.3	489	78	147	
1.00	53.0	42.6	30.8	1.2	489	78	148	
1.07	54.0	43.6	34.2	1.2	489	78	148	
1.37	54.5	44.3	50.4	1.1	660	107	202	
1.38	55.0	44.5	51.0	1.1	978	153	289	
1.47	55.0	44.6	56.0	1.0	978	155	293	
1.54	54.0	44.0	60.0	.98	635	105	199	

TABLE A 1.95

Tank Diameter : 0.4m

Impeller: Ribbon D =0.380 m P/D =.5 Nb =1.0

Material: Silicone Oil

N (r/s)	T_b (°C)	T_w (°C)	Re	Pr	Q (W)	h $\left(\frac{W}{m^2\ °C}\right)$	Nu	$(\varepsilon D^4/\nu^3)$
.027	44.5	22.2	.059	$6x10^5$	317	23.6	59.0	11.7
.030	81.2	24.6	.123	3 "	635	18.5	56.6	56.5
.058	46.1	22.2	.128	6 "	342	23.7	59.5	56
.070	75.8	24.8	.263	3 "	684	22.0	56.0	251
.124	71.7	24.0	.422	4 "	684	24.0	60.0	65
.197	74.8	26.5	.726	4 "	758	26.0	65.0	190
.286	70.7	26.2	.980	4 "	684	25.4	64.0	342

TABLE A 1.96

Tank Diameter : 0.4m

Impeller: Ribbon D =0. 38 m P/D = .5 Nb = 1.0

Material: Chocolate

N (r/s)	T_b (°C)	T_w (°C)	Re	Pr x10^5	Q (W)	h ($\frac{W}{m^2\ °C}$)	Nu	$(\varepsilon D^4/\nu^3)$
.062	38.8	31.5	.326	7.6	147	33.3	63	
.131	39.4	32.5	1.04	5.1	221	53	100	
.208	39.3	32.5	2.14	3.9	269	65	123	
.309	40.6	33.0	4.11	3.2	342	74	140	
.378	43.9	35.7	6.26	2.7	341	69	130	
.540	46.6	37.5	12.0	1.8	489	89	168	
.695	47.2	37.2	17.7	1.6	538	89	168	
.780	47.6	37.7	21.7	1.5	538	90	170	
.849	47.8	38.0	25.4	1.4	635	107	202	
.926	48.3	38.0	29.0	1.3	635	102	193	
1.01	50.5	39.7	35.1	1.2	587	90	170	
1.07	51.1	40.7	46.0	.94	635	101	191	
1.16	51.1	41.0	52.2	.89	635	104	197	
1.23	51.5	41.0	57.1	.87	684	108	204	
1.31	50.4	40.8	61.0	.86	635	108	204	

TABLE A 1.97

Tank Diameter : 0.4m

Impeller: Ribbon D =0.38 m P/D =1 Nb = 1.0

Material: Silicone Oil

N (r/s)	T_b (°C)	T_w (°C)	Re	Pr	Q (W)	h $\left(\frac{W}{m^2\ °C}\right)$	Nu	$(\varepsilon D^4/\nu^3)$
.035	63.0	21.6	.104	4×10^5	488	15.0	37.7	7.1
.062	61.0	21.9	.185	4 "	372	16.0	40.0	22.6
.100	60.0	23.0	.300	4 "	375	16.8	42.3	59.4
.140	59.0	23.0	.383	5 "	488	22.4	56.5	99.3
.181	54.0	18.8	.470	5 "	375	17.5	44.0	147
.200	57.8	22.7	.552	5 "	611	28.8	72.0	200
.286	55.4	21.7	.743	5 "	635	31.0	78.4	366
.351	54.0	21.1	.914	5 "	566	29.0	73.0	548
.44	55.5	22.7	1.15	5 "	607	31.0	78.0	860

TABLE A1.98

Tank Diameter : 0.4m

Impeller: Ribbon D =0.38 m P/D = 1 Nb = 1

Material: Lub. Oil

N (r/s)	T_b (°C)	T_w (°C)	Re	Pr x10^3	Q (W)	h ($\frac{W}{m^2\ °C}$)	Nu	$(\varepsilon D^4/\nu^3)$
.262	41.0	20.0	329	1.5	516	41.6	112	5.8×10^7
.313	39.5	20.0	429	1.5	"	43.7	121	8.6 "
.371	38.0	18.8	422	1.7	"	44.4	123	1.1×10^8
.456	36.5	20.6	456	1.9	"	53.6	148	1.3 "
.548	35.0	21.0	498	2.1	"	61.0	168	1.6 "
.614	35.5	22.5	558	2.1	"	65.6	181	2.2 "
.672	35.0	22.9	611	2.1	"	70.5	195	2.7 "
.764	33.0	21.9	619	2.3	"	76.8	212	2.7 "
.834	32.0	20.8	635	2.5	"	76.2	210	2.9 "

TABLE A 1.99

Tank Diameter : 0.4m

Impeller: Ribbon D = 0.38 m P/D = 1 Nb = 1

Material: Chocolate

N (r/s)	T_b (°C)	T_w (°C)	Re	Pr x10^5	Q (W)	h ($\frac{W}{m^2\ °C}$)	Nu	$(\varepsilon D^4/\nu^3)$
.425	54.9	41.9	10.7	1.6	440	56.0	106	7.7×10^3
.540	55.3	42.6	15.4	1.4	440	57.3	108	1.4×10^4
.656	54.7	42.3	20.9	1.3	416	55.5	105	2.41 "
.803	53.0	41.3	26.8	1.2	440	62.2	118	3.61 "
.888	49.0	41.8	27.2	1.3	440	101	191	3.55 "
1.03	57.3	45.2	44.7	.92	636	87.0	165	8.97 "
1.14	56.8	45.3	52.2	.88	587	84.0	159	1.1×10^5
1.25	56.1	44.4	58.7	.86	587	83.0	157	1.4 "
1.37	55.6	44.5	65.0	.85	684	102	193	1.7 "
1.47	55.3	44.3	75.3	.79	733	110	208	2.2 "
1.60	55.2	44.1	85.7	.75	684	102	193	2.6 "

TABLE A1.100

Tank Diameter : 0.4m

Impeller: Anchor D =0.382 m P/D = Nb =

Material: 3% CMC

N (r/s)	T_b (°C)	T_w (°C)	Re	Pr x10^3	Q (W)	h ($\frac{W}{m^2\ °C}$)	Nu	$(\varepsilon D^4/\nu^3)$
.332	47.0	23.4	59	5.6	2000	140	87	1.3×10^6
.352	46.0	24.9	62	5.7	"	157	98	1.5 "
.386	46.0	24.4	70	5.4	"	153	95	2.0 "
.406	45.3	25.4	74	5.4	"	166	103	2.2 "
.432	44.5	25.5	79	5.4	"	174	108	2.6 "
.473	43.0	26.0	88	5.4	"	195	121	3.3 "
.512	42.0	24.0	94	5.4	"	184	114	4.0 "
.556	41.0	25.3	103	5.4	"	210	130	4.8 "
.593	40.6	25.1	111	5.3	"	213	132	5.7 "
.601	40.0	26.0	113	5.3	"	237	147	5.9 "
.643	39.6	26.4	124	5.2	"	250	155	7.4 "
.684	38.5	25.5	130	5.2	"	253	157	8.2 "
.723	37.3	24.4	135	5.3	"	256	159	9.0 "
.784	36.0	23.6	149	5.3	"	266	165	11.2 "
.831	35.4	23.7	158	5.2	"	282	175	13.1 "
.863	34.7	24.7	167	5.2	"	329	204	14.5 "

TABLE A1.101

Tank Diameter : 0.4m

Impeller: Anchor D =0.348 m P/D = Nb =

Material: Silicone Oil

N (r/s)	T_b (°C)	T_w (°C)	Re	Pr x10^5	Q (W)	h ($\frac{W}{m^2\ °C}$)	Nu	$(\varepsilon D^4/\nu^3)$
.340	80.0	21.2	1.17	3.1	940	26.4	1.2	
.349	86.4	20.0	1.32	2.8	"	23.4	1.1	
.440	82.6	23.0	1.73	2.8	"	26.1	1.3	
.530	85.0	24.3	2.16	2.7	"	25.6	1.3	
.598	85.8	25.1	2.43	2.7	"	25.6	1.3	

TABLE A 1.102

Tank Diameter : 0.4m

Impeller: Anchor D =0.348 m P/D = Nb =

Material: Lub. Oil

N (r/s)	T_b (°C)	T_w (°C)	Re	Pr x10^3	Q (W)	h ($\frac{W}{m^2\ °C}$)	Nu	$(\varepsilon D^4/\nu^3)$
.324	36.5	19.5	263	1.96	380	36.9	102	2.7×10^7
.386	32.1	18.5	272	2.26	"	46.1	127	2.9 "
.459	31.0	17.2	269	2.71	"	45.7	126	2.8 "
.548	28.6	17.2	289	3.00	"	55.0	152	3.4 "
.610	30.0	17.7	348	2.80	"	69.0	190	5.1 "

TABLE A 1.103

Tank Diameter : 0.4m

Impeller: Anchor D =0.348 m P/D = Nb =

Material: 3% CMC

N (r/s)	T_b (°C)	T_w (°C)	Re	Pr x10^3	Q (W)	h ($\frac{W}{m^2\ °C}$)	Nu	$(\varepsilon D^4/\nu^3)$
.342	49.5	22.2	44	6.4	1300	79	51	.49x10^6
.421	48.6	25.2	59	5.9	"	92	60	.95 "
.483	48.0	28.1	71	5.6	"	108	70	1.49 "
.523	47.7	28.0	79	5.5	"	109	71	.92 "
.579	46.3	29.4	85	5.6	"	127	83	2.25 "
.613	45.5	28.7	90	5.6	"	128	83	2.57 "
.663	44.1	27.4	97	5.7	"	129	84	1.05 "
.692	43.6	28.0	102	5.6	"	139	90	3.42 "
.702	43.0	27.2	104	5.6	"	136	88	3.58 "
.783	42.0	28.2	116	5.6	"	156	101	4.42 "
.852	41.0	27.3	125	5.6	"	157	102	5.43 "
.903	40.6	27.9	135	5.5	"	169	110	6.64 "
.998	40.0	28.0	155	5.3	"	179	116	9.23 "
1.12	39.7	28.9	182	5.1	"	199	129	13.4 "
1.25	39.5	29.9	213	4.9	"	224	145	19.0 "

TABLE A 1.105

Tank Diameter : 0.4m

Impeller: Anchor D =0.369 m P/D = Nb =

Material: Chocolate

N (r/s)	T_b (°C)	T_w (°C)	Re	Pr x10^5	Q (W)	h ($\frac{W}{m^2\ °C}$)	Nu	$(\varepsilon D^4/\nu^3)$
.317	44	29.8	4.8	2.5	392	46	87	
.494	44	32.5	9.5	2.0	441	63	119	
.602	46	34.5	12.9	1.8	323	46.4	88	
.780	48	36.1	19.3	1.5	375	52	98.5	
.880	49	36.9	23.3	1.4	448	61	116	
1.00	49.5	38.4	28.6	1.3	483	72	136	
1.12	51	39.6	33.8	1.3	505	73.2	138	

TABLE A 1.106

Tank Diameter : 0.4m

Impeller: Anchor D =0.369 m P/D = Nb =

Material: 3% CMC

N (r/s)	T_b (°C)	T_w (°C)	Re	Pr x10^3	Q (W)	h ($\frac{W}{m^2\ °C}$)	Nu	($\varepsilon D^4/\nu^3$)
.335	49.5	24.4	53	6.4	1600	105	68	1.0x10^6
.401	48.3	26.8	69	6.0	"	123	80	1.9 "
.468	50.0	29.8	87	5.5	"	131	85	3.3 "
.532	49.0	30.7	101	5.4	"	145	94	4.7 "
.593	48.0	32.2	118	5.1	"	167	108	6.7 "
.605	47.0	30.0	116	5.4	"	157	103	6.4 "
.683	46.3	30.8	133	5.3	"	171	111	8.8 "
.756	45.5	31.9	150	5.1	"	194	126	11.7 "
.796	44.3	31.1	158	5.2	"	200	130	13.1 "
.834	43.1	30.2	165	5.2	"	206	134	14.4 "
.895	42.0	30.1	174	5.3	"	223	145	16.5 "
1.05	41.0	29.8	209	5.1	"	236	153	25.0 "
1.21	40.0	30.2	254	4.9	"	280	182	39.4 "
1.30	39.5	30.1	251	5.3	"	282	183	38.3 "

TABLE A 1.107

Tank Diameter : 0.4m

Impeller: Anchor D =0.382 m P/D = Nb =

Material: Lub. Oil

N (r/s)	T_b (°C)	T_w (°C)	Re	Pr $x10^3$	Q (W)	h $\left(\frac{W}{m^2\ °C}\right)$	Nu	$(\varepsilon D^4/\nu^3)$
.328	41	21.8	111	5.56	516	44.4	122.5	$.56x10^7$
.378	43	25.7	157	4.51	"	49.3	136	1.28 "
.465	41	26.0	157	5.56	"	56.9	157	1.27 "
.546	40	26.0	179	5.71	"	61.0	168	1.73 "
.625	39	26.7	195	6.01	"	69.3	191	2.10 "
.714	38	26.8	207	6.47	"	76.0	210	2.42 "
.800	37	25.6	212	7.07	"	74.8	206	2.56 "
.865	36	25.0	208	7.82	"	81.2	225	2.41 "

TABLE A1.108

Tank Diameter : 0.4m

Impeller:Anchor D =0.38 m P/D = Nb =

Material: Chocolate

N (r/s)	T_b (°C)	T_w (°C)	Re	Pr x10^5	Q (W)	h ($\frac{W}{m^2\ °C}$)	Nu	$(\varepsilon D^4/\nu^3)$
.170	44.7	33.6	2.2	3.1	510	76	144	
.263	42.5	34.0	4.4	2.4	280	55	103	
.309	42.8	35.0	5.6	2.2	280	59	111	
.432	46.7	37.9	9.5	1.9	392	74	140	
.525	44.5	36.0	12.8	1.7	275	54	101	
.625	45.0	37.0	16.7	1.5	283	59	110	
.695	43.6	35.7	19.7	1.4	392	82	155	
.826	43.0	34.0	25.8	1.3	392	72	136	
.849	49.6	37.0	26.9	1.3	466	61	115	

TABLE A 1.109

Tank Diameter : 0.15m

Impeller: Ribbon D = 0.113 m P/D = .5 Nb = 1.0

Material: Silicone Oil

N (r/s)	T_b (°C)	T_w (°C)	Re	Pr x10^5	Q (W)	h $\left(\frac{W}{m^2\ °C}\right)$	Nu	$(\varepsilon D^4/\nu^3)$
.072	50.8	15.9	.0153	5.4	48	15.4	14.5	
.089	48.0	15.6	.0181	5.7	47	16.5	15.6	
.103	47.3	16.0	.0210	5.8	48	17.5	16.5	
.119	46.0	15.8	.0235	5.9	45	16.8	15.8	
.140	44.9	16.6	.0269	6.1	47	18.8	17.7	
.168	43.5	16.7	.0314	6.2	48	20.3	19.1	
.181	40.3	14.8	.0323	6.6	46	20.4	19.2	
.189	40.7	14.8	.0340	6.5	48	20.8	19.6	
.199	40.3	15.9	.0355	6.6	48	22.1	20.8	
.245	39.0	16.0	.0427	6.7	47	23.0	21.7	
.256	37.1	15.4	.0431	7.0	48	25.0	23.6	
.332	38.3	15.5	.0571	6.8	48	23.9	22.5	

TABLE A 1.110

Tank Diameter : 0.15m

Impeller: Ribbon D = 0.113 m P/D = .5 Nb = 1

Material: Lub. Oil

N (r/s)	T_b (°C)	T_w (°C)	Re	Pr $\times 10^4$	Q (W)	h $\left(\frac{W}{m^2\ °C}\right)$	Nu	$(\varepsilon D^4/\nu^5)$
.912	25.9	13.0	9.2	1.7	48	42.1	43.5	
1.13	23.3	12.6	9.2	2.1	48	50.1	51.8	
1.27	23.5	13.2	10.7	2.0	46	50.9	52.7	
1.68	22.1	13.0	12.6	2.3	47	58.6	60.6	
1.90	21.2	13.1	13.4	2.3	46	64.3	66.5	
1.92	21.1	13.0	13.5	2.4	47	65.3	67.5	
2.61	20.2	13.0	17.2	2.6	47	74.3	76.9	
3.62	18.8	13.0	21.3	2.9	47	91.0	93.9	

TABLE A 1.111

Tank Diameter : 0.15m

Impeller: Ribbon D =0.135 P/D =.5 Nb = 1

Material: Silicone Oil

N (r/s)	T_b (°C)	T_w (°C)	Re	Pr x10^5	Q (W)	h ($\frac{W}{m^2\ °C}$)	Nu	$(\varepsilon D^4/\nu^3)$
.046	30.8	14.6	.0098	7.8	50	35.4	33.3	
.068	30.5	14.7	.0146	7.9	50	36.1	34.0	
.074	29.3	14.3	.0155	8.1	49	36.6	34.4	
.124	28.2	15.0	.0255	8.2	50	42.4	39.9	
.138	28.7	15.7	.0286	8.1	51	44.7	42.1	
.167	28.3	15.7	.0342	8.2	52	46.5	43.7	
.188	28.0	15.9	.0384	8.2	49	45.5	42.8	
.232	27.8	15.5	.0473	8.3	50	45.6	42.9	
.322	27.7	15.2	.0653	8.3	51	46.5	43.7	

TABLE A 1.112

Tank Diameter : 0.15m

Impeller: Ribbon D =0.135 m P/D = .5 Nb = 1

Material:Glycerol

N (r/s)	T_b (°C)	T_w (°C)	Re	Pr $x10^4$	Q (W)	h $\left(\frac{W}{m^2\ °C}\right)$	Nu	$(\varepsilon D^4/\nu^3)$
.213	20.5	12.0	4.11	.95	47	63.2	33	
.372	18.3	11.2	6.05	1.1	46	74.4	38	
.513	17.1	11.5	7.44	1.3	48	97.4	50	
.702	16.9	12.0	10.0	1.3	47	107	55	
.913	16.4	12.0	12.5	1.4	47	118	61	
1.10	15.4	11.1	13.6	1.5	47	125	65	
1.32	15.5	11.4	16.5	1.5	48	132	68	
1.54	15.4	11.6	19.1	1.5	47	140	72	
1.77	15.0	11.5	21.2	1.5	47	149	77	
1.96	14.6	11.3	22.7	1.6	47	163	84	
2.14	14.9	11.8	25.3	1.6	48	171	88	

TABLE A 1.113

Tank Diameter : 0.15m

Impeller: Anchor D =0.113 m P/D = Nb =

Material: Lub. Oil

N (r/s)	T_b (°C)	T_w (°C)	Re	Pr x10^3	Q (W)	h ($\frac{W}{m^2\ °C}$)	Nu	$(\varepsilon D^4/\nu^3)$
.772	33.2	11.8	16.6	7.8	47	24.9	25.8	
1.21	25.6	11.9	21.5	9.5	47	35.0	37.2	
1.53	21.3	11.5	15.0	1.7	46	54.2	56.0	
1.97	20.2	11.4	14.0	2.4	47	60.7	62.8	
2.24	19.3	12.1	14.6	2.6	47	73.9	76.5	
2.83	18.8	11.7	17.4	2.7	48	74.5	77.3	
3.37	18.9	12.6	19.6	2.9	48	85.3	88.4	

TABLE A 1.114

Tank Diameter : 0.15m

Impeller: Anchor D = 0.113 m P/D = Nb =

Material: Glycerol

N (r/s)	T_b (°C)	T_w (°C)	Re	Pr x10^4	Q (W)	h ($\frac{W}{m^2\ °C}$)	Nu	$(\varepsilon D^4/\nu^3)$
.510	22.1	11.1	8.95	.97	47	48.3	24.9	
.926	19.0	10.6	16.2	1.1	47	63.7	32.9	
1.25	17.5	10.6	21.8	1.2	48	79.6	41.0	
1.99	14.9	9.8	34.9	1.5	46	102	52.8	
2.52	14.7	10.4	44.1	1.6	47	123	63.4	
2.86	14.1	10.6	50.1	1.7	48	157	81.2	
3.97	14.0	10.7	69.6	1.7	47	162	83.3	
4.29	14.0	11.2	75.2	1.7	47	189	97.5	
4.79	14.0	11.3	83.9	1.7	48	195	101	
5.03	14.9	12.2	88.2	1.6	48	203	105	

TABLE A 1.115

Tank Diameter : 0.15m

Impeller: Anchor D = 0.14 m P/D = Nb =

Material: 1.5% CMC

N (r/s)	T_b (°C)	T_w (°C)	Re	Pr $\times 10^3$	Q (W)	h $\left(\frac{W}{m^2\ °C}\right)$	Nu	$(\varepsilon D^4/\nu^3)$
.636	19.5	12.1	117	.75	46	70.5	17.8	
.829	13.7	11.8	113	1.0	46	266	67	
.990	13.8	12.1	136	1.0	48	328	83	
1.21	12.7	11.5	157	1.1	47	424	107	
1.40	12.5	11.8	182	1.1	46	710	179	
1.60	12.5	12.2	208	1.1	48	1454	367	
1.74	12.4	11.9	225	1.1	47	1261	318	
1.94	12.5	12.3	257	1.1	47	2129	537	
2.06	12.7	12.6	276	1.0	47	4871	1228	

APPENDIX 2

Classification and physical properties of fluids

A2.1 Classification of Fluids

The detailed classification of fluids based on their rheological behaviour is available in the text books (1,19,51) and only a brief review will be presented in this section.

A 2.1.1 General considerations and definitions

From an engineering point of view the characteristic properties of a fluid are best described by the 'flow-curve' or 'shear diagram' which is a plot of shear stress against shear rate in laminar flow.

(a) Newtonian fluids

The most commonly encountered fluid is classed as Newtonian. This exhibit a direct proportionality between shear stress and shear rate in laminar flow, thus:

$$\tau = -\mu \frac{du}{dy} \qquad \text{----------} \qquad \text{A 2.1}$$

where $-(du/dy)$ is shear rate, τ the shear stress, and μ is the viscosity . Here, viscosity is independent of shear rate, being affected only by temperature and pressure for a given fluid system. It may be seen that the flow curve for a Newtonian fluid is a straight line through the origin of slope μ.

(b) Non-Newtonian Fluids

A non-Newtonian fluid is one in which shear rate is not always proportional to shear stress. Thus, flow behaviour can not be described by a single constant such as the viscosity of Newtonian fluids. Non-Newtonian fluids may be divided into three broad groups:-

(i) Time-independent fluids are those for which shear rate at a given point is solely dependent upon the instantaneous shear stress.

(ii) Time-dependent fluids are those for which the shear rate is a function of both the magnitude and duration of shear and possibly of the time lapse between consecutive applications of shear stress.

(iii) Visco-elastic fluids are those that show partial elastic recovery upon the removal of a deforming shear stress. Such materials posses propoerties of both viscous fluids and elastic solids.

A 2.1.2 Time independent non-Newtonian fluids

Fluids of the first type whose characteristics are independent of time may be described by a rheological equation of the form:

$$\tau = f(\dot{\gamma}) \qquad \text{---------- A 2.2}$$

This equation implies that the shear rate, $\dot{\gamma}$, at any point in the fluid is only a function of shear stress at that point. Such fluids may be termed non-Newtonian viscous fluids and divided into three distinct types depending on the nature of the function in equation A 2.2 . These are:

(1) Bingham plastics.

(2) Pseudoplastic fluids.

(3) Dilatant fluids.

and typical flow curves for these three types of fluids are shown in Figures A.2.1 and A.2.2 : and compared with that of Newtonian fluids.

(a) Bingham Plastics

A Bingham plastic is characterised by a flow curve which is a straight line having an intercept τ_y on the shear stress axis. The yield stress, τ_y, is the stress which must be exceeded before flow starts. The rheological equation for a Bingham plastic may be written:

$$\tau = \tau_y + \mu_p \dot{\gamma} \quad ; \quad \tau > \tau_y \qquad \text{---------- A 2.3}$$

where μ_p, the 'plastic viscosity' or 'co-efficient of rigidity' is the slope of the flow curve on the arith - matic co-ordinates. Examples of fluids which closely approximate an ideal Bingham plastic are slurries, oil paints, drilling muds, sewage sluges, toothpastes, paper pulp and lime suspensions. Apart from the rheological model described by equation A 2.3, there are a few other models which describe Bingham plastics of non-linear flow vurve (19).

(b) Pseudoplastic fluids

One of the most commonly encountered non-Newtonian behaviour is pseudoplasticity. Pseudoplastic fluids show no yield stress and the typical flow curve for these materials indicates that the ratio of shear stress to the shear rate, which may be termed apparent viscosity, μ_A, falls progressively with increasing shear rate and the flow curve becomes linear only at very high shear rates. This limiting slope on the arithmetic plot of $\tau - \mu$ is known as the viscosity at infinite shear and is designated ;

The logarithmic plot of $\tau - \mu$ for these materials is often found to be linear with a slope between unity and zero. As a result, an empirical functional relation known as the 'power law' is widely used to characterise

fluids of this type. This relation, which was originally proposed by Ostwald and has since been fully described by Reiner(96), may be written as:

$$\tau \propto K \dot{\gamma}^n \qquad \text{---------- A 2.4}$$

where K and n are constants for the particular fluid and for pseudoplastics n is less than unity .

n is the power law index and is the slope of the log-log curve. At $n = 1$ we have the usual Newtonian relationship ($\tau \propto \mu$) and thus n is a measure of non- Newtonian behaviour . The greater the departure from unity, the more non-Newtonian the character of the fluid.

K is the intercept at $\dot{\gamma} = 1$ on the τ axis and is a measure of the consistency of the fluid; the greater the K the more viscous the fluid and vice-versa.

n is insensitive to changes in temperature . K is temperature dependent but to a lesser degree than fluids of similar "viscosity".

The dimension of K depend on the numerical value of n,

$$K = (\tau / \dot{\gamma}^n) = (N/m^2) \Big/ (s^{-1})^n = (N.s^n/m^2)$$
$$= kg/m.s^{2-n}$$

but this is of minor significance in engineering applications.

The apparent viscosity, μ_a, for a power law fluid may be expressed in terms of n, since:

$$\mu_a = \tau / \dot{\gamma}$$

i.e.

$$\mu_a = K (\dot{\gamma})^{n-1} \quad \text{---------- A2.5}$$

and since $n < 1.0$ for pseudoplastics the apparent viscosity decreases as the shear rate increases. This type of behaviour is characteristic of suspensions of asymmetric particles or solutions of high polymers such as cellulose derivatives. This suggests that the physical interpretation of this phenomena is probably that with increasing rates of shear the asymmetric particles or molecules are progressively aligned. Complete orientation at high shear rates and complete disorientation at very low shear rates would count for the observed Newtonian behaviour in these regions (1,19,97) .

Pseudoplastic fluids have been defined as time-independent fluids and this implies that the alignment of molecules suggested above takes place instantaneously as the shear rate is increased or, at any rate, so quickly that the time-effect can not be detected with available measuring devices.

Besides the power law model, there are several empirical equations which have been proposed to describe different types of pseudoplastic fluids (1,19,97). But these equations are considerably more complicated and difficult to handle, and usually do not offer any compensating advantages over the simple power law model .

Examples of pseudoplastic fluids are: rubber solutions, adhesives, polymer solutions or melts, greases, starch suspensions, cellulose acetate, paints, detergent solutions and soap.

(c) Dilatant fluids

Dilatant fluids are similar to the pseudoplastic fluids in that they possess no yield stress but the apparent viscosity for them increases as the shear rate increases and hence are also called "shear thickening" . They are much less common than pseudoplastic fluids. The following explanation has been given (19,97) for the case of suspension of high solids content. At rest, the voidage is a minimum and just filled by the liquid content and at low shear rates the liquid lubricates the motion between particles. At higher shear rates, the material expands slightly, voidage increases and the liquid is insufficient for full lubrication causing the apparent viscosity to increase.

The "true" explanation is probably much more complicated.

Examples of dilatant fluids are: some cornflour, sugar suspensions, some gum arabic/borax solutions,starch and iron powder in low viscosity liquids.

When power law is applicable to these fluids, the treatment of both types, e.g. pseudoplastic and dilatant fluids, is much the same.

A 2.1.2 Time dependent non-Newtonian fluids

These fluids, for which the flow curve is dependent on time of application of the shear rate, are subdivided into two types:

(a) Thixotropic fluids

These fluids possess a structure, the breakdown of which depends on time and shear. Thus at a given shear rate, the shear stress falls as time increases and the structure rebuilds itself if the shear rate is removed. A well-known example of this type of behaviour is the household gel paint.

A typical flow curve is given below from Perry(98):

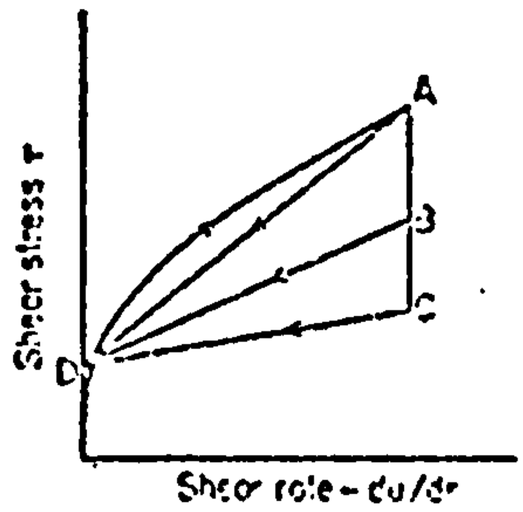

Shear diagram for thixotropic fluid.

If the shear rate is held constant after point A is reached on the up curve, the shear stress will fall vertically to a point C beyond which no further breakdown can occur at that shear rate; the down curve CD is followed on decreasing the shear rate. Any intermediate path such as ABD may be followed depending on the time allowed at the chosen shear rate. The area within the loop DAD is regarded as a measure of the amount of thixotropy.

Thixotropic materials, according to Wilkinson(97) are "rather like pseudoplastic materials in which the time required for the alignment of particles is not negligible. This time effect for pseudoplastic fluids is not observable in the apparatus normally used for the testing of these materials. The difference then is only a matter of degree."

Examples of thixotropic behaviour have been observed in the following materials: some solutions or melts of high polymer, oil well drilling muds, greases, many food materials, paints, margarine, crude oils and inks.

(b) Rheopectic fluids

These materials, of fairly rare occurrance, are occasionally referred to as antithixotropic. Shear causes a gradual formation of structure whereas so far, the properties of non-Newtonian fluids have been explained on the basis that shear destroys structure. The flow curve is given below containing a comparison with the thixotopic loop.

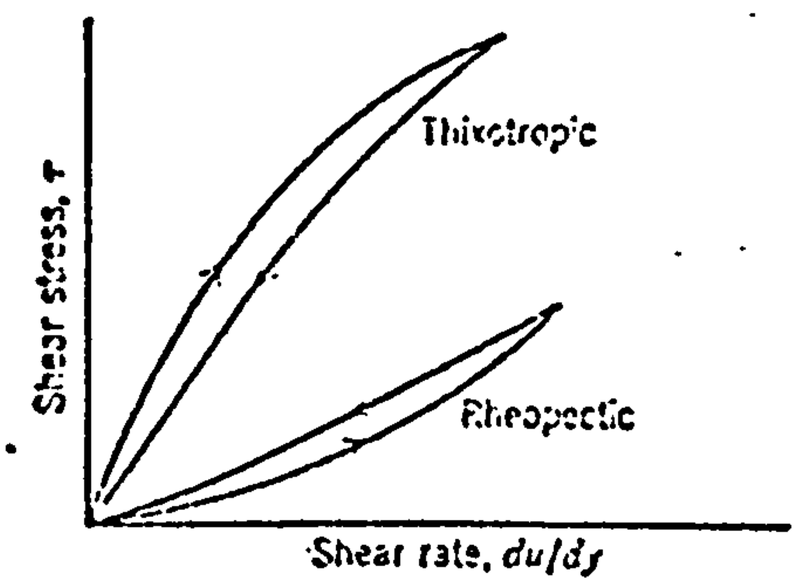

Flow curves for thixotropic and rheopectic fluids in single continuous experiments.

An example of this behaviour is that of a 42% aqueous gypsum paste. After shaking, it solidifies in 40 minutes at rest but in only 20 seconds if gently rolled.

Wilkinson(97) makes an analogy between rheopectic and dilatant materials but since there is an upper limit to the shear rate which causes rheopectic behaviour, the analogy is less strong than that between thixotropic and pseudoplastic materials.

Examples of the materials which have been observed to be rheopectic are: bentonite clay suspensions, vanadium pentaoxide suspensions, gypsum suspensions, dilute suspensions of ammonium oleate.

A2.1.3 Viscoelastic fluids

These fluids exhibit elastic recovery from deformations which occur during flow. Normal stresses occur as well as those tangiential to flow giving rise to unusual phenomena such as the "Weissenberg effect" - a 1% aqueous solution of polyacrylamide will climb up a rotating agitator shaft. In spite of the elastic effects, the steady state flow of viscoelastic fluids is very similar to that of pseudoplastic materials.

A 2.2 Flow Properties

(a) Viscosity

The viscosity of the Newtonian materials was measured in a Haake Rotovisco. The Haake Rotovisco is a rotating

fluids is shown in Fig. A2.3 .

(b) Consistency Index

The viscometric data for the non-Newtonian materials was plotted on log-log paper. Over the range of shear rates covered most of these materials followed the power law model for which:

$$\tau = K (\dot{\gamma})^n \qquad \text{---------- A2.7}$$

and the rheological parameters K and n for the fluids were evaluated. Thus for such fluids, the average apparent viscosity defined below was calculated:

$$\mu_A = K (\dot{\gamma}_A)^{n-1} = K (k_s N)^{n-1} \qquad \text{---------- A2.8}$$

where $\dot{\gamma}_A$ is the average shear rate in the vessel and k_s is the impeller shear rate constant.

Typical plots of shear stress versus shear rate are drawn in Figures A2.4 to A2.9 . In all cases K varied with temperature while great variation in the power law index,n, with temperature was not observed. The temperature dependence of the consistency index for some of the materials is shown in Fig. A2.10 .

A2.3 Thermal Conductivity

Fig. 3.10 in section 3.2.8(ii) shows the details of the thermal conductivity cell based on the steady-state hot wire method of Jamieson and Tudhope (82) whose procedure resulting to thermal conductivities accurate to within $\pm$ 5% was followed for some of the low viscosity fluids. Thermal conductivities were calculated from the equation(see also equation 3.12 in section 3.2.8(ii)):

$$k_l = \frac{C_1}{m - (C_2/k_g)} \qquad \text{---------- A2.9}$$

where k_l is the thermal conductivity of the glass and m is the rate of change of the platinum filament resistance with electrical power input. The cell constants, C_1 and C_2 were obtained from known thermal conductivities using toluene, acetone and glycerol, see Fig. A2.11, A2.12, A2.13, A2.14 . At 25°C, these values were given as

$$C_1 = 1.65 \times 10^{-3} \text{ Ohm/m } ^{\circ}C$$

and

$$C_2/kg = 9.9 \times 10^{-2} \text{ Ohm sec/J}$$

All plots of filament resistance against power input were linear which confirmed the absence of convection effects and hence the applicablity of equation A2.9 .

Thermal conductivity of some of the thick Newtonian and non-Newtonian fluids could not be measured by the steady state hot wire method as explained in section 3.2.8(ii). The main difficulty was in introducing the viscous material into the cell. In these cases the concentric cylinder apparatus shown in Fig. 3.12 and described in section 3.2.8(ii) was used to evaluate the thermal conductivities. Results are tabulated in Table A2.1

Thermal conductivity of some of the non-Newtonian polymer solutions was assumed to be the same as that of the solvent. The results are presented in Table A2.1 .

A2.4 Density

The density of the experimental fluids was measured at different temperatures by means of a specific gravity bootle. Experimental results are shown in Table A2.1 and Fig. A2.15 and A2.16 .

A2.5 Specific Heat

The specific heat of most Newtonian and non-Newtonian materials was measured in a well insulated electrical calorimeter described in section 3.2.8(iv) . The data are presented in Table A2.1

Thermal conductivity of some of the thick Newtonian and non-Newtonian fluids could not be measured by the steady state hot wire method as explained in section 3.2.8(ii). The main difficulty was in introducing the viscous material into the cell. In these cases the concentric cylinder apparatus shown in Fig. 3.12 and described in section 3.2.8(iii) was used to evaluate the thermal conductivities. Results are tabulated in Table A2.1

Thermal conductivity of some of the non-Newtonian polymer solutions was assumed to be the same as that of the solvent. The results are presented in Table A2.1 .

A2.4 Density

The density of the experimental fluids was measured at different temperatures by means of a specific gravity bootle. Experimental results are shown in Table A2.1 and Fig. A2.15 and A2.16 .

A2.5 Specific Heat

The specific heat of most Newtonian and non-Newtonian materials was measured in a well insulated electrical calorimeter described in section 3.2.8(iv) . The data are presented in Table A2.1

For the case of solutions of some of the polymers, the specific heat was assumed to be the same as that of the solvent. Results are shown in Table A2.1

Fluid used	Density (hg/m^3)	Specific Heat (kJ/kg ^oC)	Thermal Conductivity (W/m ^oC)
Chocolate	1280	4.6 at 46^oC	0.2118 at 46 ^oC
7% CMC	1060	4.2	0.595 at 45 ^oC
3% CMC	1000	4.2	0.600 at 45 ^oC
1.5% CMC	1000	4.2	0.595 at 45 ^oC
Glycerol	1250	2.35 at 43 ^oC	0.250 at 46 ^oC
Lub. Oil	see Fig. A2.16	2.18 at 40^oC	0.150 at 45 ^oC
Silicone Oil	see Fig. A2.15	1.51 at 50 ^oC	0.159 at 60 ^oC
Sugar Sol.	1483	2.5 at 50^oC	0.375 at 50 ^oC
3% Carbopol	1000	4.2	0.52 at 45 ^oC
8% Biozam R	1000	4.2	0.600 at 48 ^oC

Table A2.1 Thermal and Physical Properties of Experimental Fluids.

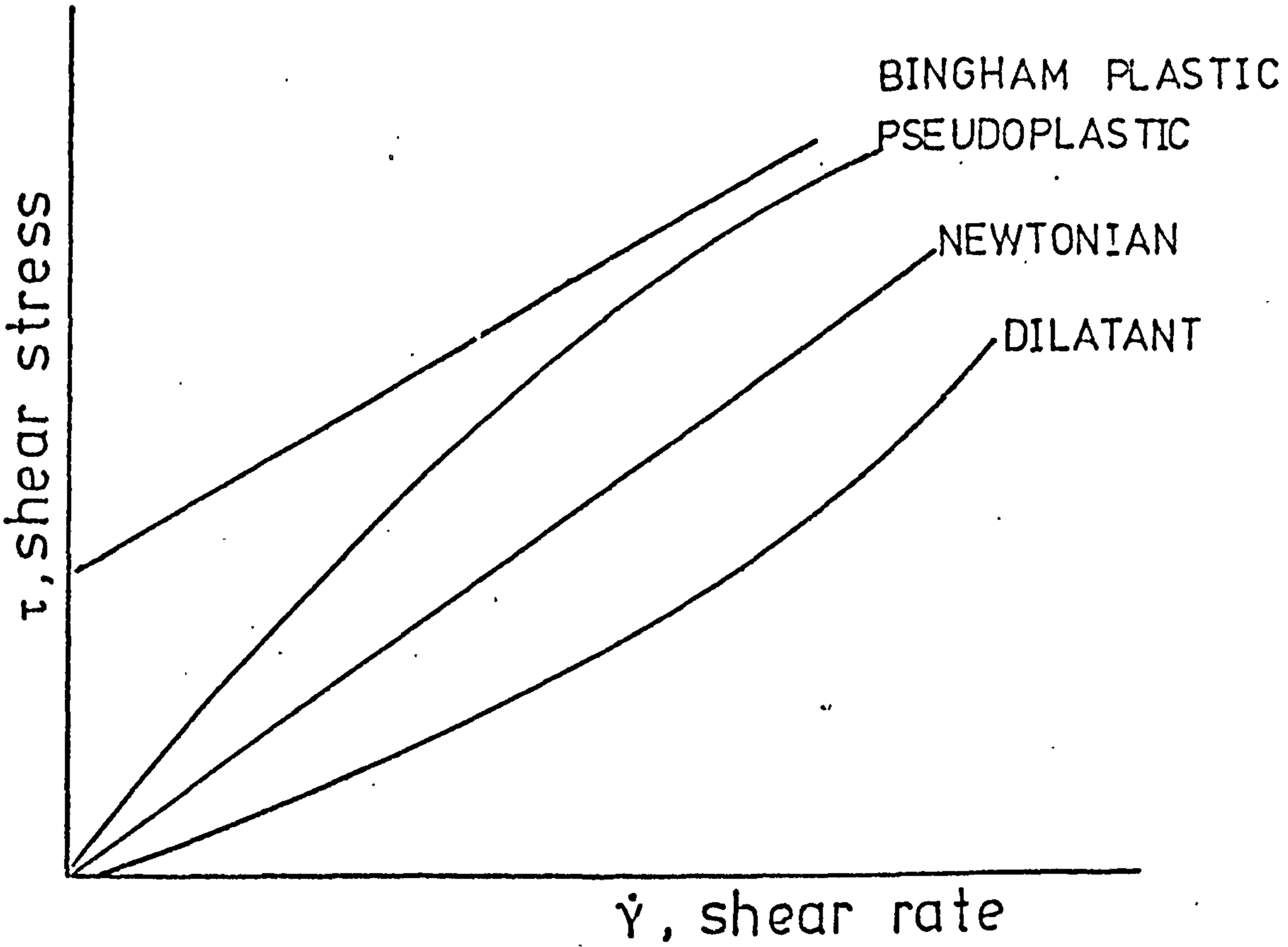

Fig A 2,1 τ-γ̇ on linear paper

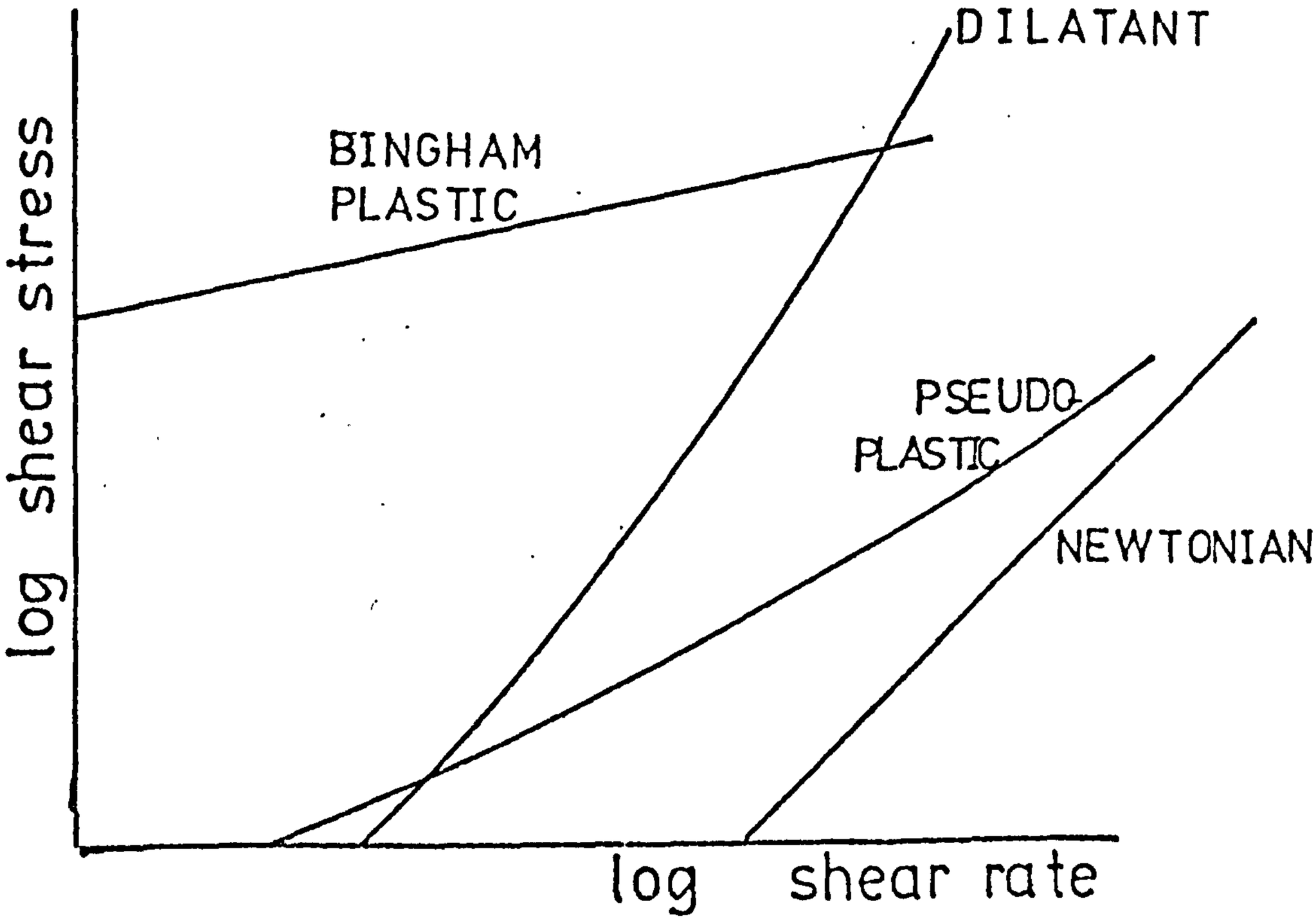

Fig A 2,2 τ-γ on log log paper

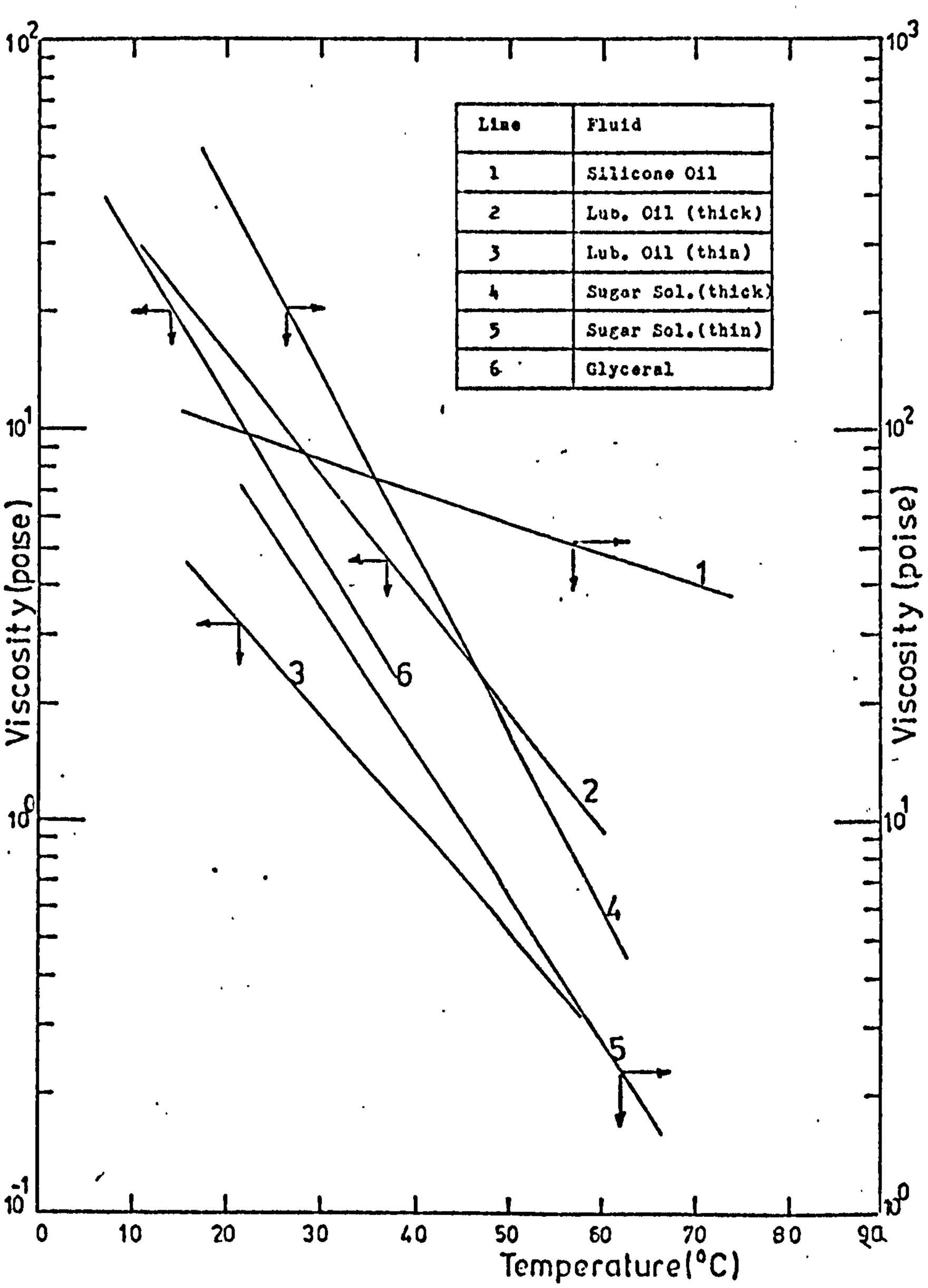

Fig. A2,3 Viscosity of Newtonian Fluids

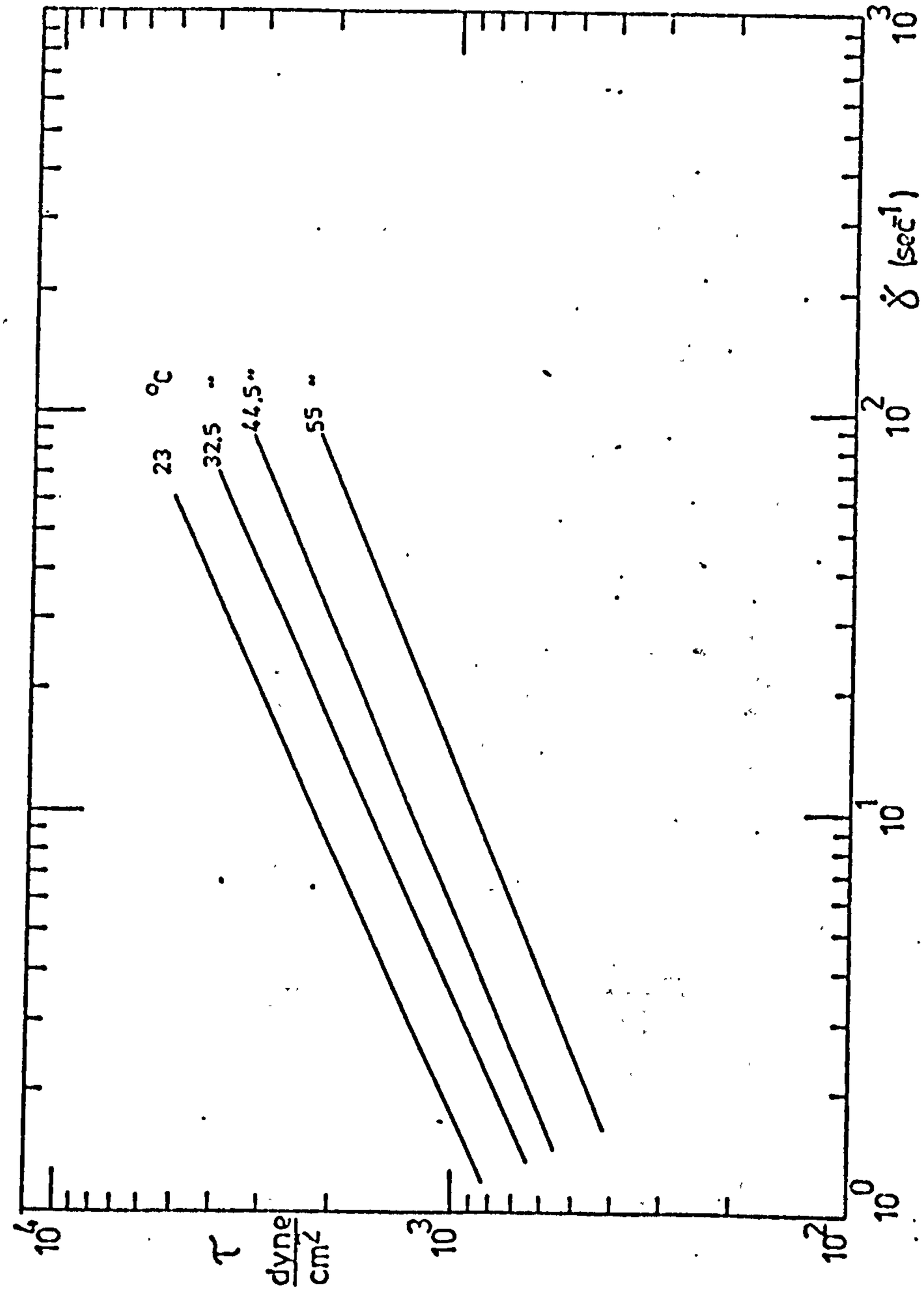
10^3
$\dot{\gamma}$ (sec^{-1})
Shear stress-Shear rate for Chocolate
10^2
10^1
10^0
23 °C
32.5 "
44.5 "
55 "
10^4
τ $\frac{dyne}{cm^2}$
10^3
10^2

Fig A2.4

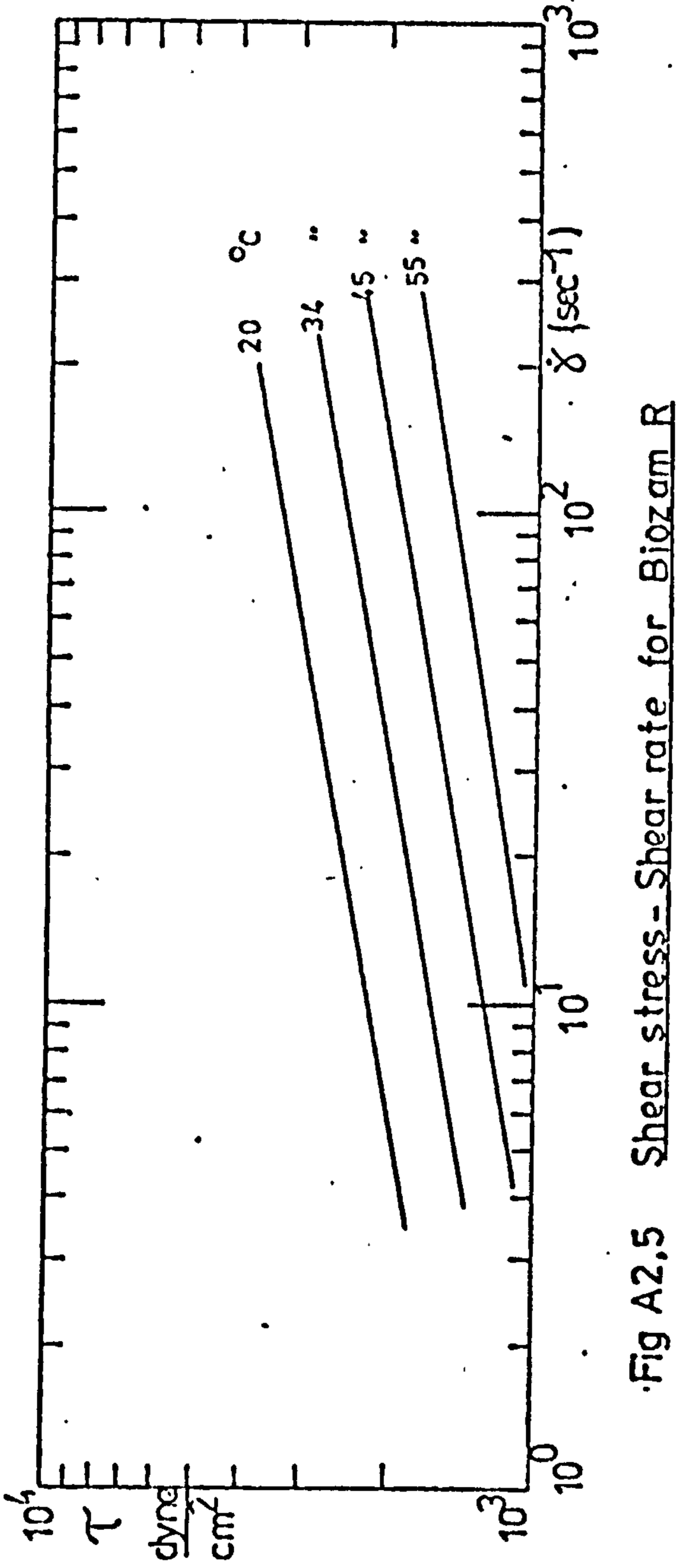

Fig A2,5 Shear stress-Shear rate for Biozam R

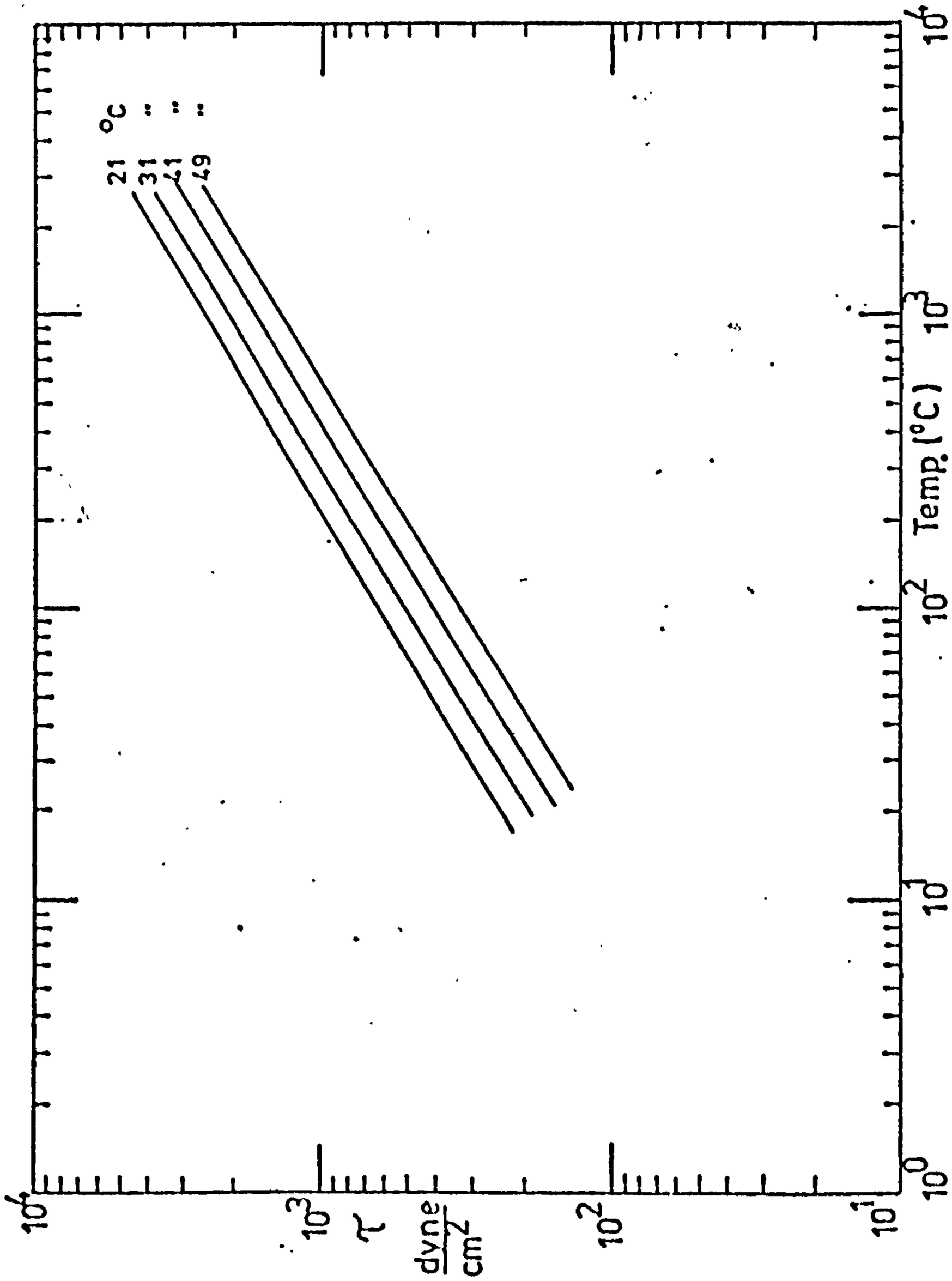

Fig A2,6 Shear stress-Sh

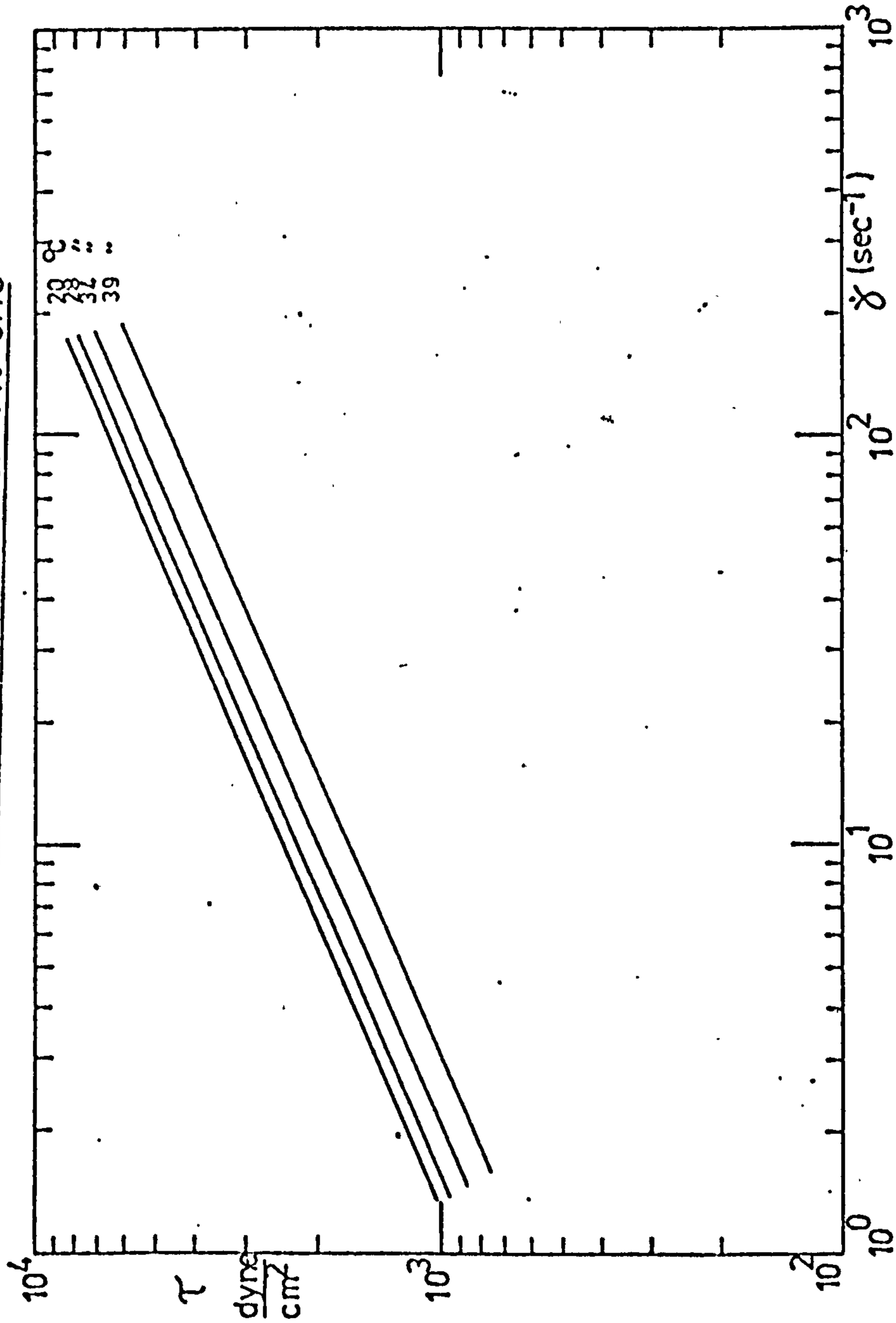

Fig A2.7 Shear stress- Sh

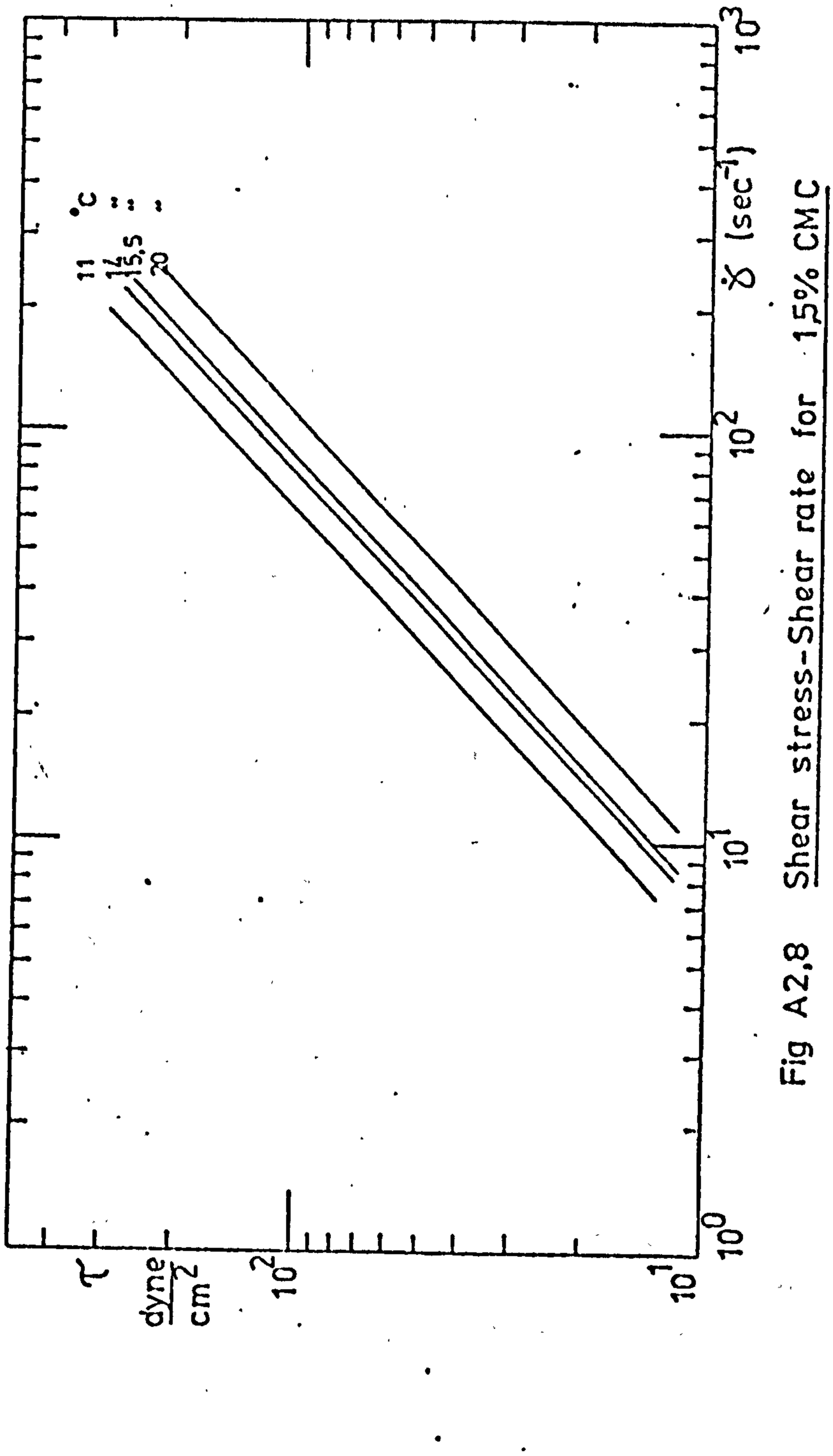

Fig A2.8 Shear stress-Shear rate for 1.5% CMC

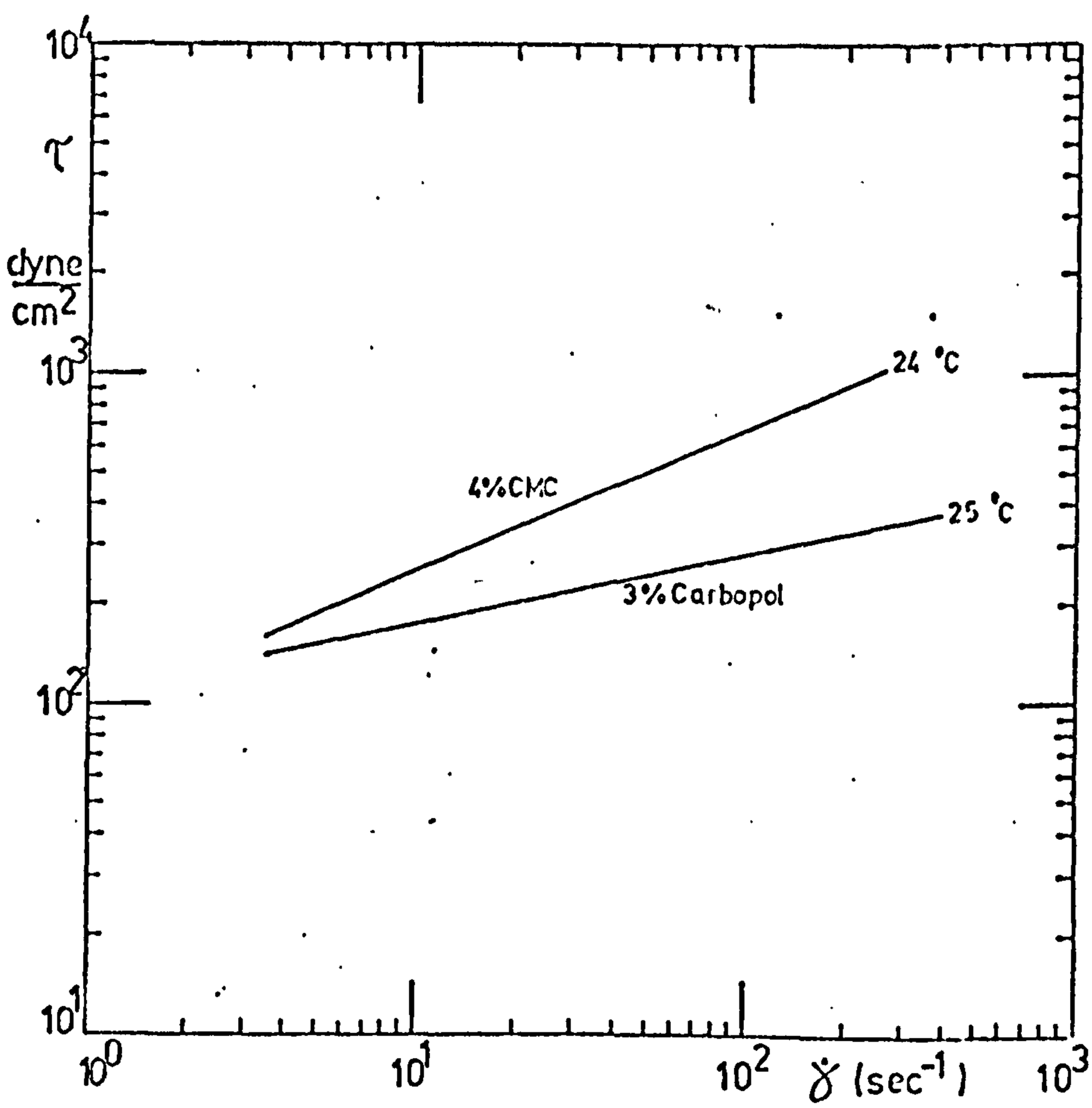

Fig A2,9 Shear stress - Shear rate for two fluids

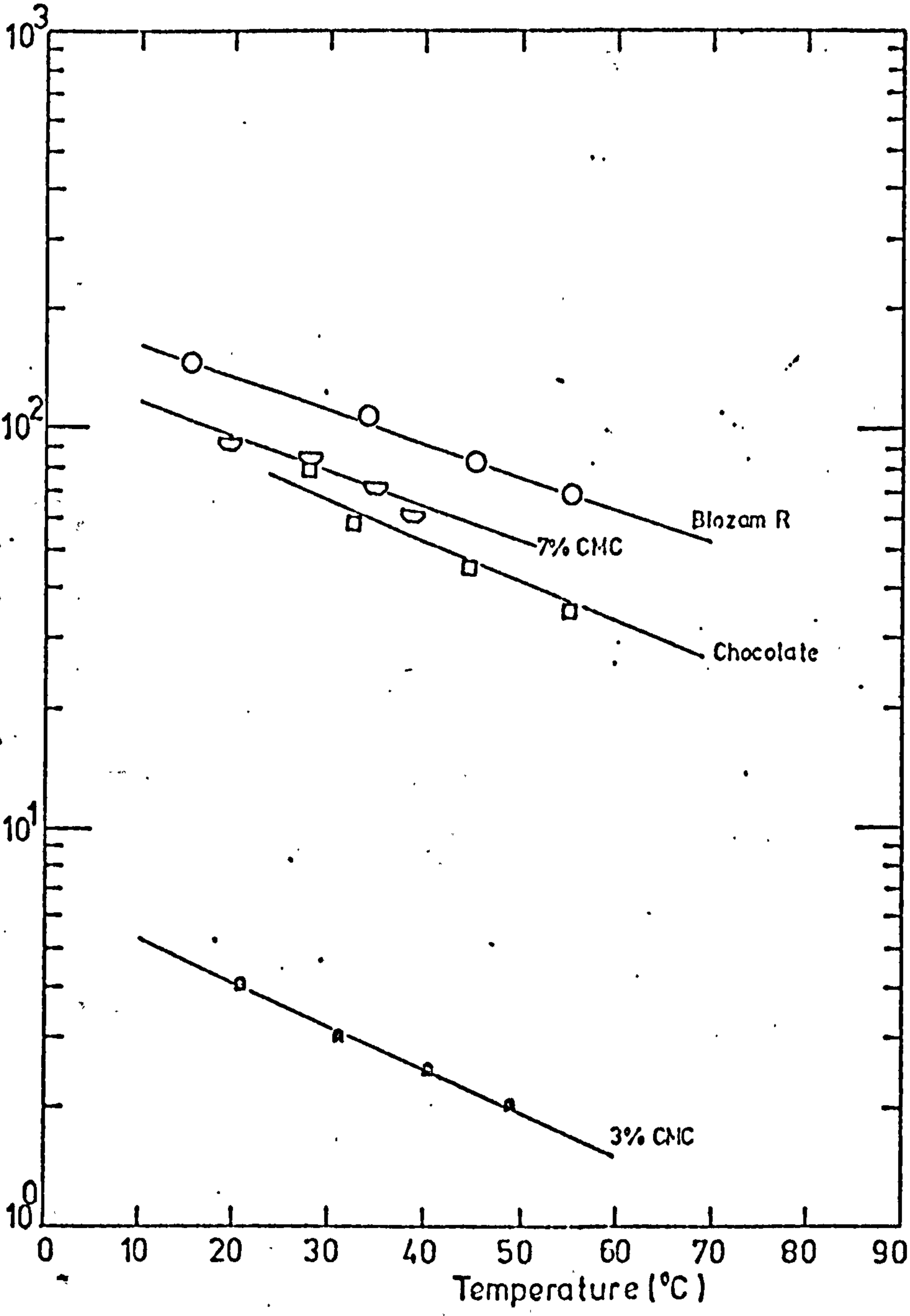

Fig A2.10 Variation of K with n for non-Newtonian Fluids used

Fig A2,11 Toluene

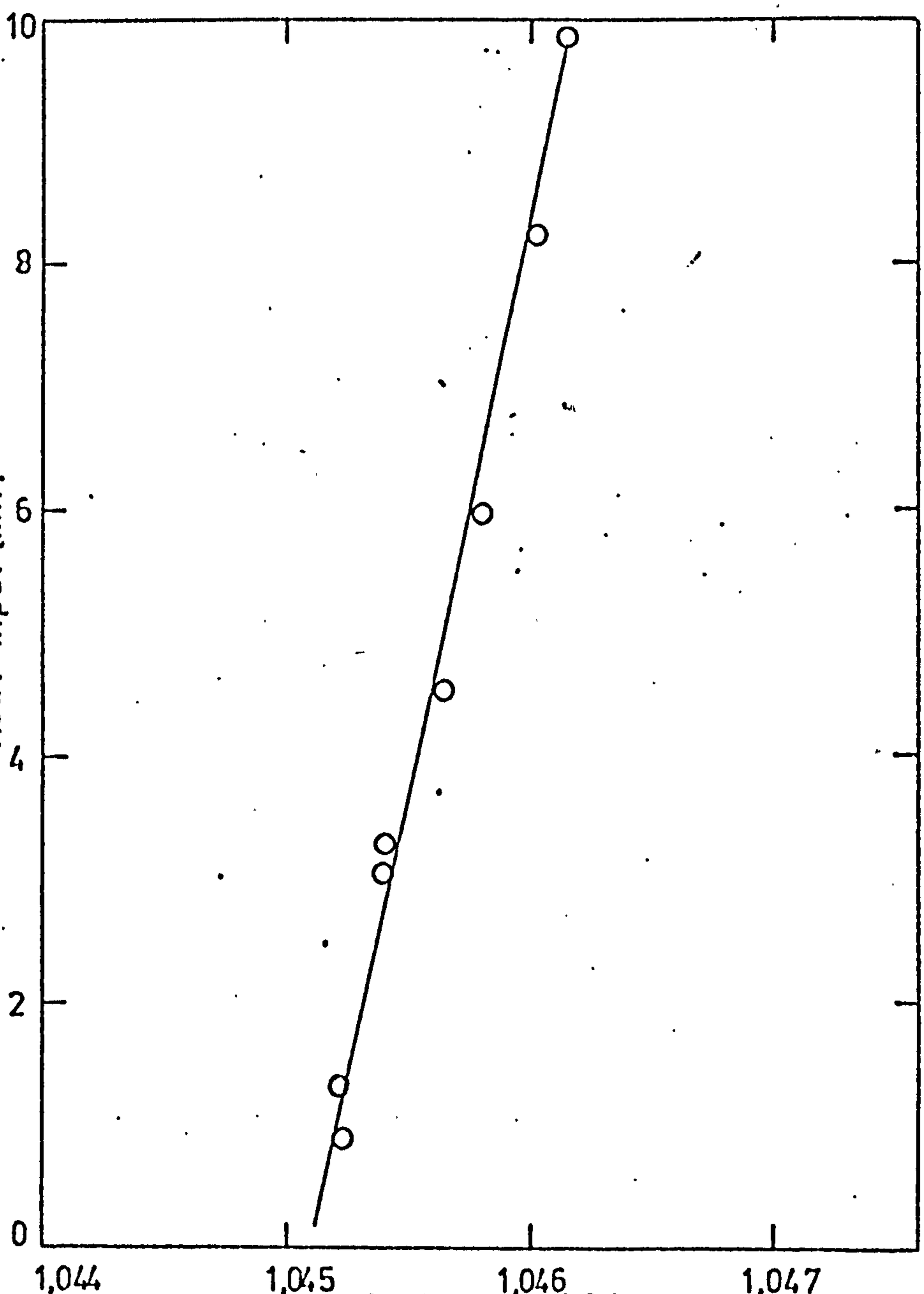

Fig A2,12 Methanol

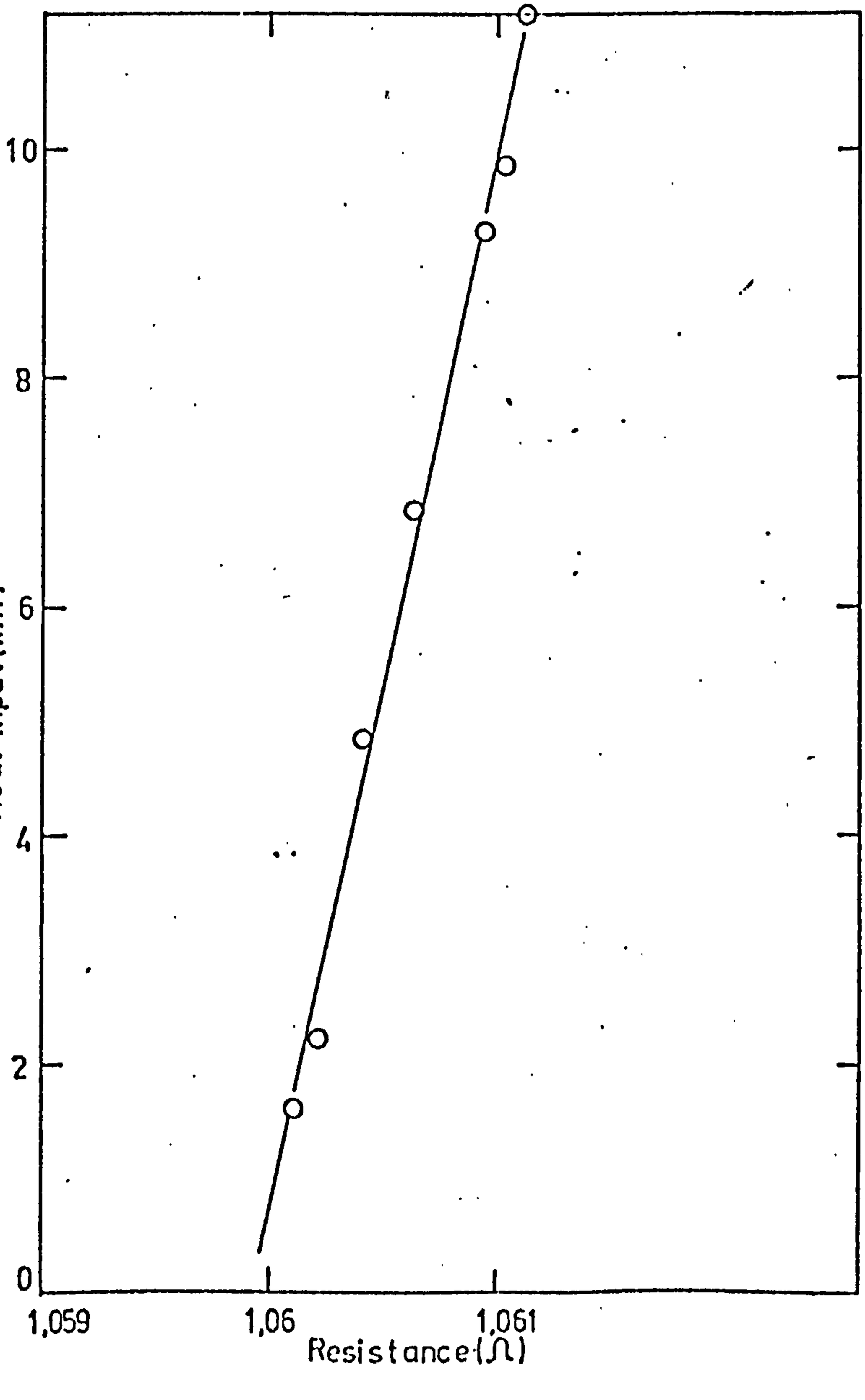

Fig A2,13 Glycerol

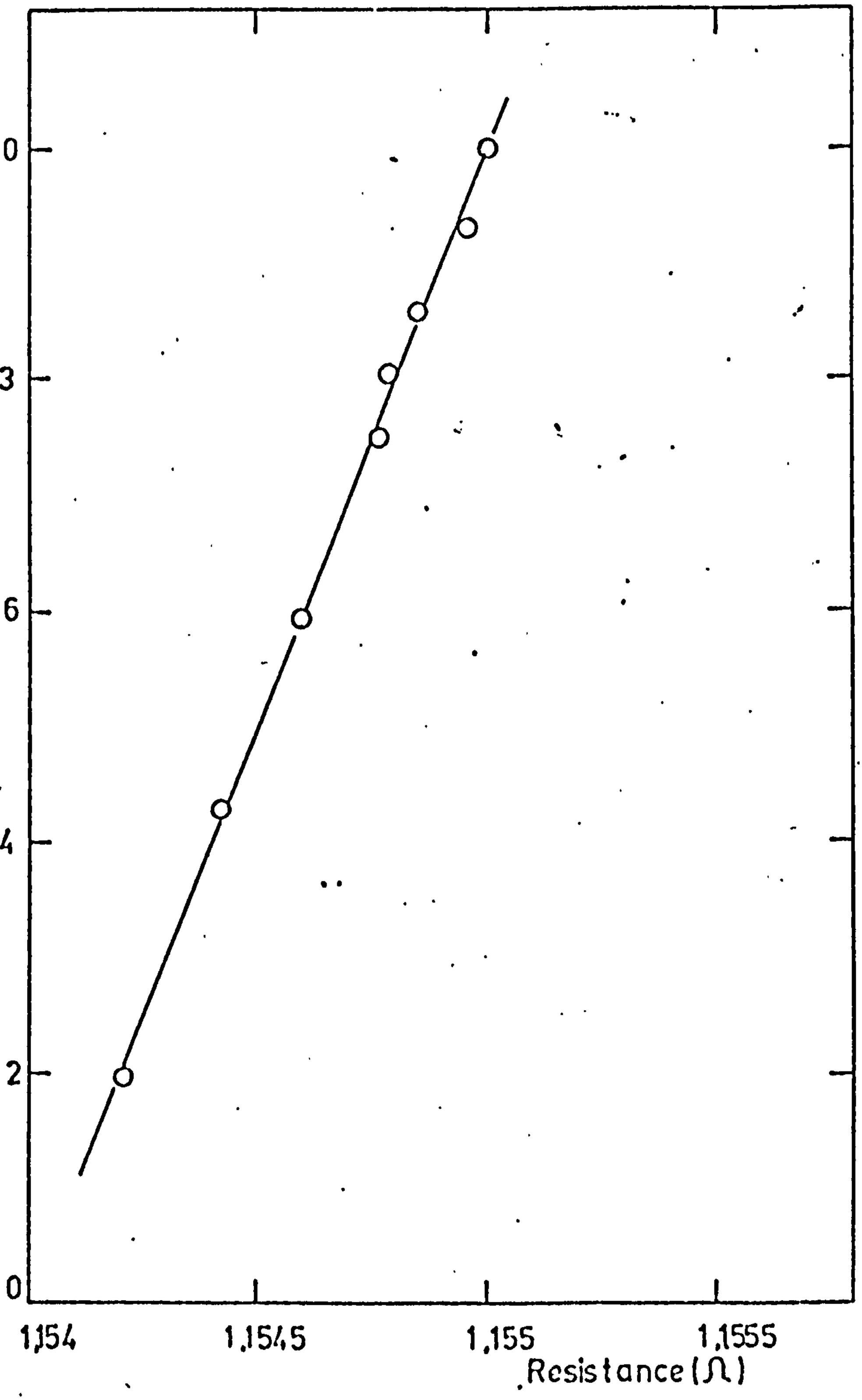

Fig A2,14 Lubricating Oil

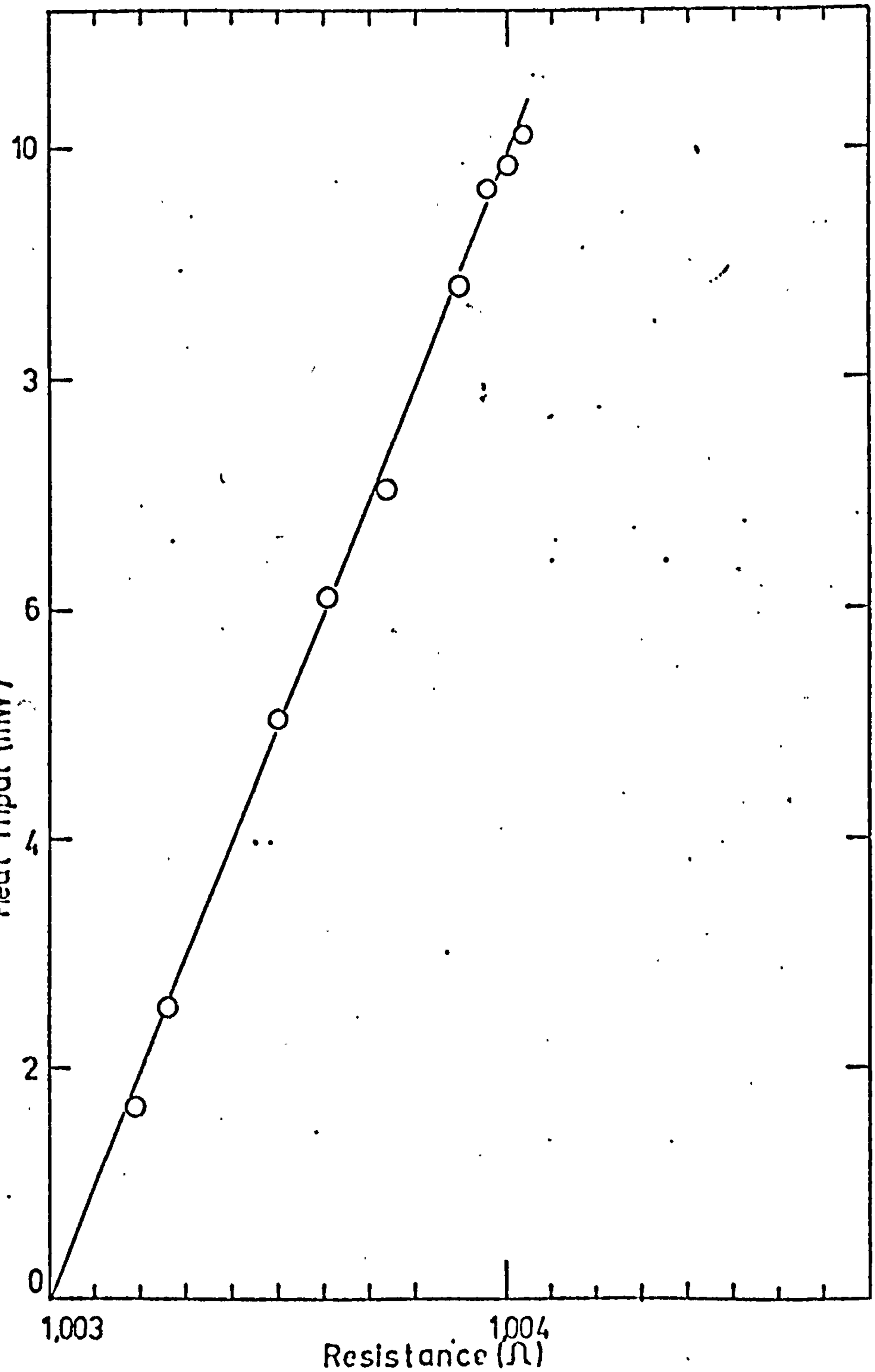

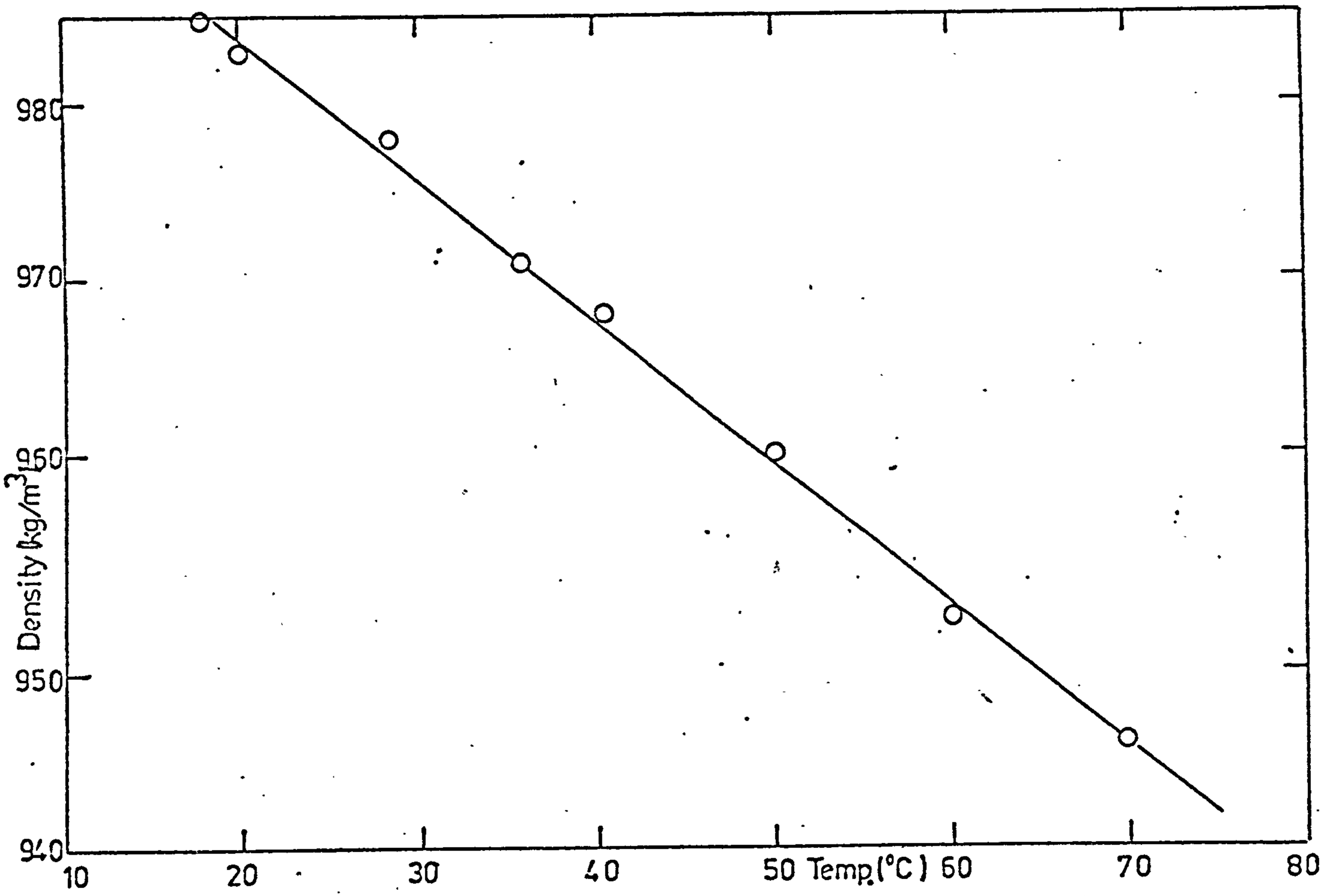

Fig A2.15 Density-Temperature variation for Silicone Oil

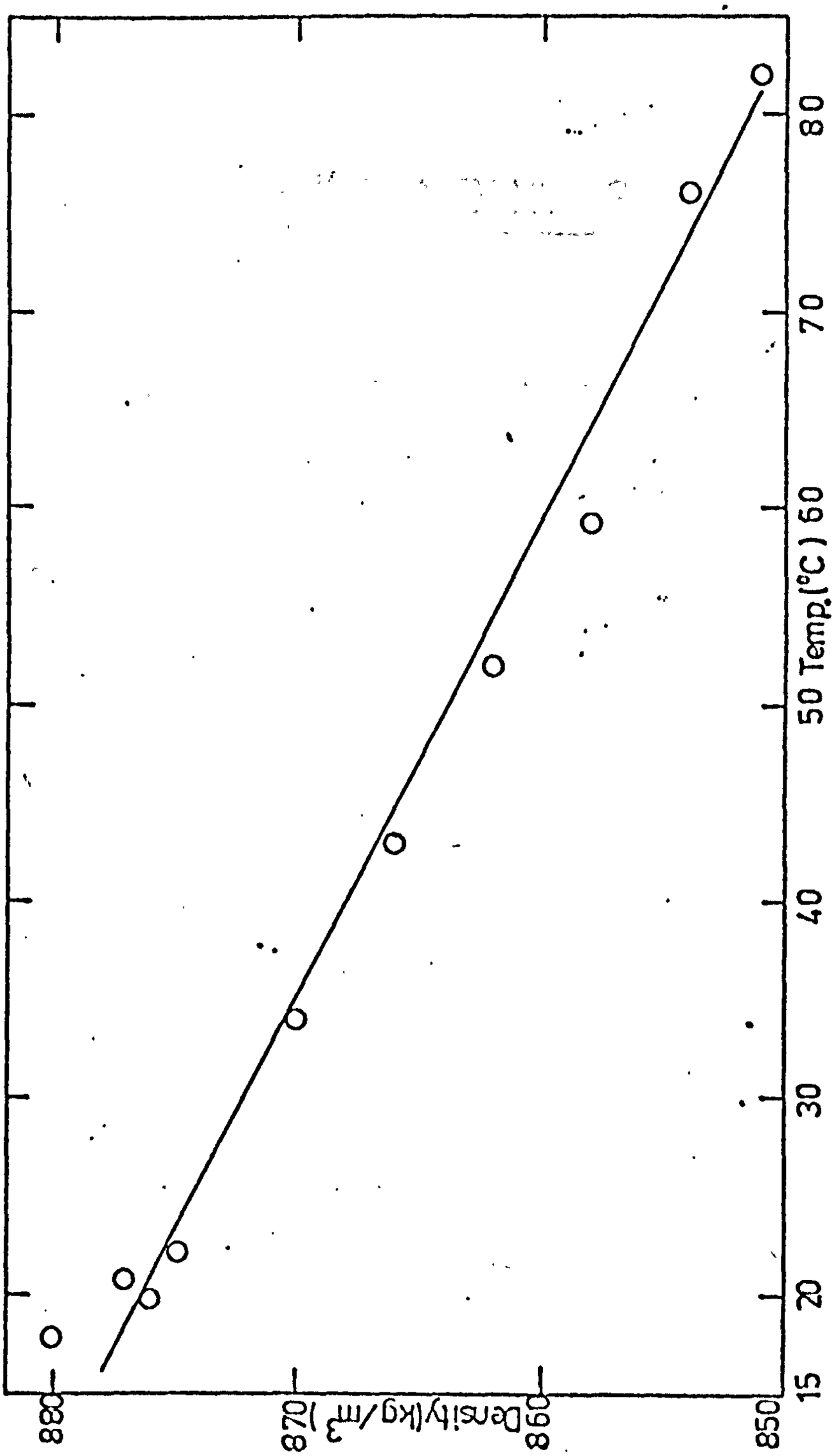

Fig A2,16 Density- Temperature variation for Lub. Oil

APPENDIX 3

Calibration of Instruments

A3.1 Calibration of cooling water rotameter used in Vessel 1

The rotameter was calibrated by the Manufacturer in liter/minute of water measured at $20^{o}C$. The calibration was checked using the method of direct weighing. The rotameter outlet was disconnected and water was allowed to flow into an empty container of known weight over a measured time. The weight of water and thus its flow rate was determined. The water flow rate was changed and the whole procedure repeated several times. The results are shown in Fig. A3.1 .

A3.2 Calibration of thermocouples

All thermocouples used in this research were calibrated by placing them in a constant temperature water bath. The temperature of the water bath was measured by a mercury-in -glass thermometer calibrated in tenths of a degree centigrade. Voltages recorded by the Kent multipoint recorder, in case of vessel 2, were noted for each temperature used in the water bath. Millivolt readings were plotted versus thermometer readings and the calibration graph is shown in Fig. A3.2 .

The digital thermometer used to measure thermocouples output with vessel 1 was calibrated in a similar way described above. It was found that the digital thermometer was accurate to $\pm$ $0.1^{o}C$.

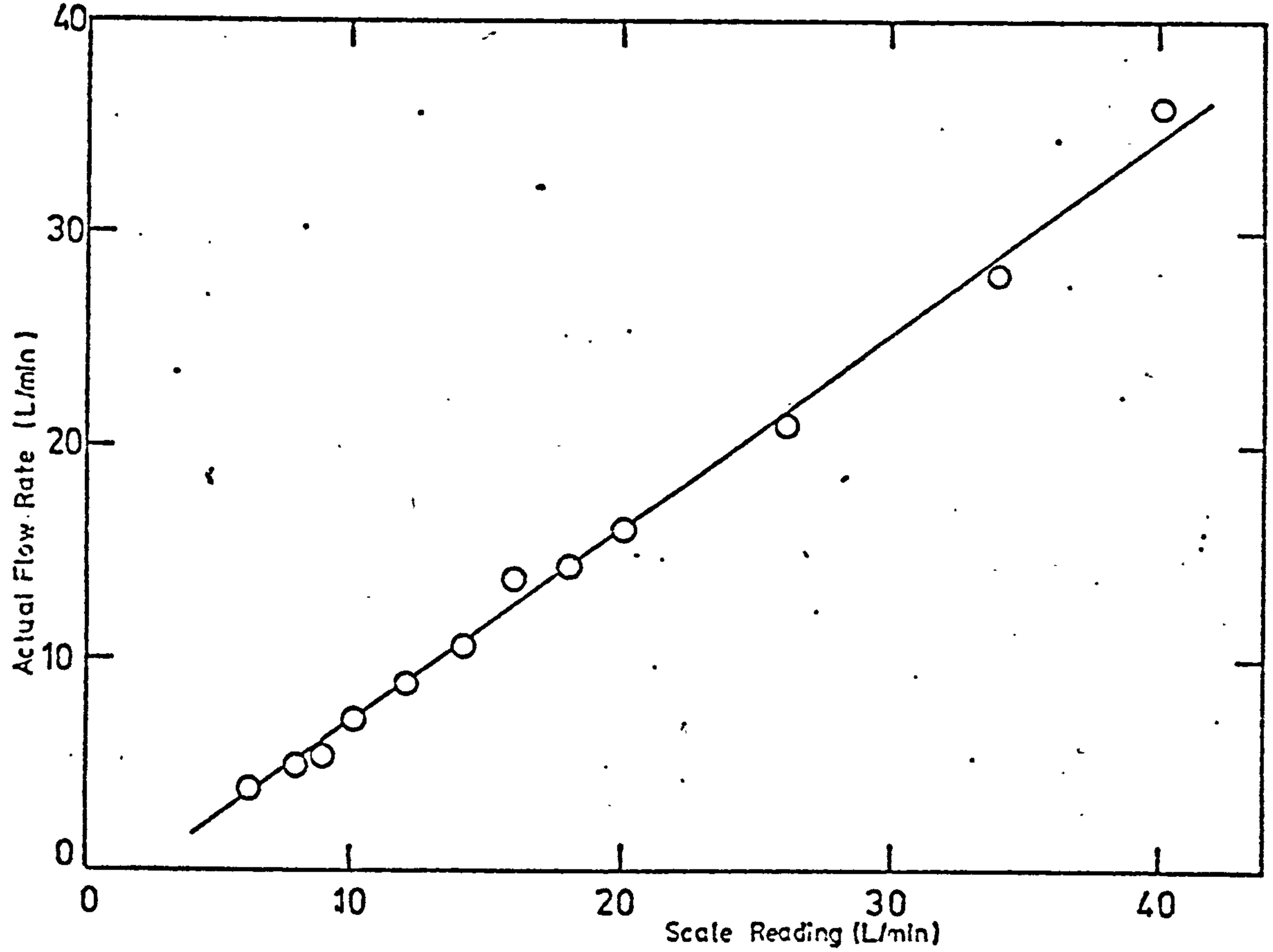

Fig A3,1 Rotameter Calibration Chart (Vessel 2)

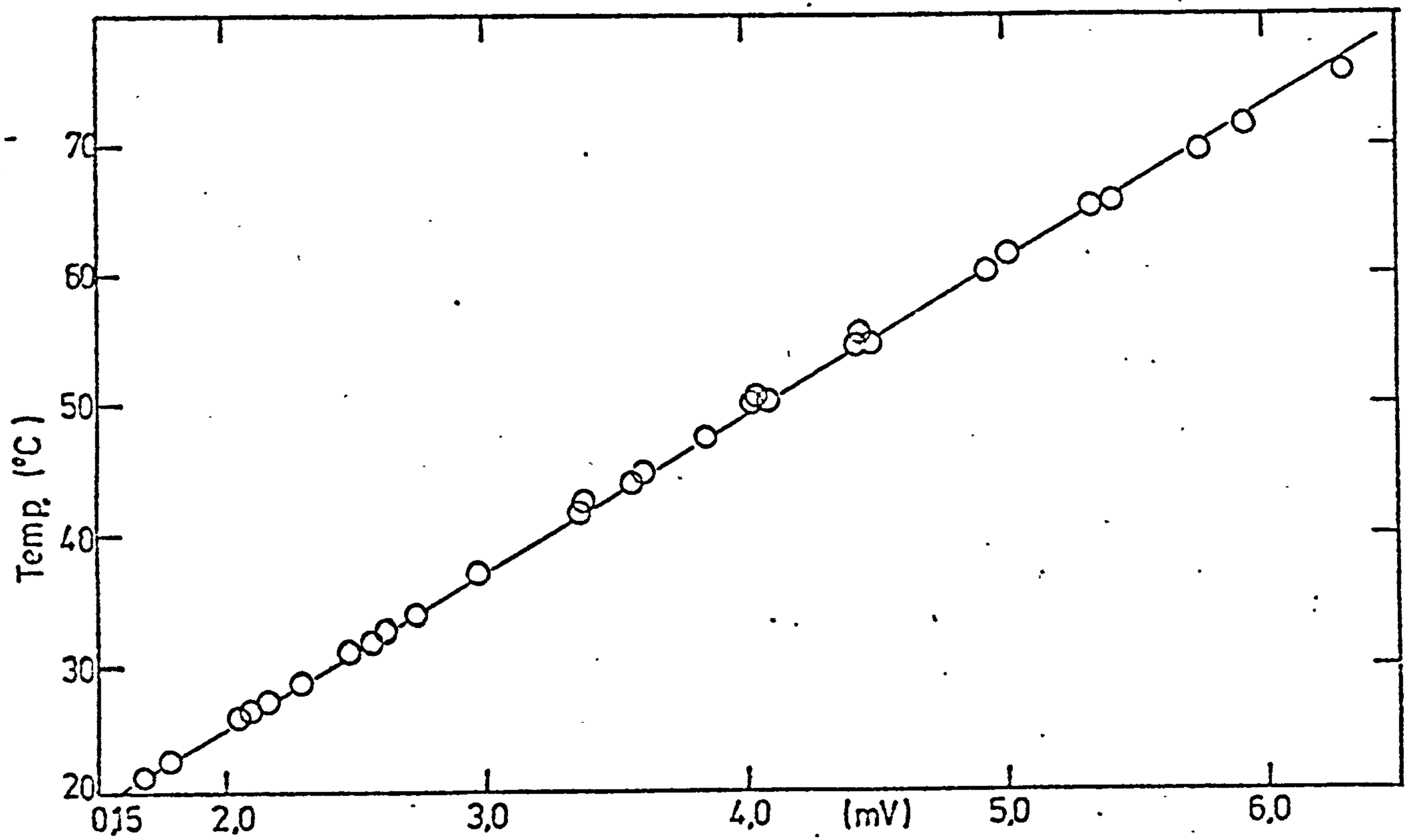

Fig A3,2 Thermocouples Calibration Chart (Vessel 2)